National Library
of Canada

Acquisitions and
Bibliographic Services Branch

395 Wellington Street
Ottawa, Ontario
K1A 0N4

Bibliothèque nationale
du Canada

Direction des acquisitions et
des services bibliographiques

395, rue Wellington
Ottawa (Ontario)
K1A 0N4

Your file Votre référence

Our file Notre référence

NOTICE

The quality of this microform is heavily dependent upon the quality of the original thesis submitted for microfilming. Every effort has been made to ensure the highest quality of reproduction possible.

If pages are missing, contact the university which granted the degree.

Some pages may have indistinct print especially if the original pages were typed with a poor typewriter ribbon or if the university sent us an inferior photocopy.

AVIS

La qualité de cette microforme dépend grandement de la qualité de la thèse soumise au microfilmage. Nous avons tout fait pour assurer une qualité supérieure de reproduction.

S'il manque des pages, veuillez communiquer avec l'université qui a conféré le grade.

La qualité d'impression de certaines pages peut laisser à désirer, surtout si les pages originales ont été dactylographiées à l'aide d'un ruban usé ou si l'université nous a fait parvenir une photocopie de qualité inférieure.

Canada

AEROELASTIC MODEL TEST OF A TALL BUILDING

A thesis submitted to the University of Ottawa
as a partial fulfilment of the requirements
for the Master of Applied Science
in Civil Engineering

Juergen Felbor

ISBN 0-315-85760-9

Canada

UNIVERSITÉ D'OTTAWA
UNIVERSITY OF OTTAWA

Abstract

An aeroelastic model test of a 500 metre tall building was carried out with the length scale of 1:200. The building response was found to be mostly buffeting due to oncoming flow turbulence. The thesis describes the test program and its results, general theory of buffeting analysis and its application to the project and some discussion on them.

Acknowlegement

The author would like to express his deepest gratitude to his research supervisor, Dr. H. Tanaka for his guidance and encouragement all through the period of this study. The opportunity to work on this subject was given to the author by participating one of his research projects based on the University's contract with Fujita Corporation Ltd., Tokyo.

The gratitude is also extended to Dr. M. Nakayama, a research engineer of Fujita Corporation, from whom the author learned a lot through working together. The technical assistance and friendship offered by staff members at the Applied Aerodynamics Laboratory, National Research Council Canada, particularly of Mr. Kevin Cooper, and of other friends at the University of Ottawa, Ms. Sandra Resende-Ide in particular, is greatly acknowledged.

For moral and financial support given by his parents and the research supervisor the author is most grateful.

Table of Contents

List of Figures and Tables

Glossary of Symbols

A	Surface area taken normal to the mean flow
B	Width of building or Background turbulence factor in buffeting calculation
C_a	Cauchy number
C_D	Drag force coefficient
C_e	Exposure factor
C_r	Generalised damping for r-th mode
E	Young's modulus
F	Gust energy ratio
$\{F\}$	Mode shape vector
Fr	Frounde number
H	Height of structure
$H(f)$	Mechanical admittance function
Iu, Iv, Iw	Intensity of turbulence for u-, v- and w-direction
I	Mass moment of inertia
$I(f)$	Joint acceptance function
K_r	Generalised stiffness
K_t	Rotational spring constant for rigid bar
L	Linear dimension of structure
Lu, Lv, Lw	Integral scales of turbulence
M_r	Generalised mass
P	Mean drag force
P_r	Generalised force
$P(t)$	Drag force
Re	Reynolds number
$R_u(s)$	Autocorrelation function of u-component
Rp	Pressure correlation coefficient
S	Scaling factors or size reduction factor in buffeting calculation
$S_u(f)$	Velocity spectrum of u-component
$S_p(f)$	Force spectrum
$S_x(f)$	Response sectrum
U	Mean wind speed in u-direction
U_{ref}	Mean reference wind speed
$Xa(f)$	Aeroynamic admittance function
X	Mean structural response
$X(t)$	Structural response
f	Frequency
f_o	Natural frequency
h	Damping ratio
h_a	aerodynamic damping
k	Stiffness per unit length of the body
m	Mass per unit length of the body
$p(t)$	Time-dependent drag force
r	f/f_o
$u(t)$	Along-wind velocity component
ρ	Air density
σ_u^2	Variance of u-component

Chapter 1. INTRODUCTION

1.1 General

Ever since the time of the Industrial Revolution a continuous development of technical challenges in the building industry has been observed. One part of this challenge can be seen as the development of new design philosophies and construction methods. At the same time, the mechanical properties of materials used for building and construction have made a remarkable progress and new materials have been also developed.

In order to satisfy both economical and aesthetic requirements as much as possible there has been a tendency to build more slender and lighter structures. With this tendency, the structures have become more and more vulnerable to wind action. This applies to bridges, towers, tall buildings as well as the structures with thin walls such as cooling towers and space structures.

It has become evident, because of this reason, that the traditional concept of dealing with the wind loading as the static wind pressure is sometimes not sufficient for the design of them. The concept of dynamic or unsteady wind forces has become more and more important for civil engineering design which was typically demonstrated by the spectacular failure of the Tacoma Narrows Bridge in 1940. It was clearly seen that the failure was not caused by the underestimation of the design wind load but was due to the dynamic action of wind which did not exist in the design process of this structure [2.1].

Research in this field has been intensified in the second half of this century partly because of an accelerated development of taller buildings and longer bridges and also by the significant development of electronic computers and the introduction of information theories as a powerful analytical tool.

Wind tunnel testing of model buildings has been done by many researchers and engineers before but it is still an important part of a design process for tall buildings, despite the fact that various mathematical models have been developed to estimate the wind induced structural response. Theoretical prediction based on some assumptions and past experience can be used as a preliminary design calculation but it can hardly replace the invaluable usefulness of wind tunnel tests.

1.2. Historical Background

Not only the understanding of the wind load itself, there have been various changes in construction technology, too. For example, the steel frames of tall buildings used to be covered with heavy masonry facade. Now they are covered with much lighter weight flooring and external cladding materials. This has produced not only lighter structures but at the same time more flexible structures with less structural damping. The decrease in rigidity resulted in lower natural frequencies which then made buildings more susceptible to the wind action. This sensitivity to wind did not necessarily result in building failures but severe damages can still occur in structures and their facade and also a possible discomfort of occupants. The following points should be considered as a part of the wind resistant design of tall buildings [2.2]:

1. Strength and stability requirements of the structural system;
2. Fatigue damages in structural members and connections caused by dynamic wind action;
3. Excessive deflection which causes cracking of partitions and external claddings, misalignment of mechanical systems and doors, and even possible permanent deformations;
4. Frequency and amplitudes of building motion which can cause discomfort to ther occupants;
5. Possible buffeting effects which may increase the wind loading on the neighbouring buildings;
6. Effects on pedestrian level wind environment;
7. Annoying accoustical disturbances;
8. Resonant vibration of various elements such as elevator hoist ropes with the building oscillation.

The Meyer Kiser Building and the Great Plain's Life Building are examples of structures which experienced a considerable permanent set due to wind though they did not collapse [2.3]. Further, an example of the Great Plain's Life Building in Lubbock shows that a building does not have to be very tall, less than 20 storeys for this case, to have wind problems. This building had a core which was somewhat off the building centre in plan so that the centre of torsion did not coincide with the geometrical centroid. It

was one of the weaknesses the building had when it was hit by a tornado.

Since the 1930s when the skyscrapers started growing, the design of tall buildings sometimes involved wind tunnel tests and even the full scale measurements were sometimes carried out after their completion. Needless to say that there have been enormous improvements since then in the experimental techniques and knowledges both for wind tunnel investigations and full scale observations.

The Empire State Building, New York, was the first tall building which involved significant wind tunnel tests. The test was carried out in a conventional aeronautical wind tunnel. It was, however, noted by Irminger and Noekkentved in Denmark [2.4] and also by Baily in Great Britain [2.5], in the same period, that there was a significant discrepancy in wind induced pressure distribution between wind tunnel model results and full scale observation on similar buildings. It was believed that at least a part of this disagreement could be attributed to the lack of simulation of turbulence which inherently exists in natural wind.

The first attempt to examine such discrepancy was tried by Bailey and Vincent in 1954 [2.6] by using a boundary layer developed on the wind tunnel wall. The results were not conclusive. Later with the formulation of the model law regarding this simulation by Jensen in 1958 [2.7], the test requirements were clarified to overcome this difficulty. For the correct modelling of the phenomena in a wind tunnel, the test has to be carried out in a turbulent boundary layer flow which has a similar turbulence structure as that of natural wind. The model law further requires that the linear scale charactrizing this boundary layer has to be scaled consistently with the linear dimensions of the building.

After the model law by Jensen, more emphasis has been given in creating the desired velocity profiles and statistical characteristics of turbulence in wind tunnels. In order to allow the use of greater linear scales for the model, various attepts were made to augment the boundary layer thickness as efficiently as possible by using screens and grids, floor roughnesses, spires and other vortex generators and the injection of jet flows and other mechanical control devices [2.8].

As the building performance, the overturning moments and base shears, sway and torsional deflections or accelerations, facade pressure distributions and overall

aerodynamic forces on the building are usually examined. The environmental aspect of the building is also an engineering focal point3 recently. This is usually examined in terms of the possible increase in local pedestrian level wind speed around the building. Some adverse effects on the neighbouring buildings, if any, can be of some concern, too. The ultimate effectiveness of wind tunnel tests can be confirmed only by the full scale comparison which is not necessarily without any difficulties [2.3].

1.3 General Characteristics of the Wind induced Building Response

By reviewing the previous studies on wind induced behaviour of structures, it becomes evident that there are various different types in wind induced dynamic response of structures. Sometimes the response amplitude monotonically increases with wind speed. Sometimes response can be observed only in a limited range of wind speed. It depends on the mechanical and geometrical characteristics of the structure and also on the conditions of wind. Natural wind is usually a turbulent flow and has random velocity fluctuations which can be described only by statistical means. The description of structural behaviour becomes more complicated because of this.

Wind induced structural vibrations can be categorized as are given in Table 2.1, for example [2.9]. This table is quite extensive and covers a wide range of structures. However, only a part of it would be usually applicable for particular types of structures. For most of the tall buildings, for example, only two categories should be usually considered; vortex induced oscillations and buffeting.

Vibrations of the first category is induced by so-called signiture turbulence which is the disturbance of air flow created by the existence of the structure itself. If the structure gives a regular fluctuation of air flow pattern which causes a similar fluctuation of aerodynamic forces and if its frequency coincides with a natural frequency of the structure, a resonant response can occur. Once the structure is in motion, the air flow pattern in the wake would be strongly influenced by this moving body and the shedding frequency may be "locked-in" to the frequency of the motion over a limited range of wind speed. Thus the apparent resonance continues in that range. However, when the motion amplitude exceeds certain limit, the continuous production of regular flow pattern would break down and the exciting force alters to a damping force [2.9].

Buffeting motion, on the other hand, is caused by randomly fluctuating wind loading due to atmospheric turbulence which inherently exists in the oncoming flow. The velocity fluctuation can be also caused by the disturbance of air flow by the existence of any objects in upstream. The resulting vibrations are characterized by the combination of wind properties and the dynamic properties of the structure. In the following chapter, a mathematical analysis of this type of wind induced motion is reviewed.

1.4 Scope of the Present Study

The subject of the thesis project is the investigation towards the dynamic response of a tall building model in turbulent wind. The experimental phase of the study included both static and dynamic calibration of the model and the examination of its behaviour in a wind tunnel. After its mechanical properties were found to be satisfactorily close to the design values, the model was placed in a wind tunnel test section and its behaviour in simulated natural winds was measured at various wind speeds and for various wind directions relative to the principal axes of the structure.

The experiment was carried out as a part of the collaborative research project between Fujita Corporation Ltd., Tokyo, and the University of Ottawa. The project is titled "Definition of Wind Loading for the Design of Super Tall Buildings", the first phase of which took place in 1991 [4.1].

The objective of this collaborative project is to study the methodology of possibly defining the wind loading in time domain for the design of very tall buildings particularly against buffeting motion due to wind turbulence. The wind induced buffeting of tall buildings has been analysed usually in frequency domain as it was explained in the previous chapter because of its stationary random characteristics over a considerably long period of time as opposed to the earthquake response calculation which is usually in time domain.

It was intended first to obtain typical time dependent wind loading functions under given conditions through pressure model test and compare the calculated response based on these aerodynamic forces with the results of the aeroelastic model test. However the sequence of the testings were reversed because of the extraneous circumstances and it was decided to carry out the aeroelastic test first, which is summarized here. The effort was also made to identify the buffeting forces from the building model response. However, this process is not included in this chapter. The resonant component in model response is generally so large that the accuracy of obtaining the buffeting force components was found to be severely limited.

The scope of this thesisproject is limited to the aeroelastic model test to predict the building response in

Chapter 2 of the thesis summarizes some of the previously carried out wind tunnel studies on tall buildings.
The intention of this summary is not to cover the whole history of the wind tunnel study but to reveal the historical development of the philosophy in wind tunnel testing of buildings.

Chapter 3 is a summary of the conventional buffeting analysis which is typically employed for the National Building Code of Canada.

Chapter 4 explains the experimental program of the study and its results and discussed and compared with the analytical prediction in Chapter 5.

Some brief concluding remarkes are given in Chapter 6.

Chapter 2. Previous Studies on Wind Induced Behaviour of Tall Buildings

As it is described in the previous section, many number of tall buildings have been tested using wind tunnels in the last 60 years. Some of these tests are referred to in this section to review the basic testing procedures. The review is not meant to cover the complete history which should be looked for elsewhere [2.10]. Its objective is to reveal the historical development of the philosophy in wind tunnel testing of buildings. Some of the most typical buildings of the century such as the Empire State Building (New York), the World Trade Centre Towers (New York), Sears Tower (Chicago) and the most recent achievement of Miglin-Beitler (Chicago). At the end of this chapter, a short summary of full scale comparisons is also given.

2.1 Empire State Building

Dryden and Hill [2.11] undertook the first significant wind tunnel study for major tall buildings. A 1:250 model building made of rolled aluminium plates of 1/4 in (6.4 mm) thick was constructed as a representative of the 1,250 ft (381 m) high prototype.

Both wind induced pressure on the building and overturning moments due to wind were examined in the 10 ft wind tunnel at the National Bureau of Standards. Pressure on the model was measured at three different elevations - 36th, 55th and 75th floors - by connecting a pressure guage to external holes with rubber tubings. In total there were 34 pressure taps on each floor level and the model was rotated through 180 degrees to study the effect of wind azimuth angle. The test was repeated at different wind speed levels. In addition to the measurement of external pressure distributions, the base overturning moments were also measured.

Another interesting observation reported in this study is the comparison of the measured overturning moments with those derived from the integration of the measured pressure values. It provides confirmation of the different measuring techniques. Comparison shows generally good agreement of the results from two techniques with the exception of some difference in the y-component for the wind direction of over 140^{o}. A full scale study on the Empire State Building for the evaluation of wind loads was also performed [2.12] which is reported in later section.

2.2 World Trade Center Towers

The World Trade Center Towers, N.Y., attracted significant attention regarding wind loading on them before and even after their construction [2.13]. The wind effects on the towers were examined at Colorado State University (CSU) whereas confirmation test was carried out at the National Physical Laboratory (NPL), England. Wind effects on plaza level environment were tested at the University of Western Ontario (UWO). This was the first major tall building project in which a proper simulation of natural wind turbulence was introduced.

2.2.1 Wind Load on Towers

A model of the twin towers including the low-rise plaza level buildings and the surroundings was tested at CSU with the shear flow turbulence as a simulation of natural wind. A geometric scale of 1:500 was used for the model simulation. About 250 pressure taps were connected to a Scanivalve pressure measuring system. The distance between two towers was varied to provide a guideline for placing the two towers relative to each other. The pressure measured at CSU was confirmed by another study at NPL. A static wind load of 55 psf (1 psf = 48 Pa) for the top 100 ft and 45 psf for the remaining portion of the tower was recommended from the wind tunnel test results for the 100 year wind of 140 mph (60 m/s). Viscoelastic damping units were suggested to limit the maximum deflection to 3/8 in (9.5 mm) per storey at the same bench-mark wind speed.

2.2.2 Dynamic Response of the Towers

The study at NPL consisted of two parts; pressure test which more or less confirmed the results at CSU and the prediction of wind induced response using a 1:400 scale aeroelastic model which is reported in [2.14]. The building model was constructed of a light timber frame covered with thin plywood, designed as a rigid body with proper mass simulation and the required stiffness. Variable damping was provided by the system under the wind tunnel floor via an extended aluminium tube from the model going through gimbal.

Its response to wind was observed in an idealized smooth flow and two kinds of turbulent flow; homogeneous

turbulence and shear flow turbulence both created by grids installed at the front end of the wind tunnel test section.

Both an isolated tower and twin towers were tested and it was concluded that the Towers are unlikely to experience any adverse wind effects from aerodynamic instability for wind speeds below 100 mph (160 km/h or 45 m/s), either as a single tower or as the completed twin-tower configuration. However, in order to limit amplitudes at the tower top to less than 10 ft for wind speeds up to 150 mph a very high damping (approximately 12 % of critical) needs to be provided.

2.2.3 Pressure Study for the Plaza Level

Wind engineering study for the plaza level of the project consisted of two parts; measurement of wind induced pressure on the plaza level buildings for the design of exterior claddings and pedestrian level environmental wind conditions around the towers. These experiments were carried out at the Boundary Layer Wind Tunnel Laboratory, the University of Western Ontario [2.15].

Using a linear scale of 1:400, the four main buildings and the surroundings were modelled. There were 45 pressure taps on each building model. The upstream terrain conditions for the site varies depending on the wind direction. Three different exposure conditions were simulated in the wind tunnel. They are: Exposure I representing the open water fetch, typical of the wind coming across the Upper Bay and along the Hudson River, Exposure II representing the fetch typical of the wind coming across the Hudson River from Jersey City, and Exposure III representing Manhattan fetch, typical of the wind coming over heavily built-up terrain. All three exposure conditions were physically modelled in the wind tunnel with the surrounding topography of a radius of 1,600 ft. in order to include the local flow characteristics. Such a precise terrain simulation was one of the novel points of this particular study.

Isolated pressure signals were collected by tubing with a Scanivalve pressure transducer. Mean, rms and peak pressure coefficients are based on the wind speed at the top of the main towers. For the design of window panels and exterior cladding elements, gust factors were obtained. A summary of the measured peak factors (the ratio of dynamic peak to the root-mean-square) showed the average value of

about 4.5 for all building elements. The positive peak pressure factors were about 4 to 5 whereas the maximum peak suction factor was typically in excess of 7 for some locations. The largest pressure, suction and their fluctuations were observed by the wind coming from the SW quadrant, which is over the exposure I.

2.2.4 Environment Study for the Plaza Level

Flow visualization and velocity measurement were both carried out to establish the acceptable pedestrian level wind conditions. The flow visualization was performed by generating smokes in the wind tunnel whereas the velocity measurement was done by using a hot wire anemometry system. All three flow regimes as discussed in the previous section were considered.

For each wind azimuth angle, 20 observation points were chosen at a full-scale elevation of 6 to 12 ft. The results indicate generally greater wind speeds near the immediate vicinity of the main towers. The passage ways, especially between the US Custom Building, the Towers and the Hotel building show the highest mean speed ratios and particularly for WNW to SSW winds. The peak values of the wind speed ratio is found to be from 0.4 to 1.2 for the positions examined.

2.3 Sears Tower, Chicago

To this date, the 443 m tall Sears Tower holds the title of the world tallest office building. The proposed Miglin-Beitler Tower (585 m) upon its completion will move the Sears Tower to the second place. A comprehensive wind engineering study was performed at the University of Western Ontario [2.16]. The project comprised of the study of local wind climate, measurement of wind induced pressure loads and determination of wind induced dynamic response of the building and the prediction of wind loads based on these results [2.17].

This particular project more or less established the pattern of the wind engineering study of tall buildings at UWO where a number of major tall buildings have been tested. These include Federal Reserve Bank Buildings both in New York and in Boston; Bank of Montreal Tower, Toronto; John Hancock Tower, Boston; First National City Corporation

Building, New York, and so on. This pattern continued until a high frequency force balance was introduced.

2.3.1 Local Wind Climate Study

The local wind climate at the site of Sears Tower was established based on two approaches. First of all, the meteorological data from the surface and upper level observations in the Chicago area were used to establish the general climate of the area. Secondly, using a 1:2000 scale topographical model of the Chicago area, the detailed wind condition at the site was examined. For the topographical modelling, the surrounding area extended over a circle with a full scale radius of 400 m centred approximately at the tower site. Two types of upstream terrain, open water and urban terrain, were considered. Vertical profiles of mean and rms wind speeds at the site were established normalized by the gradient wind speed.

A 1:400 scale wind tunnel study was also performed to establish further details of the upstream flow regimes. Based on this exercise, three flow conditions were identified as a good choice. They are represented by the power law exponents of 0.56, 0.40 and 0.13. These conditions correspond to the winds coming from NE direction, NW or SW direction and SE direction, respectively.

Full scale wind data from six locations were used to evaluate the probability of exceedance for a given wind speed from a particular direction. The macro-scale spectra were also established which provide the time domain variation of mean wind speed averaged over intervals of time long enough compared to time scales associated with turbulent velocity fluctuations. The effective cycling rate for the Chicago area was found to be 0.11 cycles/hour; i.e., the number of events becomes about 960 per annum. This was based on the frequencies associated with the macro-scale variations in velocity spectra.

2.3.2 Pressure Study

Two different models with the linear scales of 1:400 and 1:2000 were fabricated to evaluate the wind induced external pressure distribution on the Sears Tower. The 1:2000 model was used for finding the scale effect on the measured pressure and also to correlate the local wind

statistics influenced by the local topography. The detailed pressuer study was performed by using the 1:400 model with 183 pressure taps. The model was tested for various wind directions using all three exposures discussed in the previous section.

The peak pressure factors were examined for selected tap locations. These factors are very useful for the design of window glass panels and other exterior cladding elements. It is worth to notice that the peak suction coefficients were sometimes found to exceed 10.

The comparison of results from the 1:2000 model and the 1:400 model confirmed that the scale effect, if any, is negligibly small. The pressure results obtained from the 1:400 model were extensively used with the topographical wind speed data obtained from the 1:2000 model for the wind load predictions. The peak pressure of 25 psf and 60 to 70 psf (1 psf = 48 Pa) peak suction were predicted for the 100 year wind.

2.3.3 Aeroelastic Study

A multi-degree of freedom aeroelastic model of the Sears Tower was constructed to a scale of 1:400. The model was mounted on a flexible base designed to represent the rotational flexibility of the foundation. The model consisted of seven rigid floor plates, a base plate and columns to simulate the building stiffness. Including the three degrees of freedom at the base, the model had a total of 24 degrees of freedom. At the full scale height of 1,165 ft, the top floor acceleration was monitored. Structural damping was assumed to be 0.5 and 1.0% of critical. Measurements were carried out in three different flow regimes as developed in the wind climate study. The measured results suggest the peak factor of approximately 3.5.

The measured mean base moment coefficients from the aeroelastic test agreed well with the calculated values from the pressure study. The measured mean pressure values were integrated over the building surface and the base moments were taken at the level of 105 ft (= 32 m) below the plaza level.

2.4 Bank of China, Hong Kong

When it is completed, the Bank of China building will become the tallest structure in Hong Kong and also the tallest building in the world outside North America. Its unusual geometry and local high incident of typhoon winds pointed to the need for a wind engineering study. An extensive study of typhoon conditions in Hong Kong has been reported elsewhere [2.18-2.19] and the following informations are gathered from Davenport et al.[2.20].

First, the wind records were synthesized to obtain the profile of the hourly mean wind speed. Secondly, a 1:500 pressure model was tested at the Boundary Layer Wind Tunnel Laboratory (BLWTL) to predict the static loads for various return periods. Hong Kong wind climate can be devided into two types of winds: winds associated with typhoons and those which are free from typhoons. Always the structural design for safety and strength is governed by typhoon winds of typically about 48 m/s, whereas the occupant comfort and other serviceability are designed based on non-typhoon wind climate of the order of 28 m/s. Both values are given at the gradient height and correspond to the return period of 50 years.

The largest suction for the 100 year wind was about 6.6 kPa occurring on a joint corner of the building. Generally the East elevation has higher peak suction values than other elevations. This is not only because of the unusual building shape but because of the prevailing wind direction. The 50 year suction of 5.9 kPa was observed as opposed to the code value of 5.3 kPa. This is a case in which the conservativeness of the code was not enough for covering the unusual high loads caused by unusual building configurations. For the final design of cladding and other external elements, the code has been generally adopted except at those locations where it was exceeded by the wind tunnel predictions.

Another approach taken in this study was the use of force balance technique developed by Tschanz [2.21] for the measurement of wind loads and response prediction. It is a simple approach compared with the conventional aeroelastic modelling. It has several advantages such as simplicity in modelling without including the details of the structural dynamic properties. Construction of simpler models reduces the model cost. It should be noted also that structural properties are not vitally important during initial design process because of the anticipated changes in the final design and/or actual construction of the building.

A comparison of the results obtained by using the new force balance technique vs the conventional aeroelastic testing is shown on the next page:

Source	50 yr moments (10^6 kN m)			100 yr accelerations (milli-g)		
	X	Y	T	X	Y	T
Force Balance	5.18	4.86	0.28	6.8	5.5	8.4
Aeroelastic	3.42	3.00	3.16	5.1	4.4	10.6
H.K. Code	14.6	10.2	----	---	---	---

The base bending moments calculated from the Hong Kong Code are also included as a reference. In general, the moments obtained from the aeroelastic model study are smaller than those indicated by the force balance technique. In reality, the major structural components were designed to meet the requirements of the code of practice.

2.5 New Miglin-Beitler Tower, Chicago

The Chicago Planning Commission has approved the construction of the New Miglin-Beitler Tower [2.22]. Upon successful completion with the design height of 585 m, it will be the tallest building in the world. Wind tunnel studies for the evaluation of design wind loading were carried out by RWDI Consulting Engineers, Guelph. Static and dynamic analysis were carried out but findings are not disclosed yet. A unique character of this building is the height-to-width ratio, which is about 14. Considering only the occupied building space, the ratio reduces to 8.25.

2.6 Brief Summary of Development in Wind Tunnel Studies

Looking over the history as above, it has been clearly seen that the whole issue has come through the following steps:

1. Appreciation of wind loads in design
2. Testing with conventional aeronautical wind tunnels
3. Dynamic response measurement by aeroelastic models
4. Consideration of flow turbulence
5. Better simulation of natural winds
6. Cross checking of force/pressure and response
7. Introduction of high frequency balance

8. Integration with the meteorological parameters and prediction of building performance

The elaboration of the above step No.7 by pressure measurement using high speed scanning system has been recently proposed and applied to some structures. This will make it possible to evaluate two-dimensional aerodynamic forces at various heights of buildings and is expected to open another horizon to this field of research.

2.7 Full Scale Comparison of Wind Tunnel Test Results

The only way to truly verify the wind tunnel test results is to compare them with the behaviour of the real buildings. Since the full scale information can be obtained only after the construction of the structures, they cannot be used for the design of them. However, full scale data have vital importance for the validation of physical and numerical modelling and simulation. Unfortunately, the full scale measurements are relatively costly and they often provide obscure outputs which does not allow straightforward comparison because of various reasons. Thus, only few studies have been made so far [2.30].

Some of these rare and yet precious measurements are summarized here. The buildings are the Empire State Building, the Commerce Court Tower and the Allied Bank Plaza which may represent the construction of 1930s, '60s and '80s, respectively.

2.7.1 Empire State Building

Full scale measurement of wind induced pressure on the Empire State Building was carried out by Rathbun in 1930s [2.12]. In this experiment, one anemometer, 30 manometers, 28 cameras with operating mechanisms, 22 extensometers, 1 collimator with its target and 1 plumb-bob were used. Pressure signals were measured at 10 stations on each of three floors using manometer boards and flash cameras.

As it was mentioned before, Dryden and Hill [2.11] performed wind tunnel measurement for the same building. However, no attempts were made by Rathbun to compare his full scale values with the wind tunnel test results, presumably because they appeared to agree very little. In

1969, Dalgliesh [2.24] made several comparisons using those results.

Generally speaking, the wind tunnel values are higher than the full scale data and this may be due to the difference of the way to take the reference pressure between them. More seriously, Dryden and Hill assumed that the wind flow would be uniform at 200 ft (= 61 m) or more above ground and based on this assumption they used an aeronautical type wind tunnel for the measurement. The results could have been, of course, significantly different if one considers the boundary layer wind tunnel profile with the wisdom of hindsight. Much of the scatter and difference of results must have been caused by gustiness of wind due to surrounding topography whereas in the wind tunnel measurement this was not considered either. In any event, the change in wind direction causes significant change in pressure reading for both cases. The agreement seems to be better when the wind is normal to building walls rather than the angled flow cases.

Another comparison was attempted by Davenport [2.25] in terms of the overturning base moments after more recent boundary layer wind tunnel tests on the Empire State Building model was carried out using the base balance technique. A model of the building machined from a stiff foamed plastic was mounted on an ultrasensitive high frequency balance to measure the base shears, moments and torques. The agreement between them is remarkable. This provides a very important full scale confirmation of a model test.

2.7.2 Commerce Court Building

One of the most successful, and detailed full scale comparison was made on this building by Dalgliesh et al. [2.26-2.29]. This is a 57 storey office building (239 m tall) located in downtown Toronto and has a rectangular cross section of 36 m x 70 m. The design wind load was based on the model test carried out at the University of Western Ontario [2.30]. The full scale measurements were undertaken by Dalgliesh and other members of the Division of Building Research, National Research Council Canada in 1973-79. Surface wind induced pressure was measured simultaneously at 32 points on the building. The building internal pressure was also measured at one point and used as the reference for the calculation.

Pressures were collected for all ports at a sampling rate of 120 samples per minute over a period of 5 minutes. The agreement of the mean pressure coefficients was found to be better than that of rms values. One reason for this was attributed to the fact that winds from the south had not been frequent enough or strong enough to provide sufficiently reliable rms data.

Wind tunnel testing of both pressure model and aeroelastic model of the Commerce Court Tower was repeated at the National Research Council Canada [2.28, 2.31]. There were some minor differences between the NRC study and that of UWO but the general tendency is found to be quite similar.

2.7.3 Allied Bank Plaza

Full scale observation of the top floor acceleration of the Allied Bank Plaza has been reported [2.32] as a comparison with the wind tunnel test results. The measurement was done by using two kinemetric Model VM-1 accelerometers with a range of 0.1 mg to 1.0 g. The measurement was not successful in the beginning when wind speed was in the range of 35 to 45 mph (1 mph = 0.447 m/s). However, the area was later hit by a tropical storm with wind gusts of 56 mph and also by Hurricane Alica with fastest mile speed of 90 mph (equivalent to approximately 70 mph or 31 m/s) and some data were obtained. A possible fluctuation of wind speed and wind yaw angle was expected to be less than 2.5 m/s and 5^{o}, respectively.

In addition to the direct comparison of the wind induced parameters, it would be useful if the design wind loading criteria are validated. This was attempted for this building through the acceleration measurement. The lateral force acting on each floor can be estimated by the product of the weight at each floor, the top floor peak acceleration and the mode shape factor which normalized at the top floor. Using this concept, the estimated base shear and moment from the wind tunnel test results can be compared with the observation during Hurricane Alicia and the Houston Building Code (C_p = 1.4 assumed) as follows:

	Wind Tunnel		Full scale	Houston
First Mode	100 yrs	50 yrs	(Alicia)	Code
Base Shear (Kips)	5,600	4,900	4,500	12,500
Base Moment (ft-K)	3.5×10^6	3.1×10^6	2.7×10^6	7.1×10^6

Second Mode

Base Shear (Kips)	4,200	3,500	3,000	9,500
Base Moment(ft-K)	2.6×10^6	2.2×10^6	1.8×10^6	5.4×10^6

(1 Kip = 4.45 kN, 1 ft-K = 1.36 kN-m)

In general the agreement is found to be satisfactory. The full scale monitoring programme also started after the structure was completed. However, the interior constructions and windows still remained to be finished then. The calculation on the other hand is assuming a fully occupied, completed building. Having this in mind, the agreement between full scale observation and wind tunnel data are found to be good. This comparison shows that the code values are by and large conservative and overestimating both the moment and shear typically by a factor of two.

Chapter 3. BUFFETING ANALYSIS OF STRUCTURES

3.1 Mathematical Tools for Buffeting Analysis

The mathematical analysis of buffeting described in this chapter is based on a theory of random vibration which predicts the root-mean-square (rms) response of structures through a frequency domain analysis. It is accomplished by relating the frequency components of aerodynamic forces and those of the structural response by considering the structure's sensitivity to each frequency, which is given by the frequency response function.

It is, through this analysis, generally assumed that the statistical characteristics of wind are independent of the averaging period. It means that the fluctuating aerodynamic excitation and the induced structural motion are both stationary, ergodic random processes. This assumption is known to be reasonable as long as the averaging time is taken to be around ten minutes to one hour in case of ordinary wind storms [3.1].

3.1.1 Formulation of Aerodynamic Properties

(1) Formulation of Aerodynamic Forces

A turbulent flow can be discribed as a flow with three time-depemdent velocity components U(t), V(t) and W(t) in mutually perpendicular directions.

As a simple example to show the essential process of the buffeting analysis, a simple point structure consisting of a mass and a linear elastic restoring mechanism shall be considered. It is further assumed that the point mass can move only in drag direction.

First of all, the along-wind velocity component is to be separated into its mean value and the time-dependent fluctuating part as follows:

$$U(t) = \overline{U} + u(t) \tag{3.1}$$

The resulted drag force per unit length of the body is

$$P(t) = \bar{P} + p(t)$$
$$= (\rho\bar{U}^2/2)BC_D + \rho\bar{U}BC_D \cdot u(t) \qquad (3.2)$$

where B = the dimension of the body projected normal to the mean wind
C_D = the drag force coefficient; and
ρ = the air density

(2) Velocity and Force Spectra

Because of the stationary random characteristics of the wind turbulence, buffeting analysis is usually treated in frequency domain rather than in time domain by describing the contribution of fluctuating velocity and forces in terms of frequency spectra which are obtained by applying the Fourier analysis.

The fundamental procedure of calculating the spectral density function is to apply the Fourier Transform to the autocorrelation function which is calculated directly from the data. However, the most popular method now is the application of the Fast Fourier Transform (FFT) [3.2] which calculates the spectral density function directly from the data. The autocorrelation for this case is calculated by applying the Inverse Fourier Transform to the spectral density function. Their relationship for a time series u(t), for example, is

$$S_u(f) = F[R_u(s)]$$
$$R_u(s) = F^{-1}[S_u(f)] \qquad (3.3)$$

where F[ ] is the operator for the Fourier Transform and $R_u(s)$ is the autocorrelation which is given as a function of time lag "s". Because of the assumed stationarity for u(t), the above relationship becomes as follows:

$$S_u(f) = 4\int_0^\infty R_u(s)\cos(2\pi fs)\,ds$$
$$R_u(s) = \int_0^\infty S_u(f)\cos(2\pi fs)\,df \qquad (3.4)$$

Once the spectral density is defined, the variance of u(t) is given by

$$\sigma_u^2 = R_u(0) = \int_0^\infty S_u(f)df \tag{3.5}$$

As the analytical form of the spectral density function of u-component velocity, various expressions have been proposed by von Karman, Davenport, Harris, Hino, Kaimal and others [2.8]. All of these expressions incorporate the basic requirements such as the Kolmogorov's similarity rule, which requires $S_u(f)$ to be proportional to $f^{-5/3}$ in the inertia subrange. Davenport, for example, has established a universal function as follows [3.3]:

$$fS_u(f)/\sigma_u^2 = (2/3)X^2/(1+X^2)^{4/3} \tag{3.6}$$

where $X = Lf/\bar{U}$ (L = 1,200m = Davenport's length scale)
f = frequency

Fig.3.1 shows measured results of u-component spectra in high winds. Using the velocity spectrum given by (3.6), the force spectrum for the fluctuating part p(t) of (3.2) is expressed as follows:

$$S_p(f) = (\rho\bar{U}B)^2[X_a(f)]^2S_u(f) \tag{3.7}$$

where $[X_a(f)]^2$ is the aerodynamic admittance function which is explained in the following section.

(3) Aerodynamic Admittance Function

The aerodynamic admittance function is a transfer function which expresses effectiveness of various frequency components of the velocity spectra to the aerodynamic forces. It is a function of the structure's geometrical form, its dimension and of the characteristics of the turbulence.

Fig.3.2 shows the aerodynamic admittance function of a square plate situated normal to the flow with homogeneous turbulence. Due to the fact that smaller turbulent eddies which have shorter wavelength or higher frequencies have

lower coherence than larger eddies, the magnitude of the aerodynamic admittance function decreases with the increase in frequency.

For a flat plate placed normal to a turbulent flow as depicted in Fig.3.3, Davenport [3.3] has given an expression as follows:

$$[X_a(f)]^2 = \int_0^B \int_0^B \int_0^D \int_0^D R_u(r_y) R_u(r_z) d(y_1/B) d(y_2/B) d(z_1/D) d(z_2/D) \tag{3.8}$$

in which $R_u(r) = \exp[-kfr/\bar{U}]$ expresses the velocity correlation coefficient at two points separated by the distance r, r_y between y_1 and y_2 and r_z between z_1 and z_2.

The value of k is suggested to be 7 to 8 by Davenport. For a square plate, $B = D = (A)^{1/2}$, (3.8) becomes

$$[X_a(f)]^2 = [2(kz-1 + e^{-kz})/(kz)^2]^2 \tag{3.9}$$

where $z = fB/\bar{U}$ and $k = 7$.

Vickery [3.4] gave another empirical expression as

$$[X_a(f)]^2 = [1 + (2z)^{4/3}]^{-2} \tag{3.10}$$

These equations compare reasonablly well with the experimental results and are widely in use for practical purpose.

3.1.2 Response Calculation

The structural response can be also expressed as a combination of the mean value and a fluctuating part as

$$X(t) = \bar{X} + x(t) \tag{3.11}$$

Furthermore, it is well-known that the spectral density function of input to a linear system and the corresponding output, $S_p(f)$ and $S_x(f)$ respectively, are related by the frequency response function of the system, H(f), by [3.5]

$$S_x(f) = [H(f)/k]^2 S_p(f) \tag{3.12}$$

where $$[H(f)]^2 = \{(1 - r^2)^2 + (2hr)^2\}^{-1} \tag{3.13}$$

k = stiffness per unit length of the body
r = f/f_0
f_0 = natural frequency (Hz)
h = the damping ratio (% of critical)

H(f) is sometimes called the mechanical admittance function and/or the dynamic magnification factor. The damping ratio should include both structural damping and aerodynamic damping which, for this case, is approximately given, according to the quasi-steady aerodynamics [3.6], by

$$h_a = \rho B \bar{U} C_D / (4\pi f_0 m) \tag{3.14}$$

where m = mass per unit length of the body.

3.1.3 Modal Analysis

For the dynamic analysis of an elastic structure, a linear superposition of vibration modes is usually applicable. During this process, the structural response is assumed to be a combination of response in many different natural modes in which each mode can be considered as a single-degree-of-freedom system. The dynamic properties of the original system are then presented in matrix form using those of the equivalent SDOF systems [3.7].

Referring to Fig.3.4, the equations of motion for a n-storey shear building are given by

$$[M]\{\ddot{Y}\} + [C]\{\dot{Y}\} + [K]\{Y\} = \{P(t)\} \tag{3.15}$$

where

$$[M] = \begin{bmatrix} m_1 & 0 & \cdots & 0 \\ 0 & m_2 & \cdots & 0 \\ \vdots & \vdots & \ddots & \vdots \\ 0 & 0 & \cdots & m_n \end{bmatrix} \quad \{Y\} = \begin{bmatrix} y_1 \\ y_2 \\ \vdots \\ y_n \end{bmatrix} \quad \{P(t)\} = \begin{bmatrix} p_1(t) \\ p_2(t) \\ \vdots \\ p_n(t) \end{bmatrix}$$

$$[C] = \begin{bmatrix} c_1+c_2 & -c_2 & 0 & \cdots & 0 \\ -c_2 & c_2+c_3 & -c_3 & \cdots & 0 \\ 0 & -c_3 & c_3+c_4 & \cdots & 0 \\ \vdots & \vdots & \vdots & \ddots & \vdots \\ 0 & 0 & 0 & & c_n \end{bmatrix}$$

$$[K] = \begin{bmatrix} k_1+k_2 & -k_2 & 0 & \cdots & 0 \\ -k_2 & k_2+k_3 & -k_3 & \cdots & 0 \\ 0 & -k_3 & k_3+k_4 & \cdots & 0 \\ \vdots & \vdots & \vdots & \ddots & \vdots \\ 0 & 0 & 0 & & k_n \end{bmatrix}$$

[M], [K] and [C] are the mass, stiffness and damping matrices respectively, and $\{\ddot{Y}\}$, $\{\dot{Y}\}$, $\{Y\}$ and $\{P(t)\}$ are the acceleration, velocity, displacement and the external force vectors respectively.

For the free vibration analysis, the damping effect can be ignored and the force vector is equal to zero. Eq.(3.15) hence becomes

$$[M]\ \{\ddot{Y}\} + [K]\ \{Y\} = \{0\} \tag{3.16}$$

Assuming the solutions of (3.16) in the form

$$\{Y\} = \{F\}\ e^{iwt} \tag{3.17}$$

the subtitution of (3.17) into (3.16) gives

$$([K] - w^2\ [M])\ \{F\} = \{0\} \tag{3.18}$$

From the condition to have a nontrivial solution set, which is given by putting the determinant of the coefficient matrix equal to zero, w_r (r=1,2,...,n) become the solutions of (3.19). Eq.(3.18) then provides

$$([K] - w_r^2\ [M])\ \{F_r\} = \{0\} \quad (r=1,2,\ldots,n) \tag{3.19}$$

where $\{F_r\}$ is the r-th mode shape vector and w_r is the corresponding natural circular frequency. The vibration mode shape matrix [F] and natural circular frequency vector {w} are defined as follows:

$$[F] = [\{F_1\},\{F_2\},\ldots,\{F_n\}] = \begin{bmatrix} F_{11} & F_{12} & \cdots & F_{1n} \\ F_{21} & F_{22} & & \vdots \\ \vdots & \vdots & \ddots & \vdots \\ \vdots & \vdots & \cdots & \vdots \\ F_{n1} & \cdots & \cdots & F_{nn} \end{bmatrix}$$

$$\{w\}^T = \{w_1, w_2, \ldots, w_n\}$$

Next, the forced motion is considered. Since (3.15) is a set of coupled differential equations, it will be more convenient to transform it into a set of uncoupled differential equations. By introducing the linear transformation of coordonates

$$\{Y\} = [F]\ \{q(t)\} \tag{3.20}$$

where $\{q\}^T = \{q_1, q_2, \ldots, q_n\}$

Using (3.20), (3.15) yields as follows:

$$[M]\ [F]\ \{\ddot{q}\} + [C]\ [F]\ \{\dot{q}\} + [K]\ [F]\ \{q\} = \{P(t)\} \tag{3.21}$$

By premultiplying the transpose of the r-th mode shape vector $\{F_r\}^T$ to (3.21),

$$\{F_r\}^T\ [M]\ [F]\ \{\ddot{q}\} + \{F_r\}^T\ [C]\ [F]\ \{\dot{q}\} + \{F_r\}^T\ [K]\ [F]\ \{q\} = \{F_r\}^T\ \{P(t)\} \tag{3.22}$$

Because of the orthogonality property of the mode shape functions

$$\{F_r\}^T\ [M]\ \{F_s\} = \begin{cases} M_r & (r = s) \\ 0 & (r \neq s) \end{cases} \tag{3.23}$$

and

$$\{F_r\}^T\ [K]\ \{F_s\} = 0 \tag{3.24}$$

By assuming a similar reduction to the damping term, (3.22) becomes

$$M_r\ddot{q}_r + C_r\dot{q}_r + K_r q_r = P_r(t) \tag{3.25}$$

or

$$\ddot{q}_r + 2h_r w_r \dot{q}_r + w_r^2 q_r = P_r(t)/M_r \tag{3.25A}$$

which is a set of n-uncoupled differential equations where

$$M_r = \{F_r\}^T [M] [F] \quad : \text{generalised mass} \tag{3.26}$$

$$K_r = \{F_r\}^T [K] [F] = w_r^2 M_r \quad : \text{generalised stiffness} \tag{3.27}$$

$$C_r = \{F_r\}^T [C] [F] = 2h_r w_r M_r \quad : \text{generalised damping} \tag{3.28}$$

$$P_r(t) = \{F_r\}^T \{P(t)\} \quad : \text{generalized force} \tag{3.29}$$

Using the above equations the building deflection at the height z is generally given by

$$x(z,t) = \sum_r F_r(z)\, q_r(t) \tag{3.30}$$

For structures with light damping, the variance of its response can be approximated by

$$\sigma_x^2(z) = \sum_i \sum_j \bar{q}_i\, \bar{q}_j\, F_i(z)\, F_j(z) \doteq \sum_r \bar{q}_r^2 F_r^2 \tag{3.31}$$

3.2 Buffeting Analysis of Tall Buildings

3.2.1 Calculation Procedure [3.8-3.10]

The following analysis for vertical structures applies only when the structure undergoes vibration with small amplitudes. It is also assumed that the structure does not experience any aerodynamic instablility or vortex-induced oscillations.

(1) Mean response

In the atmospheric boundary layer, the mean wind speed varies with height and its variation is often expressed by the power law by taking the gradient wind speed as a reference. However, since only the wind below the building height H would have any influence on the building behaviour, it may be more convenient for the present analysis to give it as follows:

$$\bar{U}(z) = \bar{U}(H)[z/H]^{a} \tag{3.32}$$

Since the fundamental mode shape of a tall building is often rectilineal, as the first approximation for its deflection analysis, it is acceptable to treat the building as if it is a rigid bar with the mass distribution m(z) and supported at its base by an equivalent torsional spring with the stiffness K_t. With this mathematical model, the mean deflection of the building at any height z due to distributed drag force P(z) is given as follows:

$$X(z) = (z/K_t)\int_0^H z\bar{P}(z)dz \tag{3.33}$$

The equivalent rotational spring constant K_t can be expressed by using the natural frequency f_0 (Hz)

$$K_t = J(2\pi f_0)^2 \tag{3.34}$$

where the mass moment of inertia with respect to the building base is given by

$$J = \int_0^H m(z) z^2 dz \tag{3.35}$$

The mean wind pressure $\bar{P}(z)$ can be calculated with the following expression:

$$\bar{P}(z) = (\rho C_D B/2)[\bar{U}(z)]^2 \tag{3.36}$$

(2) Dynamic Response

As it was already given in the previous section, the boundary layer wind profile is given by

$$\bar{U}(z) = \bar{U}(H)(z/H)^a \tag{3.32}$$

and the dynamic response of the building is

$$x(z,t) = \sum_r F_r(z) q_r(t) \tag{3.30}$$

Introducing the generalised quantities M_r, K_r, C_r and $P_r(t)$ the equation of motion for the r-th mode becomes

$$\ddot{q}_r + 2h_r w_r \dot{q}_r + w_r^2 q_r = P_r(t)/M_r \tag{3.25A}$$

and the mean-square response is

$$\sigma(z)^2 = \sum_i \sum_j \bar{q}_i \bar{q}_j F_i(z) F_j(z) = \sum_r \bar{q}_r^2 F_r^2(z) \tag{3.37}$$

where the mean squared response for the r-th mode is given by

$$\bar{q}_r^2 = \int_0^\infty [H_r(f)/K_r]^2 Sp_r(f) df \tag{3.38}$$

The force spectum $Sp_r(f)$ is, considering (3.29), given by

$$Sp_r(f) = \int_0^H\int_0^H S_p(z_1,z_2;f)F_r(z_1)F_r(z_2)dz_1dz_2 \qquad (3.39)$$

where

$$S_p(z_1,z_2;f) = [S_p(z_1,f)S_p(z_2,f)]^{1/2}R_p(z_1,z_2;f) \qquad (3.40)$$

The force spectrum $S_p(z,f)$ at the height z is given by

$$S_p(z,f) = 4\bar{P}(z)^2[X_a(f)]^2S_u(z,f)/\bar{U}(z)^2 \qquad (3.41)$$

where $X_a(f)$ is the aerodynamic admittance function given by (3.8) and the velocity spectrum can be taken at z = H.

The velocity correlation coefficient is approximated by

$$R_p(z_1,z_2;f) = R_u(z_1,z_2;f) = \exp[-C_vfr/\bar{U}] \qquad (3.42)$$

in which r is the distance between z_1 and z_2. From (3.41)

$$[S_p(z_1,f)S_p(z_2,f)]^{1/2} = 4(P/U)_1(P/U)_2[X_a(f)]^2S_u(f) \qquad (3.43)$$

where $(P/U)_z = (\rho C_D B/2)\bar{U}(z) = (P/U)_H\bar{U}(z)/\bar{U}_H$

and $(P/U)_H = (\rho C_D B/2)\bar{U}_H$, $\bar{U}_H = \bar{U}(H)$

Applying (3.43), the spectrum for the generalised force $P_r(t)$ can be rewriten as follows:

$$S_{pr}(f) = 4S_u(f)[X_a(f)/\bar{U}_H]^2\bar{P}_H^2\int_0^H\int_0^H R_u(z_1,z_2,f)F(z_1)F(z_2)x$$
$$x\ (\bar{U}_1/\bar{U}_H)(\bar{U}_2/\bar{U}_H)dz_1dz_2 \qquad (3.44)$$

or

$$Sq_r(f) = 4S_u(f)[X_a(f)/\bar{U}_H]^2\ \bar{P}_H^2[J_r(f)]^2 \qquad (3.45)$$

where $J_r(f)$ is the joint acceptance function for the case and is given by

$$[J(f)]^2 = \int_0^H\int_0^H (\bar{U}_1/\bar{U}_H)(\bar{U}_2/\bar{U}_H)\exp[-C_v fr/\bar{U}_m]F(z_1)F(z_2)dz_1dz_2 \tag{3.46}$$

where r is the distance between z_1 and z_2 and $\bar{U}_m$ is the mean wind speed at the middle height of z_1 and z_2. According to Davenport [3.1], the above analysis is valid only if the following assumptions are applicable:

1) The structure is sufficiently slender so that the force at each section is uniquely determined by the velocity incident upon the section (strip theory);

2) The turbulence spectra are invariant with height;

3) The aerodynamic coefficient C_D and its slope do not vary with height; and

4) A narrow band velocity correlation is given by

$$\text{correlation} = \exp[-kfr/\bar{U}] \tag{3.47}$$

Since $\bar{U}(z)/\bar{U}_H$ can be defined by a power law exponent, assuming a rectilinear mode shape of the buildings, (3.46) can be approximated by the following expression:

$$\int_0^H\int_0^H (U_1/U_H)(U_2/U_H)\ldots. = \{1+(C_v/3)(fH/\bar{U}_H)\}^{-1}(1+a)^{-2} \tag{3.48}$$

where C_v indicates the effective width of a gust expressed in terms of wavelength U/f and its value is said to be approximately 0.3.

The above equations describe only the along-wind response of vertically extended structures. If both the vertical and horizontal extension of the structure need to be considered, since the wind forces work over the whole width of the building, the following expression for the generalised force spectrum can be considered:

$$S_q(f) = 4\bar{P}_H^2[J_v(f)]^2[J_h(f)]^2 S_u(f)/\bar{U}_H^2 \tag{3.49}$$

where $[J_h(f)]^2 = [1 + 10(fB/\bar{U}_H)]^{-1}$ (3.50)

and $[J_v(f)]^2$ is the same as given in (3.48).

The coefficient of variance given by the rms over the mean is expressed by

$$(\sigma_x/\bar{X})^2 = \{4(1+a)/\bar{U}\}^2 \int_0^\infty [H(f)]^2 [J_v(f)]^2 [J_h(f)]^2 S_u(f) df \quad (3.51)$$

which is equal to

$$\doteqdot 16(1+a)^2 I_u^2 [J_v(f_0)]^2 [J_h(f_0)]^2 S_u(f_0)/\sigma_u^2 \int_0^\infty [H(f)]^2 df + \int_0^\infty [J_v(f)]^2 df + \int_0^\infty [J_v(f)]^2 [J_h(f)]^2 S_u(f)/\sigma_u^2 df \quad (3.52)$$

where I_u is the intesity of turbulence given by (4.1) and

$$\int_0^\infty [H(f)]^2 df = \pi f_0/4h$$

$$\int_0^\infty [J_v(f)]^2 [J_h(f)]^2 S_u(f)/\sigma_u^2 df = \int_0^L [f S_u(f)/\sigma_u^2] d(\ln f)$$

where $L = 3\bar{U}_H/8H$

3.2.2 Description in the National Building Code [3.11]

The buffeting calculation given in the National Building Code of Canada is based on the mathematical analysis given in this chapter. The code actually allows three different approaches for determining the design wind loads; the simple procedure, the detailed procedure and the performance of dedicated wind tunnel tests. In this section, the detailed procedure in the code is briefly summarized since the experimental results in the next chapter are later compered with the calculation along this approach.

Essentially the procedure is the determination of the gust effect factor C_g. For the calculation of the gust factor, the following parameters are required:

1) Exposure factor = C_e
2) Surface roughness = K
3) Background turbulence factor = B
4) Size reduction factor = S
5) Gust energy ratio = F
6) Cycling rate = n
7) Peak factor = g_p

The exposure factor C_e is based on the mean wind speed profile, which varies considerably with the terrain roughness K over which the wind has been blowing before it reaches the building. Three categories are established:

Exposure A : open level terrain with only scattered buildings, trees or other obstruction, open water or shorelines thereof;

Exposure B : suburban and urban areas, wooded terain or centres of large towns; and

Exposure C : centers of large cities with heavy concentration of tall buildings.

The representative numbers for C_e and K are defined for each exposure. For the calculation of the reference wind speed U_H the local climatic data are used as (units are in SI)

$$\bar{U}_{ref} = q_{ref}/(650\times10^{-6}) \qquad \bar{U}_H = \bar{U}_{ref} \times (C_{eH})^{1/2}$$

where q_{ref} is the reference wind pressure. For the present calculation to compare with the wind tunnel test results, U_H is directly given.

The backround turbulence factor is the integration of the response spectra over the whole freqency range except around the natural frequency, which corresponds to the second line of (3.52). It is expressed by the following integration and is given as the function of the building height and its aspect ratio, or the width to height ratio:

$$B = 4/3 \int_0^h (1+zH/457)^{-1}(1+zW/122)^{-1}z(1+z^2)^{4/3}dz$$

$$= B(W/H,H) \qquad \text{where} \qquad h = 914/H$$

The size reduction factor S and the gust energy ratio F relate to the integration of the resonant peak which is the first line of (3.52). They are as follows:

$$S = (\pi/4)(1+ 8f_0H/3\bar{U}_H)^{-1}(1+ 10f_0W/\bar{U}_H)^{-1} = S(W/H, f_r)$$

$$F = X_0^2/(1+X_0^2)^{4/3} = F(f_0/\bar{U}_H) \quad \text{where} \quad X_0 = 1220(f_0/\bar{U}_H)$$

$f_0/\bar{U}_H$ and $f_r = f_0\bar{H}/U_H$ are called the wave number and the reduced frequency, respectively. The peak factor g_p is then given by

$$g_p = s + 0.577/s$$

where $s = [2\ln(nT)]^{1/2}$, $T = 3600$ sec (averaging time)
and $n = f_0SF/(SF+B)$ = cycling rate.

Finally, using these parameters the gust factor

$$C_g = 1 + g_p[(KB/C_e) + (SF/h)]$$

is obtained. This represents the ratio of the peak to the mean response. The mean response for tall, slender buildings can be obtained by the method described in the previous section.

Chapter 4. EXPERIMENT

This chapter describes an aeroelastic model test of a tall building. The project started its planning stage in 1990. The model was designed by a project engineer and constructed at the Applied Aerodynamics Laboratory, National Research Council Canada in 1990-91. Having finished the static and dynamic calibration, with which the present author started being involved in the project, the model was moved to the 9m x 9m wind tunnel and the actual testing with wind took place in May 1991. The transfer of the obtained data from NRCC to the University was completed by the end of 1991.

4.1 Aeroelastic Model

4.1.1 Prototype Building

A 500 metre tall building with an octahedral tapered cross-section shown in Fig.4.1 was considered to be the prototype structure for the study. The building is assumed to be homogeneous in terms of mass distribution and has the density of 150 kg/m3. The fundamental natural periods of 10 and 9 seconds in two principal sway directions and less than 8 seconds in torsion are assumed. The expected vibration mode for the lowest frequency is linearly proportional to the height and the structural damping is 1.0 to 1.5 % of critical in all three directions. The building foundation is assumed to be rigid and no soil-structure interaction is to be considered.

The building is assumed to be situated in a homogeneous and moderately built-up suburban area and the wind characteristics should be typically defined by the power-law exponent of approximately 0.20 [3.11].

4.1.2 Similitude Requirements

An aeroelastic model of the prototype building was constructed as a seven-mass "equivalent model" to a geometrical scale of 1:200 (Fig.4.2). A computer model was first made to calculate the required stiffness with the following assumptions:

1) The kinetic energy corresponding to each mass displacement in the first sway mode is approximately the same.

2) The flexibility of the building is provided only by the bending of supporting columns.

3) The flexibility of the floor plates can be ignored.

The similarity principles required for the wind tunnel testing is to keep the following dimensionless parameters consistent between the model and full scale structure:

a) Reynolds number: $\bar{U}L/n$ (= Re)

b) Density ratio: ρ_a/ρ_s

c) Cauchy number: $E/\rho_a U^2$ (= Ca)

d) Structural damping: h_s

e) Frounde number: $\bar{U}/(gL)^{1/2}$ (= Fr)

in which

$\bar{U}$ = mean wind speed (m/s)
L = representative linear dimension of structure (m)
ρ_s = density of structural material (kg/m^3)
ρ_a = air density (kg/m^3)
E = Young's modulus of structural material (N/m^2)
h_s = structural damping ratio (% of critical)
g = acceleration due to gravity (=9.81 m/s^2)
n = kinematic viscosity of air (=15.2x10^{-6} m^2/s)

The similarity of the mean velocity distribution and statistical properties of the turbulence are also required for a complete simulation of the flow field around the structure.

In the present study, requirements a) and e) above are relaxed because of the following reasons:

1) The influence of gravitational field on the wind induced response of the structure is likely to be negligible except for the P-delta effect which will be adequately covered as long as the mass distribution and the mode shapes are properly simulated.

2) It is impracticable to achieve the Reynolds number similarity in wind tunnel tests. There will be some influence on the result due to this distorsion in similitude. However, there is a good reason to belive that this influence will be negligibly small for the present building configuration.

Consequently, the time scale $S_T = (T)_m/(T)_p$ is decided only by the choice of the model frequency as follows:

$$S_T = 1/S_f = (f)_p/(f)_m \qquad (4.1)$$

where the subscripts p and m stand for prototype and model quantities, respectively. The requirement c) can be replaced by the consistency of the reduced velocity $U_r = U/Lf$, as long as the second requirement b), or mass ratio, is held [3.9].

The resulted scaling factors are as follows:

Length	$S_L = 5 \times 10^{-3}$
Density	$S_\rho = 1$
Mass	$S_m = S_L^3 = 0.125 \times 10^{-6}$
Mass moment of inertia	$S_J = S_m S_L^2 = 3.12 \times 10^{-12}$
Time	$S_T = 17.5 \times 10^{-3}$ (*)
Velocity	$S_U = S_L / S_T = 0.286$
Force	$S_F = S_m S_L / S_T^2 = 2.04 \times 10^{-6}$
Moment	$S_M = S_F S_L = 10.2 \times 10^{-9}$

(*) based on the dynamic calibration test results.

4.1.3 Model Characteristics

The model consists of seven floor plates, four supporting columns for each floor and the surface plexiglass skin which gives the geometric configuration of the building. The floor plates are made of aluminum whereas the columns are of steel (Photo 4.1). The diagram to show the model dimensions is given in Fig.4.3. It can be seen that the dimensions of the columns in X-direction are smaller than in Y-direction, so that a higher stiffness in X-direction is expected. The definition of the coordinate system and the numbering of the floors are shown in Fig.4.4. The model displacement in two sway directions and torsion were detected through strain measurement by wire strain gauges attached to the lower portion of the steel columns at each floor. The required Wheatstone bridge for the strain measurement is shown in Fig.A.5. The principle of measurement with wire strain gauges is briefly summarized in Appendix A.

The model is firmly fixed on a 0.8 metre diameter steel plate which was placed on a pedestal (Fig.4.2) prepared under the wind tunnel floor seperated from it to avoid the transmission of mechanical vibration from the wind tunnel shell to the model.

4.2 Calibration of Model

4.2.1 Static Calibration

(1) Experimental Set-up

The purpose of the static calibration is to measure the mass, mass moment of inertia and stiffness of each floor and also of the assembled model to make sure that they are in agreement with the design values.

First the mass and mass moment of inertia of each floor plate were measured. The pendulum method applied for the measuremant of the moments of inertia is briefly explained in Appendix B.

Next, the measurement of each floor stiffness was carried out. Four columns with a floor plate on them were rigidly attached to the prepared base plate and a horizontal loading was applied at the mid-height of the floor plate. The experimental set-up for this measurement is seen in Photo 4.2.

The same procedure was repeated when the assembled model was tested. In addition to control the strain gauge outputs, a pair of the Kaman transducers were installed at each floor. Each pair consisted of an excitation pole (slave) and a sensor pole receiving the signal (master). For each floor, up to four different load steps were applied. An additional combined load was applied in X- and Y-directions at the same time for the confirmation of the test results.

The measured data were analysed by a HP45 data analyser which scanned the strain gauges with the sampling frequency of 500 Hz.

(2) Data Analysis

The calibration results were found to be very close to the design values which assured the good material quality and satisfactory workmanship.

According to Appendix A, the strain gauge outputs dE_k of the columns are reduced to the relative displacements in all three directions, X-, Y- and torsion. When the

assembled model is subjected to the lateral loads, not only the relative displacements but also the absolute displacement of each mass is hence also found from dE_k. It means that the absolute deflection of each storey in X-, Y-direction or torsion is found from the corresponding strain gauge bridge output voltage of the columns located below this floor.

The voltage outputs have to be converted into displacements with the units in cm (10^{-2} m) or radian. The conversion was done by dividing the voltage readings by calibration factors.

The stiffness was measured by dividing the applied load by the relative displacement for each floor. The results of the measured stiffness are compared with the design values together with the measured masses in Table 4.1 - 4.2.

4.2.2 Dynamic Calibration

(1) Instrumental Set-up

The task of the dynamic calibration is to investigate the dynamic properties of the model and compare them with the predicted values from the model design. As mentioned in the previous chapter, a model is characterized by the following parameters:

$\{F_r\}$ = r-th mode shape vector
w_r = natural circular frequency for r-th mode
h_r = modal damping for r-th mode
and $[M]$ = mass matrix

The mass matrix is known from the design calculation and also confirmed by the static calibration. Other factors are obtained by the dynamic calibration.

The dynamic calibration of the model was carried out after its assembly and again briefly after its installation in the wind tunnel (Photo 4.3). Thin rubber films were attached between seven modules to increase the structural damping of the model which was found to be too low otherwise.

The view of the dynamic calibration set-up is seen in Photo 4.4. In order to excite the model, a loose string was

attached to the building to connect it with a mechanical shaker. The connection consisted of a thin fishing line with a mass attached to the middle of it. The system was found to work very effectively.

(2) Testing Procedure

First, the model was excited with a white noise input. A spectral analysis of the strain gauge and accelerometer output signals provided typical dynamic response characteristics of the model as shown in Fig.4.6. The spectral peaks show the location of natural frequencies. The spectral analysis was carried out by the use of a HP spectrum analyser.

In order to obtain the mode shapes $F_{k,r}$ a simple harmonic excitation at each natural frequency $f_r = w_r/2\pi$ was appllied to the model so that the dynamic response of the model would be observed mostly in the r-th mode. The r-th mode shape is found under the steady vibration at this frequency.

The structural damping was obtained by cutting off the previous excitation to give a free vibration trace of the model motion. The motion of the model for this case will give a clear indication of both natural frequency and structural damping of each vibration mode.

Improvement of the accuracy in measurement was also attempted by applying the spectral analysis to the strain gauge outputs recorded on the Data Recorder, TEA XR-7000, too. For a higher accuracy measurement of the mode shapes, a bandpass filter was applied to isolate the response at the natural frequency from the noise with neighbouring frequencies. This was done by isolating a part of the spectrum when it was obtained by the white noise excitation. The method is shown in Fig.4.7. Fig.4.8 presents the result of a bandpass filtered random signal. The results are not conclusive except for the lower modes, since it was not easy to clearly identify the natural frequencies in 6th and 7th modes.

In case of the modal damping good results were obtained for the lower frequencies, see Fig.4.9. In case of the higher modes the interaction between modes were observed as seen in Fig.4.10. This made the identification of damping a little more difficult. The situation was improved by applying a digital filter as shown in Fig.4.11.

The obtained results for all three directions are listed in Tables 4.3 - 4.5. For each mode, both calculated and measured natural frequencies f_r, both calculated and measured mode shapes $\{F_r\}$ and measured modal dampings h_r are given. For the calculated values, the stiffness matrix [K] from the static calibration of each storey and the mass matrix [M] from the design calculation were employed. The results of the dynamic calibration by and large agree well with the calculation results. A graphical comparison between the measured and calculated natural frequencies is given in Fig.4.12 - 4.14. The obtained mode shapes are compared in Fig.4.15 - 4.17.

It is noticed that the results for the lower modes show generally better agreement. The torsional modes show poorer agreement. However, the torsional modes are considered to be less important for this particular project. The dynamic calibration confirms that the model was more or less as it was designed.

4.3 Facilities and Equipment

4.3.1 Wind Tunnel and Data Acquisition System

The aerodynamic test was carried out at the 9m x 9m V/STOL Wind Tunnel of the Institute of Aerospace Research, National Research Council Canada. It is located near the Ottawa International Airport in Gloucester, Ontario. The wind tunnel is a horizontal, closed circuit facility and its general feature is illustrated in Fig.4.18. Its test section is approximately 9.1m high, 9.1m wide and 22.9m long. The wind tunnel blockage ratio with the present model is less than 1.0%. The obtainable maximum wind speed is approximately 60 m/s.

The experimental data were collected through a Neff 500/620 A/D converter. The Neff front end is DMA interfaced to a Micro Vax 3400/DEC 11-44, real time data acquisition system. A flow chart of the acquisition system is shown in Fig.4.19.

The strain readings from the test were all converted to displacement readings in three directions at all seven mass levels and stored on magnetic tapes with VAX binary code. The outputs were also recorded as a backup through a TEA XR-7000 Data Recorder.

4.3.2 Flow Conditions

(1) Flow Measurement

The flow measurement was carried out to establish the flow characteristics at the wind tunnel test section.

The wind tunnel used for this project was constructed for aeronautical purposes and is designed to produce a uniform flow with low turbulence through a relatively large test section. In order to obtain a turbulent boundary layer which simulates the characteristics of natural wind with a power law exponent of approximately 0.20, the flow conditions were altered by installing a row of four triangular spires which are 3.5m high and 0.4m wide at their base. These spires were installed across normal to the mean air flow at the entrance of the test section. In addition to these, a small wooden board of 0.15m high was installed across the floor at 4.0m upstream side of the model location (Fig.4.20).

The spires were designed based on the semi-theoretical equations developed by Irwin [4.2] and the flow conditions including the effect of the board were confirmed by a preliminary flow test with a scale of 1:10 at the 0.9m x 0.9m wind tunnel of IAR/NRCC prior to the project.

The turbulent flow is typically characterised by the following statistical quantities:

1) Mean wind profiles
2) Intensities and scales of turbulence
3) Spectral density functions
4) Cross-spectra and coherence

Intensities and scales are most frequently quoted to identify the turbulence characteristics but these quantities are actually derived from the spectra and cross-correlations.

A list of the flow measurement is given in Table 4.6.

(2) Instrumental Set-up

The flow measurement was carried out using the TSI 1241 hot-film anemometry system with the cross-type sensors (51×10^{-6}m) showen in Photo 4.5. The instrumental set-up in

the wind tunnel is shown in Fig.4.21. One probe gives the reference readings in both u- and v-directions whereas another probe moves vertically or horizontally to measure the space correlations. In addition, two Pitot tubes were installed, one at the model hight next to the hot-film sensor and another on the wind tunnel wall also at the same hight for a general reference reading.

(3) Turbulent Boundary Layer Characteristics

The magnitude of mean wind velocity generally increases with height. The rate of this increase is mostly decided by the roughness of the ground terrain. The variation of mean velocity with height can be considered to be caused generally by retardation of the air flow near the ground level due to surface friction. At certain height above ground the stream velocity becomes nearly constant and this is called the gradient height, as showen in Fig.4.22 [3.9].

The mean wind speed in the boundary layer at any height z can be approximately expressed by the power law :

$$U(z) = U_g(z/z_g)^a \qquad (4.2)$$

where "a" is an exponent depending upon the roughness of the terrain and is assumed to be about 0.20 in this case which would represent a moderately built-up suburban terrain.

The turbulence can be expressed by statistical characteristics of u-, v-, and w-component of the velocity vector measured at any point (x,y,z). In turbulent flow, all three components are functions of both the time and space coordinates.

The mean velocity vector $(\overline{U},\overline{V},\overline{W})$ at any location can be defined as the time avarage of the general velocity vector over a period of time, T. T becomes the sampling time for the measurement, shown in Fig.4.22. For the present case, the coordinate system (x,y,z) is taken in such a way that $\overline{V} = \overline{W} = 0$. Also assumed is a stationary and ergodic nature of velocity fluctuations.

By using the standard deviation or the root-mean-square values, the intensities of turbulence are defined as

$$I_u(z) = \sigma_u(z) \; / \; \overline{U}(z)$$

$$I_v(z) = \sigma_v(z) \; / \; \bar{U}(z) \qquad (4.3)$$

$$I_w(z) = \sigma_w(z) \; / \; \bar{U}(z)$$

The space correlation describes the similarity of the turbulence at two different locations separated by the distance r. The correlation coefficient becomes +1 when two signals have a complete correlation, for a comletely out-of-phase correlation it becomes -1 and 0 for a perfectly random association. The space correlations of u-component are defined as follows:

$$R_u(r_y) = E[u(y,z) \times u(y+r_y,z)] \qquad (4.4)$$

$$R_u(r_z) = E[u(y,z) \times u(y,z+r_z)]$$

$R_u(r_x)$ is not measured for the present project. Other correlation functions of v- and w-components can be defined in similar manner. The correlation coefficients are given by deviding the correlation functions by corresponding variances. For example

$$R_u(r_z) = R_u(r_z) \; / \; \sigma_z^2 < 1 \qquad (4.5)$$

The scales of turbulence are defined by the area under the correlation curves. The scales of turbulence were calculated for $L_u{}^y$, $L_u{}^z$, $L_v{}^y$ and $L_v{}^z$.

(4) Analysis of the Results

The output file from the flow measurement contains the time histories of u- and v-components measured over one minute with a sampling rate of 500 Hz. The mean values of measured v-components are nearly zero as expected. The mean, root-mean-square (rms), maximum and minimum values were calculated for each run.

Table 4.7 shows the actual results of the flow measurement. H indicates the hight of the model, which is 2.5m, U_H stands for the wind speed measured at the height of the model. Fig.2.23 shows the mean wind speed profile at the model location and Fig.4.24 gives the profile of turbulece intensity. The power law exponent was found to be 0.19 which is comparable to the target value of 0.20.

The velocity spectra were calculated by applying a standard Fast Fourier Transform program [3.2]. The results are shown in dimensionless form, spectral density times frequency devided by the variance, against the wave length wich is frequency over the mean speed. The obtained spectra agree generally well with the empirical expressions such as by von Karman, except the scale for v-component seems to be greater than expected. Figs.4.27 shows velocity spectra of u- and v-components. The estimated length scales from the measured spectral peaks at z/H = 0.26 using Fig.4.27 are

$$L_u^x = 1.00 \text{ m} \qquad L_v^x = 0.90 \text{ m}$$

The measured lateral and vertical space correlation coefficients are shown in Figs.4.25 and 4.26. They did not show too much difference at different elevations. The indicated length scales at the height of z/H = 0.76 are

$$L_u^z = 0.28 \text{ m} \qquad L_v^z = 0.20 \text{ m}$$

$$L_u^y = 0.27 \text{ m} \qquad L_v^y = 0.40 \text{ m}$$

4.4 Experimental Procedure

Since the building is not mechanically symmetric, wind induced response is excpected to be different in two sway directions. The coordinate system is defined in such a way that the stiffer sway direction corresponds to x-axis. A wind of azimuth angle 0^o is towards positive X, with increasing angle in clockwise rotation, and 90^o corresponds to a wind towards negative Y. Photo 4.6 shows the model installed at the test section of the wind tunnel.

The building behaviour was examined for winds at every 5^o of the azimuth angle for the quadrant of 0^o to 45^o and also at 90^o under various wind speed levels corresponding to the range of 12 to 100 m/s in full scale at the building top (z = 500m). For the wind speed reading, a Pitot static reference pressure was calibrated to the wind speed at the top level of the model building. All the test run numbers are summarized in Table 4.8.

The outputs of the building response were given in time domain for each floor in X-, Y- and torsional directions. Original readings were all in voltage corresponding to the

strain readings at the gauge locations. These data were converted into displacement readings with the units of 10^{-2}m (cm) in both sways and radian in torsion.

At each set of azimuth angle and wind speed, the time histories of all 21 displacement outputs were recorded for a sampling period of 60 seconds with the sampling rate of 500 Hz, which correspond to the period of approximately one hour and the frequency of 8.75 Hz in full scale. Thus each file contains 30,000 sample points for each 21 channels. The total number of cases is 87.

All of these time histories have been converted to the IBM binary code and stored on ten magnetic tapes. Fig.4.28 shows sample time histories, which represent X, Y and torsional response at the top mass level for the wind angle of 0^{o} (X-direction) for the period of approximately 33 seconds. Full scale equivalence to this case is the mean wind speed of 42 m/s at the building top for the period of about a half of an hour. The deflection observed in X, Y and torsion directions in full scale are approximately 0.7 m and 0.2^{o}, respectively. The statistical summary of mean, rms and peak response for each run are given in the Final Report of the project [4.3].

Chapter 5. RESULTS AND DISCUSSION

5.1 General

All through the experiment, the building response was generally in all three directions and they were mostly caused by the oncoming flow turbulence. It was sometimes noticed that the model movement in X- and Y-directions increased its magnitude alternatively rather than concurrently. It was more difficult to draw general conclusions for torsional motion because it was often coupled with one of the sway motion.

The mean and rms response in all three directions for each angle are summarized in Figs.5.1 and 5.2. It can be seen from these plots against reduced wind speed that most of the wind induced dynamic response observed in this experiment was buffeting caused by the wind turbulence. One of the typical response characteristics in case of buffeting is a gradual increase of its magnitude with the increase of wind speed which can be clearly seen for all three directions in most of the experimental cases. The buffeting motion is a random process caused by the oncoming flow turbulence. The response of the building for this case is controlled only by the building properties.

But this was not the only response characteristic observed in this experiment. In some cases, especialy for Y-direction at 0^{o}, 5^{o} and for X-direction at 90^{o}, vortex induced vibrations were observed. This is indicated by the response curves with its drop of displacement at a certain wind speed and a slow recovery by further increasing wind speed. The wind speed range for this phenomenon was between the reduced velocity of 8 to 11.

It is expected that the mean response in each direction should be proportional to the dynamic pressure or the square of the wind speed, and indeed it is. The mean response in torsion, however, is expected to be negligibly small because of the symmetric building configuration. The dynamic component expressed in terms of the rms response would have a power slightly in excess of a square law [5.1]. It is assumed, hence, the following functional relationships between response and wind speed:

$$\begin{aligned} \text{Mean response} &= C_m(a) * (U_r)^2 \\ \text{RMS response} &= C_s(a) * (U_r)^{K(a)} \end{aligned} \qquad (5.1)$$

where

a = wind azimuth angle
U_r = $\overline{U}/(fB)$ = reduced velocity
f = natural frequency in each direction
B = model width at the mid-height

Coefficients C_m, C_s and the power exponent K can be obtained by applying a regression analysis. Calculated parameters are listed in Table 5.1 and also shown in Figs.5.3 and 5.4. It is interesting to find that the mean deflection in Y-direction for small angles such as 5^o, 10^o is slightly positive rather than negative. This must be attributed to the cross sectional shape of the model building and the resulted pressure distribution around it.

$K_x(20^o)$ for the rms response was relatively a small number, which resulted very high $C_x(20^o)$ correspondingly. This is because there is a change of curvature in the response curve vs wind speed for this angle as seen in Fig.5.2. The increase of response magnitude against wind speed to become more gradual in higher speed range. This observation is consistent with some other cases [5.1] but why so at this particular angle for this building is not immediately clear.

Wind induced buffeting response observed in this series of testing agrees, by and large, very well with the preliminary test results reported elsewhere [5.2], which confirms the previous knowledge of tall building response characteristics [5.1, 5.3].

5.2 Peak Factors

The peak factor is defined as a ratio of the peak dynamic response to the rms [5.4]. Its value is expected to be approximately 3.6 if the buffeting response amplitude has the Gaussian type histogram whereas it will be given by 1.4 if the response fluctuatuion is simply harmonic. The statistical summary for the calculation of the peak factor is given in Table 5.2.

As evidenced in Fig.5.5, the peak factor is between 3 and 4 for most of the cases, meaning that a typical random buffeting is observed here.

5.3 Mode Shapes

By taking the ratios of C_m calculated in Section 5.1 at each floor to the C_m of the top floor, actual response mode shape should be depicted. Fig.5.6 shows the response mode shapes in two sway directions. It is obvious from these that the first mode of vibration is predominant in both sway modes. Since the mean response in torsion is expected to be nearly zero anyways, this method does not make too much sense when it is applied to torsion.

5.4 Response Spectra

Fig.5.7 gives the response spectra for various cases obtained by applying the Fast Fourier Transform procedure. The program used for this analysis is given in Appendix C. As it is clear from them, the building response is mostly in the first mode of vibration and the resonant component with this mode as opposed to the response due to background turbulence is predominant. Buffeting due to turbulence is seen as a substantial part of the spectra only when wind speed is very low.

In many cases, the spectral peaks exist at the lowest natural frequency of each mode. However, sometimes, particularly when vortex excitation exists in one mode, the other modes of vibration seem to be "absorbed" into it. For example, in case of angle = 90^o, at U_r=13-16 in Y-mode, the X-frequency gives the spectral peak, whereas in case of 0^o at U_r=12-16 in X-mode, the peak is found at the Y-frequency.

5.5 Correlation between Modes

Fig.5.8 gives the correlation of response at various levels to that of the top floor. The result shows clearly that the first mode of vibration in all three directions is predominant. It is interesting to note that the correlation becomes higher when the building shows tendency towards vortex excition.

Fig.5.9 shows the correlation between three different modes. It is observed that the torsional response tends to be highly correlated with the X-sway. This was also evidenced by the existence of torsional spectral peak at the X-frequency.

5.6 Aerodynamic Damping

Fig.5.10 gives the response autocorrelation functions obtained by applying the Inverse Fourier Transform to the spectra. The autocorrelation readings in some low speed cases did not make too much sense because of the poor resolution.

The damping of the system can be read from the decay of autocorrelation functions [3.9]. Since more than one natural frequencies coexist in many cases, the autocorrelation functions are not necessarily simply decaying in exponential manner and the reading of its damping is not so straight forward. However, if the reading of the system damping is reliable, and the total damping can be assumed to be linear sum of structural and aerodynamic dampings, the aerodynamic damping for given angle and wind speed could be estimated by applying this method. It should be kept in mind that the accuracy of autocorrelations largely depends upon the length of the record. For the present case this must have certainly cause some inaccuracy.

Fig.5.11 is an example of aerodynamic dampings calculated through this procedure. The figure lists the cases of across-wind response in X and Y and they are expected to be very similar, if not identical. Also plotted are the amplitude response of these cases. They seem to correspond very with as far as these cases are concerned.

5.7 Comparison with Theoretical Prediction

It was attempted to compare the theoretical prediction of building buffeting with the experimental results. For the mean response the inverted pendulum model as explained in the preceding sections was applied.

The mass per unit length of the building is

$$\begin{array}{lll} \text{at the top} : & m_H = 1{,}472 \times 150 = 220{,}8 \times 10^3 & [\text{kg/m}] \\ \text{at the base} : & m_0 = 6{,}272 \times 150 = 940{,}8 \times 10^3 & [\text{kg/m}] \end{array}$$

Hence the mass distribution for a given height is given by

$$m(z) = 150\ (6{,}272 - 4{,}800\ z/H) \quad [\text{kg/m}]$$

For a building vibrating in a SDOF manner the overturning moment is given by

$$M_{ot} = \int_0^H z\bar{P}(z)dz \qquad (5.2)$$

where $\bar{P}(z) = (\rho U_z^2/2)B(z)C_D$ and $U_z = \bar{U}_H(z/H)^a$

Substiuding the above equations into (5.2) it becomes

$$M_{ot} = (\rho BC_D\bar{U}_H^2/2H^2a)\int_0^H z^{1+2a}dz = \rho BH^2C_D\bar{U}_H^2/4(1+a) \qquad (5.3)$$

The mean displacement is given by

$$\bar{X}_H = M_{ot}H/K_t \qquad (5.4)$$

where K_t is the equivalent spring constant. The magnitude of this stiffness is given by

$$K_t = J(2\pi f_0)^2 \qquad (5.5)$$

where J is the mass moment of inertia given by

$$J = \int_0^H m(z)z^2dz \qquad (5.6)$$

Using the mass distribution given for the height z above, the mass moment of inertia becomes

$$J = 1{,}018.67 \times 150\ H^3 \quad [kg\text{-}m^2]$$

The equivalent spring stiffness is

<u>X-dir</u>:	$f_0 = 0.10$ Hz	$K_t = 402.1 \times 150\ H^3$ [N m]
<u>Y-dir</u>:	$f_0 = 0.11$ Hz	$K_t = 496.5 \times 150\ H^3$ [N m]

The mean displacement from this given as

$$\bar{X}_H = (\rho B C_D \bar{U}_H^2)/4(1+a)/K_t \qquad (5.7)$$

where

C_D = 1.0 [5.2]
ρ = 1.25 kg/m^3
B = 60 m (at mid-height)
a = 0.19 (from the flow measurment)
H = 500 m

Therefore X-direction : $\bar{X}_H = 16.16 \times 10^{-3} \times \bar{U}_H^2$

Y-direction : $\bar{Y}_H = 13.09 \times 10^{-3} \times \bar{U}_H^2$

Obtained results for several wind speeds are shown in Table 5.3 and 5.4. The mean displacement is given in dimensionless format X/H and Y/H.

The gust factor was calculated according to the description given in Chapter 3. For the exposure factor the measured power law exponent a=0.19 was used. The exposure factor at the building height is approximately

$$C_{eH} = (500/11)^{0.38} \times 0.8 = 3.41$$

Corresponding roughness factor K was assumed to be 0.09.

The aspect ratio of the building is, using the width at the mid-height for W, W/H=0.12 and H=500 m. The background turbulence factor is then B=0.3.

The peak response is obtained by multiplying the mean response with the gust effect factor C_g. The rms response is given by

$$\sigma_x = (X/H - \bar{X}/H)/g_p \qquad (5.8)$$

In order to compare the calculated response values with the experimental counterparts, the wind tunnel test results were taken from Figs.5.1 and 5.2. For the X-direction the case with the azimuth angle of 0^o was used whereas the case of 90^o was used for the Y-direction. The results are given in Tables 5.3 and 5.4 together with the predicted values.

The predicted and measured values compare very well. Although the measured response for lower wind speeds tend to be a little higher than predicted. The tendency changes in higher wind speed and predicted values surpass the experimental values.

Chapter6. Concluding Remarks

An aeroelastic model of a 500 meter tall building was costructed to a linear scale of 1:200 using the concept of seven mass equivalent model. The test was carried out at the 9m x 9m NRCC Wind Tunnel. The wind induced deflection of the model at each mass level was detected. Main findings from the test are summarized and discussed from various aspects in Chapter 5. It is emphasized here that

1. Under the given conditions, the substantial part of the building response was found to be buffeting response in the fundamental modes with lowest natural frequencies.

2. Strong tendency towards vortex induced oscillation was observed only in limited number of cases and was not so clearly evidenced as it would be expected in smooth air flow.

3. Aerodynamic damping has been estimated from the test results via their autocorrelation function for some cases. These results corresponded well with the measured dynamic response.

4. Theoretical calculation based on a frequency domain analysis of buffeting showed a good agreement with the experimental results.

References:

2.1 Aynsly, R.M., Melbourne, W. and Vickery, B.J., Architectural Aerodynamics, Applied Science Publisher, 1977.

2.2 Bungales, T., Structural Analysis and Design of Tall Buildings, McGraw-Hill, 1988.

2.3 Davenport, A.G., Tall Buildings: an Anatomy of Wind Risk, Proc. NBRI Conference, Johanesburg, South Africa, 1975.

2.4 Irminger, I.O.V. and Nokkentved, C., Wind-pressure on Buildings, Experimental Research (2nd series), Ingenioervidenskabelige Skrifter (A) No.42, 1936.

2.5 Bailey, A., Wind Pressure on Buildings, Institution of Civil Engineers, Selected Engineering Paper No.139, London, 1933.

2.6 Bailey, A. and Vincent, N.D.G, Wind Pressure on Buildings Including Effects of Adjacent Buildings, Proc. ICE, (20) 1943, pp.243-275.

2.7 Jensen, M., Shelter Effects Investigation into the Aerodynamics of Shelter and its Effects on Climate and Crops, Danish Technical Press, Copenhagen, 1954.

2.8 Plate, E.J. (ed.), Engineering Meteorology, Elsevier, Amsterdam, 1982.

2.9 Lawson, T.V., Wind Effects on Buildings, Vol.1, Design Application, Applied Science Publishers, London, 1980.

2.10 Taranath, B.S., Structural Analysis and Design of Tall Buildings, McGraw-Hill, 1988.

2.11 Dryden, H.L. and Hill, G.C., Wind Pressures on a Model of the Empire State Building, Bureau of Standards Journal of Research (10) 1933, pp.493-523.

2.12 Rathbun, C.J., Wind Forces on a Tall Building, Trans. ASCE (105) Paper No.2056, 1940, pp.1-82.

2.13 Feld, L.S., Superstructure for 1,350 feet World Trade Center, Civil Engineering, ASCE, 1971, pp.66-70.

2.14 Whitebread, R.E. and Scruton, C., An Investigation of the Aerodynamic Stability of a Model of the Proposed Tower Blocks for the World Trade Center, New York (Part I), NPL Aero Rept. 1156, National Physical Laboratory, July 1965.

2.15 Davenport, A.G., Isyumov, N., Fader, D.J. and Bowen, C.F.P., Study of Wind Effects on the World Trade Center, New York; Exterior Pressure on Plaza Buildings and Airflow in Plaza, BLWT-6-70, University of Western Ontario, 1970.

2.16 Davenport, A.G., Isyumov, N. and Jandali, T., A Study of Wind Effects for the Sears Project, BLWT-5-71, University of Western Ontario, 1971.

2.17 Davenport, A.G., On the Statistical Prediction of Structural Performance in the Wind Environment, Meeting Preprint 1420, ASCE National Structural Meeting, Baltimore, Maryland, 1971.

2.18 Lythe, G.R., Surry, D. and Davenport, A.G., Wind Profiles over Selected Sites in the Hong Kong Area, BLWT-SS22-81, University of Western Ontario, 1981.

2.19 Georgiou, P.N., Mikitiuk, M.J., Surry, D. and Davenport, A.G., Wind Climate for Hong Kong, BLWT-SS2-84, University of Western Ontario, 1984.

2.20 Davenport, A.G. et al., The Wind Engineering Study for the Bank of China, Proc. 4th International Conference on Tall Buildings, Hong Kong, 1988, pp.143-147.

2.21 Tschanz, T., The Base Balance Measurement Technique and Applications to Dynamic Wind Loading of Structures, Ph.D. Thesis submitted to the University of Western Ontario, 1982.

2.22 -----, World's Tallest Tower Approved in Chicago, Civil Engineering, ASCE, 1990, p.18.

2.23 Davenport, A.G., Perspectives on the Full Scale Measurement of Wind Effects, Journal of Industrial Aerodynamics (1) 1975, pp.23-54.

2.24 Dalgliesh, W.A., Experiences with Wind Pressure Measurements on a Full Scale Building, Proc. Technical Meeting Concerning Wind Loads on Buildings and Structures, NBS Bldg. Sc. (30) Gaithersburg, Md., 1969, pp.61-71.

2.25 Davenport, A.G., The Response of Super Tall Buildings to Wind, Second Century of the Skyscraper, Van Nostrand Reinhold, 1988, pp.705-725.

2.26 Dalgliesh, W.A., Comparison of Model/Full Scale Wind Pressures on a High Rise Building, Journal of Industrial Aerodynamics (1) 1975, pp.55-66.

2.27 Dalgliesh, W.A., Comparison of the Model and Full Scale Tests of the Commerce Court Building in Toronto, Proc. International Workshop on Wind Tunnel Modeling Criteria and Techniques in Civil Engineering, Gaithersburg, Maryland, 1982, pp.575-589.

2.28 Dalgliesh, W.A., Templin, J.T. and Cooper, K.R., Comparisons of Wind Tunnel and Full Scale Building Surface Pressures with Emphasis on Peaks, Proc. 5th International Conference on Wind Engineering, Fort Collins, Colorado, July 1979, pp.553-565.

2.29 Dalgliesh, W.A. and Rainer, J.H., Measurements of Wind Induced Displacements and Accelerations of 57-storey Building in Toronto, Proc. 3rd Colloquium on Industrial Aerodynamics, Aachen, F.R.Germany, June 1978, pp.67-78.

2.30 Davenport, A.G., Hogan, M. and Isyumov, N., A Study of Wind Effects on the Commerce Court Tower, BLWT-7-69, University of Western Ontario, 1969.

2.31 Templin, J.T. and Cooper, K.R., Design and Performance of a Multi-degree-of-freedom Aeroelastic Building Model, Journal of Wind Engineering and Industrial Aerodynamics (8) 1981, pp.157-175.

2.32 Halvarson, R. and Isyumov, N., Comparison of the Predicted and Measured Dynamic Behaviour of Allied Bank Plaza, Building Motion in Wind, ASCE, 1986, pp.23-41.

3.1 Davenport, A.G., The Treatment of Wind Loading on Tall Buildings, Proc. Symp. on Tall Buildings with Particular Reference to Shear Wall Structures, University of Southampton, 1966, pp.3-44.

3.2 Brigham, E.O., The Fast Fourier Transform, Prentice-Hall, 1976.

3.3 Davenport, A.G., Gust Loading Factors, Proc. ASCE (93) ST3, 1967.

3.4 Vickery, B.J., On the Reliability of Gust Loading Factors, US Dept. of Commerce, NBS Bldg. Ser. (30) 1969.

3.5 Blevins, R.D., Flow Induced Vibration, Van Nostrand Reinhold, 1977.

3.6 Lawson, T.V., Wind Effects on Buildings, Vol.1: Design Applications, Applied Science Publishers, London, 1980.

3.7 Paz, M., Structural Dynamics: Theory and Computation (3rd ed.), Van Nostrand Reinhold, 1991.

3.8 Ruscheweyh, H., Dynamische Windwirkung an Bauwerken, Band 2: Praktische Anwendungen, Bauverlag Gmbh, Wiesbaden und Berlin, 1982.

3.9 Tanaka, H., Course material for CVG 5153 "Wind Engineering", University of Ottawa, Ottawa, 1991.

3.10 Simiu, E. and Scanlan, R.H., Wind Effects on Structures: An Introduction to Wind Engineering, John Wiley & Sons, 1978.

3.11 ----------, Supplement to the National Building Code of Canada 1985, NRCC No.23178, 1985.

4.1 Research Agreement between the University of Ottawa and Fujita Corporation, Tokyo, August 1990.

4.2 Irwin, H.P.A, Design and Use of Spires for Natural Wind Simulation, NAE-LTR-LA 233, National Research Council Canada, August 1979.

4.3 Tanaka, H., Resende-Ide, S. and Felbor, J., Aeroelastic Model Test of a Proposed Building, Rept. prepared for Fujita Corporation Ltd., Tokyo, 1992.

5.1 Davenport, A.G, The Interaction of Wind and Structures, Chapt.12 of Engineering Meteorology (ed. E.J. Plate) Elsevier, 1982.

5.2 Nakayama, M., Personal Communication with the University Team Tall Building Project, November 1990 and March 1991.

5.3 Isyumov, N., Wind Tunnel Modelling for Evaluating Wind Effects on Buildings and Structures, Proc. Int. Symp. on Experimental Mechanics, Univ. of Waterloo, 1972.

5.4 Davenport, A.G., Note on the Distribution of the Largest Value of a Random Function with Application to Gust Loading, Proc. ICE (24) 1964, pp.187-196.

Table.2.1 Wind Response Characteristics of Structures

Type of building	Type of wind	Stiffness of building	Type of excitation	Flow pattern	Secondary building present?	Resultant force / moment	Resultant motion	Name of motion	Section:
Streamlined	Steady	Stiff Flexible	None Static instability	Attached for limited wind direction range	No	Steady	None	None	3 (introduction)
				Attached up to stall incidence	No	Divergent or periodic at natural frequency		Divergence stall flutter	6 (introduction)
Bluff	Steady	Stiff	Static instability	Fluctuating separation	No	Random	Negligible	Fluctuating separation	3.2
				Flow switching	No	Irregular	Negligible	Flow switching	3.7
				Vortex shedding	No	Periodic (Strouhal No.)	Negligible	Vortex shedding	3.5
		Stiff to flexible		Names and patterns as above, with increased motion of building which can cause 'lock-in' at one of the natural frequencies of the building, leading to amplification of motion in those instances					6.12
	Steady	Flexible	Galloping or dynamic instability	Movement causes Reynolds number changes	No	Δ drag only	Along-wind oscillation	Drag saddle galloping	6.4
						Δ drag and Δ lift	Compound oscillation	Stranded cable galloping	6.6
				Movement causes incidence changes	No	Periodic torsion at natural frequency: unstable ranges of incidence	Periodic rotation at natural frequency	Torsional galloping	6.10
					No		Resonance at natural frequency	Cross-wind galloping of sharp-edged buildings	6.8
					Yes			Twin conductor galloping	6.7
				Movement through windspeed gradient caused by upwind building	Yes	Quasi-static forces which are functions of position wrt upwind building	Oscillation occurs above critical value of frequency parameter	Wake galloping	6.9
	Fluctuating	Stiff / Flexible	Buffeting	Atmospheric turbulence	No	Random	Random / Resonant	Atmospheric buffeting along-wind	5.4 to 5.8
								Atmospheric buffeting cross-wind	5.12 to 5.13
				Wake turbulence	Yes	Random	Random / Resonant	Wake buffeting along-wind	
								Wake buffeting cross-wind	5.9
				Atmospheric turbulence	No	Random	Random / Resonant	Atmospheric torsional buffeting	5.14
				Wake turbulence	Yes	Random	Random / Resonant	Wake torsional buffeting	5.14
	Steady or fluctuating	Flexible	Flutter	Flexure-torsion	No	Bending / Torque	Flexure / Twist with phase lag	Flat plate flutter	6.15
				Velocity gradients in two planes at right angles	Yes	Periodic	Elliptic periodic at natural frequency	Suspension bridge deck flutter	6.15
								Wake induced flutter	6.14

(from [2.9])

Table.4.1 Floor Masses (unit: kg)

Mass	Measured values				Required
	Floor	Skin	Columns	Total	
No.7 (top)	0.656	0.330	0.177	1.164	1.17
No.6	0.788	0.303	0.379	1.471	1.48
No.5	1.004	0.365	0.518	1.887	1.89
No.4	1.357	0.453	0.693	2.503	2.50
No.3	1.917	0.598	0.986	3.501	3.51
No.2	2.790	0.937	1.800	5.527	5.29
No.1 (base)	11.016	4.603	2.799	18.418	18.77

Table.4.2 Floor Stiffnesses

	X-dir (kN/m)		Y-dir (kN/m)		Tors (kN m)	
	Meas'd	Req'd	Meas'd	Req'd	Meas'd	Req'd
No.7	28.5	29.1	23.4	23.6	0.38	0.38
No.6	49.9	57.4	44.3	46.5	0.87	0.90
No.5	74.3	82.2	60.4	66.6	1.51	1.54
No.4	90.2	104.2	75.2	84.4	2.21	2.38
No.3	95.1	116.1	79.4	94.0	3.25	3.33
No.2	101.7	119.8	84.7	97.0	4.68	4.82
No.1	79.1	85.8	63.9	69.5	5.16	4.89

Table.4.3 Dynamic Characteristics in X-direction

Mode	1st	2nd	3rd	4th	5th	6th	7th
req.fq(Hz)	6.65	13.2	21.3	30.4	39.3	48.4	57.6
meas.f(Hz)	6.26	13.3	22.1	31.8	41.4	51.1	----
damping(%)	1.23	1.15	0.90	1.00	0.99	0.92	----

Required Modes

No.7 (top)	1.00	1.00	1.00	1.00	-0.70	-0.37	0.14
No.6	0.93	0.73	0.29	-0.46	1.00	1.00	-0.58
No.5	0.85	0.46	-0.21	-0.77	0.30	-0.67	1.00
No.4	0.77	0.20	-0.47	-0.35	-0.61	-0.41	-0.89
No.3	0.66	-0.03	-0.47	0.30	-0.43	0.72	0.43
No.2	0.53	-0.25	-0.21	0.55	0.54	-0.30	-0.10
No.1 (base)	0.37	-0.37	0.21	-0.14	-0.07	0.02	0.01

Obtained Modes

No.7 (top)	1.00	1.00	1.00	1.00	-0.54	0.09	----
No.6	0.95	0.78	0.45	-0.27	1.00	1.00	----
No.5	0.86	0.42	-0.23	-0.92	0.31	-0.35	----
No.4	0.78	0.16	-0.53	-0.55	-0.68	-0.44	----
No.3	0.66	-0.13	-0.56	0.31	-0.51	0.59	----
No.2	0.51	-0.36	-0.23	0.67	0.70	-0.20	----
No.1 (base)	0.32	-0.53	0.24	-0.20	-0.11	0.08	----

Table.4.4 Dynamic Characteristics in Y-direction

Mode	1st	2nd	3rd	4th	5th	6th	7th
req.fq(Hz)	5.98	11.8	19.2	27.4	35.4	43.5	51.9
meas.f(Hz)	5.70	12.2	20.1	29.2	38.2	46.4	----
damping(%)	0.97	1.05	1.21	1.25	1.24	1.07	----

Required Modes

No.7 (top)	1.00	1.00	1.00	1.00	-0.69	-0.37	0.14
No.6	0.93	0.73	0.29	-0.46	1.00	1.00	-0.58
No.5	0.85	0.46	-0.21	-0.77	0.29	-0.67	1.00
No.4	0.77	0.21	-0.47	-0.35	-0.60	-0.41	-0.89
No.3	0.66	-0.03	-0.47	0.30	-0.43	0.72	0.43
No.2	0.53	-0.24	-0.21	0.55	0.54	-0.30	-0.10
No.1 (base)	0.37	-0.37	0.21	-0.14	-0.07	0.02	0.01

Obtained Modes

No.7 (top)	1.00	1.00	1.00	1.00	-0.93	-0.02	----
No.6	0.95	0.81	0.50	-0.33	1.00	1.00	----
No.5	0.85	0.44	-0.23	-1.18	0.17	-0.61	----
No.4	0.78	0.21	-0.49	-0.85	-0.97	-0.50	----
No.3	0.65	-0.10	-0.54	0.27	-0.77	0.65	----
No.2	0.50	-0.35	-0.21	0.72	0.83	-0.28	----
No.1 (base)	0.32	-0.45	0.25	-0.25	-0.12	0.05	----

Table.4.5 Dynamic Characteristics in Torsion

Mode	1st	2nd	3rd	4th	5th	6th	7th
req.fq.(Hz)	8.71	15.0	23.0	32.2	41.4	50.5	60.0
meas.f.(Hz)	11.3	19.3	29.9	41.3	54.3	----	----
damping (%)	1.39	1.64	1.57	2.18	1.63	----	----

Required Modes

No.7 (top)	1.00	1.00	1.00	1.00	-0.75	-0.40	0.16
No.6	0.90	0.69	0.28	-0.41	1.00	1.00	-0.64
No.5	0.79	0.43	-0.16	-0.65	0.27	-0.61	1.00
No.4	0.69	0.20	-0.35	-0.26	-0.51	-0.33	-0.86
No.3	0.57	0.01	-0.33	0.22	-0.33	0.53	0.38
No.2	0.44	-0.14	-0.13	0.35	0.39	-0.21	-0.08
No.1 (base)	0.29	-0.20	0.12	-0.09	-0.05	0.02	0.00

Obtained Modes

No.7 (top)	1.00	1.00	1.00	1.00	-0.83	-0.50	----
No.6	0.89	0.71	0.32	-1.30	1.00	1.00	----
No.5	0.74	0.36	-0.23	-1.30	0.32	-0.42	----
No.4	0.63	0.14	-0.42	-0.53	-0.39	-0.25	----
No.3	0.47	-0.10	-0.36	0.29	-0.21	0.55	----
No.2	0.31	-0.23	-0.10	0.47	0.56	-0.36	----
No.1 (base)	0.15	-0.25	0.19	-0.16	-0.07	0.13	----

Table 4.6 List of Flow Runs

Lateral Correlations:

RUN #	PT #	REF HT (mm)	dz (mm)	dy (mm)
44*	1,2,3	630	0	25
	5,6,7	1490		
	8,9,10	1900		
	14,15,16	1900	0	50
	17,18,19	1490		
	20,21,22	630		
	23,24,25	630	0	100
	26,27,28	1490		
	29,30,31	1900		
	32,33,34	1900	0	200
	35,36,37	1490		
	38,39,40	630		
	41,42,43	630	0	400
	44,45,46	1490		
	47,48,49	1900		

* PT # 4, 11, 12 and 13 are unavailable.

Vertical Correlations:

RUN #	PT #	REF HT (mm)	dz (mm)	dy (mm)
46	1,2,3	630	25	0
	4,5,6		50	
	7,8		100	
	9,10,11		200	
	12,13,14		400	
48	1,2,3	1490	25	0
	4,5,6		50	
	7,8,9		100	
	10,11,12		200	
	13,14,15		400	
50	1,2,3	1900	25	0
	4,5,6		50	
	7,8,9		100	
	10,11,12		200	
	13,14,15		400	

Table.4.7 Results of Flow Measurement

	z/H	U	U/Utop	u'/U	v'/U	smth U/Uo
1	0.025	6.409	0.475	0.250	0.212	0.475
2	0.042	6.594	0.489	0.258	0.199	0.504
3	0.083	7.555	0.560	0.233	0.174	0.561
4	0.125	8.550	0.634	0.213	0.154	0.634
5	0.167	9.510	0.705	0.190	0.135	0.693
6	0.179	9.808	0.728	0.182	0.129	0.742
7	0.250	10.870	0.806	0.119	0.095	0.796
8	0.333	11.370	0.843	0.085	0.072	0.838
9	0.417	11.590	0.860	0.079	0.067	0.860
10	0.500	11.800	0.875	0.076	0.062	
11	0.512	11.670	0.866	0.072	0.060	
12	0.513	11.790	0.875	0.082	0.066	0.874
13	0.529	11.850	0.879	0.082	0.067	
14	0.571	12.060	0.895	0.079	0.062	0.874
15	0.583	12.130	0.900	0.075	0.060	0.902
16	0.613	12.190	0.904	0.078	0.064	0.911
17	0.654	12.370	0.918	0.079	0.060	0.915
18	0.667	12.310	0.913	0.069	0.055	0.917
19	0.667	12.350	0.916	0.078	0.061	
20	0.738	12.570	0.932	0.076	0.055	
21	0.750	12.720	0.944	0.066	0.047	0.938
22	0.762	12.640	0.938	0.062	0.047	
23	0.821	12.920	0.958	0.070	0.049	0.960
24	0.904	13.270	0.984	0.055	0.038	0.982
25	0.988	13.510	1.002	0.038	0.028	0.997
26	1.000	13.480	1.000	0.038	0.028	0.999
27	1.071	13.390	0.993	0.025	0.021	
28	1.154	13.610	1.010	0.016	0.014	1.012
29	1.238	13.960	1.036	0.011	0.009	1.029
30	1.250	13.980	1.037	0.012	0.011	1.037

Table.4.8 List of Runs

The following 4 pages list all the wind tunnel runs to identify the RUN number, POINT number and corresponding wind speed etc. for each file. Listed for each file are as follows:

Angle = Wind azimuth angle which is 0^{o} for X-direction, increasing in clockwise direction and 90^{o} for negative Y-direction

RUN # and POINT # = numbers to identify the files

Wind Vel = mean wind speed (m/s) at the building top height

V_x, V_y, V_t = reduced velocities in three directions which are used for the regression analysis (Section 6.1)

B = 0.3 m, average width of the building

f_x, f_y, f_t = lowest natural frequencies in three modes

V_{mh} = "nominal" wind speed (m/s) at the building height

V_{mh} values were provided by NRCC but later it was found to be slightly off because of the conversion used. V_{mh} is listed only for angles of 0^{o} and 5^{o} since these numbers were used for the calculation of velocity spectra and auto-correlations for these angles.

In the last page, there are 16 files identified as $V_{modl} = 0$. These data were not used for the regression analysis.

"Wind Vel": Wind Speed at model height (m/s)
"Vmh" was used for Spectra and Auto-Correlation Graphs.
B=0.3 fx=6.25 Hz fy=5.70 Hz fx=11.29 Hz

Angle=0	Point	Wind Vel	Vx=V/fxB	Vy=V/fyB	Vt=V/ftB	Vmh
RUN=100	1	3.458	1.845	2.022	1.021	3.426
RUN=100	2	3.478	1.855	2.034	1.027	3.446
RUN=100	3	5.157	2.751	3.016	1.523	5.136
RUN=100	4	5.166	2.755	3.021	1.525	5.144
RUN=100	5	8.938	4.767	5.227	2.639	8.924
RUN=100	6	8.942	4.769	5.229	2.640	8.928
RUN=100	7	11.942	6.369	6.983	3.526	11.930
RUN=100	8	11.940	6.368	6.982	3.525	11.930
RUN=100	9	13.796	7.358	8.068	4.073	13.790
RUN=100	10	13.805	7.363	8.073	4.076	13.800
RUN=103	1	13.771	7.345	8.053	4.066	13.820
RUN=103	2	13.785	7.352	8.062	4.070	13.830
RUN=103	3	15.456	8.243	9.038	4.563	15.500
RUN=103	4	15.468	8.250	9.046	4.567	15.510
RUN=103	5	16.759	8.938	9.800	4.948	16.790
RUN=103	6	16.764	8.941	9.803	4.949	16.800
RUN=103	7	18.451	9.840	10.790	5.448	18.480
RUN=103	8	18.449	9.839	10.789	5.447	18.480
RUN=103	9	20.629	11.002	12.064	6.091	20.660
RUN=103	10	20.636	11.006	12.068	6.093	20.670
RUN=103	11	24.140	12.874	14.117	7.127	24.170
RUN=103	12	24.151	12.880	14.123	7.130	24.180
RUN=103	13	28.068	14.970	16.414	8.287	28.090
RUN=103	14	28.083	14.977	16.423	8.291	28.110

Angle=5	Point	Wind Vel	Vx=V/fxB	Vy=V/fyB	Vt=V/ftB	Vmh
RUN=106	1	3.464	1.847	2.026	1.023	3.628
RUN=106	2	3.453	1.842	2.019	1.019	3.617
RUN=106	3	5.221	2.784	3.053	1.541	5.330
RUN=106	4	5.249	2.799	3.069	1.550	5.357
RUN=106	5	9.027	4.814	5.279	2.665	9.089
RUN=106	6	9.034	4.818	5.283	2.667	9.097
RUN=106	7	12.041	6.422	7.042	3.555	12.090
RUN=106	8	12.051	6.427	7.047	3.558	12.100
RUN=106	9	13.928	7.428	8.145	4.112	13.970
RUN=106	10	13.933	7.431	8.148	4.114	13.970
RUN=108	1	15.604	8.322	9.125	4.607	15.630
RUN=108	2	15.607	8.324	9.127	4.608	15.630
RUN=108	3	16.893	9.010	9.879	4.988	16.920
RUN=108	4	16.886	9.006	9.875	4.986	16.910
RUN=108	5	18.579	9.909	10.865	5.485	18.600
RUN=108	6	18.578	9.908	10.864	5.485	18.600
RUN=108	7	20.751	11.067	12.135	6.127	20.770
RUN=108	8	20.757	11.070	12.138	6.128	20.780
RUN=108	9	24.300	12.960	14.210	7.174	24.320
RUN=108	10	24.301	12.960	14.211	7.175	24.320
RUN=108	11	28.208	15.044	16.496	8.328	28.230
RUN=108	12	28.218	15.050	16.502	8.331	28.230

Angle=45	Point	Wind Vel	Vx=V/fxB	Vy=V/fyB	Vt=V/ftB
RUN=111	1	3.561	1.899	2.082	1.051
RUN=111	2	3.570	1.904	2.088	1.054
RUN=111	3	5.268	2.810	3.081	1.555
RUN=111	4	5.261	2.806	3.077	1.553
RUN=111	5	9.036	4.819	5.284	2.668
RUN=111	6	9.024	4.813	5.277	2.664
RUN=111	7	12.055	6.429	7.050	3.559
RUN=111	8	12.065	6.435	7.056	3.562
RUN=111	9	13.942	7.436	8.153	4.116
RUN=111	10	13.946	7.438	8.156	4.118
RUN=111	11	15.593	8.316	9.119	4.604
RUN=111	12	15.601	8.321	9.123	4.606
RUN=114	1	5.238	2.794	3.063	1.547
RUN=114	2	5.255	2.803	3.073	1.552
RUN=114	3	9.022	4.812	5.276	2.664
RUN=114	4	9.028	4.815	5.280	2.665
RUN=114	5	12.043	6.423	7.043	3.556
RUN=114	6	16.874	8.999	9.868	4.982
RUN=114	7	16.884	9.005	9.874	4.985
RUN=114	8	18.559	9.898	10.853	5.479
RUN=114	9	18.576	9.907	10.863	5.484
RUN=114	10	20.673	11.026	12.089	6.104
RUN=114	11	20.680	11.029	12.094	6.106
RUN=114	12	24.269	12.943	14.192	7.165
RUN=114	13	24.285	12.952	14.202	7.170
RUN=114	14	28.210	15.045	16.497	8.329
RUN=114	15	28.215	15.048	16.500	8.330

Angle=20	Point	Wind Vel	Vx=V/fxB	Vy=V/fyB	Vt=V/ftB
RUN=116	1	3.536	1.886	2.068	1.044
RUN=116	2	3.549	1.893	2.075	1.048
RUN=116	3	9.024	4.813	5.277	2.664
RUN=116	4	9.029	4.815	5.280	2.666
RUN=116	5	13.917	7.422	8.139	4.109
RUN=116	6	13.926	7.427	8.144	4.112
RUN=116	7	16.871	8.998	9.866	4.981
RUN=116	8	16.875	9.000	9.868	4.982
RUN=116	9	20.711	11.046	12.112	6.115
RUN=116	10	20.719	11.050	12.116	6.117
RUN=116	11	28.165	15.021	16.471	8.316
RUN=116	12	28.189	15.034	16.485	8.323

Angle=15	Point	Wind Vel	Vx=V/fxB	Vy=V/fyB	Vt=V/ftB
RUN=118	3	8.043	4.290	4.704	2.375
RUN=118	4	8.102	4.321	4.738	2.392
RUN=118	5	13.440	7.168	7.860	3.968
RUN=118	6	13.566	7.235	7.933	4.005
RUN=118	7	16.548	8.826	9.677	4.886
RUN=118	8	16.571	8.838	9.691	4.893
RUN=118	9	20.465	10.915	11.968	6.042
RUN=118	10	20.701	11.041	12.106	6.112
RUN=118	11	28.153	15.015	16.464	8.312
RUN=118	12	28.169	15.023	16.473	8.317

Angle=30	Point	Wind Vel	Vx=V/fxB	Vy=V/fyB	Vt=V/ftB
RUN=120	1	3.121	1.665	1.825	0.921
RUN=120	2	3.228	1.722	1.888	0.953
RUN=120	3	8.782	4.684	5.136	2.593
RUN=120	4	8.803	4.695	5.148	2.599
RUN=120	5	13.778	7.348	8.057	4.068
RUN=120	6	13.805	7.363	8.073	4.076
RUN=120	7	16.796	8.958	9.822	4.959
RUN=120	8	16.798	8.959	9.823	4.960
RUN=120	9	20.670	11.024	12.088	6.103
RUN=120	10	20.636	11.006	12.068	6.093
RUN=120	11	28.064	14.967	16.412	8.286
RUN=120	12	28.074	14.973	16.418	8.289

Angle=25	Point	Wind Vel	Vx=V/fxB	Vy=V/fyB	Vt=V/ftB
RUN=124	1	3.447	1.838	2.016	1.018
RUN=124	2	3.492	1.862	2.042	1.031
RUN=124	3	8.983	4.791	5.253	2.652
RUN=124	4	8.996	4.798	5.261	2.656
RUN=124	5	13.890	7.408	8.123	4.101
RUN=124	6	13.878	7.402	8.116	4.097
RUN=124	7	16.826	8.974	9.840	4.968
RUN=124	8	16.845	8.984	9.851	4.973
RUN=127	1	20.701	11.041	12.106	6.112
RUN=127	2	20.729	11.055	12.122	6.120
RUN=127	3	28.094	14.983	16.429	8.295
RUN=127	4	28.070	14.971	16.415	8.288

Angle=10	Point	Wind Vel	Vx=V/fxB	Vy=V/fyB	Vt=V/ftB
RUN=129	1	3.945	2.104	2.307	1.165
RUN=129	2	3.964	2.114	2.318	1.170
RUN=129	3	9.091	4.849	5.316	2.684
RUN=129	4	9.047	4.825	5.291	2.671
RUN=129	5	13.901	7.414	8.129	4.104
RUN=129	6	13.915	7.421	8.137	4.108
RUN=129	7	16.834	8.978	9.844	4.970
RUN=129	8	16.858	8.991	9.858	4.977
RUN=129	9	20.638	11.007	12.069	6.093
RUN=129	10	20.644	11.010	12.073	6.095
RUN=129	11	28.043	14.956	16.399	8.280
RUN=129	12	28.047	14.958	16.402	8.281

Angle=35	Point	Wind Vel	Vx=V/fxB	Vy=V/fyB	Vt=V/ftB
RUN=131	1	3.766	2.009	2.202	1.112
RUN=131	2	3.738	1.994	2.186	1.104
RUN=131	3	9.110	4.859	5.327	2.690
RUN=131	4	9.137	4.873	5.343	2.698
RUN=131	5	13.928	7.428	8.145	4.112
RUN=131	6	13.876	7.401	8.115	4.097
RUN=131	7	16.770	8.944	9.807	4.951
RUN=131	8	16.880	9.003	9.871	4.984
RUN=131	9	20.692	11.036	12.101	6.109
RUN=131	10	20.656	11.017	12.080	6.099
RUN=131	11	28.031	14.950	16.392	8.276
RUN=131	12	28.052	14.961	16.405	8.282

Angle=40	Point	Wind Vel	Vx=V/IxB	Vy=V/IyB	Vt=V/ItB
RUN=133	1	3.947	2.105	2.308	1.165
RUN=133	2	3.951	2.107	2.311	1.167
RUN=133	3	9.149	4.879	5.350	2.701
RUN=133	4	9.161	4.886	5.357	2.705
RUN=133	5	13.972	7.452	8.171	4.125
RUN=133	6	13.974	7.453	8.172	4.126
RUN=133	7	16.887	9.006	9.875	4.986
RUN=133	8	16.891	9.009	9.878	4.987
RUN=133	9	20.686	11.033	12.097	6.107
RUN=133	10	22.001	11.734	12.866	6.496
RUN=133	11	27.997	14.932	16.373	8.266
RUN=133	12	28.084	14.978	16.423	8.292
RUN=133	13	27.349	14.586	15.994	8.075

Angle=90	Point	Wind Vel	Vx=V/IxB	Vy=V/IyB	Vt=V/ItB
RUN=135	1	3.956	2.110	2.313	1.168
RUN=135	2	3.976	2.121	2.325	1.174
RUN=135	3	5.530	2.949	3.234	1.633
RUN=135	4	5.527	2.948	3.232	1.632
RUN=135	5	9.160	4.885	5.357	2.704
RUN=135	6	9.176	4.894	5.366	2.709
RUN=135	7	12.138	6.474	7.098	3.584
RUN=135	8	12.137	6.473	7.098	3.583
RUN=135	9	13.984	7.458	8.178	4.129
RUN=135	10	13.982	7.457	8.177	4.128
RUN=135	11	15.630	8.336	9.140	4.615
RUN=135	12	15.633	8.338	9.142	4.616
RUN=137	1	16.903	9.015	9.885	4.991
RUN=137	2	16.905	9.016	9.886	4.991
RUN=137	3	18.561	9.899	10.854	5.480
RUN=137	4	18.561	9.899	10.854	5.480
RUN=137	5	20.697	11.038	12.104	6.111
RUN=137	6	20.652	11.014	12.077	6.097

The following points were not used on exponential curve fitting:

Vmodl=0	Point	Wind Vel	Angle
RUN=100	11	0	0
RUN=103	15	0	0
RUN=108	13	0	5
RUN=111	13	0	45
RUN=114	16	0	45
RUN=116	13	0	20
RUN=118	1	0	15
RUN=118	2	0	15
RUN=118	13	0	15
RUN=120	13	0.711	30
RUN=125	1	0.741	25
RUN=127	5	1.239	25
RUN=129	13	1.142	10
RUN=131	13	1.703	35
RUN=133	14	1.712	40
RUN=135	13	1.734	90

Table.5.1 List of Regression Coefficients

The following 3 pages list the regression coefficients for the equations given in Section 5.1.

The first page is the list of C-coefficients for the mean response in X- and Y- directions which are defined by

$$\text{Mean of } x(t) = C_x(a)*(V_r)^2$$

$$\text{Mean of } y(t) = C_y(a)*(V_r)^2$$

where a = wind azimuth angle
$V_r = V/Bf$ = reduced velocity

The mean response in torsion is not included because they are considered to be "nearly zero".

The last two pages list K- and C-coefficients defined for the root-mean-square response as follows:

$$\text{RMS of } x(t) = C_x(a)*(V_r)**K_x(a)$$

$$\text{RMS of } y(t) = C_y(a)*(V_r)**K_y(a)$$

$$\text{RMS of } 0(t) = C_t(a)*(V_r)**K_t(a)$$

K- and C-coefficients are calculated for each of seven masses.

Mean for K=2

Angle	Cx1	Cx2	Cx3	Cx4	Cx5	Cx6	Cx7
0	0.001370	0.002135	0.002730	0.003192	0.003537	0.003939	0.004169
5	0.001319	0.002030	0.002577	0.003023	0.003338	0.003707	0.003918
10	0.001295	0.001963	0.002474	0.002871	0.003168	0.003518	0.003716
15	0.001303	0.001962	0.002466	0.002858	0.003153	0.003504	0.003698
20	0.001293	0.001940	0.002430	0.002803	0.003082	0.003416	0.003599
25	0.001373	0.002056	0.002572	0.002961	0.003249	0.003587	0.003772
30	0.001355	0.002025	0.002531	0.002917	0.00320	0.003545	0.003729
35	0.001356	0.002021	0.002527	0.002914	0.003203	0.003553	0.003743
40	0.001295	0.001920	0.002400	0.002767	0.003044	0.003380	0.003563
45	0.001247	0.001842	0.002299	0.002651	0.002919	0.003248	0.003422
90	0.000021	0.000069	0.000095	0.000102	0.000080	0.000031	0.000038

Angle	Cy1	Cy2	Cy3	Cy4	Cy5	Cy6	Cy7
0	0.000110	0.000153	0.000204	0.000225	0.000222	0.000216	0.000207
5	0.000262	0.000476	0.000646	0.000784	0.000842	0.000927	0.000952
10	0.000155	0.000337	0.000501	0.000628	0.000681	0.000747	0.000774
15	0.000191	0.000194	0.000178	0.000184	0.000199	0.000212	0.000227
20	0.000474	0.000633	0.000753	0.000891	0.000976	0.001090	0.001150
25	0.000705	0.000990	0.001222	0.001473	0.001622	0.001826	0.001928
30	0.000845	0.001211	0.001503	0.001808	0.001982	0.002220	0.002338
35	0.001009	0.001458	0.001817	0.002180	0.002383	0.002659	0.002792
40	0.001104	0.001596	0.001983	0.002371	0.002585	0.002873	0.003008
45	0.001241	0.001797	0.002239	0.002675	0.002911	0.003229	0.003381
90	0.001324	0.001961	0.002478	0.002973	0.003234	0.003603	0.003785

Angle	Kx1	Kx2	Kx3	Kx4	Kx5	Kx6	Kx7
0	2.039027	2.004461	2.000789	1.996927	2.008076	2.044711	2.055896
5	2.276065	2.301229	2.304290	2.305727	2.308123	2.312782	2.317513
10	2.243024	2.283848	2.296927	2.300414	2.302031	2.303586	2.308275
15	2.413273	2.431552	2.442784	2.460884	2.465615	2.465859	2.467824
20	1.832077	1.849640	1.862689	1.874512	1.885117	1.895730	1.906782
25	2.610790	2.618853	2.645902	2.656758	2.662349	2.666197	2.669545
30	2.769462	2.784363	2.809130	2.820178	2.824907	2.828007	2.830630
35	2.606531	2.620080	2.651114	2.661104	2.666326	2.669850	2.672157
40	2.754123	2.758008	2.791395	2.803505	2.809213	2.813576	2.816357
45	2.635807	2.662462	2.675418	2.683919	2.688985	2.695556	2.701530
90	4.226012	4.182959	4.183251	4.194715	4.205960	4.218152	4.227757

Angle	Cx1	Cx2	Cx3	Cx4	Cx5	Cx6	Cx7
0	0.000408	0.000704	0.000917	0.001094	0.001180	0.001189	0.001223
5	0.000185	0.000268	0.000342	0.000401	0.000443	0.000490	0.000514
10	0.000200	0.000279	0.000345	0.000402	0.000445	0.000494	0.000518
15	0.000171	0.000251	0.000310	0.000355	0.000390	0.000433	0.000456
20	0.000628	0.000929	0.001151	0.001312	0.001419	0.001544	0.001594
25	0.000147	0.000222	0.000268	0.000307	0.000335	0.000370	0.000388
30	0.000110	0.000163	0.000197	0.000225	0.000247	0.000272	0.000286
35	0.000141	0.000208	0.000248	0.000284	0.000311	0.000342	0.000360
40	0.000105	0.000159	0.000187	0.000213	0.000232	0.000255	0.000267
45	0.000133	0.000191	0.000237	0.000272	0.000298	0.000326	0.000339
90	2.07E-05	3.54E-05	4.55E-05	5.21E-05	5.63E-05	6.07E-05	6.27E-05

Angle	Ky1	Ky2	Ky3	Ky4	Ky5	Ky6	Ky7
0	4.431134	4.430254	4.435619	4.445678	4.452894	4.465463	4.474253
5	3.284225	3.266296	3.263650	3.271188	3.279113	3.292917	3.303911
10	2.037782	1.931014	1.901856	1.919046	1.943834	1.994199	2.026337
15	1.794383	1.708205	1.694920	1.715630	1.737969	1.781308	1.809775
20	1.600811	1.523917	1.521231	1.549168	1.574772	1.619818	1.648053
25	1.541750	1.465923	1.464220	1.490754	1.515289	1.558489	1.587322
30	2.570603	2.585248	2.607086	2.623581	2.632295	2.648483	2.656991
35	2.738478	2.773017	2.806418	2.843558	2.857032	2.869342	2.876445
40	2.896973	2.946416	2.992947	3.023825	3.034701	3.045418	3.050886
45	2.802125	2.824653	2.834775	2.848474	2.855907	2.865669	2.873702
90	2.635333	2.599500	2.591795	2.597681	2.603092	2.602005	2.606144

Angle	Cy1	Cy2	Cy3	Cy4	Cy5	Cy6	Cy7
0	2.55E-05	3.90E-05	4.99E-05	5.92E-05	6.36E-05	6.89E-05	7.10E-05
5	0.000097	0.000151	0.000194	0.000231	0.000248	0.000268	0.000275
10	0.000469	0.000862	0.001167	0.001357	0.001404	0.001408	0.001381
15	0.000801	0.001415	0.001852	0.002134	0.002216	0.002251	0.002223
20	0.001371	0.002381	0.003044	0.003452	0.003559	0.003601	0.003558
25	0.001459	0.002506	0.003191	0.003628	0.003750	0.003813	0.003763
30	0.000168	0.000238	0.000288	0.000334	0.000357	0.000383	0.000395
35	0.000096	0.000128	0.000151	0.000166	0.000175	0.000190	0.000196
40	0.000063	0.000081	0.000092	0.000102	0.000109	0.000118	0.000122
45	0.000073	0.000101	0.000125	0.000145	0.000155	0.000168	0.000173
90	0.000092	0.000145	0.000190	0.000224	0.000237	0.000263	0.000273

Angle	Kt1	Kt2	Kt3	Kt4	Kt5	Kt6	Kt7
0	2.118099	2.196530	2.303259	2.388112	2.421303	2.438381	2.489925
5	2.419125	2.553859	2.648647	2.701729	2.723043	2.738936	2.778234
10	2.505417	2.595735	2.689863	2.706033	2.720385	2.741788	2.790319
15	2.196531	2.281917	2.337310	2.331701	2.348258	2.385928	2.447933
20	2.059587	2.118563	2.162445	2.170198	2.186363	2.219825	2.268574
25	2.100343	2.108820	2.132360	2.114213	2.129091	2.162361	2.226509
30	2.164836	2.266418	2.311220	2.271137	2.263567	2.275083	2.324580
35	2.288242	2.296470	2.309727	2.265699	2.264456	2.284779	2.333988
40	2.408716	2.430461	2.441765	2.365051	2.355186	2.377133	2.426874
45	2.403479	2.407954	2.416316	2.387134	2.395635	2.424182	2.470914
90	3.385705	3.411600	3.502621	3.672240	3.735803	3.780359	3.716230

Angle	Ct1	Ct2	Ct3	Ct4	Ct5	Ct6	Ct7
0	1.53E-05	2.00E-05	2.18E-05	2.34E-05	2.61E-05	3.05E-05	3.08E-05
5	5.72E-06	6.67E-06	7.52E-06	8.76E-06	1.01E-05	1.18E-05	1.22E-05
10	3.42E-06	4.26E-06	4.80E-06	6.18E-06	7.28E-06	8.51E-06	8.57E-06
15	5.70E-06	7.19E-06	8.65E-06	1.17E-05	1.38E-05	1.56E-05	1.54E-05
20	7.74E-06	1.04E-05	1.28E-05	1.69E-05	1.99E-05	2.28E-05	2.30E-05
25	6.86E-06	1.01E-05	1.30E-05	1.83E-05	2.18E-05	2.53E-05	2.48E-05
30	6.27E-06	7.75E-06	9.47E-06	1.38E-05	1.70E-05	2.03E-05	2.03E-05
35	4.54E-06	6.57E-06	8.41E-06	1.23E-05	1.51E-05	1.79E-05	1.79E-05
40	3.68E-06	5.13E-06	6.58E-06	1.02E-05	1.28E-05	1.50E-05	1.50E-05
45	3.98E-06	5.62E-06	7.16E-06	1.03E-05	1.24E-05	1.45E-05	1.44E-05
90	2.13E-06	3.05E-06	3.66E-06	4.59E-06	5.37E-06	6.20E-06	7.02E-06

Table.5.2 Stastistical Summary of Test Results

The following 11 pages list the statistical summary of the measured data, for each azimuth angle in the highest wind speed.

There are three groups of numbers which correspond to the displacements in X- and Y-sway motions and in torsion. The first to the seventh lines in each group correspond to the response of the first (lowest) to the seventh (top) masses of the model. The meaning of nine columns are as follows:

1st column: Summation of all N readings (= S_X)
2nd column: Summation of all N readings squared (= S_{XX})
3rd column: Mean value which is given by S_X/N (= m)
4th column: RMS given by $[S_{XX}/(N-1)-S_X^2/N(N-1)]^{1/2}$ (= s)
5th column: Maximum reading of the file (= pp)
6th column: Minimum reading of the file (= np)
7th column: Peak factor g_1 = (pp - m)/s
8th column: Peak factor g_2 = (m - np)/s
9th column: Peak factor g_3 = (pp - np)/(2s)

in which N = 30,000

These tables are from [4.3]

RUN=103 POINT=13 VMODEL= 28.068 AIR DENSITY= 1.240

X									
1	0.48122500E+04	0.16092195E+04	0.29371643E+00	0.10931778E+00	0.69432205E+00	-0.11651285E-01	3.664597	-2.793394	3.228995
2	0.74997461E+04	0.39222593E+04	0.45774817E+00	0.17281258E+00	0.10355196E+01	-0.37702456E-01	3.343341	-2.866982	3.105159
3	0.95919492E+04	0.64222500E+04	0.58544612E+00	0.22189844E+00	0.13091640E+01	-0.92684925E-01	3.261482	-3.056042	3.158762
4	0.11215043E+05	0.87985156E+04	0.68451190E+00	0.26166087E+00	0.15494423E+01	-0.12571484E+00	3.305539	-3.096476	3.201007
5	0.12425180E+05	0.10810844E+05	0.75837278E+00	0.29106265E+00	0.17311916E+01	-0.14502829E+00	3.342300	-3.103803	3.223051
6	0.13845687E+05	0.13425082E+05	0.84507370E+00	0.32443625E+00	0.19197817E+01	-0.15897530E+00	3.312539	-3.094748	3.203643
7	0.14639746E+05	0.15019809E+05	0.89353919E+00	0.34399319E+00	0.20173120E+01	-0.17070454E+00	3.266845	-3.093791	3.180318
Y									
1	0.42463330E+03	0.12943435E+04	0.25917560E-01	0.27988112E+00	0.81283210E+00	-0.67949855E+00	2.811603	-2.520412	2.666007
2	0.57448389E+03	0.25166143E+04	0.35063714E-01	0.39036101E+00	0.11718130E+01	-0.93704277E+00	2.912045	-2.490275	2.701159
3	0.71810547E+03	0.39947637E+04	0.43829679E-01	0.49184823E+00	0.14728117E+01	-0.12602110E+01	2.905331	-2.651305	2.778318
4	0.73515405E+03	0.59817734E+04	0.44870242E-01	0.60258377E+00	0.17193947E+01	-0.16023540E+01	2.778907	-2.733601	2.756256
5	0.68004810E+03	0.73554961E+04	0.41506842E-01	0.66876626E+00	0.18226900E+01	-0.17886829E+01	2.663385	-2.736666	2.700027
6	0.56363501E+03	0.97399961E+04	0.34401551E-01	0.77028233E+00	0.19633045E+01	-0.20844812E+01	2.504149	-2.750786	2.627469
7	0.50673755E+03	0.11180965E+05	0.30928805E-01	0.82554036E+00	0.20961838E+01	-0.22572689E+01	2.501699	-2.771757	2.636729
T									
1	0.14169204E+02	0.53767391E-01	0.86481939E-03	0.15918359E-02	0.63266829E-02	-0.45894049E-02	3.431170	-3.426373	3.428773
2	0.17244705E+02	0.12049288E+00	0.10525333E-02	0.24993713E-02	0.88350847E-02	-0.62903836E-02	3.113802	-2.937904	3.025856
3	0.17240524E+02	0.21172351E+00	0.10522781E-02	0.34374422E-02	0.11431564E-01	-0.84625520E-02	3.019479	-2.767996	2.893738
4	0.32257141E+02	0.39109313E+00	0.19688196E-02	0.44716187E-02	0.16378440E-01	-0.10285214E-01	3.222462	-2.740401	2.981431
5	0.43223175E+02	0.58674055E+00	0.26381332E-02	0.53715743E-02	0.21224946E-01	-0.12059502E-01	3.460217	-2.736187	3.098202
6	0.54597672E+02	0.87918377E+00	0.33323774E-02	0.65237246E-02	0.27631588E-01	-0.14840838E-01	3.724744	-2.785711	3.255228
7	0.52165421E+02	0.10673866E+01	0.31839246E-02	0.74171461E-02	0.31245507E-01	-0.18282261E-01	3.783339	-2.894130	3.338735

RUN=108 POINT=11 VMODEL= 28.208 AIR DENSITY= 1.190

X									
1	0.46768477E+04	0.14966636E+04	0.28545213E+00	0.99331915E-01	0.60867220E+00	-0.76222241E-01	3.253940	-3.641068	3.447504
2	0.72175586E+04	0.35824045E+04	0.44052482E+00	0.15681851E+00	0.94075024E+00	-0.94975889E-01	3.189837	-3.414780	3.302306
3	0.91838633E+04	0.58114570E+04	0.56053853E+00	0.20125169E+00	0.12038412E+01	-0.92517972E-01	3.196507	-3.244973	3.220740
4	0.10698773E+05	0.79068828E+04	0.65300131E+00	0.23704559E+00	0.14217129E+01	-0.88911176E-01	3.242885	-3.129830	3.186357
5	0.11833848E+05	0.96856406E+04	0.72228074E+00	0.26358944E+00	0.15962191E+01	-0.13025939E+00	3.315528	-3.234348	3.274937
6	0.13151250E+05	0.11974863E+05	0.80268860E+00	0.29425156E+00	0.18199043E+01	-0.18856657E+00	3.456959	-3.368733	3.412846
7	0.13910246E+05	0.13407047E+05	0.84901404E+00	0.31222153E+00	0.19558945E+01	-0.22310245E+00	3.545176	-3.433830	3.489503
Y									
1	0.10187185E+04	0.61143408E-03	0.62177643E-01	0.18290699E+00	0.71458322E+00	-0.44674760E+00	3.566870	-2.702426	3.174646
2	0.18875308E+04	0.12311013E+04	0.11520571E+00	0.24874049E+00	0.96740210E+00	-0.68123209E+00	3.426045	-3.201881	3.313963
3	0.25985439E+04	0.19960017E+04	0.15860254E+00	0.31112605E+00	0.12471638E+01	-0.91258752E+00	3.498777	-3.442945	3.470861
4	0.31704556E+04	0.30027827E+04	0.19350922E+00	0.38188785E+00	0.15236101E+01	-0.11143761E+01	3.482960	-3.424788	3.453875
5	0.34146272E+04	0.36747744E+04	0.20841229E+00	0.42528307E+00	0.16685228E+01	-0.12279425E+01	3.433265	-3.377408	3.405337
6	0.37631E4.E+04	0.48473281E+04	0.22968531E+00	0.49306881E+00	0.18851757E+01	-0.14372578E+01	3.357523	-3.380750	3.369137
7	0.38706550E+04	0.55205859E+04	0.23624599E+00	0.53024030E+00	0.19850826E+01	-0.15858612E+01	3.298196	-3.436378	3.367290
T									
1	0.11600090E-02	0.25477719E-01	0.70801331E-03	0.10265564E-02	0.45965463E-02	-0.33779419E-02	3.787939	-3.980253	3.884095
2	0.13742243E-02	0.52808017E-01	0.83875982E-03	0.15873816E-02	0.61020255E-02	-0.49170405E-02	3.315689	-3.625969	3.470830
3	0.15295901E-02	0.93160450E-01	0.93358755E-03	0.21942584E-02	0.81726760E-02	-0.59042424E-02	3.299105	-3.116237	3.207672
4	0.26298899E-02	0.17834377E-00	0.16051668E-02	0.28825719E-02	0.11525884E-01	-0.65882802E-02	3.441623	-2.842404	3.142014
5	0.33140854E-02	0.26505601E+00	0.20227572E-02	0.34766251E-02	0.15018087E-01	-0.79454444E-02	3.737914	-2.867205	3.302562
6	0.38523590E-02	0.38230772E-00	0.23512933E-02	0.42306334E-02	0.19284874E-01	-0.10886606E-01	4.002610	-3.129530	3.566071
7	0.34798304E-02	0.44572753E-00	0.21239566E-02	0.47639497E-02	0.21896292E-01	-0.14014348E-01	4.150407	-3.387589	3.768998

RUN=129 POINT=11 VMODEL= 28.043 AIR DENSITY= 1.177

X									
1	0.46846562E+04	0.14424092E+04	0.28592873E+00	0.79264522E-01	0.54989278E+00	-0.72578371E-01	3.330166	-4.522920	3.926543
2	0.71047227E+04	0.33292954E+04	0.43363786E+00	0.12313914E+00	0.89514434E+00	-0.10086393E+00	3.747845	-4.340632	4.044239
3	0.89627695E+04	0.53045703E+04	0.54704404E+00	0.15655547E+00	0.11772118E+01	-0.12400872E+00	4.025204	-4.286357	4.155779
4	0.10409984E+05	0.71667891E+04	0.63537502E+00	0.18364847E+00	0.14033117E+01	-0.13020617E+00	4.181558	-4.168732	4.175144
5	0.11491559E+05	0.87429375E+04	0.70138907E+00	0.20416301E+00	0.15711851E+01	-0.12159550E+00	4.260302	-4.031016	4.145658
6	0.12763387E+05	0.10795789E+05	0.77901530E+00	0.22816885E+00	0.17658434E+01	-0.10599703E+00	4.324990	-3.878760	4.101873
7	0.13492664E+05	0.12075180E+05	0.82352686E+00	0.24252343E+00	0.18790140E+01	-0.11260676E+00	4.352101	-3.859971	4.106036
Y									
1	0.64416846E+03	0.32909180E+03	0.39316922E-01	0.13616711E+00	0.45777643E+00	-0.46484619E+00	3.073132	-3.702532	3.387832
2	0.14104622E+04	0.67097119E+03	0.86087763E-01	0.18314958E+00	0.63338077E+00	-0.55126500E+00	2.988229	-3.479958	3.234093
3	0.20984897E+04	0.11183792E+04	0.12808162E+00	0.22772503E+00	0.80392295E+00	-0.60562313E+00	2.967795	-3.221889	3.094841
4	0.26254304E+04	0.16904980E+04	0.16024351E+00	0.27839988E+00	0.97982550E+00	-0.68720549E+00	2.943902	-3.043999	2.993949
5	0.28335813E+04	0.20600459E+04	0.17294806E+00	0.30956417E+00	0.10957546E+01	-0.79041493E+00	2.980986	-3.111998	3.046492
6	0.30966287E+04	0.26986553E+04	0.18900317E+00	0.35916358E+00	0.12796421E+01	-0.95576882E+00	3.036605	-3.187325	3.111967
7	0.31967024E+04	0.30719687E+04	0.19511122E+00	0.38657314E+00	0.13718863E+01	-0.10562344E+01	3.044120	-3.237019	3.140571
T									
1	0.93545687E+00	0.71613528E-02	0.57095749E-04	0.65868115E-03	0.26163813E-02	-0.25089313E-02	3.885468	-3.895704	3.890585
2	-0.25538015E+01	0.17036576E-01	-0.15587168E-03	0.10077676E-02	0.34870778E-02	-0.36966957E-02	3.614870	-3.513532	3.564200
3	-0.46717811E+00	0.32105867E-01	-0.28514289E-04	0.13996044E-02	0.46499521E-02	-0.44512898E-02	3.342705	-3.160016	3.251362
4	0.53145838E+01	0.58420658E-01	0.32437639E-03	0.18602968E-02	0.63882470E-02	-0.55679642E-02	3.259624	-3.167418	3.213522
5	0.86315489E+01	0.88454008E-01	0.52682776E-03	0.22630887E-02	0.81786253E-02	-0.66154487E-02	3.381129	-3.155986	3.268559
6	0.10779358E+02	0.13433093E+00	0.65791979E-03	0.27868485E-02	0.10436047E-01	-0.82325041E-02	3.508668	-3.190135	3.349403
7	0.44717445E+01	0.16352963E+00	0.27293363E-03	0.31475653E-02	0.11557650E-01	-0.98817796E-02	3.585219	-3.226212	3.405716

RUN=118 POINT=11 VMODEL= 28.153 AIR DENSITY= 1.156

X									
1	0.47014922E+04	0.14094514E+04	0.28695631E+00	0.60683068E-01	0.45074618E+00	0.74782789E-01	2.699102	-3.496420	3.097763
2	0.70856680E+04	0.32095613E+04	0.43247485E+00	0.94138920E-01	0.68177426E+00	0.13320225E+00	2.648207	-3.179052	2.913630
3	0.89180195E+04	0.50869844E+04	0.54431272E+00	0.11920315E+00	0.87711293E+00	0.16613168E+00	2.791874	-3.172575	2.982224
4	0.10347684E+05	0.68535469E+04	0.63157248E+00	0.13937265E+00	0.10393801E+01	0.19141632E+00	2.926023	-3.158124	3.042073
5	0.11426305E+05	0.83617305E+04	0.69740629E+00	0.15487236E+00	0.11555872E+01	0.21764934E+00	2.958442	-3.097756	3.028099
6	0.12704262E+05	0.10344031E+05	0.77540660E+00	0.17348212E+00	0.12966747E+01	0.25599921E+00	3.004737	-2.994011	2.999372
7	0.13419328E+05	0.11550812E+05	0.81905079E+00	0.18483394E+00	0.13991499E+01	0.26947230E+00	3.138488	-2.973363	3.055923
Y									
1	-0.83196069E+03	0.25541315E+03	-0.50778851E-01	0.11406785E+00	0.28798324E+00	-0.39321023E+00	2.969829	-3.001997	2.985913
2	-0.84088818E+03	0.45098096E+03	-0.51323742E-01	0.15777540E+00	0.38232380E+00	-0.51123267E+00	2.748511	-2.914959	2.831736
3	-0.75881470E+03	0.68261450E+03	-0.46314374E-01	0.19879860E+00	0.51555985E+00	-0.59443337E+00	2.826348	-2.757156	2.791752
4	-0.77323657E+03	0.99871460E+03	-0.47194615E-01	0.24234879E+00	0.66142207E+00	-0.73334616E+00	2.923953	-2.831256	2.877604
5	-0.83036060E+03	0.12156208E+04	-0.50681189E-01	0.26764029E+00	0.74549049E+00	-0.82520020E+00	2.974782	-2.893880	2.934330
6	-0.87372168E+03	0.15878647E+04	-0.53327739E-01	0.30672044E+00	0.86395204E+00	-0.96161711E+00	2.990605	-2.961293	2.975949
7	-0.94033130E+03	0.18169277E+04	-0.57393268E-01	0.32803810E+00	0.91243434E+00	-0.10258818E+01	2.956448	-2.952366	2.954406
T									
1	-0.42851629E+01	0.62220059E-02	-0.26154541E-03	0.55800891E-03	0.17252970E-02	-0.25127293E-02	3.560592	-4.034315	3.797452
2	-0.95850401E+01	0.17486691E-01	-0.58502425E-03	0.85152406E-03	0.25941140E-02	-0.39231405E-02	3.733468	-3.920166	3.826817
3	-0.13758722E+02	0.33353891E-01	-0.83976565E-03	0.11535308E-02	0.37849538E-02	-0.50317794E-02	4.009183	-3.634071	3.821628
4	-0.94507074E+01	0.43627176E-01	-0.57682535E-03	0.15265008E-02	0.54331981E-02	-0.57745576E-02	3.937123	-3.404996	3.671061
5	-0.72940168E+01	0.59674516E-01	-0.44519128E-03	0.18558709E-02	0.67181997E-02	-0.65011121E-02	3.859854	-3.263113	3.561484
6	-0.64670563E+01	0.88139772E-01	-0.39471779E-03	0.22856381E-02	0.84351860E-02	-0.77833980E-02	3.863211	-3.232654	3.547935
7	-0.13266895E+02	0.12022084E+00	-0.80974703E-03	0.25850367E-02	0.94967186E-02	-0.93778670E-02	3.986969	-3.314506	3.650738

RUN=116 POINT=11 VMODEL= 28.165 AIR DENSITY= 1.161

X									
1	0.47403672E+04	0.14563354E+04	0.28932905E+00	0.71949422E-01	0.49230421E+00	0.22536449E-01	2.821080	-3.708057	3.264569
2	0.71213047E+04	0.32986174E+04	0.43464994E+00	0.11140841E+00	0.75390488E+00	0.61212704E-01	2.865626	-3.351966	3.108796
3	0.89355625E+04	0.52039766E+04	0.54538345E+00	0.14206928E+00	0.96206582E+00	0.90916932E-01	2.932951	-3.198907	3.065929
4	0.10319426E+05	0.69565039E+04	0.62984776E+00	0.16698736E+00	0.11266069E+01	0.11218971E+00	2.974831	-3.099983	3.037405
5	0.11363633E+05	0.84477070E+04	0.69358110E+00	0.18588853E+00	0.12845049E+01	0.12020481E+00	3.178914	-3.084517	3.131715
6	0.12612406E+05	0.10422332E+05	0.76980019E+00	0.20866013E+00	0.14777212E+01	0.13048446E+00	3.392698	-3.063909	3.228304
7	0.13302234E+05	0.11611168E+05	0.81190395E+00	0.22249597E+00	0.15898190E+01	0.13251132E+00	3.496310	-3.053505	3.274905
Y									
1	-0.20344592E+04	0.42781763E+03	-0.12417352E+00	0.10340941E+00	0.37037516E+00	-0.51628679E+00	4.782434	-3.791852	4.287143
2	-0.27160110E+04	0.79439478E+03	-0.16577214E+00	0.14493752E+00	0.47799778E+00	-0.78751761E+00	4.441706	-4.289748	4.365726
3	-0.32146541E+04	0.11885937E+04	-0.19620687E+00	0.18452889E+00	0.59004396E+00	-0.10523462E+01	4.260855	-4.639595	4.450222
4	-0.37875166E+04	0.17216577E+04	-0.23117167E+00	0.22725415E+00	0.66695505E+00	-0.13148546E+01	3.952080	-4.768590	4.360337
5	-0.41406328E+04	0.20908386E+04	-0.25272417E+00	0.25248581E+00	0.69080025E+00	-0.14584970E+01	3.736939	-4.775604	4.256272
6	-0.45936055E+04	0.26765286E+04	-0.28037143E+00	0.29113472E+00	0.69948453E+00	-0.17775469E+01	3.365644	-5.142550	4.254097
7	-0.48485195E+04	0.30308005E+04	-0.29593015E+00	0.31211656E+00	0.71730721E+00	-0.19615726E+01	3.246341	-5.336601	4.291472
T									
1	-0.61254959E+01	0.76394007E-02	-0.37387060E-03	0.57141297E-03	0.17704999E-02	-0.22839073E-02	3.752750	-3.342655	3.547701
2	-0.11353297E+02	0.20407189E-01	-0.69295010E-03	0.87488396E-03	0.25863869E-02	-0.37541827E-02	3.748310	-3.499015	3.623661
3	-0.15861786E+02	0.38485136E-01	-0.96812658E-03	0.11881760E-02	0.35009261E-02	-0.51889047E-02	3.761271	-3.552316	3.656793
4	-0.11438622E+02	0.48656873E-01	-0.69815805E-03	0.15755969E-02	0.52439459E-02	-0.64498708E-02	3.771334	-3.650496	3.710916
5	-0.94206610E+01	0.65508723E-01	-0.57499134E-03	0.19151876E-02	0.64921044E-02	-0.76368228E-02	3.690027	-3.687277	3.688653
6	-0.90569324E+01	0.95800817E-01	-0.55279117E-03	0.23541404E-02	0.81433244E-02	-0.92763975E-02	3.693965	-3.705644	3.699806
7	-0.15804296E+02	0.13085598E+00	-0.96461759E-03	0.26564561E-02	0.83039179E-02	-0.10614280E-01	3.489059	-3.632531	3.560796

RUN=127 POINT= 3 VMODEL= 28.094 AIR DENSITY= 1.187

X									
1	0.50189844E+04	0.16749082E+04	0.30633450E+00	0.91585934E-01	0.55581445E+00	0.11211068E-02	2.723998	-3.332535	3.028267
2	0.75418359E+04	0.38042031E+04	0.46031713E+00	0.14247650E+00	0.86518562E+00	-0.27311966E-02	2.841651	-3.249997	3.045824
3	0.94603789E+04	0.60055430E+04	0.57741570E+00	0.18205053E+00	0.11104946E+01	0.22941935E-02	2.928191	-3.159130	3.043660
4	0.10911727E+05	0.80237695E+04	0.66599894E+00	0.21489590E+00	0.12989254E+01	0.17341249E-01	2.945270	-3.018474	2.981871
5	0.11992609E+05	0.97188281E+04	0.73197079E+00	0.23960906E+00	0.14422722E+01	0.35041902E-01	2.964417	-2.908607	2.936511
6	0.13279504E+05	0.11898789E+05	0.80868554E+00	0.26884305E+00	0.16340313E+01	0.44901140E-01	3.069990	-2.841004	2.955496
7	0.13947031E+05	0.13214367E+05	0.85125923E+00	0.28618813E+00	0.17627840E+01	0.32351945E-01	3.185054	-2.861429	3.023241
Y									
1	-0.30142261E+04	0.69694604E+03	-0.18397373E+00	0.93233049E-01	0.93323231E-01	-0.50646234E+00	2.974235	-3.458951	3.216593
2	-0.42355039E+04	0.13640911E+04	-0.25851464E+00	0.12817454E+00	0.14900464E+00	-0.70559019E+00	3.179408	-3.488021	3.333714
3	-0.52075586E+04	0.20863857E+04	-0.31784415E+00	0.16223323E+00	0.23358607E+00	-0.87003762E+00	3.398996	-3.403701	3.401347
4	-0.62633047E+04	0.30397170E+04	-0.38228178E+00	0.19847596E+00	0.31219870E+00	-0.10318947E+01	3.499065	-3.273005	3.386035
5	-0.68873789E+04	0.36861770E+04	-0.42037225E+00	0.21971923E+00	0.34707969E+00	-0.11639376E+01	3.492875	-3.384161	3.438517
6	-0.77455312E+04	0.47043750E+04	-0.47274971E+00	0.25227749E+00	0.39564228E+00	-0.13683529E+01	3.442209	-3.550071	3.496140
7	-0.81784375E+04	0.52792930E+04	-0.49917221E+00	0.27028507E+00	0.41639000E+00	-0.14745359E+01	3.387394	-3.608647	3.498020
T									
1	-0.63571672E+01	0.89910291E-02	-0.51008095E-03	0.53721876E-03	0.14696165E-02	-0.24356772E-02	3.685086	-3.584380	3.634733
2	-0.13828250E+02	0.22688370E-01	-0.84400922E-03	0.82004676E-03	0.21739439E-02	-0.35318183E-02	3.680221	-3.277629	3.478923
3	-0.14826712E+02	0.34105487E-01	-0.90507278E-03	0.11236339E-02	0.35469660E-02	-0.47353841E-02	3.962178	-3.408860	3.685518
4	-0.90165987E+01	0.42201363E-01	-0.55032945E-03	0.15076611E-02	0.54857098E-02	-0.53144395E-02	4.003575	-3.159934	3.581756
5	-0.62240334E+01	0.58735270E-01	-0.37988485E-03	0.18549429E-02	0.70290715E-02	-0.62310286E-02	3.994168	-3.154351	3.574261
6	-0.53977203E+01	0.88549604E-01	-0.32945070E-03	0.23053710E-02	0.88157579E-02	-0.76098666E-02	3.966913	-3.158022	3.562470
7	-0.12205026E+02	0.11931837E-00	-0.74493559E-03	0.25938572E-02	0.96733309E-02	-0.92094317E-02	4.016515	-3.263284	3.639901

RUN=120 POINT=11 VMODEL= 28.064 AIR DENSITY= 1.152

X									
1	0.48992617E+04	0.15557705E+04	0.29902720E+00	0.74430048E-01	0.60273778E+00	0.46756655E-01	4.080482	-3.389363	3.734923
2	0.73327656E+04	0.35016946E+04	0.44755650E+00	0.11584699E+00	0.88348585E+00	0.79530299E-01	3.762975	-3.176829	3.469902
3	0.91843594E+04	0.55066328E+04	0.56056881E+00	0.14785874E+00	0.11022024E+01	0.72668374E-01	3.663182	-3.299773	3.481476
4	0.10601852E+05	0.73578867E+04	0.64708567E+00	0.17427504E+00	0.12710829E+01	0.58613729E-01	3.580531	-3.376684	3.478607
5	0.11658113E+05	0.89148828E+04	0.71155477E+00	0.19445676E+00	0.13931017E+01	0.48562065E-01	3.504876	-3.409460	3.457169
6	0.12904082E+05	0.10946457E+05	0.78760266E+00	0.21864057E+00	0.15381927E+01	0.38437672E-01	3.432986	-3.426468	3.429727
7	0.13574945E+05	0.12135559E+05	0.82854891E+00	0.23282123E+00	0.16197309E+01	0.59767440E-03	3.398238	-3.556167	3.477201
Y									
1	-0.35315073E+04	0.87917700E+03	-0.21554607E+00	0.84858894E-01	0.71357965E-01	-0.47650898E+00	3.380954	-3.075256	3.228106
2	-0.50876445E+04	0.18258997E+04	-0.31052518E+00	0.12255275E+00	0.65108001E-01	-0.73527384E+00	3.065073	-3.465843	3.265458
3	-0.63359180E+04	0.28578083E+04	-0.38671374E+00	0.15773636E+00	0.87339640E-01	-0.97390366E+00	3.005352	-3.722603	3.363976
4	-0.76353359E+04	0.41762891E+04	-0.46602392E+00	0.19422793E+00	0.12345004E+00	-0.12416334E+01	3.034959	-3.993295	3.514125
5	-0.83766211E+04	0.50357266E+04	-0.51126838E+00	0.21439177E+00	0.13893473E+00	-0.13995380E+01	3.032780	-4.143708	3.587992
6	-0.93869336E+04	0.63607695E+04	-0.57293296E+00	0.24491233E+00	0.16051465E+00	-0.16422501E+01	2.994735	-4.366120	3.680427
7	-0.93986211E+04	0.70969570E+04	-0.60416389E+00	0.26106340E+00	0.17806363E+00	-0.17862577E+01	2.996312	-4.527994	3.762153
T									
1	-0.86163940E+01	0.96526481E-02	-0.52590296E-03	0.55910298E-03	0.16238929E-02	-0.30146446E-02	3.845079	-4.451311	4.148192
2	-0.12408967E+02	0.21716204E-01	-0.75738318E-03	0.86710323E-03	0.24809747E-02	-0.42520091E-02	3.734685	-4.030231	3.882457
3	-0.12169804E+02	0.31432722E-01	-0.74278587E-03	0.11691251E-02	0.33837548E-02	-0.51431209E-02	3.629594	-3.763782	3.646689
4	-0.49463940E+01	0.40066879E-01	-0.30190381E-03	0.15344329E-02	0.47875866E-02	-0.56471489E-02	3.316853	-3.483530	3.400192
5	-0.11515455E+01	0.56337081E-01	-0.70284761E-04	0.18530546E-02	0.59720874E-02	-0.64497851E-02	3.260760	-3.442694	3.351728
6	0.68473017E+00	0.83204269E-01	0.41792606E-04	0.22532083E-02	0.76759346E-02	-0.78967698E-02	3.388120	-3.523225	3.455673
7	-0.45528164E+01	0.10559207E+00	-0.27788174E-03	0.25234893E-02	0.85355453E-02	-0.93671083E-02	3.492555	-3.601848	3.547202

RUN=131 POINT=11 VMODEL= 28.031 AIR DENSITY= 1.170

X									
1	0.49498672E+04	0.16149221E+04	0.30211592E+00	0.85401773E-01	0.58080226E+00	-0.35704415E-01	3.263238	-3.955659	3.609448
2	0.73952578E+04	0.36293396E+04	0.45137072E+00	0.13335264E+00	0.90373409E+00	-0.58372952E-01	3.392234	-3.822523	3.607379
3	0.92697852E+04	0.57236328E+04	0.56578279E+00	0.17098093E+00	0.11713238E+01	-0.87932944E-01	3.541570	-3.823325	3.682446
4	0.10706094E+05	0.76653437E+04	0.65344810E+00	0.20214742E+00	0.13756247E+01	-0.11559743E+00	3.572524	-3.804379	3.688450
5	0.11781762E+05	0.93077383E+04	0.71910167E+00	0.22582108E+00	0.15176029E+01	-0.13385892E+00	3.535991	-3.777152	3.656570
6	0.13067367E+05	0.11478090E+05	0.79756880E+00	0.25387985E+00	0.16860285E+01	-0.15913224E+00	3.499528	-3.768322	3.633924
7	0.13767660E+05	0.12767328E+05	0.84031129E+00	0.27043903E+00	0.17744751E+01	-0.17963666E+00	3.454248	-3.771449	3.612849
Y									
1	-0.43615859E+04	0.12701123E+04	-0.26621008E+00	0.81572950E-01	0.38855847E-01	-0.51952720E+00	3.739792	-3.105406	3.422599
2	-0.63221016E+04	0.26640283E+04	-0.38587046E+00	0.11706513E+00	0.56562517E-01	-0.79313427E+00	3.779374	-3.478951	3.629162
3	-0.78860742E+04	0.41633047E+04	-0.48132777E+00	0.14977622E+00	0.57518762E-01	-0.10660696E+01	3.597676	-3.904102	3.750887
4	-0.94691836E+04	0.60165078E+04	-0.57795310E+00	0.18218338E+00	0.17319135E-01	-0.13264303E+01	3.267433	-4.108372	3.687901
5	-0.10351086E+05	0.72012969E+04	-0.63178015E+00	0.20096928E+00	-0.26311185E-01	-0.14646187E+01	3.012743	-4.144108	3.578424
6	-0.11561477E+05	0.90252891E+04	-0.70565653E+00	0.23002636E+00	-0.69650531E-01	-0.16637535E+01	2.764926	-4.165161	3.465043
7	-0.12140512E+05	0.99832031E+04	-0.74099803E+00	0.24546272E+00	-0.46277739E-01	-0.17904730E+01	2.830247	-4.275495	3.552871
T									
1	-0.99918146E+01	0.10305304E-01	-0.60985191E-03	0.50703273E-03	0.12045375E-02	-0.26576244E-02	3.578445	-4.038738	3.808592
2	-0.12329473E+02	0.18855248E-01	-0.75253122E-03	0.76456834E-03	0.21837666E-02	-0.37244316E-02	3.840465	-3.887030	3.863745
3	-0.13479814E+02	0.28220538E-01	-0.82274247E-03	0.10225470E-02	0.31815816E-02	-0.48294254E-02	3.916027	-3.918333	3.917182
4	-0.43676996E+01	0.32020502E-01	-0.26658317E-03	0.13723788E-02	0.52371100E-02	-0.59266500E-02	4.010329	-4.124272	4.067303
5	0.87423253E+00	0.46707395E-01	0.53358919E-04	0.16876371E-02	0.65748133E-02	-0.69161206E-02	3.864250	-4.129725	3.996988
6	0.43112898E+01	0.72610855E-01	0.26314007E-03	0.20887407E-02	0.82859360E-02	-0.82296431E-02	3.840971	-4.065982	3.953478
7	0.24906349E+00	0.89581132E-01	0.15201629E-04	0.23383112E-02	0.90489089E-02	-0.96845217E-02	3.863346	-4.148173	4.005761

RUN=133 POINT=11 VMODEL= 27.997 AIR DENSITY= 1.163

X									
1	0.47783555E+04	0.14886963E+04	0.29164767E-00	0.76189458E-01	0.66987997E+00	-0.64831138E-01	4.964365	-4.678846	4.821606
2	0.70872344E+04	0.32916362E+04	0.43257046E+00	0.11742759E+00	0.10091782E+01	-0.76836765E-01	4.910325	-4.338054	4.624188
3	0.88682734E+04	0.51672930E+04	0.54127645E+00	0.14969188E+00	0.12906027E+01	-0.10055339E+00	5.005791	-4.287673	4.646729
4	0.10240012E+05	0.69098867E+04	0.62500072E+00	0.17641419E+00	0.15257797E+01	-0.12823653E+00	5.106046	-4.269709	4.687875
5	0.11278556E+05	0.84002187E+04	0.68839455E+00	0.19703811E+00	0.17057505E+01	-0.14113802E+00	5.163244	-4.210011	4.686625
6	0.12527109E+05	0.10383652E+05	0.76459408E+00	0.22173589E+00	0.19077368E+01	-0.14880824E+00	5.155424	-4.119325	4.637373
7	0.13221547E+05	0.11584660E+05	0.80697918E+00	0.23634642E+00	0.20214949E+01	-0.15300846E+00	5.138709	-4.061782	4.600245
Y									
1	-0.48318359E+04	0.15302593E+04	-0.29491186E+00	0.80168903E-01	0.41730184E-01	-0.60813564E+00	4.199160	-3.907048	4.053103
2	-0.70110781E+04	0.32199590E+04	-0.42792225E+00	0.11581922E+00	0.26384905E-01	-0.88827533E+00	3.922554	-3.974755	3.948654
3	-0.87287695E+04	0.50074375E+04	-0.53276181E+00	0.14763445E+00	0.12393400E-01	-0.11652040E+01	3.692601	-4.283839	3.988218
4	-0.10443664E+05	0.71913437E+04	-0.63743067E+00	0.18057942E+00	-0.24637505E-02	-0.14571495E+01	3.516274	-4.539381	4.027826
5	-0.11386668E+05	0.85655234E+04	-0.69498706E+00	0.19948322E+00	0.59199706E-02	-0.16190977E+01	3.513614	-4.632523	4.073067
6	-0.12663160E+05	0.10642004E+05	-0.77289796E+00	0.22840399E+00	0.66185176E-01	-0.18585224E+01	3.673679	-4.753085	4.213384
7	-0.13250148E+05	0.11688992E+05	-0.80872488E+00	0.24373585E+00	0.12461871E+00	-0.19728823E+01	3.829324	-4.776305	4.302815
T									
1	-0.10391746E+02	0.10747507E-01	-0.63426164E-03	0.50368975E-03	0.10951466E-02	-0.25513549E-02	3.433478	-3.806099	3.619789
2	-0.11430944E+02	0.17315596E-01	-0.69768936E-03	0.75506535E-03	0.17041208E-02	-0.34012208E-02	3.180930	-3.580526	3.380726
3	-0.81001635E+01	0.20504061E-01	-0.49439468E-03	0.10035455E-02	0.26321274E-02	-0.40125549E-02	3.115476	-3.505731	3.310602
4	0.21076756E+01	0.28960355E-01	0.12864231E-03	0.13233130E-02	0.46981424E-02	-0.47394894E-02	3.453073	-3.678744	3.565910
5	0.82775135E+01	0.46785850E-01	0.50521921E-03	0.16126044E-02	0.63134544E-02	-0.58693364E-02	3.601772	-3.952954	3.777365
6	0.12846409E+02	0.74350893E-01	0.78408257E-03	0.19807755E-02	0.82357898E-02	-0.76462403E-02	3.762013	-4.256070	4.009046
7	0.95193644E+01	0.86166799E-01	0.58101583E-03	0.22185408E-02	0.91718063E-02	-0.90801008E-02	3.872269	-4.354716	4.113493

RUN=114 POINT=14 VMODEL= 28.210 AIR DENSITY= 1.167

X									
1	0.45920117E+04	0.14406299E+04	0.28027415E+00	0.96830308E-01	0.64753604E+00	-0.13522947E+00	3.792840	-4.291049	4.041945
2	0.67973437E+04	0.31936316E+04	0.41487694E+00	0.15100449E+00	0.92774737E+00	-0.18493128E+00	3.396391	-3.972121	3.684256
3	0.85060039E+04	0.50352734E+04	0.51916528E+00	0.19441813E+00	0.12258711E+01	-0.21776402E+00	3.634978	-3.790435	3.712707
4	0.98279570E+04	0.67588437E+04	0.59985089E+00	0.22958487E+00	0.14678621E+01	-0.23756915E+00	3.780786	-3.647540	3.714162
5	0.10842156E+05	0.82497656E+04	0.66175270E+00	0.25615054E+00	0.16462240E+01	-0.24304414E+00	3.843330	-3.532285	3.687807
6	0.12060277E+05	0.10232027E+05	0.73610091E+00	0.28753072E+00	0.18439837E+01	-0.24355805E+00	3.853092	-3.407145	3.630118
7	0.12751629E+05	0.11454969E+05	0.77829766E+00	0.30563742E+00	0.19491968E+01	-0.28254443E+00	3.831004	-3.470915	3.650961
Y									
1	-0.54260352E+04	0.19657825E+04	-0.33117890E+00	0.10150379E+00	0.57255179E-01	-0.68490237E+00	3.826793	-3.484830	3.655811
2	-0.79029336E+04	0.41860977E+04	-0.48235679E+00	0.15110409E+00	0.66731453E-01	-0.10732841E+01	3.633841	-3.910729	3.772285
3	-0.98715820E+04	0.65647070E+04	-0.60251355E+00	0.19405586E+00	0.73976159E-01	-0.14096479E+01	3.486056	-4.159288	3.822671
4	-0.11808125E+05	0.94348086E+04	-0.72071075E+00	0.23755950E+00	0.72287560E-01	-0.17218647E+01	3.338103	-4.214329	3.776217
5	-0.12858363E+05	0.11210402E+05	-0.78481221E+00	0.26134771E+00	0.70807934E-01	-0.18832712E+01	3.273876	-4.203053	3.738464
6	-0.14274012E+05	0.13869852E+05	-0.87121654E+00	0.29586416E+00	0.85568309E-01	-0.20927067E+01	3.233865	-4.128550	3.681206
7	-0.14920199E+05	0.15198316E+05	-0.91065669E+00	0.31359529E+00	0.99973679E-01	-0.21950588E+01	3.222719	-4.095730	3.659226
T									
1	-0.86712179E+01	0.10308966E-01	-0.52924897E-03	0.59086899E-03	0.15027791E-02	-0.32836397E-02	3.439050	-4.661592	4.050320
2	-0.76075420E+01	0.15320294E-01	-0.46432740E-03	0.84824557E-03	0.24631734E-02	-0.41151978E-02	3.451241	-4.304025	3.877633
3	-0.58412180E+01	0.21640494E-01	-0.35651959E-03	0.10926099E-02	0.33827061E-02	-0.48041269E-02	3.422287	-4.070624	3.746456
4	0.60267134E+01	0.35491958E-01	0.36784122E-03	0.14251573E-02	0.54534338E-02	-0.59427209E-02	3.568441	-4.427974	3.998209
5	0.13482596E+02	0.60038327E-01	0.82291220E-03	0.17389851E-02	0.72541423E-02	-0.72298124E-02	3.698266	-4.630701	4.164485
6	0.19468903E+02	0.98336816E-01	0.11882875E-02	0.21424883E-02	0.94198808E-02	-0.90288222E-02	3.842071	-4.768805	4.305440
7	0.18172806E+02	0.11290902E+00	0.11091800E-02	0.23793876E-02	0.10167591E-01	-0.99781975E-02	3.807033	-4.659760	4.233397

RUN=137 POINT= 6 VMODEL= 20.652 AIR DENSITY= 1.158

X									
1	-0.27345657E+02	0.19499971E+03	-0.16690465E-02	0.10908610E+00	0.33863890E+00	-0.34788221E+00	3.119626	-3.173760	3.146693
2	-0.71603653E+02	0.45804541E+03	-0.43703392E-02	0.16715103E+00	0.47733402E+00	-0.54580206E+00	2.881850	-3.239176	3.060511
3	-0.11688287E+03	0.74820557E+03	-0.71339644E-02	0.21358544E+00	0.60943216E+00	-0.71193260E+00	2.886742	-3.299844	3.093292
4	-0.16093604E+03	0.10289536E+04	-0.98227561E-02	0.25041890E+00	0.71210271E+00	-0.84067327E+00	2.882871	-3.317842	3.100355
5	-0.14176949E+03	0.12618052E+04	-0.86529218E-02	0.27738822E+00	0.78841567E+00	-0.93043596E+00	2.873476	-3.323079	3.098276
6	-0.24347458E+02	0.15604927E+04	-0.14860509E-02	0.30862361E+00	0.87734985E+00	-0.10302744E+01	2.847597	-3.333469	3.090534
7	0.46066772E+02	0.17441372E+04	0.28116927E-02	0.32627016E+00	0.92462438E+00	-0.10820560E+01	2.825304	-3.325058	3.075180
Y									
1	-0.31289834E+04	0.66919067E+03	-0.19097799E+00	0.66119850E-01	0.17183803E-01	-0.39485627E+00	3.148249	-3.083466	3.115857
2	-0.46342070E+04	0.14700322E+04	-0.28284955E+00	0.98592043E-01	0.20239808E-01	-0.58221066E+00	3.074176	-3.036362	3.055268
3	-0.58555078E+04	0.23571743E+04	-0.35739183E+00	0.12705356E+00	0.24151389E-01	-0.74571514E+00	3.003011	-3.056375	3.029693
4	-0.70269375E+04	0.33971619E+04	-0.42889023E+00	0.15297371E+00	0.36357835E-01	-0.88605565E+00	3.041359	-2.988523	3.014940
5	-0.76462187E+04	0.40208066E+04	-0.46668816E+00	0.16617584E+00	0.37726913E-01	-0.95519859E+00	3.035429	-2.939719	2.987575
6	-0.85320586E+04	0.49988828E+04	-0.52075553E+00	0.18418300E+00	0.34699537E-01	-0.10662050E+01	3.015778	-2.961453	2.988615
7	-0.89705352E+04	0.55246211E+04	-0.54751801E+00	0.19344890E+00	0.29303908E-01	-0.11172457E+01	2.981779	-2.945107	2.963442
T									
1	-0.25442638E+01	0.26634207E-02	-0.15528954E-03	0.37209666E-03	0.13411453E-02	-0.14870807E-02	4.021628	-3.579153	3.800391
2	-0.37387924E+01	0.57648197E-02	-0.22819778E-03	0.54754061E-03	0.18391376E-02	-0.21990077E-02	3.775675	-3.599385	3.687529
3	-0.32473501E+01	0.97951777E-02	-0.23482362E-03	0.73670968E-03	0.27113492E-02	-0.28398414E-02	3.999095	-3.536016	3.767555
4	-0.33641214E+01	0.20220853E-01	-0.20532968E-03	0.10918309E-02	0.38927167E-02	-0.42667910E-02	3.753367	-3.719862	3.736616
5	-0.36697102E+01	0.31766899E-01	-0.22398133E-03	0.13743523E-02	0.47943257E-02	-0.52885376E-02	3.651396	-3.685048	3.668223
6	-0.49303284E+01	0.48462294E-01	-0.30092336E-03	0.16933763E-02	0.58794990E-02	-0.62639415E-02	3.649761	-3.521377	3.585570
7	-0.61363277E+01	0.55712476E-01	-0.37453161E-03	0.18056422E-02	0.63450448E-02	-0.66040307E-02	3.721432	-3.450017	3.585726

Table 5.3 Predicted vs Measured Response in X-direction

U_H (m/s)	20	40	60	80
U_r	3.33	6.67	10.0	13.3

Calculated Values:

$\bar{X}/H$ (10^{-3})	0.21	0.84	1.88	3.34
σ_x'/H (10^{-3})	0.04	0.28	0.86	1.78
g_p	3.4	3.5	3.6	3.6
$\hat{X}/H$ (10^{-3})	0.34	2.82	4.98	9.76
C_g	1.62	2.18	2.65	2.92

Measured Values:

$\bar{X}/H$ (10^{-3})	0.19	0.74	1.67	2.96
σ_x'/H (10^{-3})	0.03	0.21	0.48	0.83
g_p	2.6	2.0	2.3	3.1
$\hat{X}/H$ (10^{-3})	0.28	1.17	2.77	5.52
C_g	1.50	1.58	1.66	1.86

Table 5.4 Predicted vs Measured Response in Y-direction

U_H (m/s)	20	40	60	80
U_r	3.03	6.06	9.09	12.1

Calculated Values:

$\bar{Y}/H$ (10^{-3})	0.17	0.67	1.52	2.71
σ_y/H (10^{-3})	0.03	0.28	0.65	1.38
g_p	3.5	3.5	3.6	3.6
$\hat{Y}/H$ (10^{-3})	0.27	1.45	3.82	7.66
C_g	1.59	2.16	2.51	2.83

Measured Values:

$\bar{Y}/H$ (10^{-3})	0.17	0.66	1.49	2.77
σ_y/H (10^{-3})	0.02	0.14	0.41	0.95
g_p	3.1	4.0	3.3	2.6
$\hat{Y}/H$ (10^{-3})	0.23	1.21	2.83	5.20
C_g	1.35	1.83	1.90	1.88

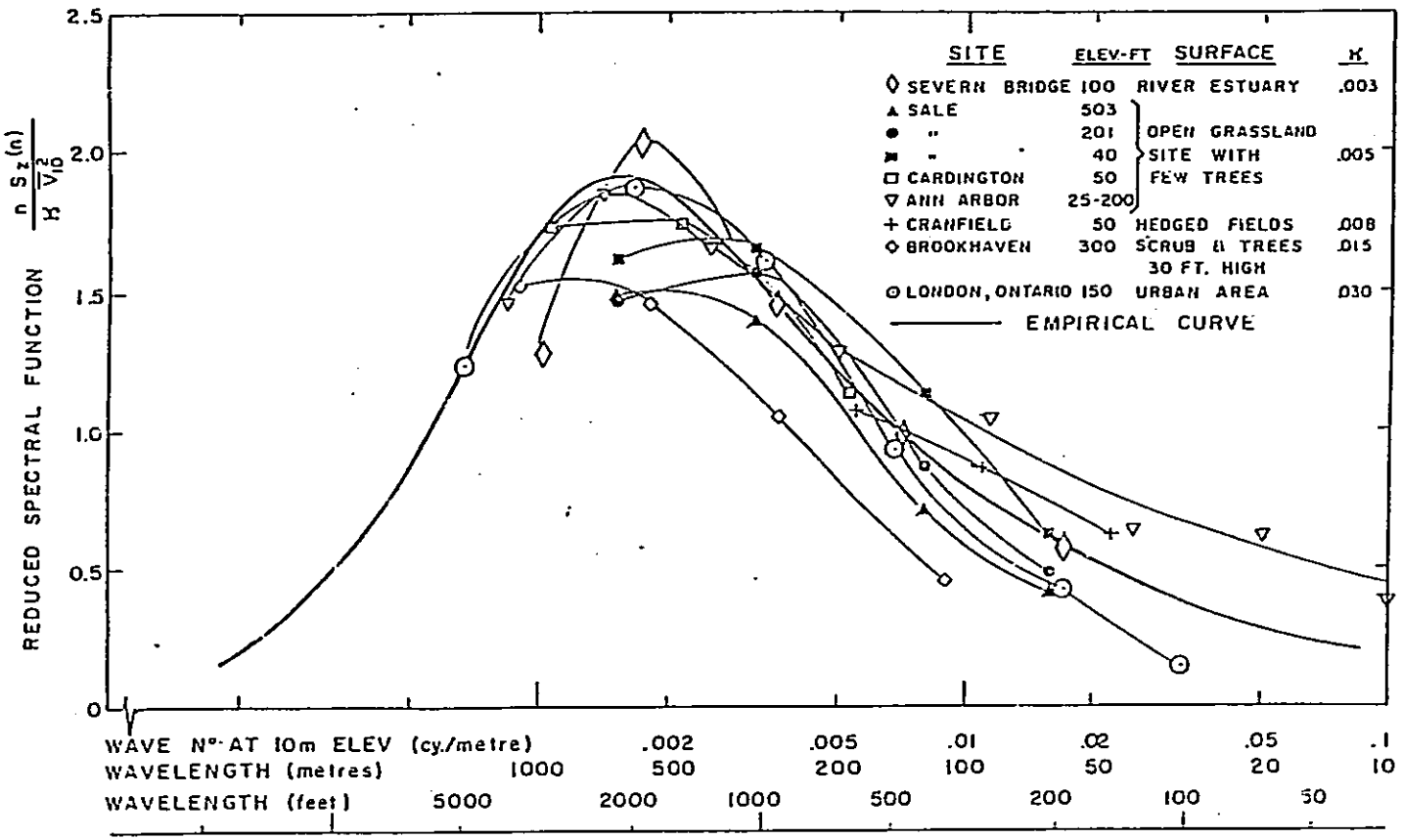

Fig.3.1 Spectra of Along-Wind Velocity Component

(from [3.1])

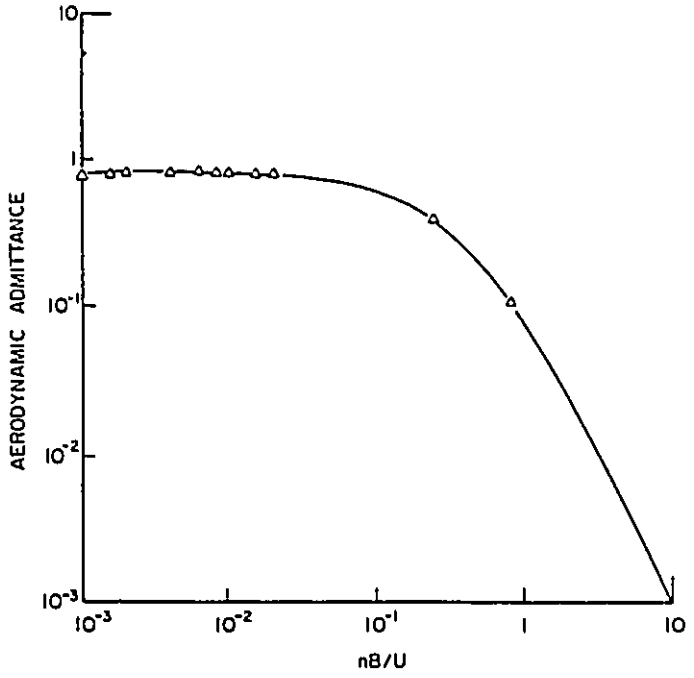

Fig.3.2 Aerodynamic Admittance Function

(from [3.5])

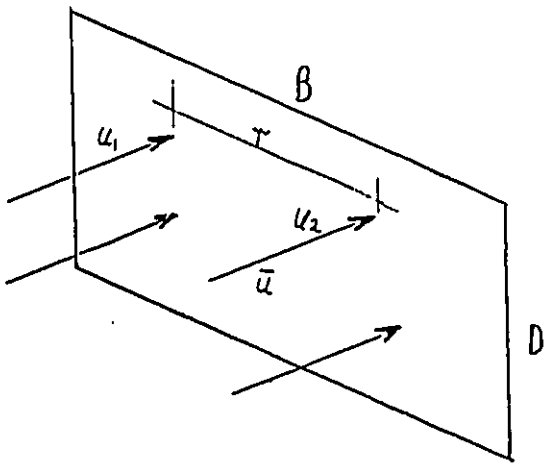

Fig.3.3 Flat Plate Placed Normal to a Turbulent Flow

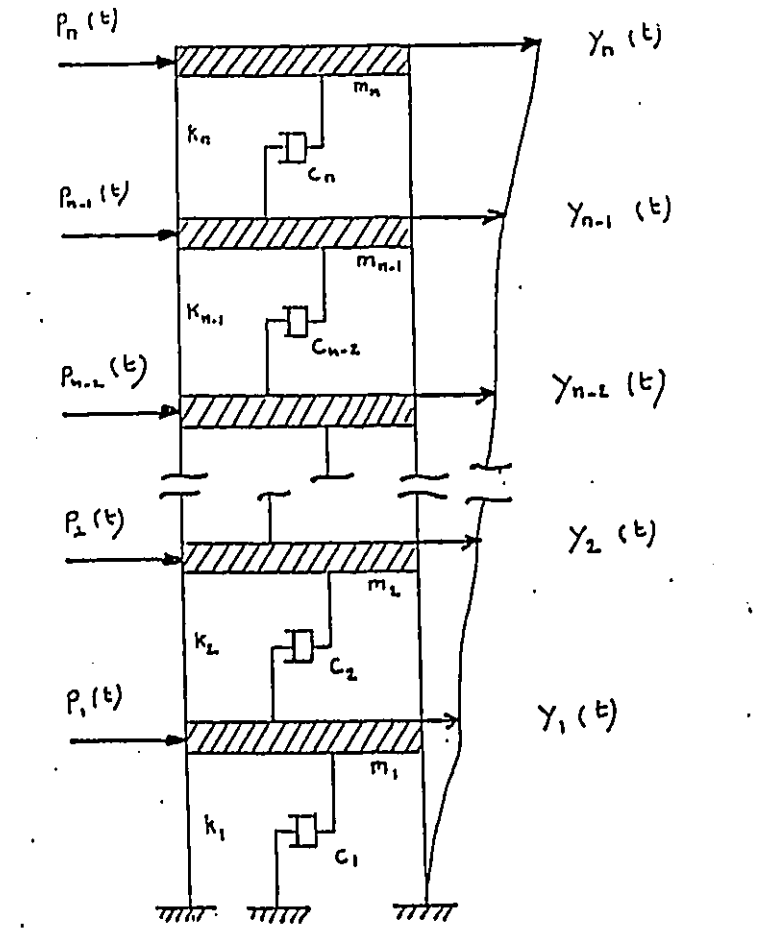

Fig.3.4 Schematic Diagram of MDOF System

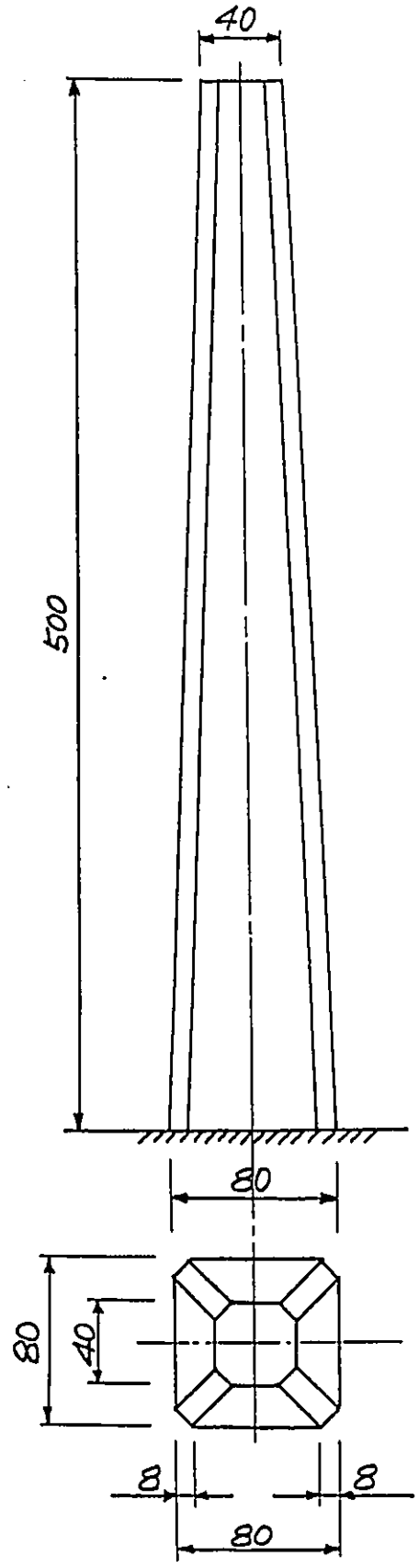

(unit: metre)

Fig.4.1 Prototype Building

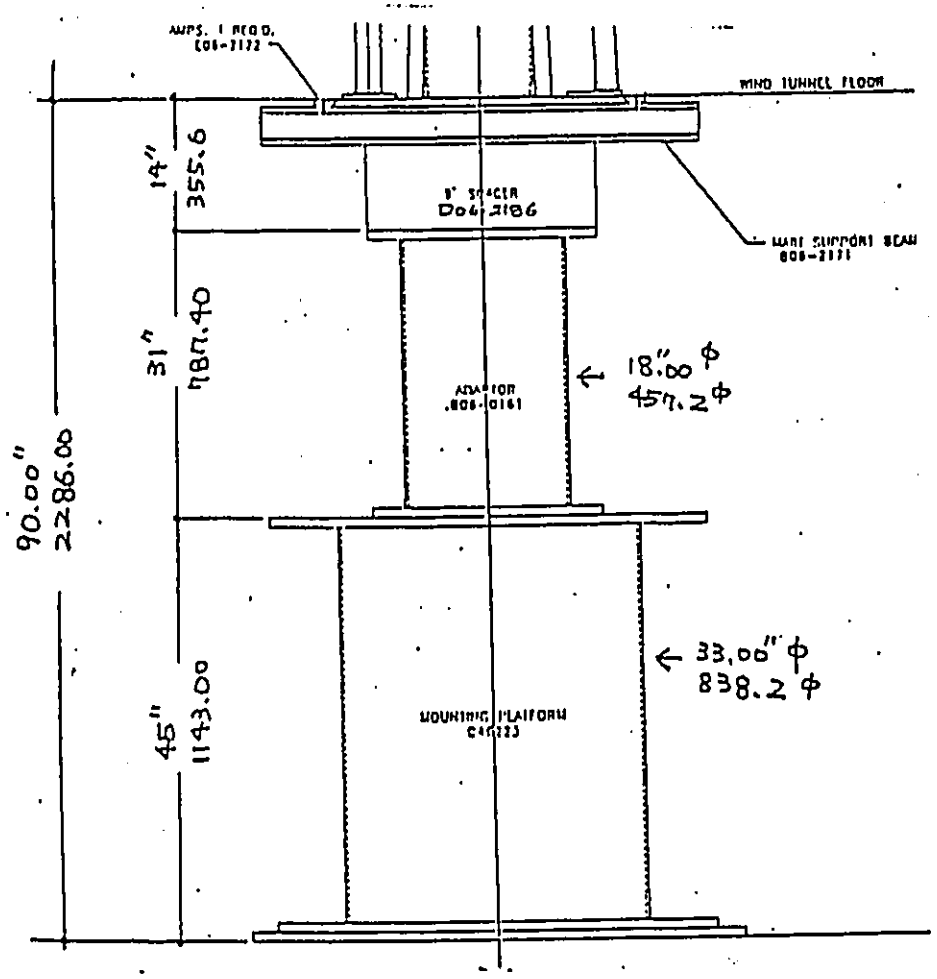

(from [4.3])

Fig.4.2 Pedestal under the Wind Tunnel Floor

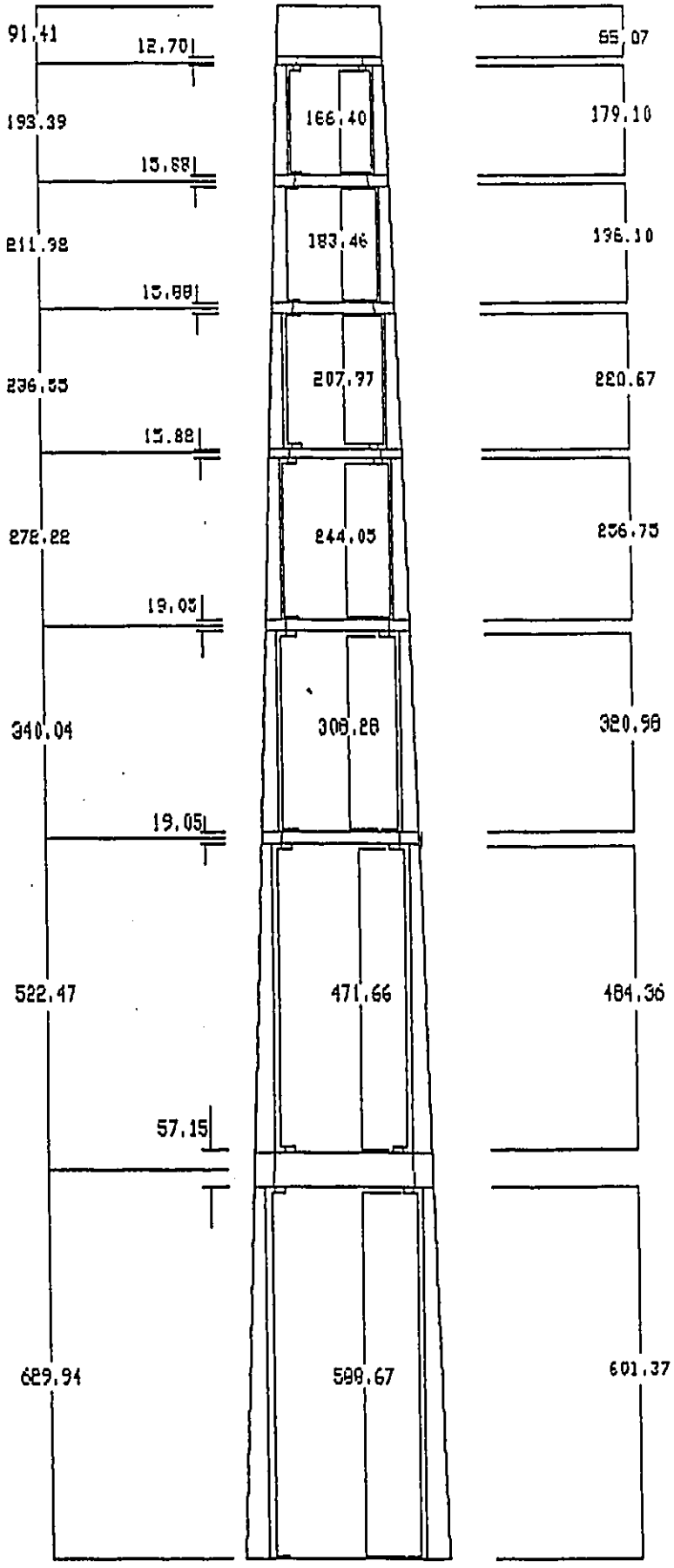

Model
Dimensions

(in 10^{-3} m)

Fig.4.3 General Feature of the Model

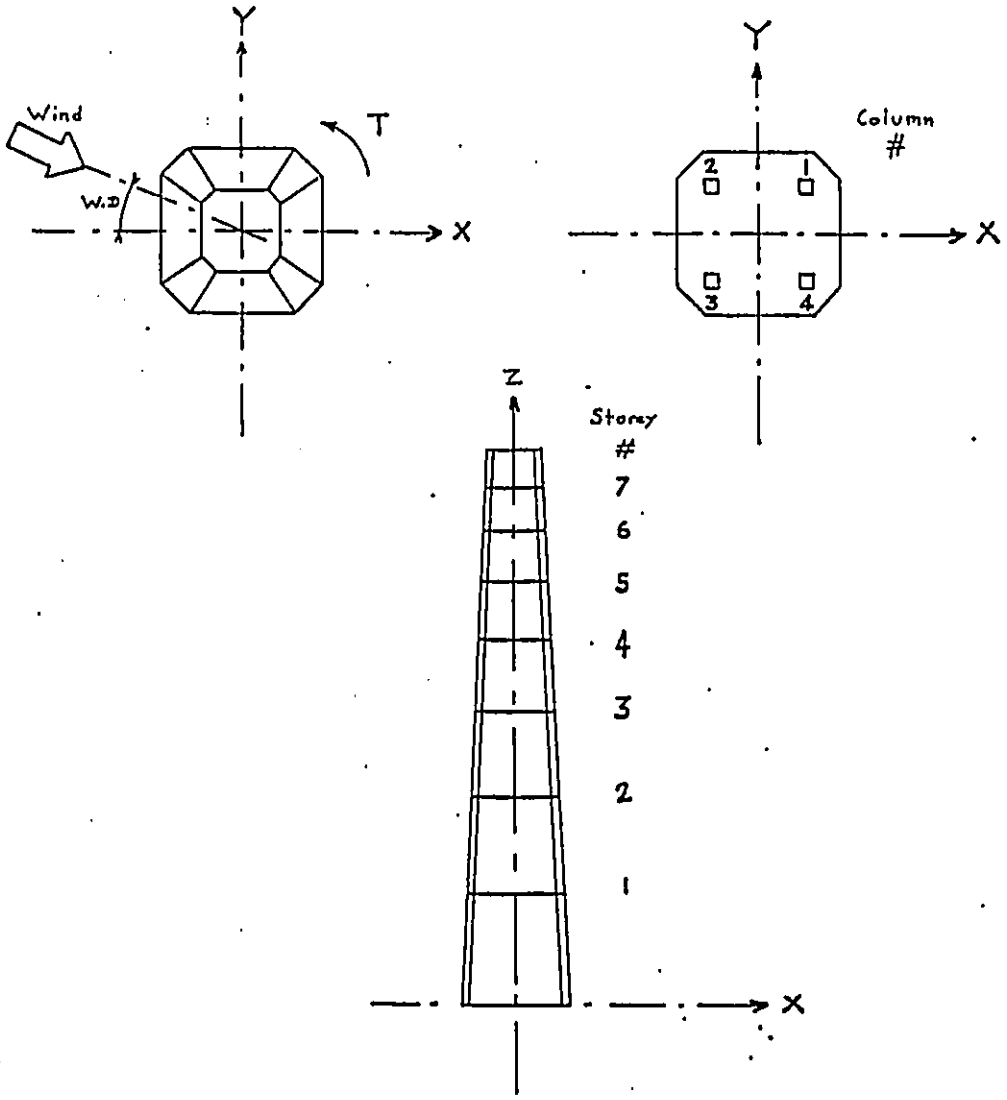

Fig.4.4 Coordinate System and Floor Numbering

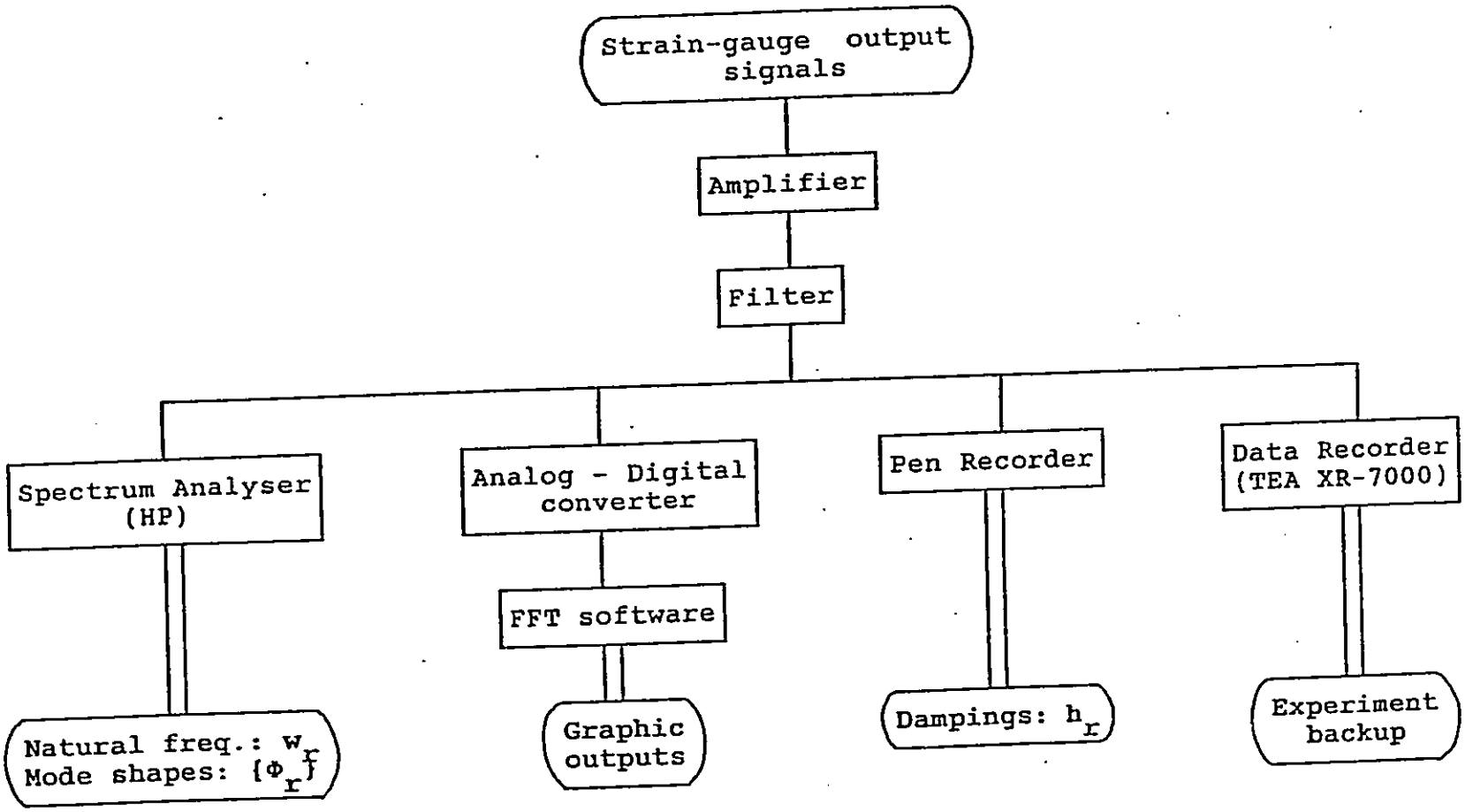

Fig.4.5 Dynamic Calibration Set-up (data acquisition system)

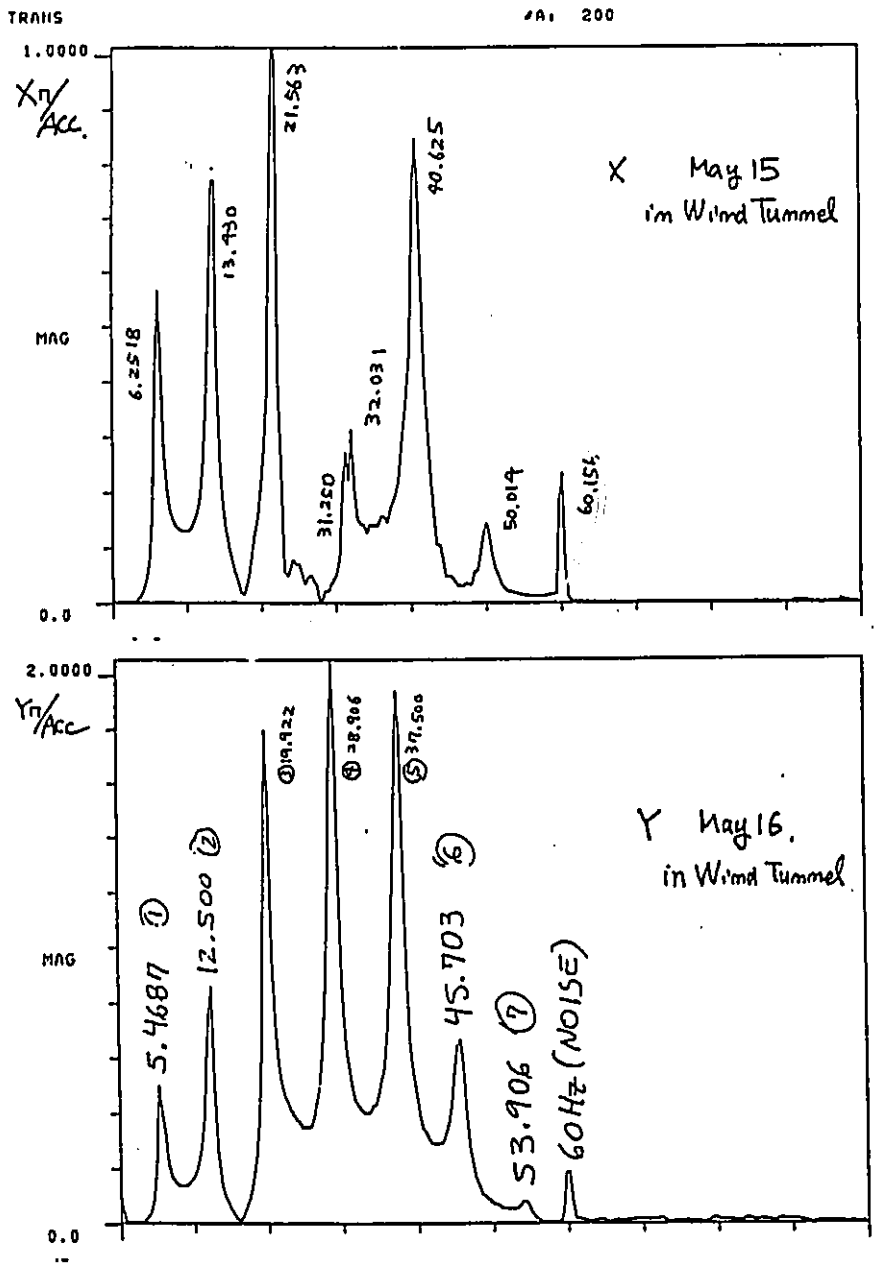

Fig.4.6 Dynamic Response Characteristics (X-dir, Y-dir)

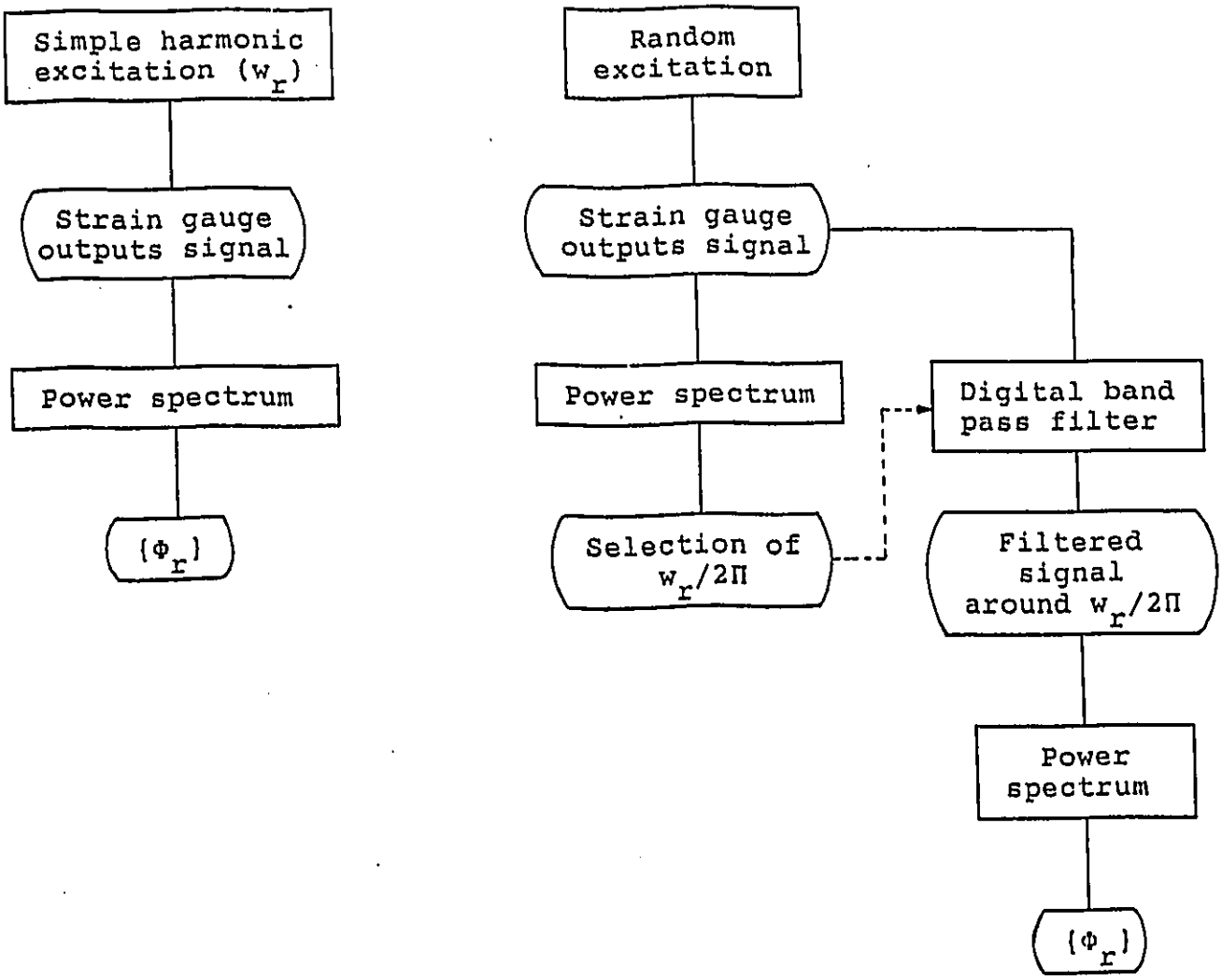

* Determination of $\{\Phi_r\}$ from a simple harmonic excitation.

* Determination of $\{\Phi_r\}$ from a white noise excitation

Fig.4.7 Comparison of Two Methods for $\{F_r\}$

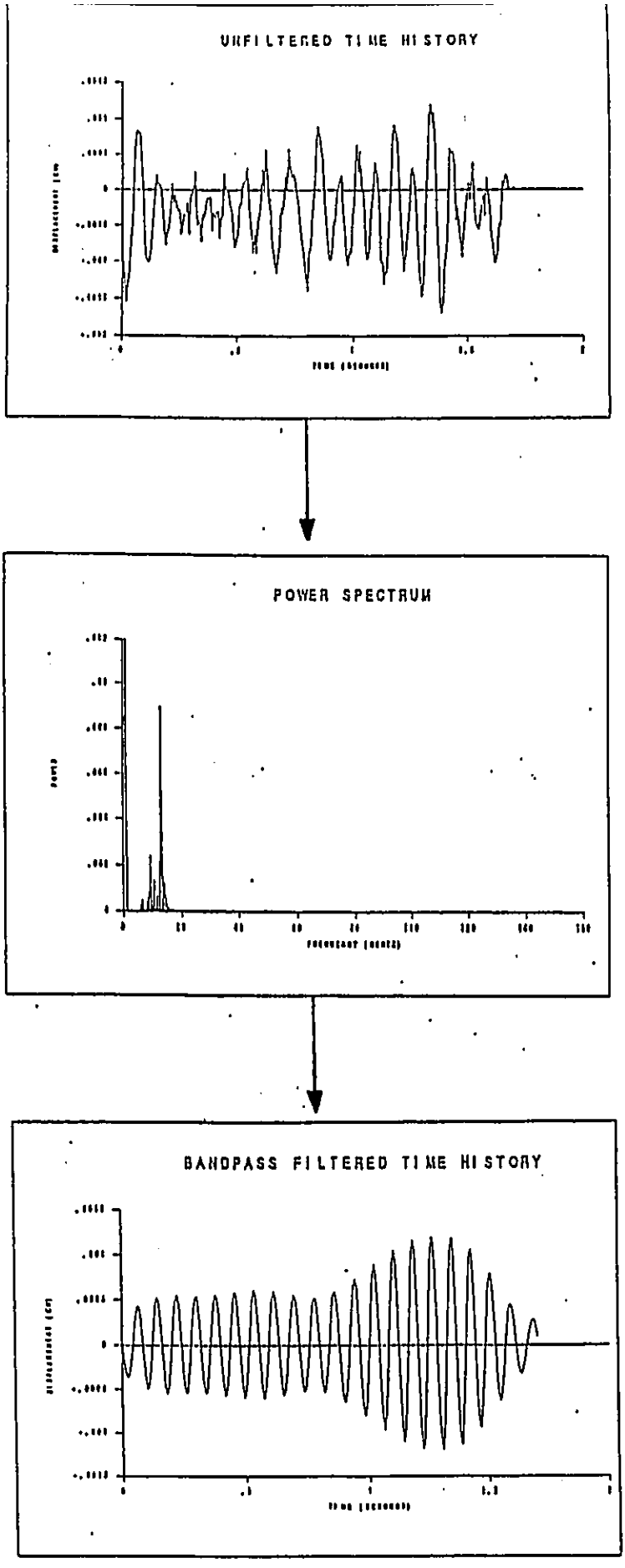

Fig.4.8 Bandpass Filter Processing

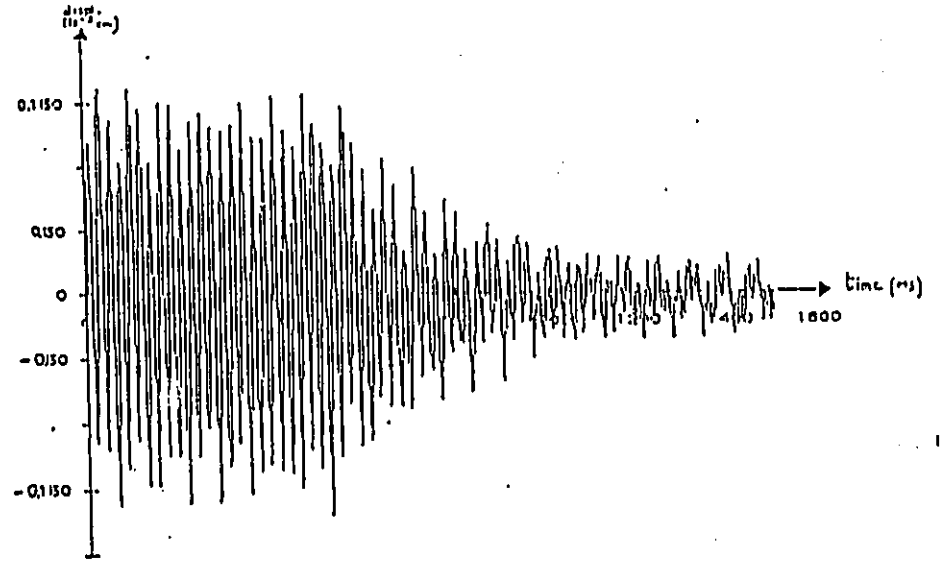

Fig.4.9 Recording of Model Damping

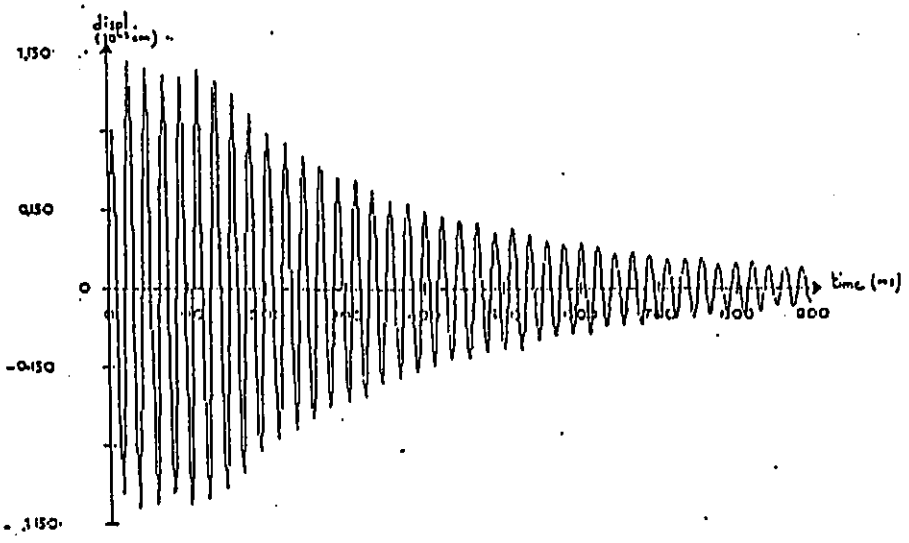

Fig.4.10 Recording of 7-th Strain Gauge Output

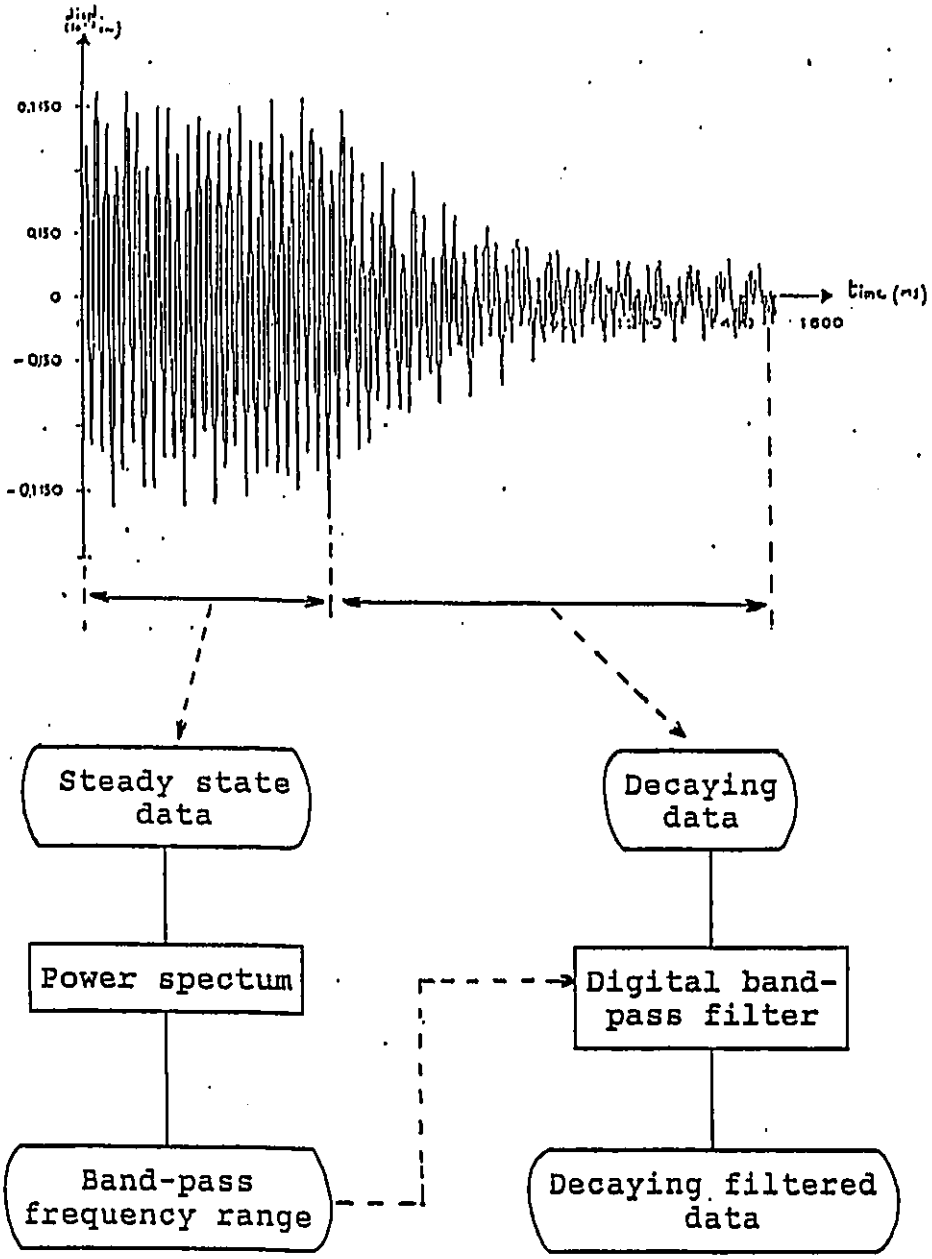

Fig.4.11 Improvement of Model Damping Determination

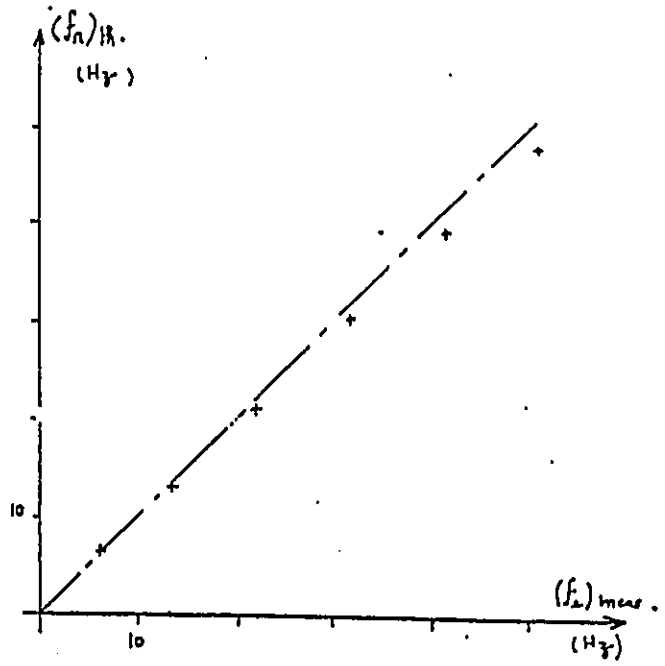

Fig.4.12 Natural Frequency in X-direction

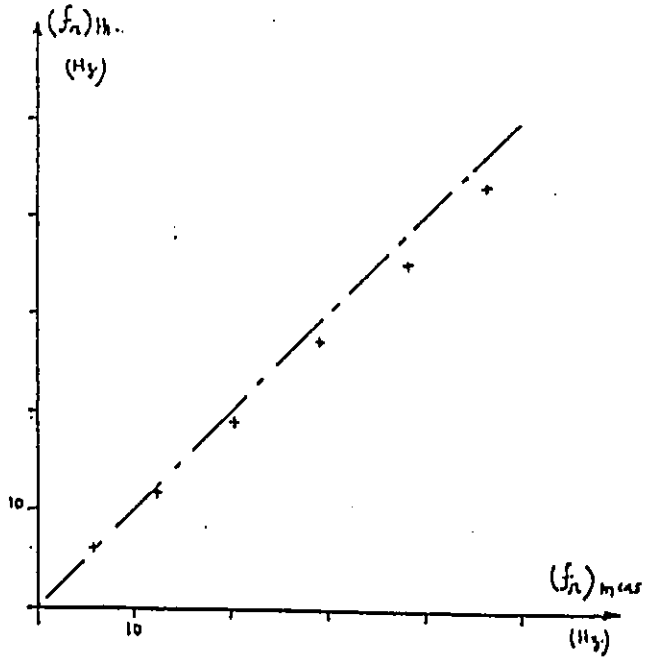

Fig.4.13 Natural Frequency in Y-direction

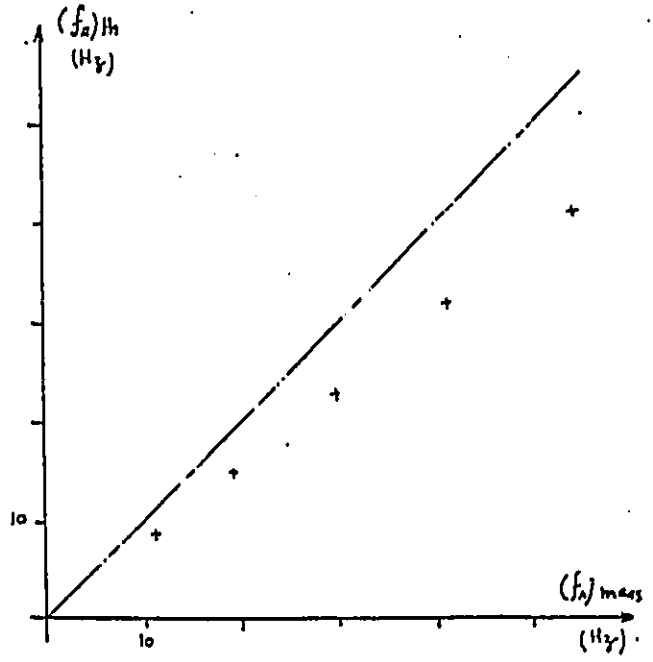

Fig.4.14 Natural Frequency in Torsion

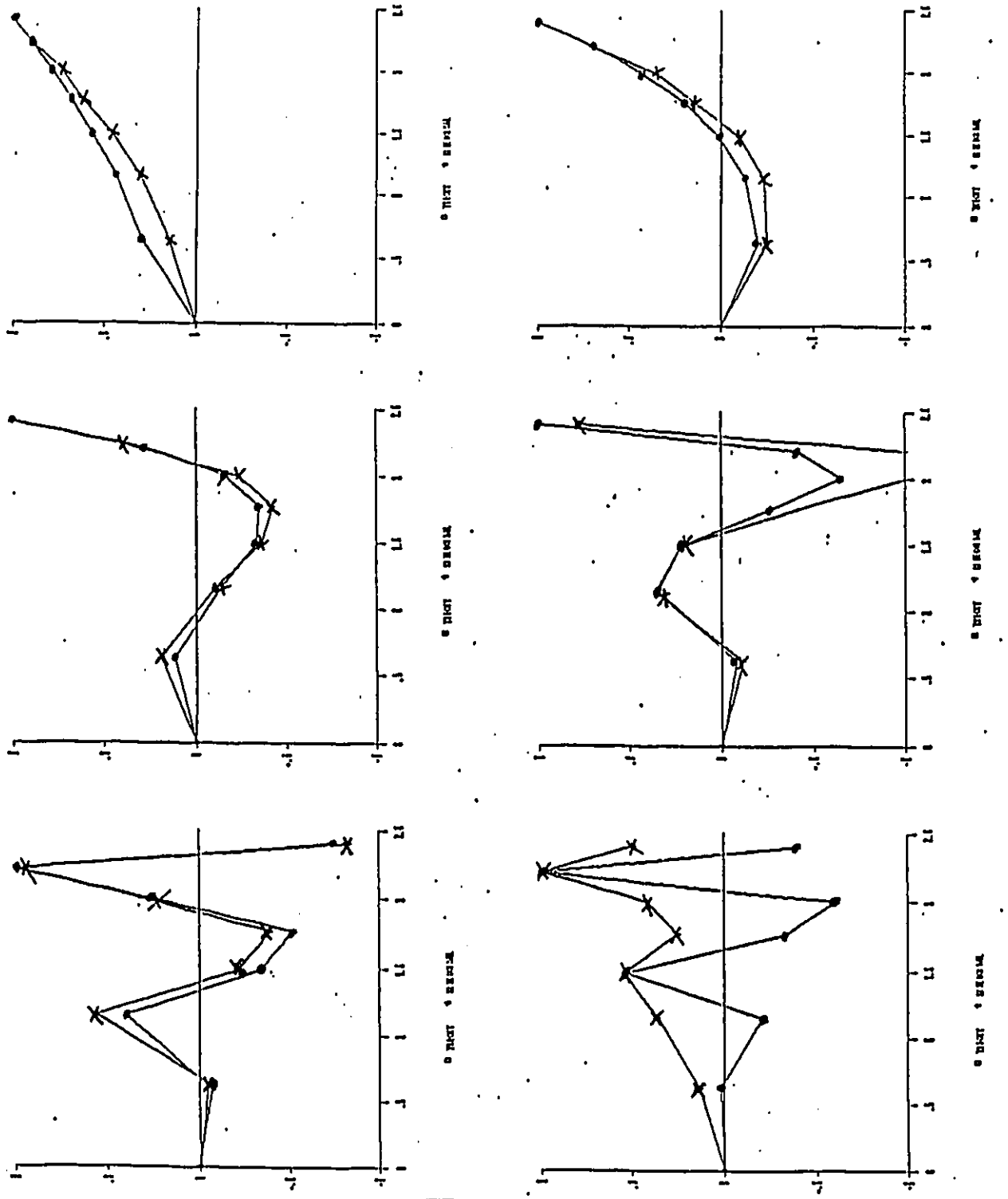

● : calculated results
x : measured results

Fig.4.17 Vibration Mode Shape in Torsion

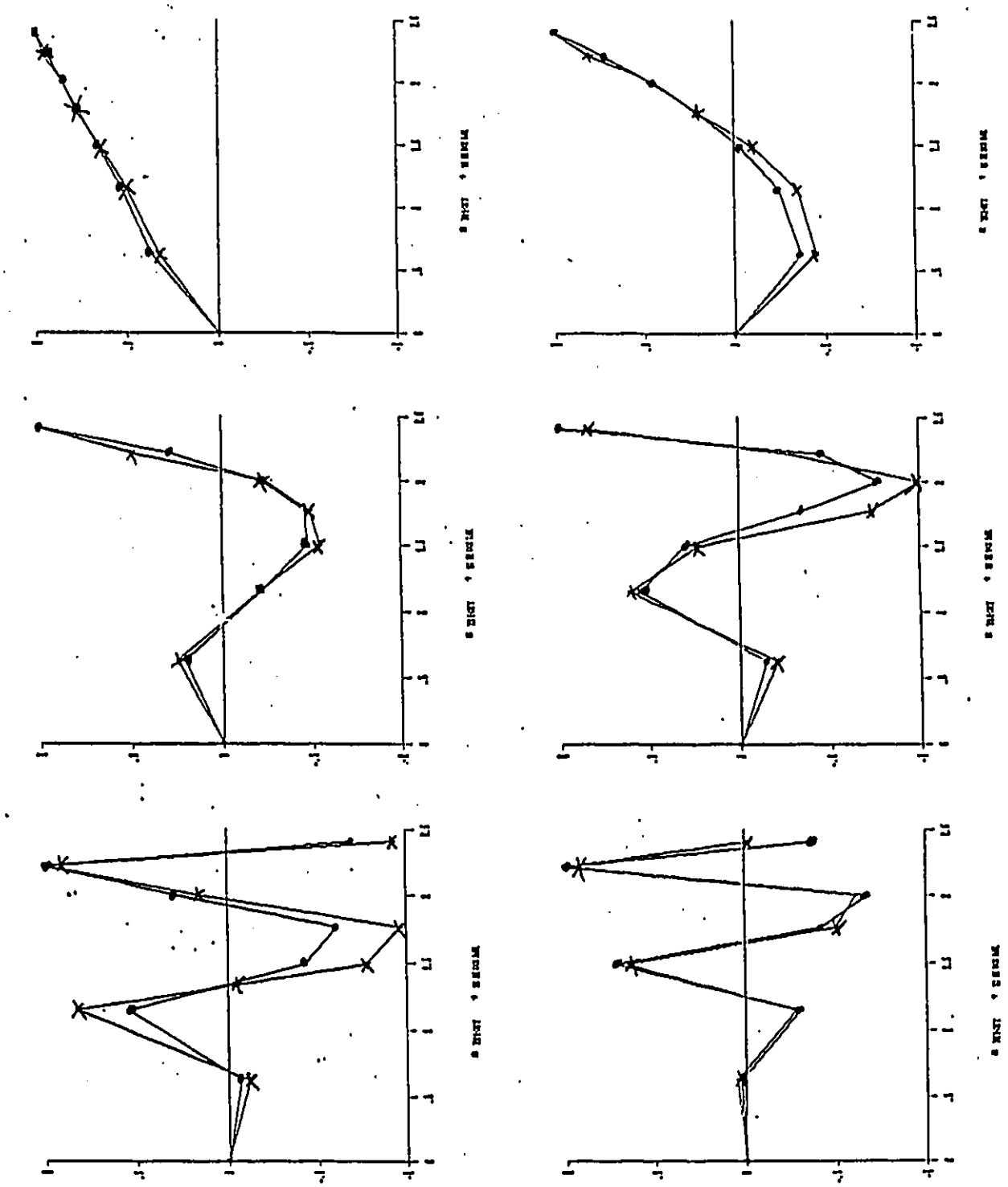

● : calculated results
x : measured results

Fig.4.16 Vibration Mode Shape in Y-direction

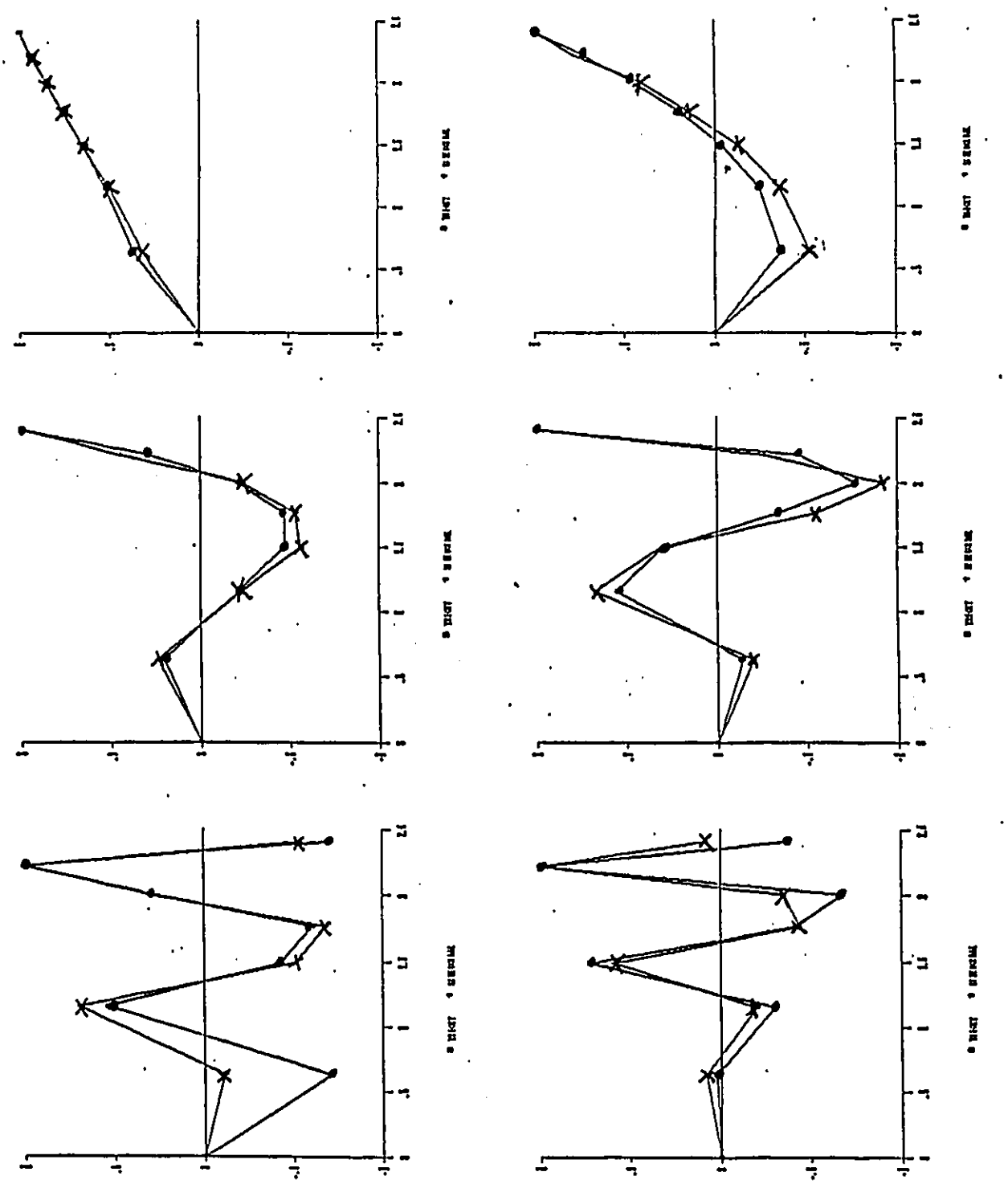

● : calculated results
x : measured results

Fig.4.15 Vibration Mode Shape in X-direction

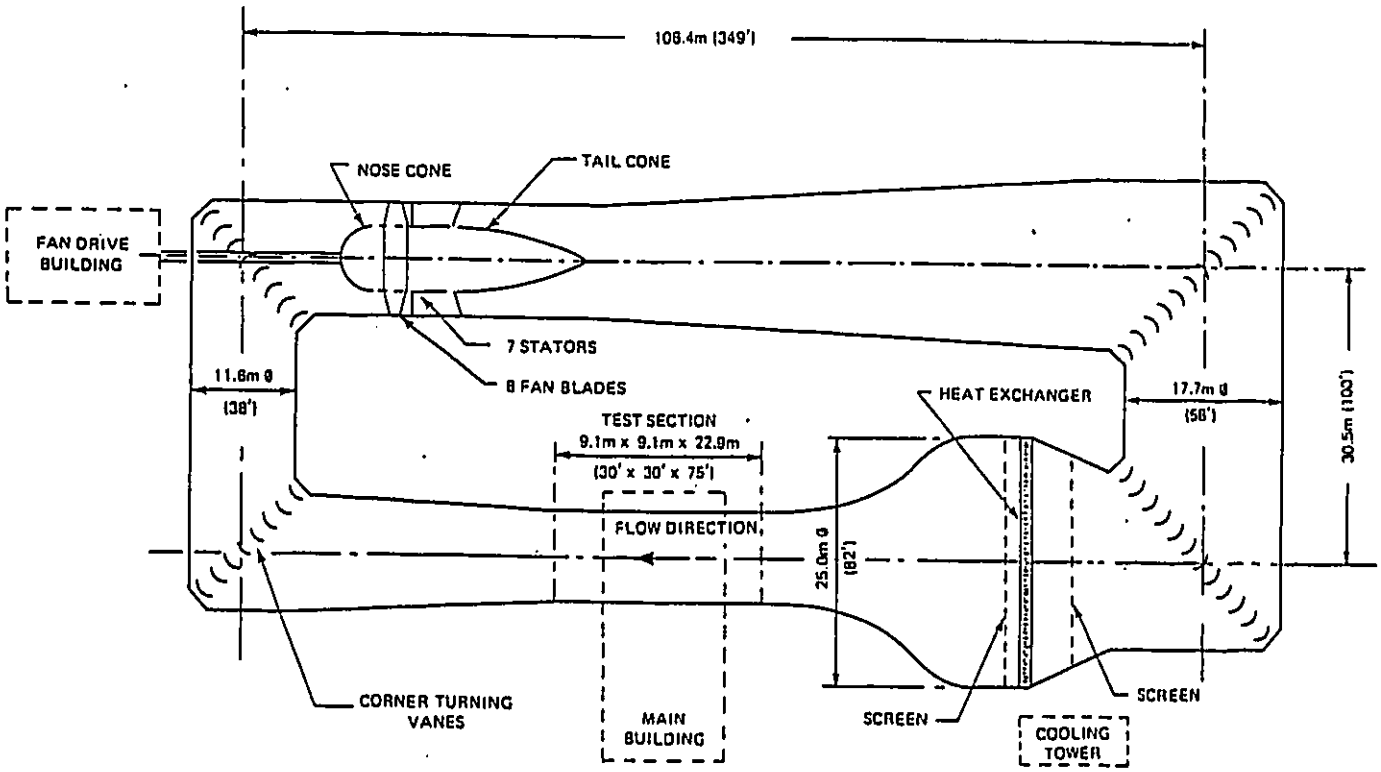

(from [4.3])

Fig.4.18 NRCC 9 m x 9 m Wind Tunnel

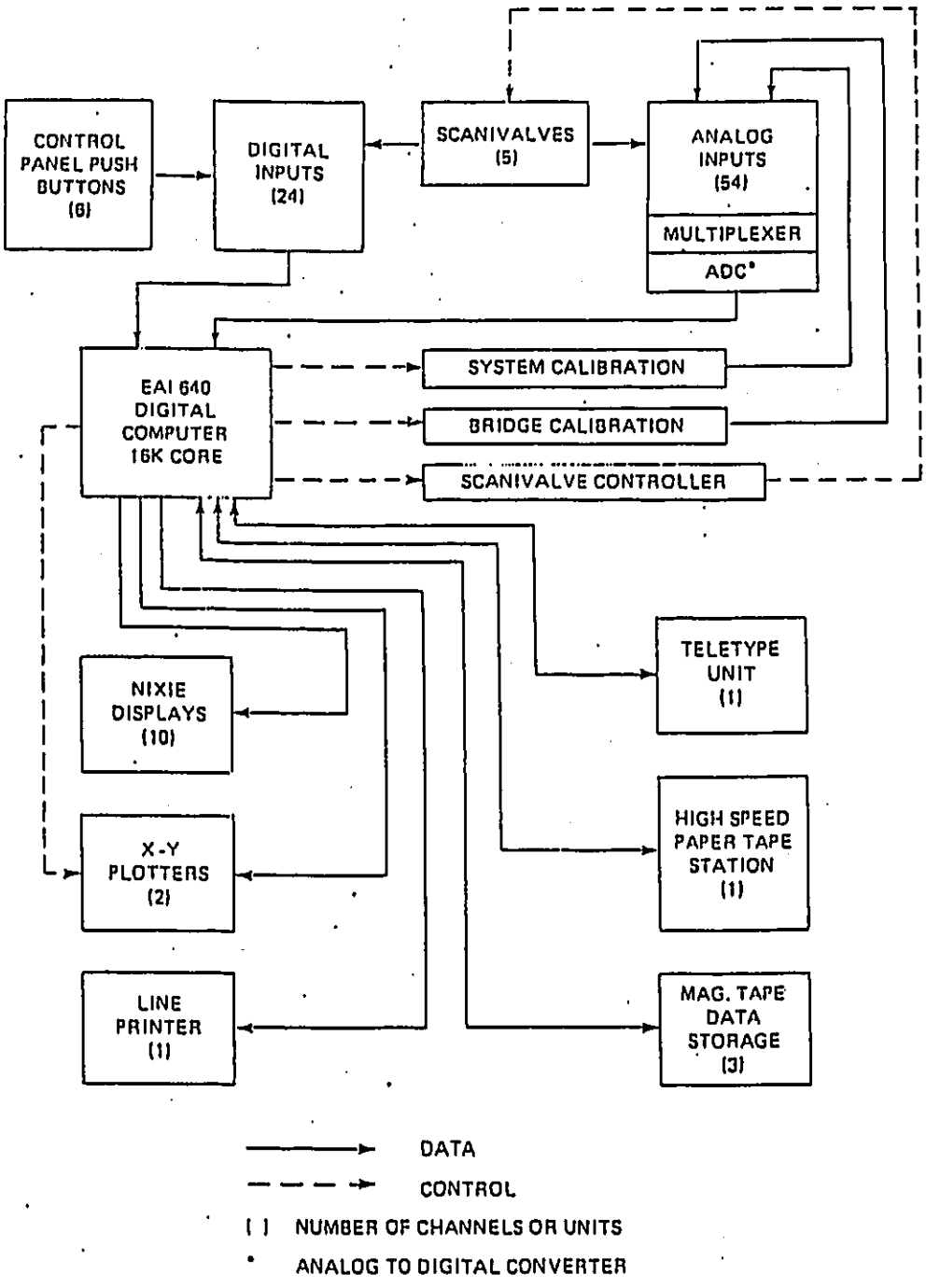

Fig.4.19 Flow Chart of Data Acquisition System

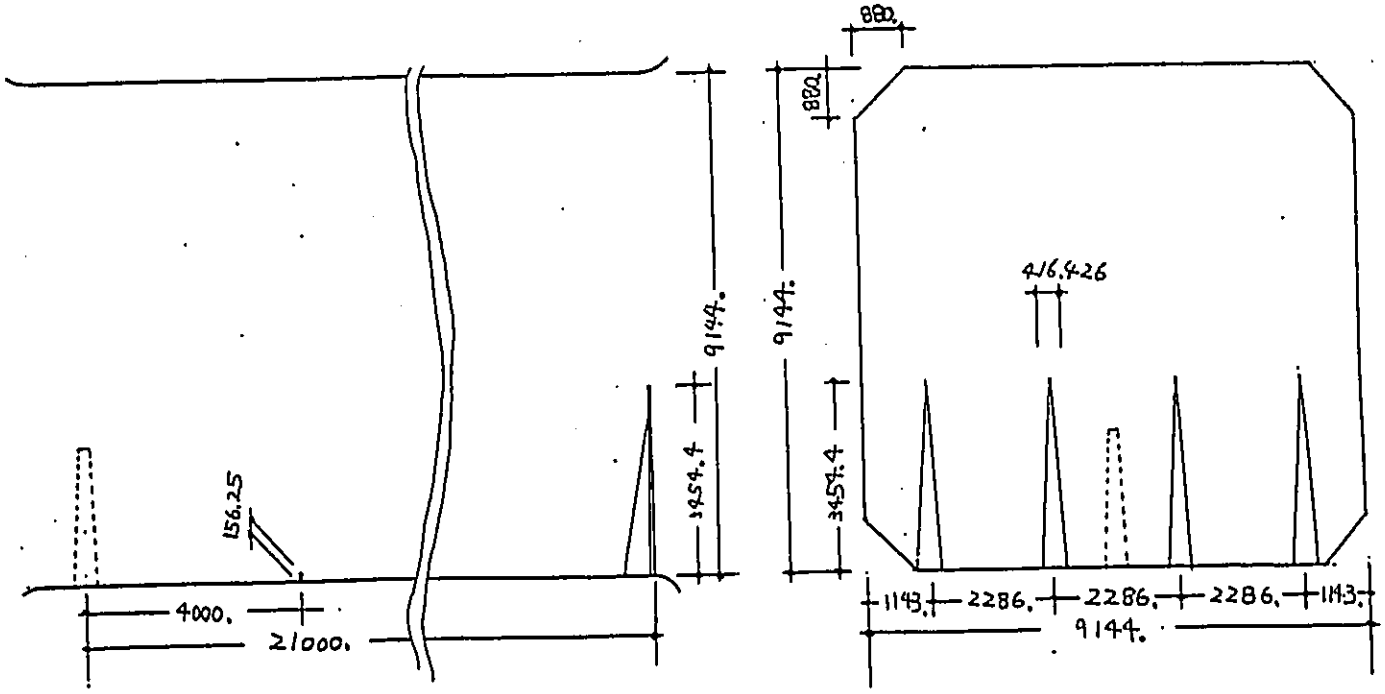

Fig.4.20 Spires and Board in the Wind Tunnel

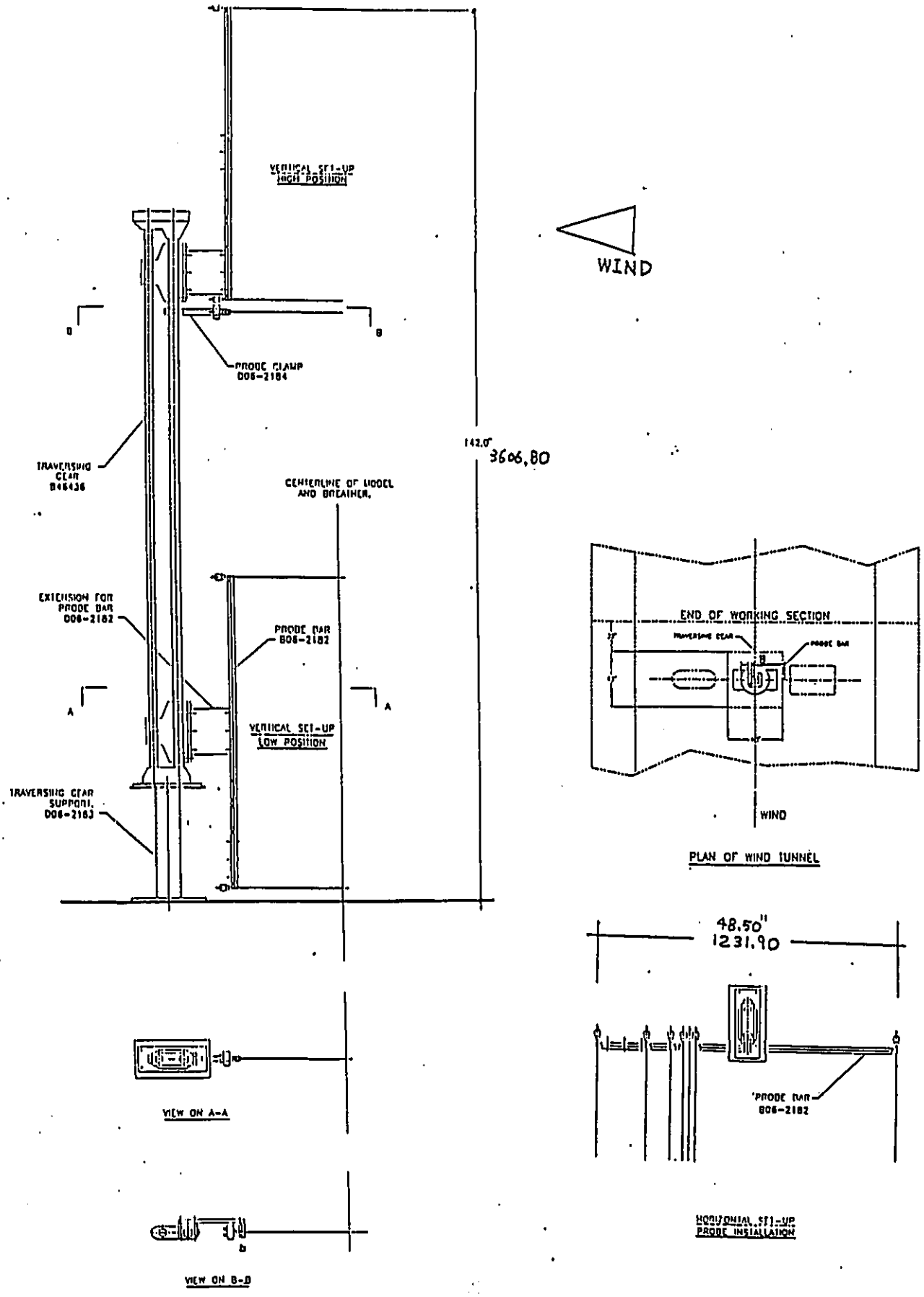

Fig.4.21 Instrumental Set-up for the Flow Measurement

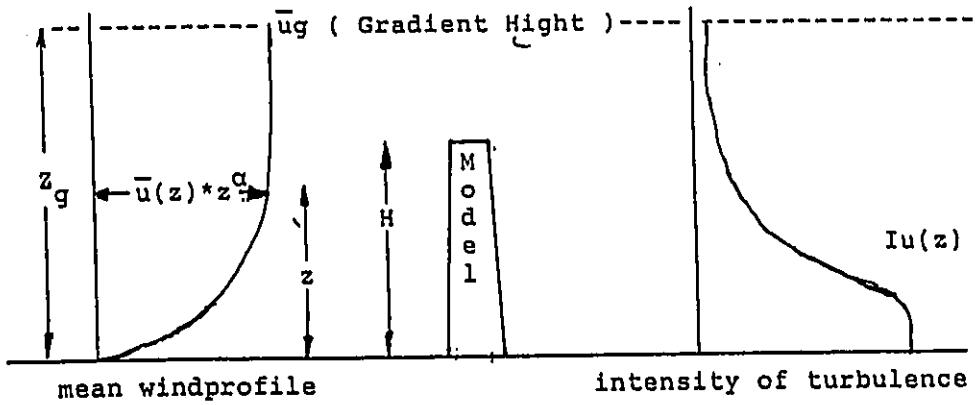

Fig.4.22 Boundary Layer Wind Profile

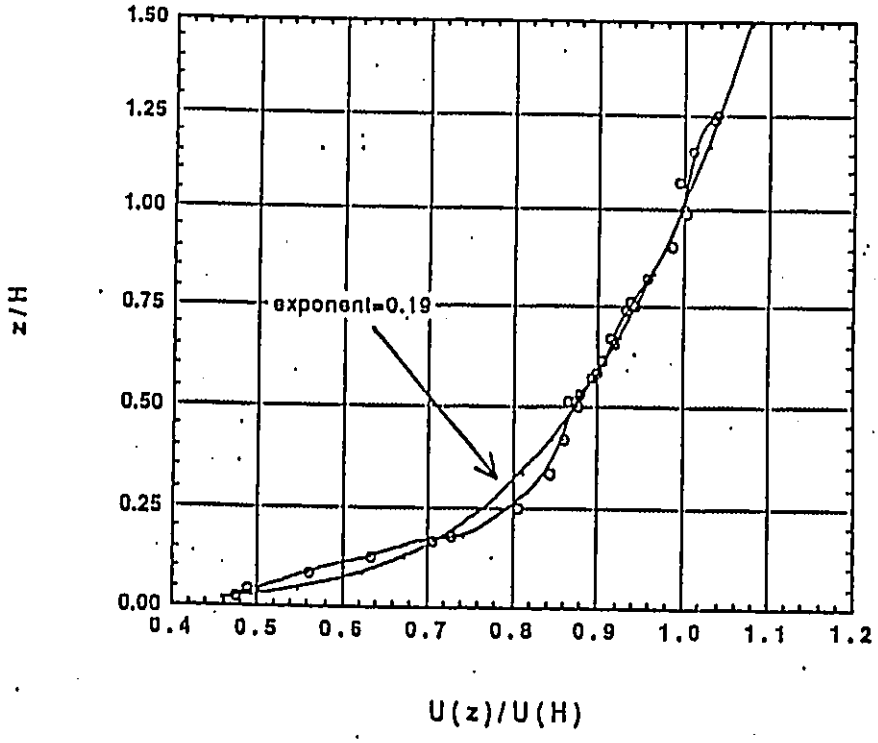

Fig.4.23 Mean Wind Speed Profile at Model Location

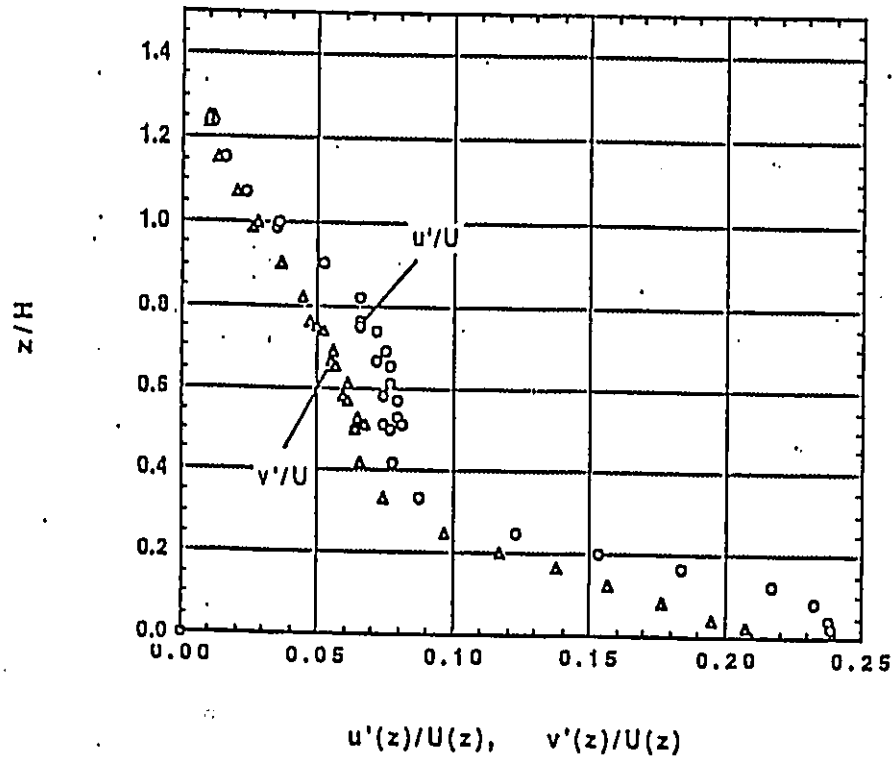

Fig.4.24 Profile of Turbulence Intensity

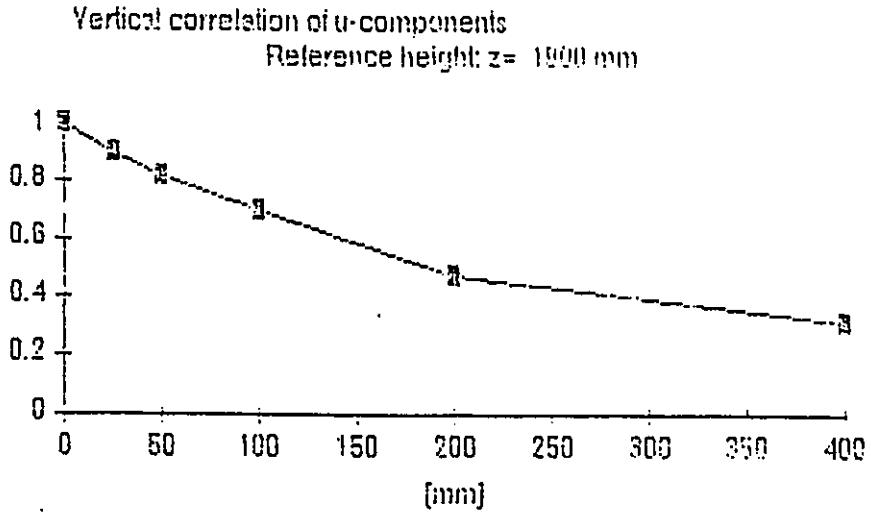

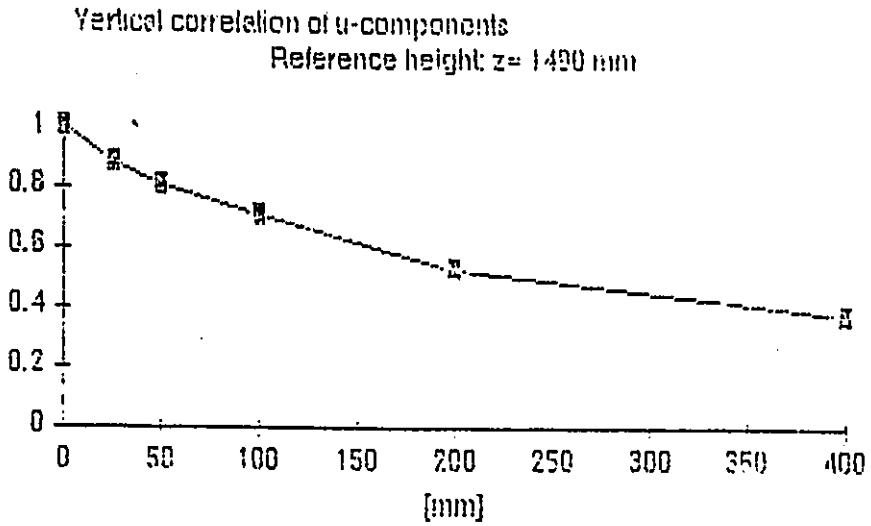

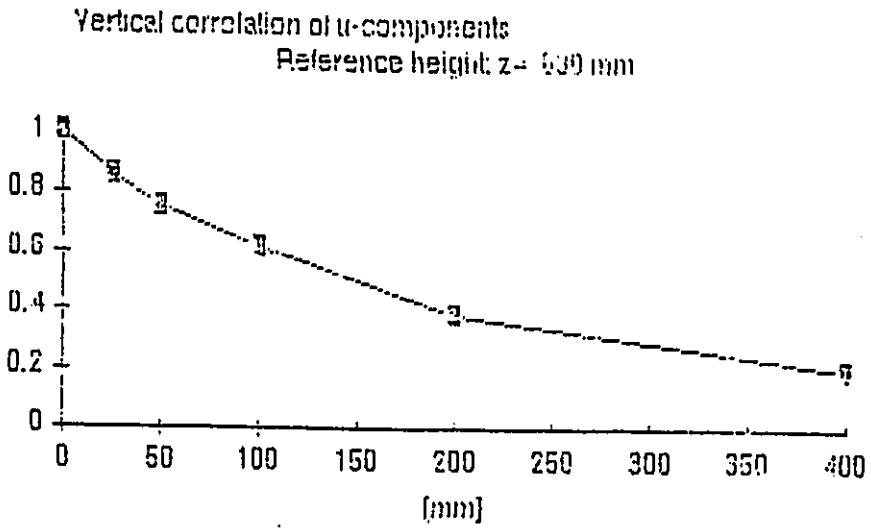

(from [4.3])

Fig.4.25.a Vertical Correlation of u(t)

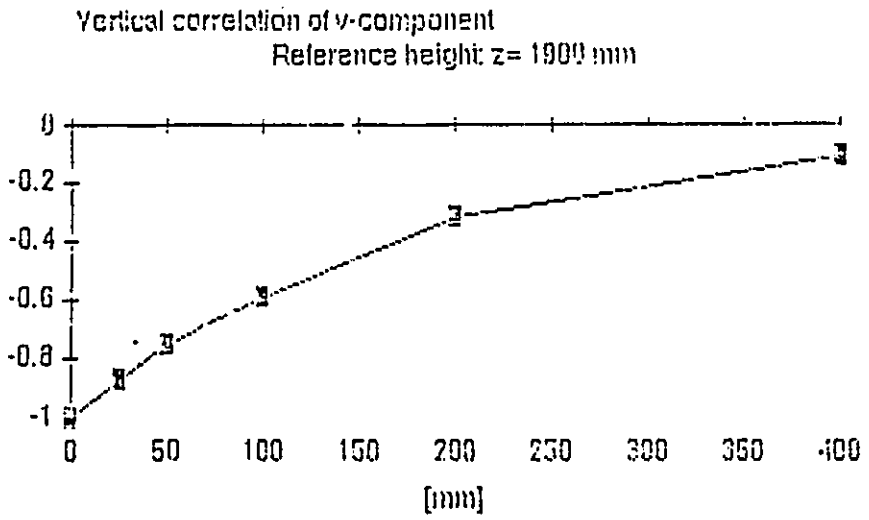

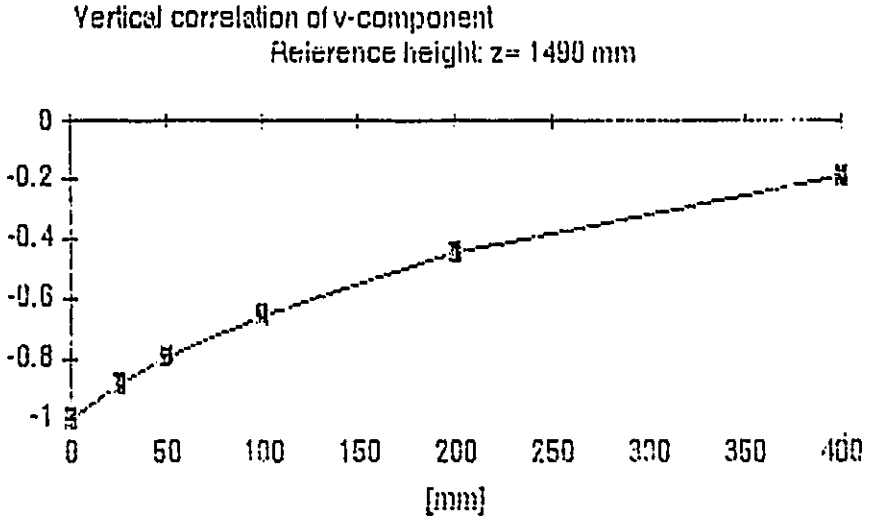

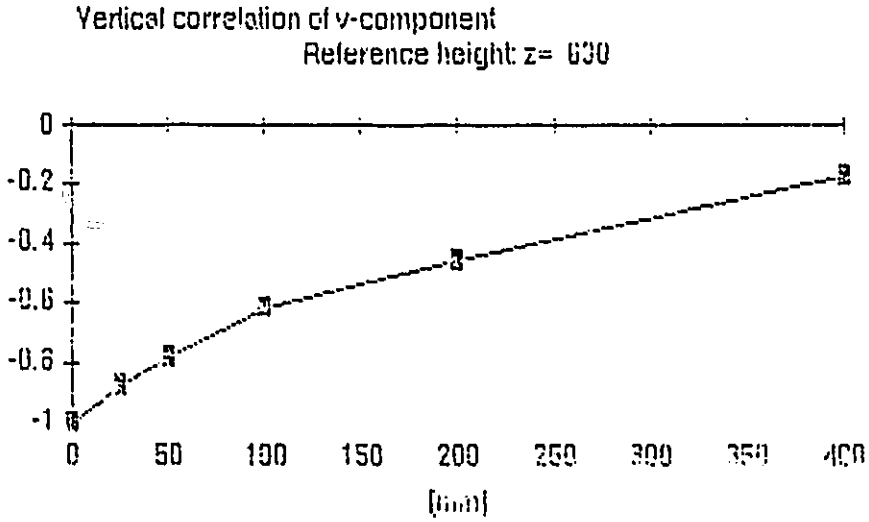

(from [4.3])

Fig.4.25.b Vertical Correlation of v(t)

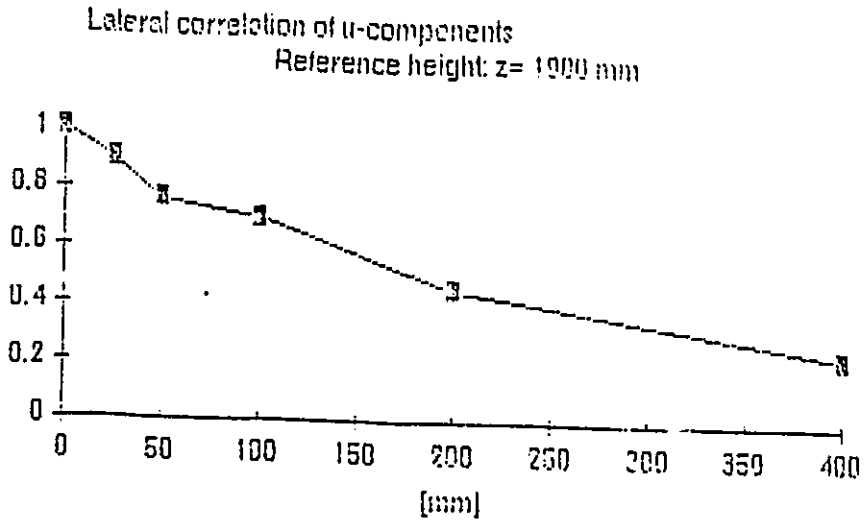

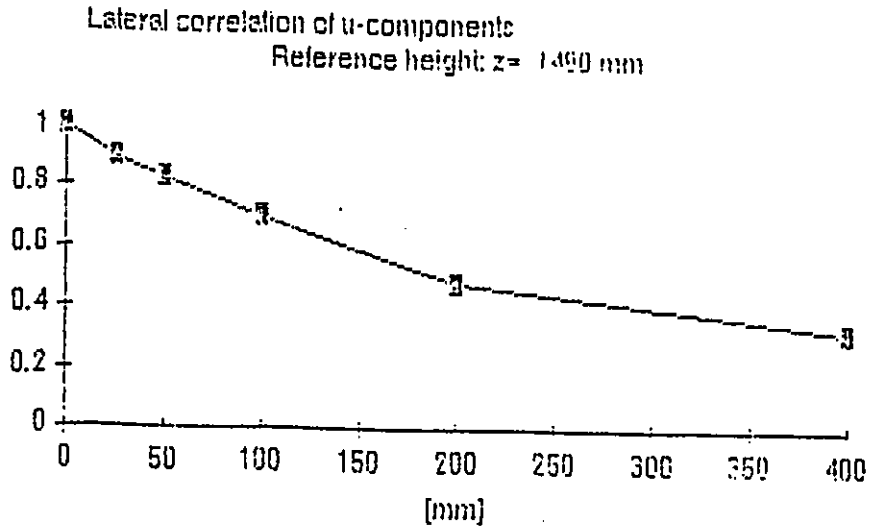

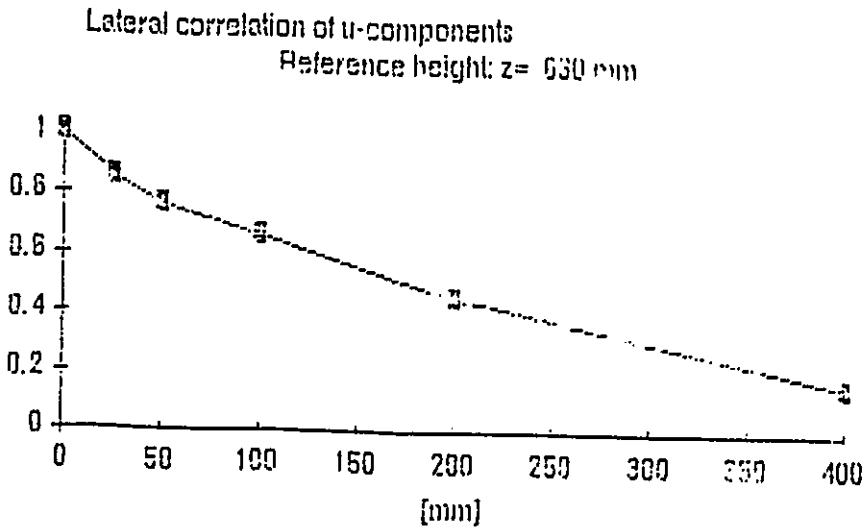

(from [4.3])

Fig.4.26.a Lateral Correlation of u(t)

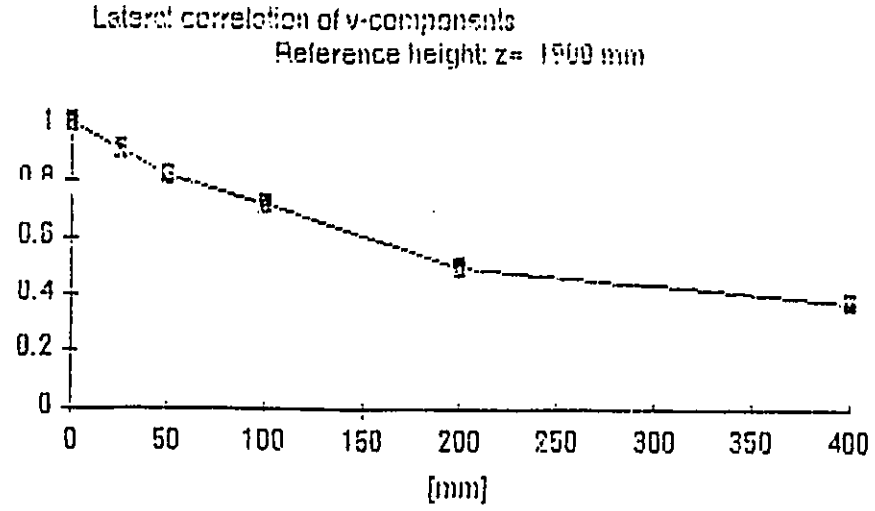

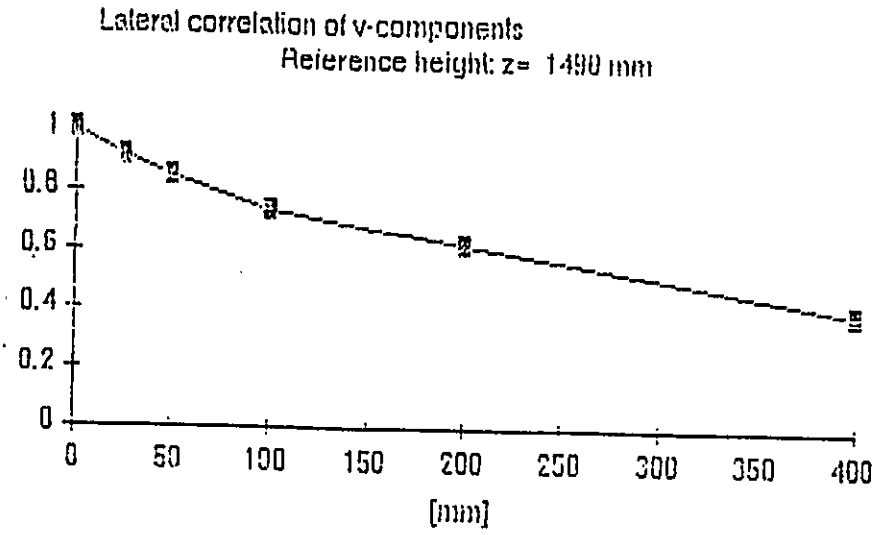

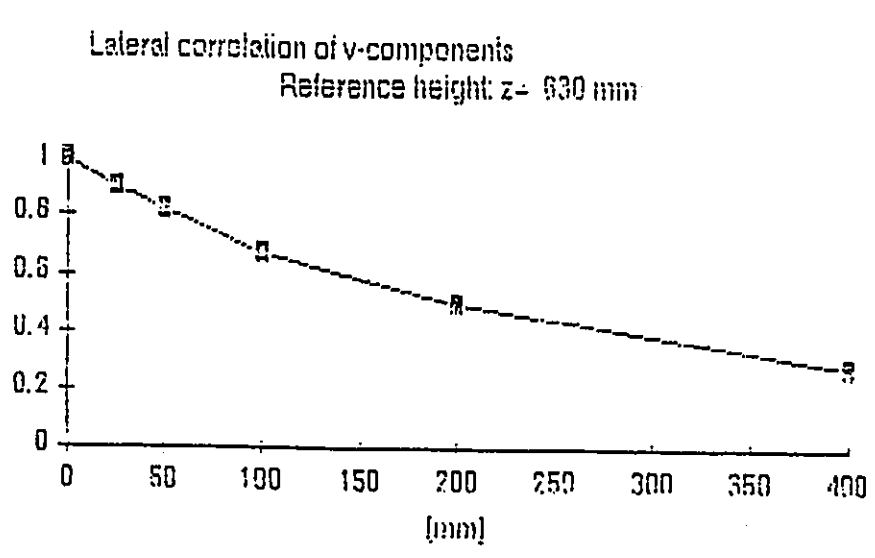

(from [4.3])

Fig.4.26.b Lateral Correlation of u(t)

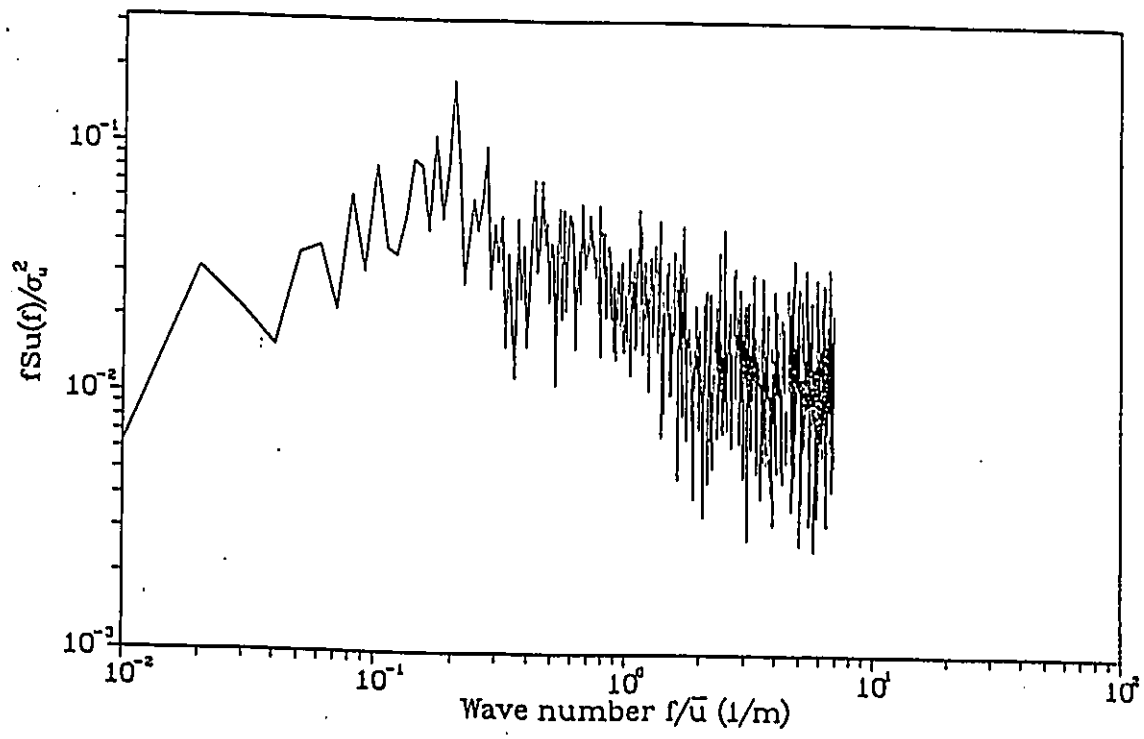

Spectrum of u-component

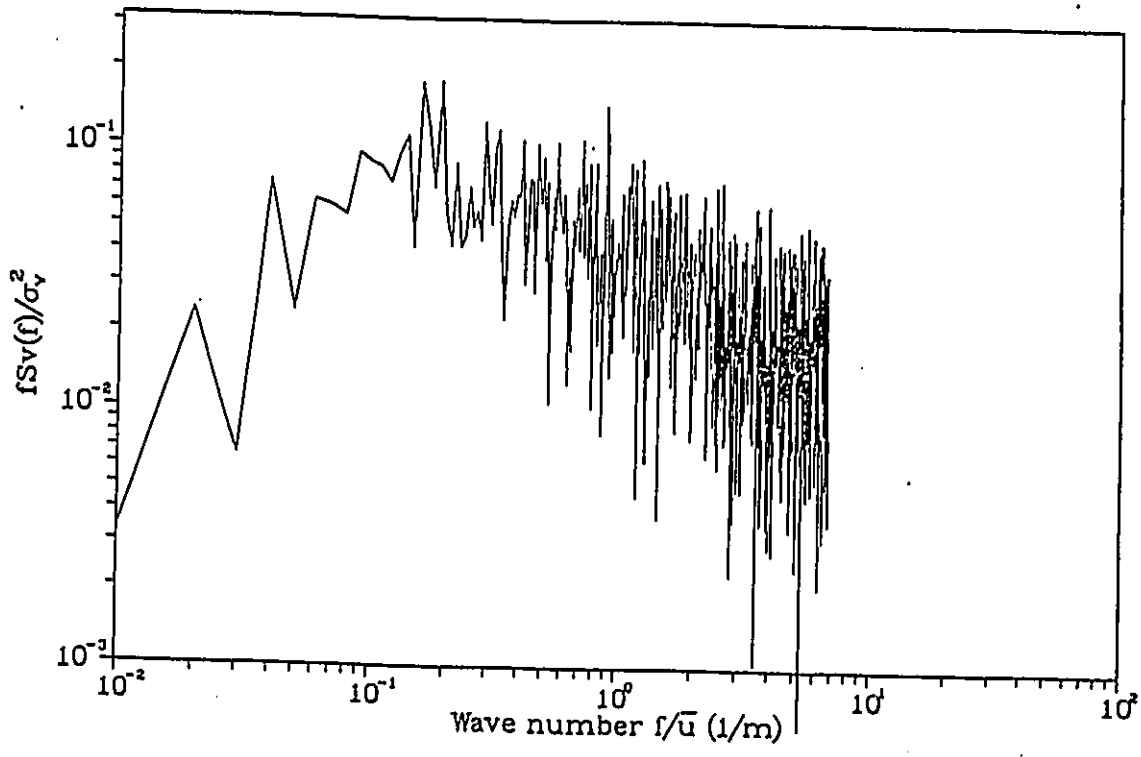

Spectrum of v-component

(from [4.3])

Fig.4.27 Velocity Spectra

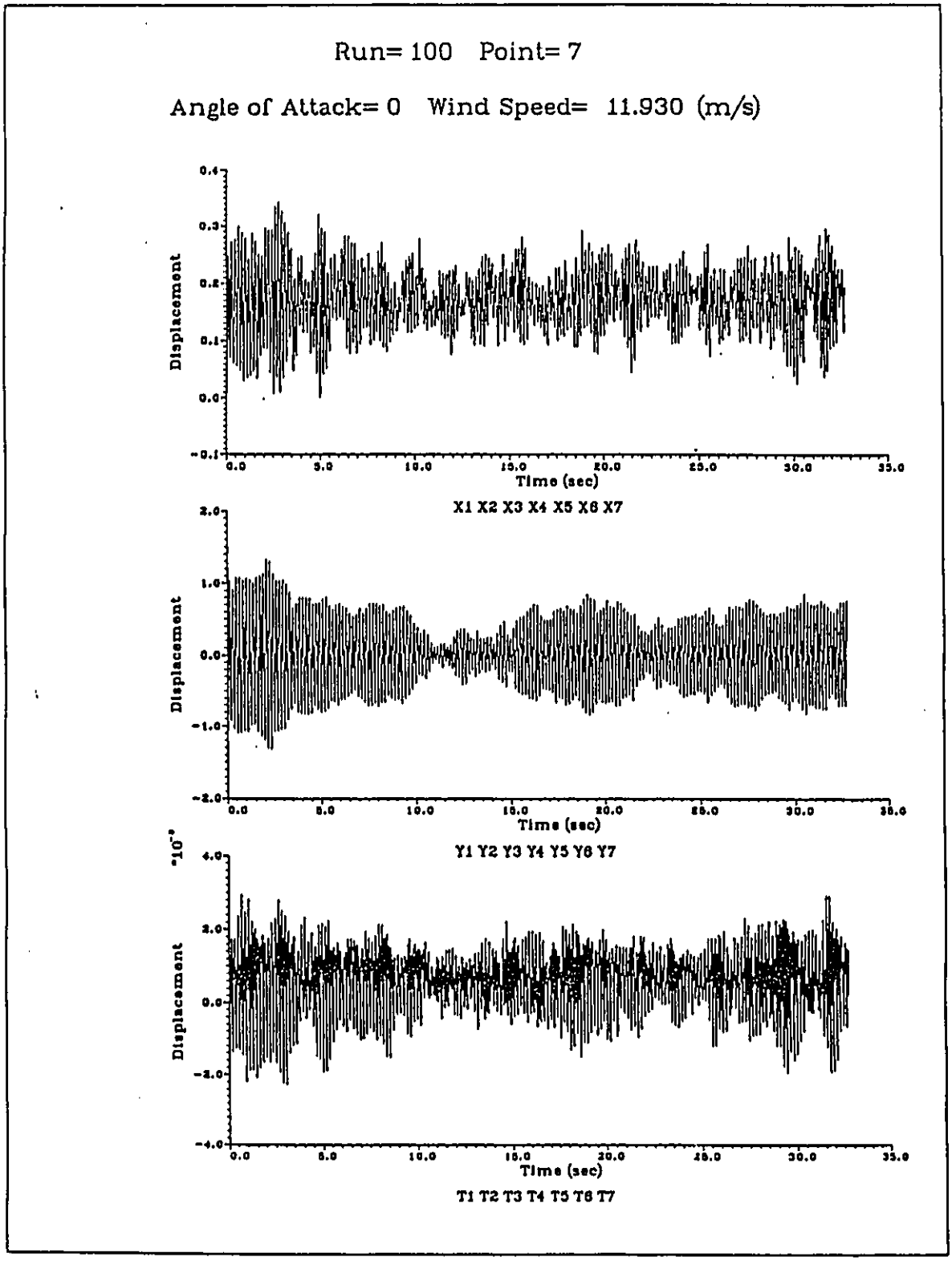

(from [4.3])

Fig.4.28 Sample of Response Histories (Top Floor)

Notes on Figs. 5.1 and 5.2

There are 66 figures in the following 22 pages showing both mean and root-mean-square response of the model plotted against reduced velocity. Each page shows either mean or rms response in all three directions for a given wind azimuth angle.

Displacements are given in 10^{-2} m (cm) for X- and Y-sway motion and radian for torsion. Reduced velocity for each case is given by the same definition as in Table 5.1, namely

V_r in X-sway $= V_H/(f_x B)$

V_r in Y-sway $= V_H/(f_y B)$

V_r in torsion $= V_H/(f_t B)$

where V_H = Mean wind speed at the building top
B = Average width of the building (= 0.3 m)
f_x, f_y and f_t = natural frequencies

Displacements are identified by three letters in which

x, y and t = direction of displacement
m and s = mean and rms
numbers = number of mass module, 7 being the top

Fig.5.1 and Fig.5.2 are from [4.3]

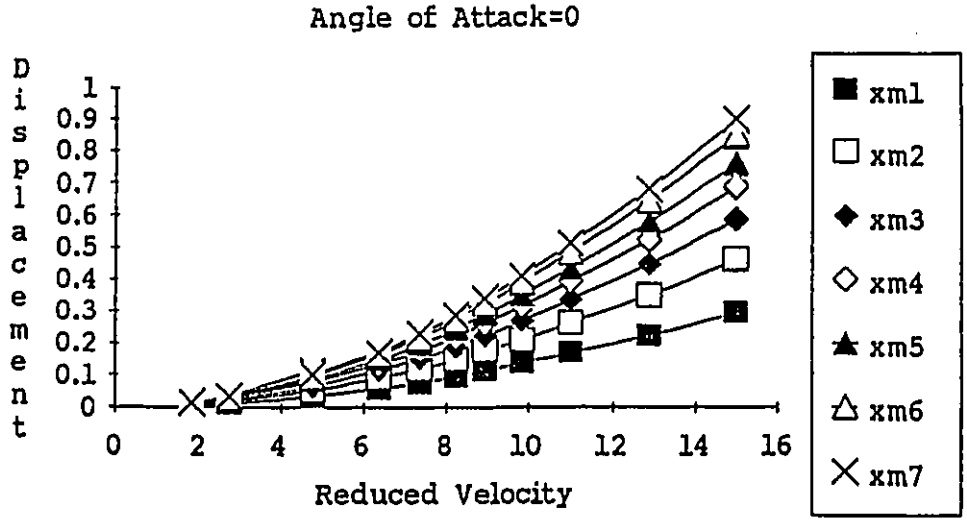

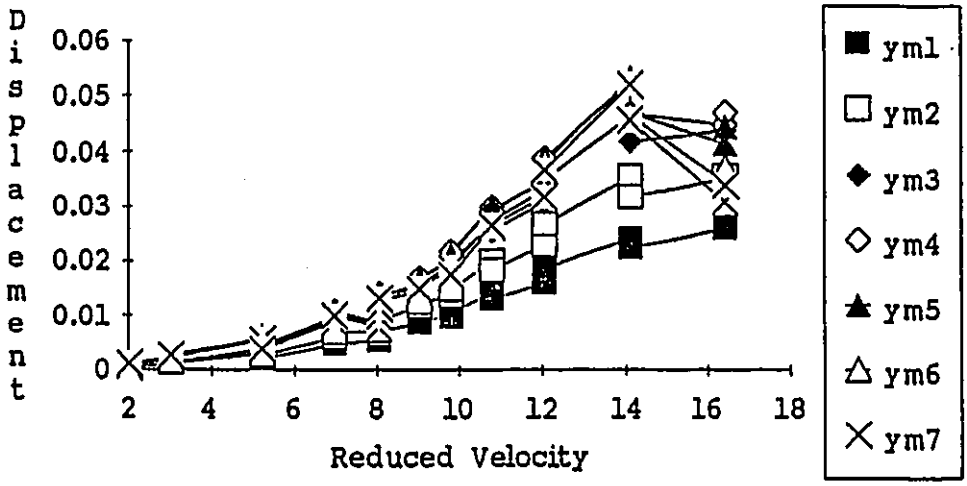

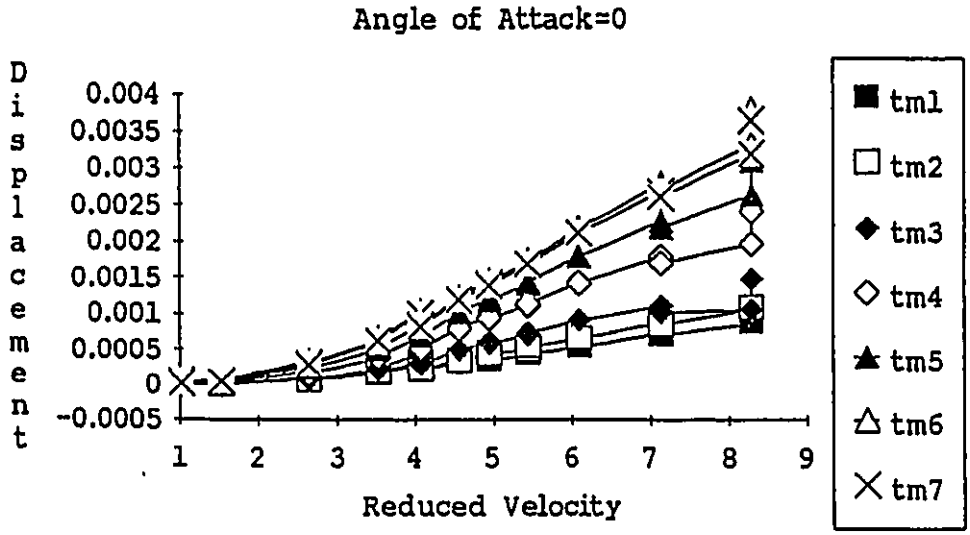

Fig.5.1 Mean Displacements vs. Reduced Velocity

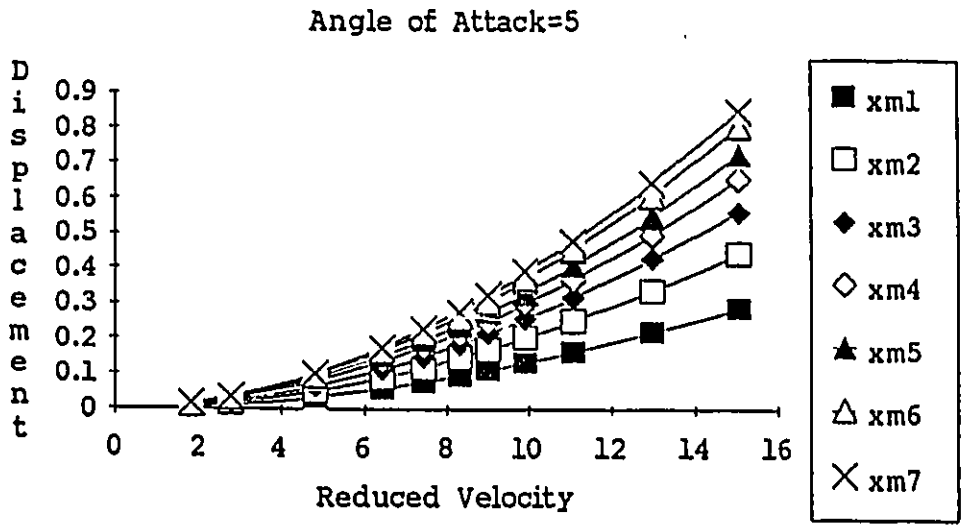

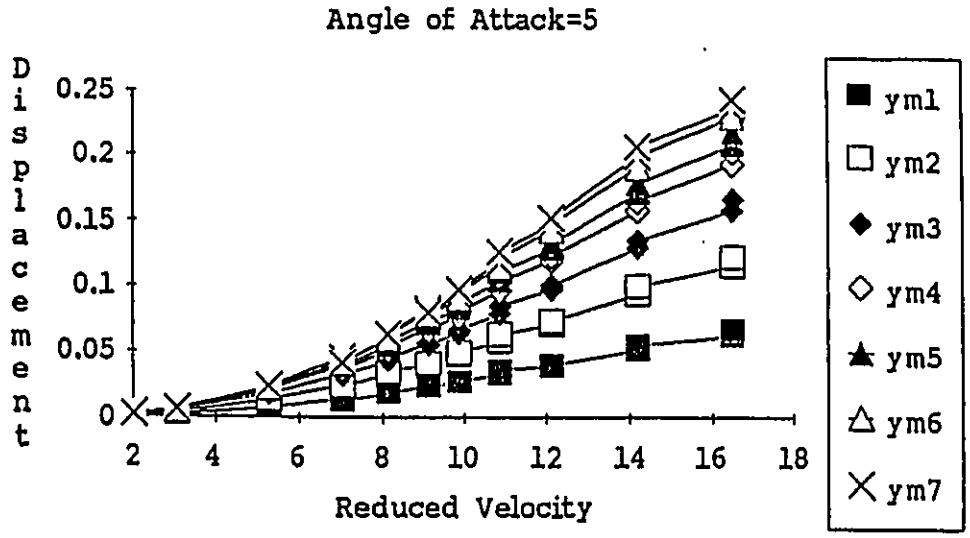

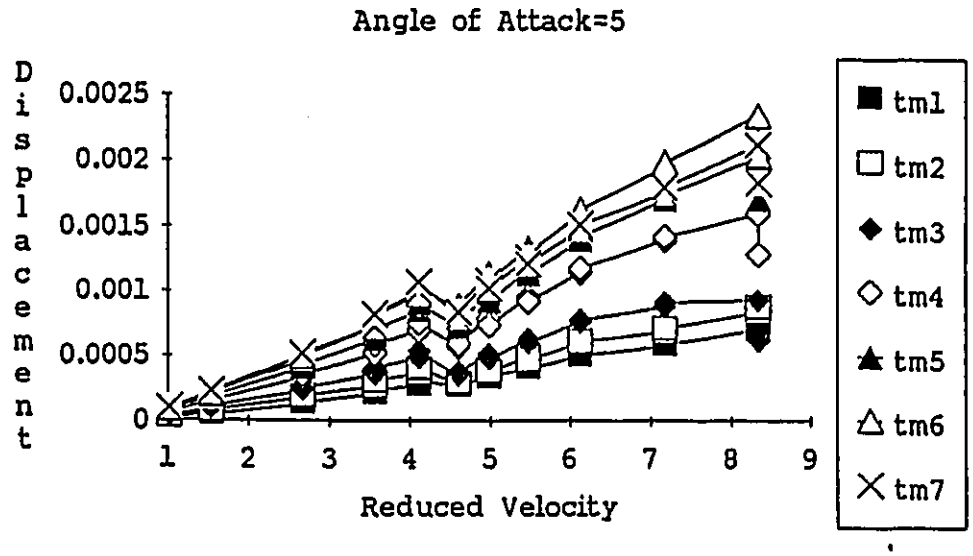

Fig.5.1 Mean Displacements vs. Reduced Velocity

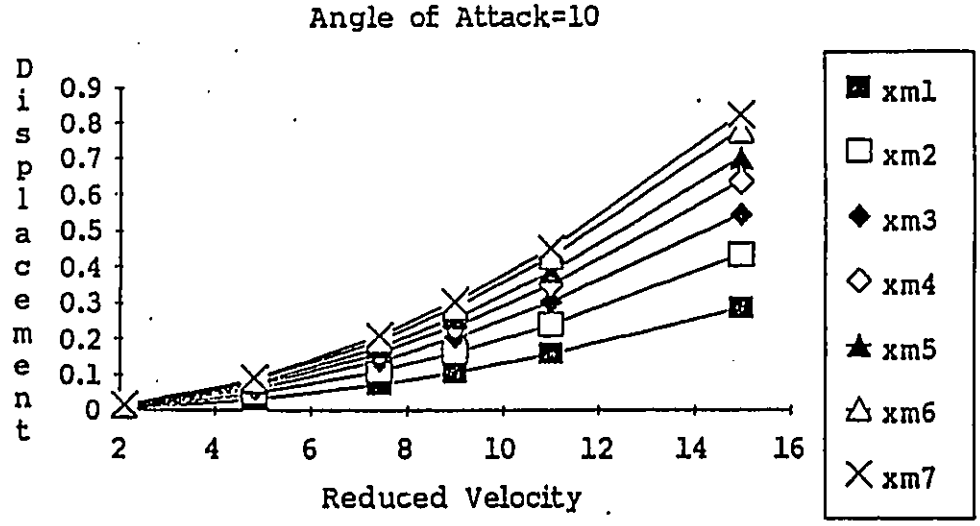

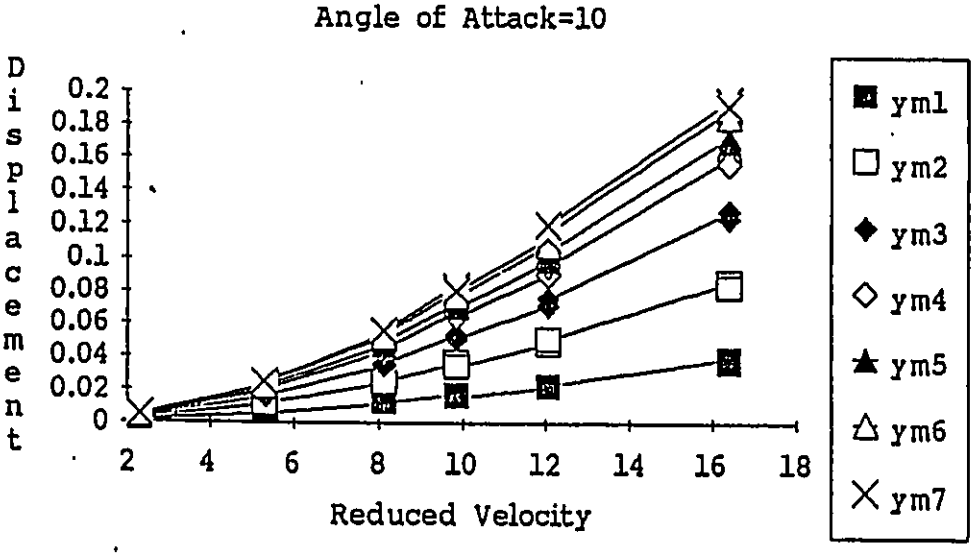

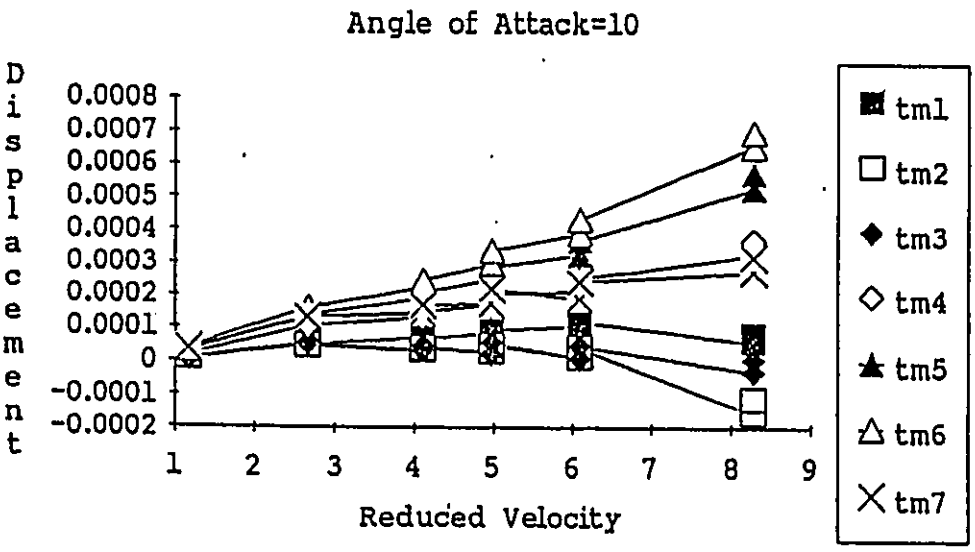

Fig.5.1 Mean Displacements vs. Reduced Velocity

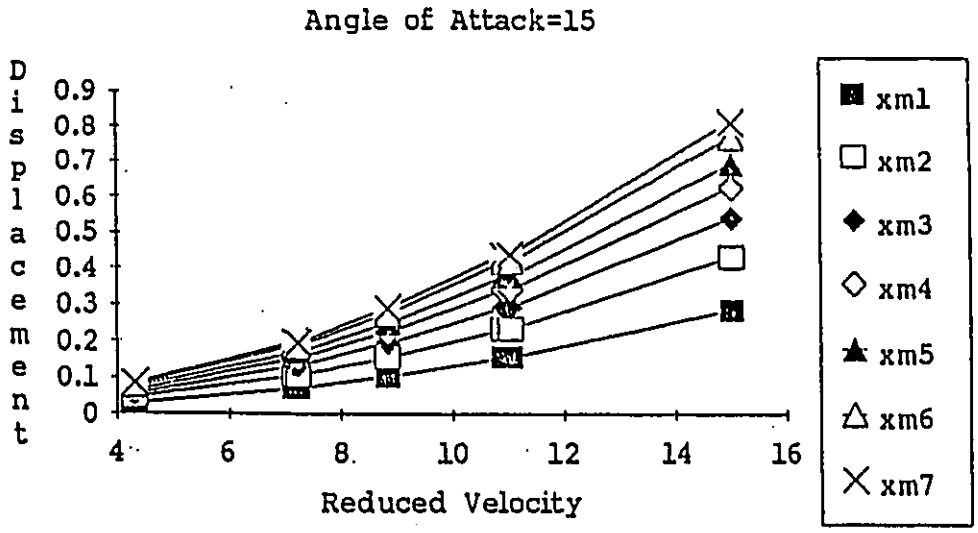

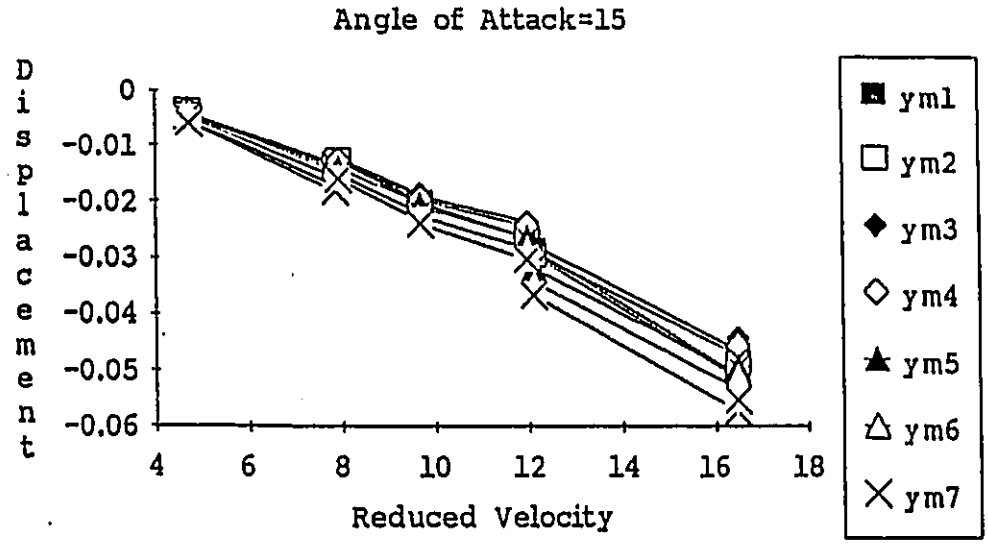

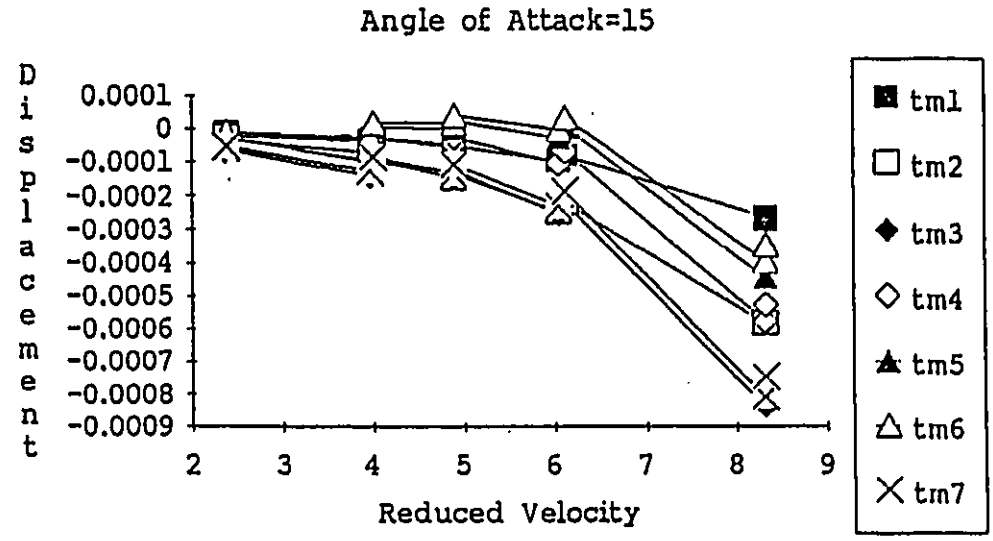

Fig.5.1 Mean Displacements vs. Reduced Velocity

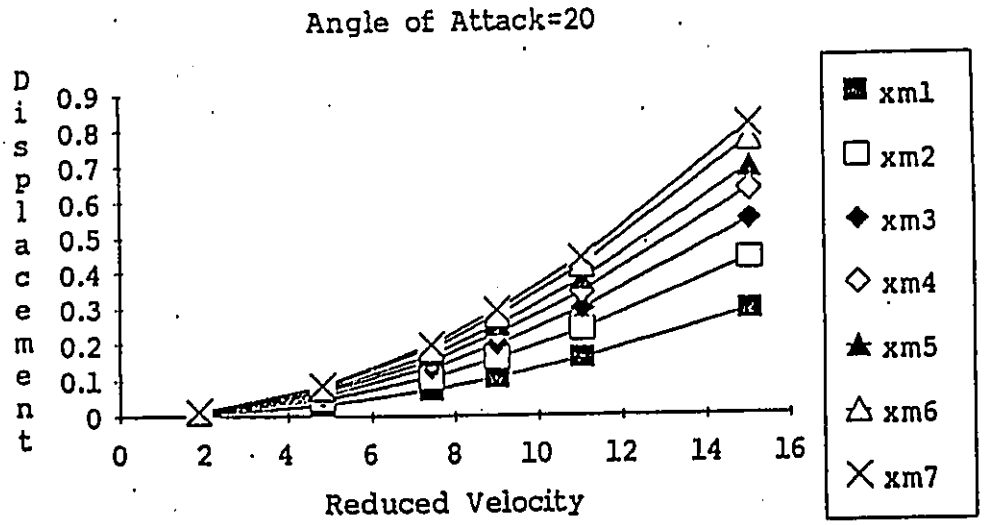

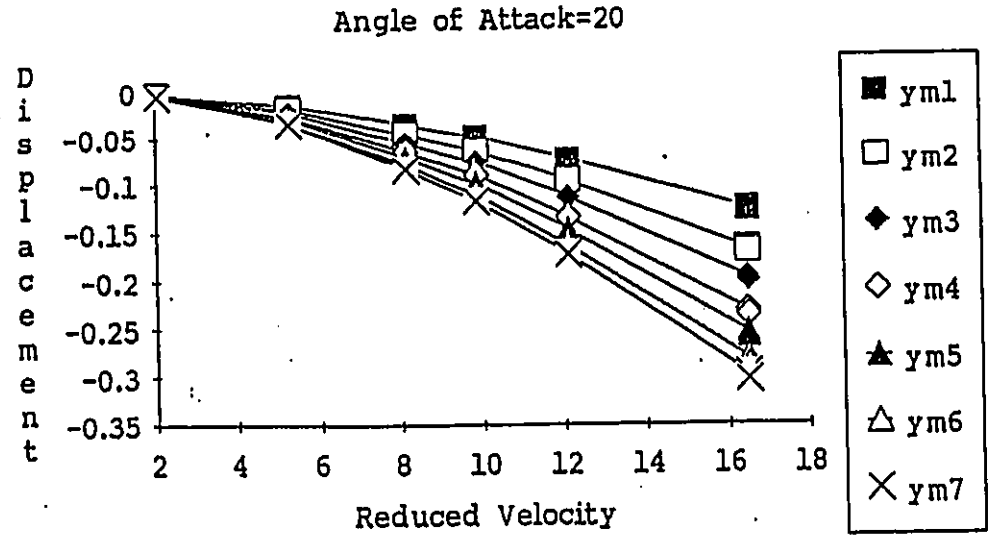

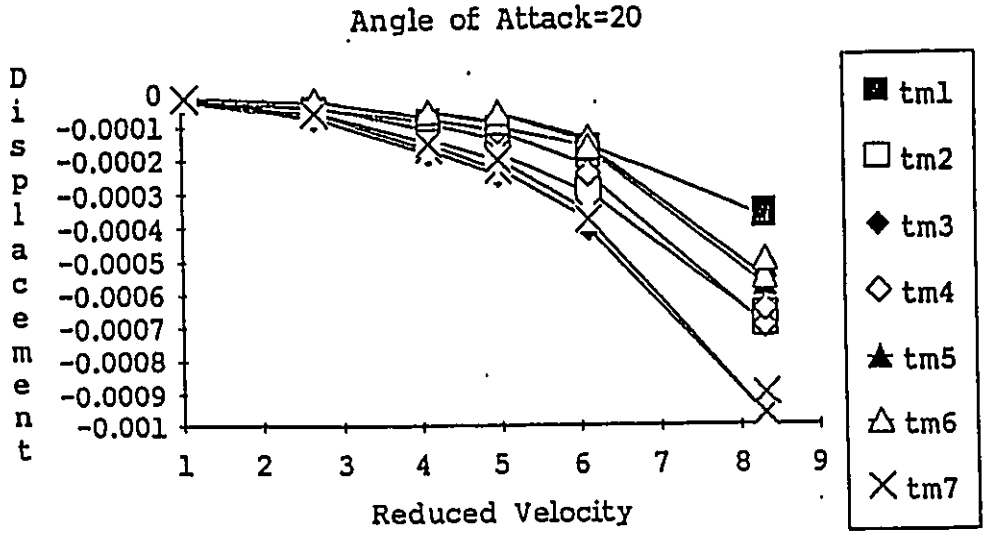

Fig.5.1 Mean Displacements vs. Reduced Velocity

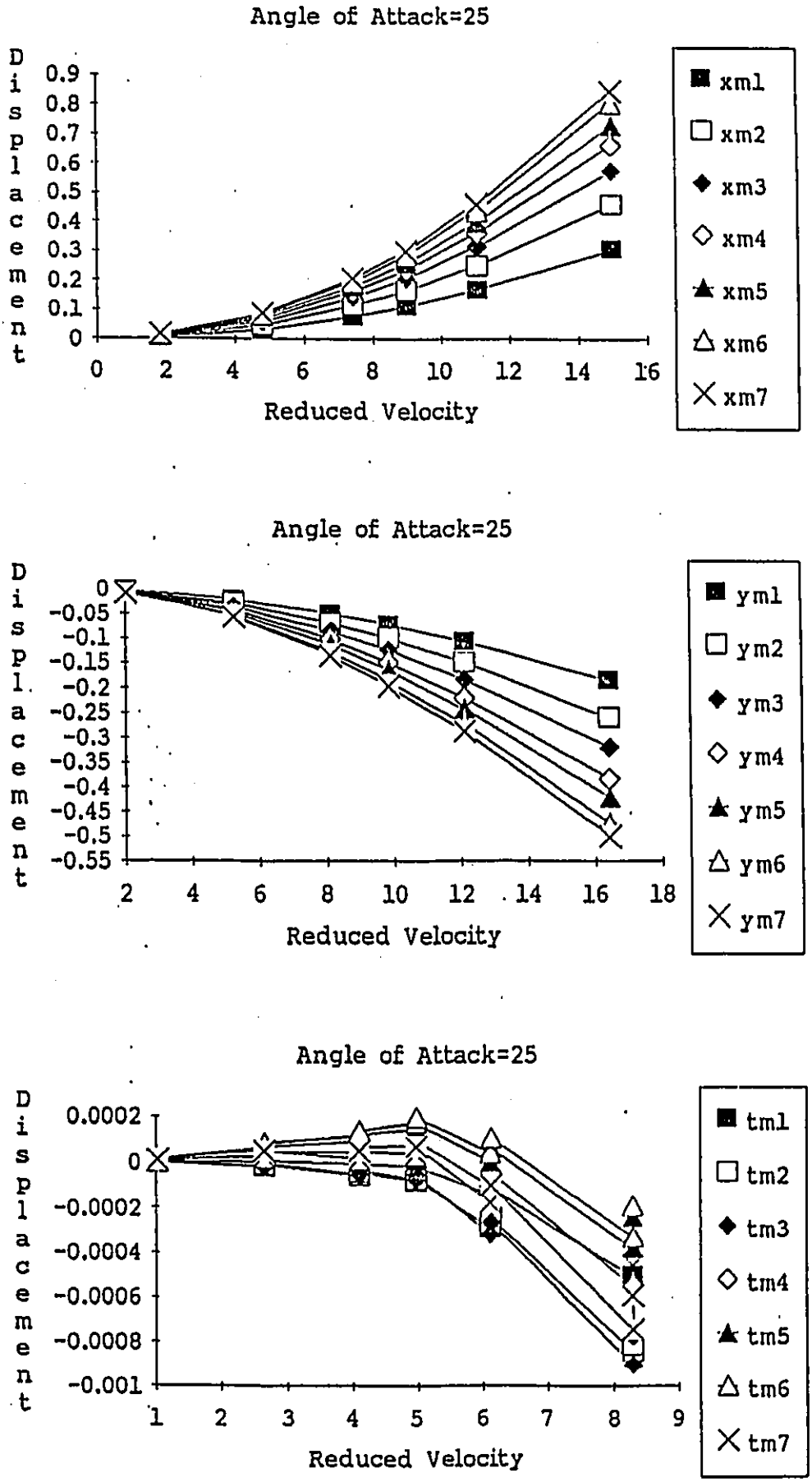

Fig.5.1 Mean Displacements vs. Reduced Velocity

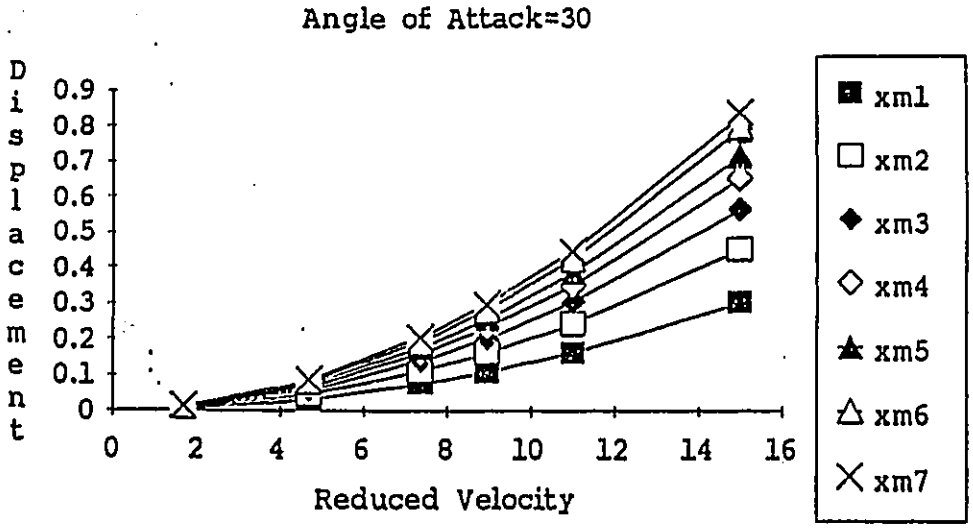

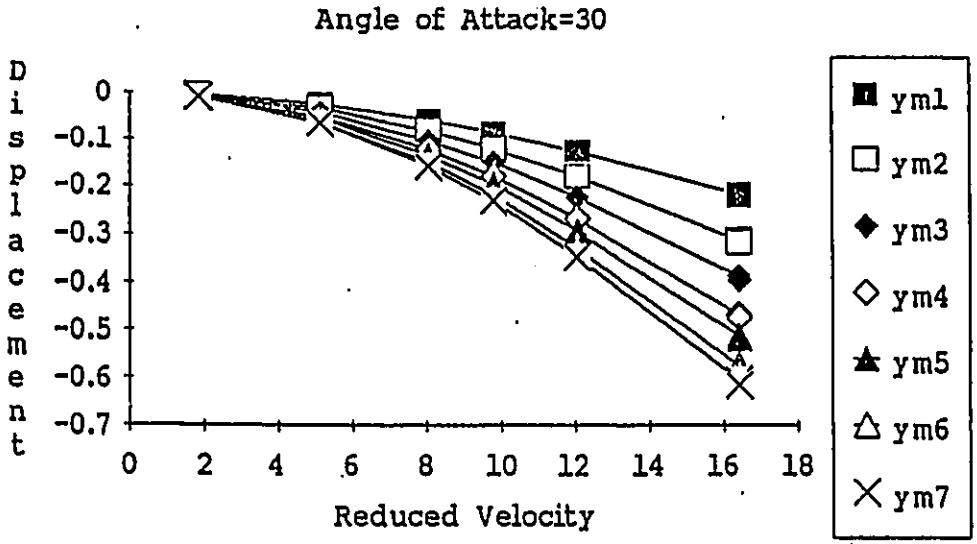

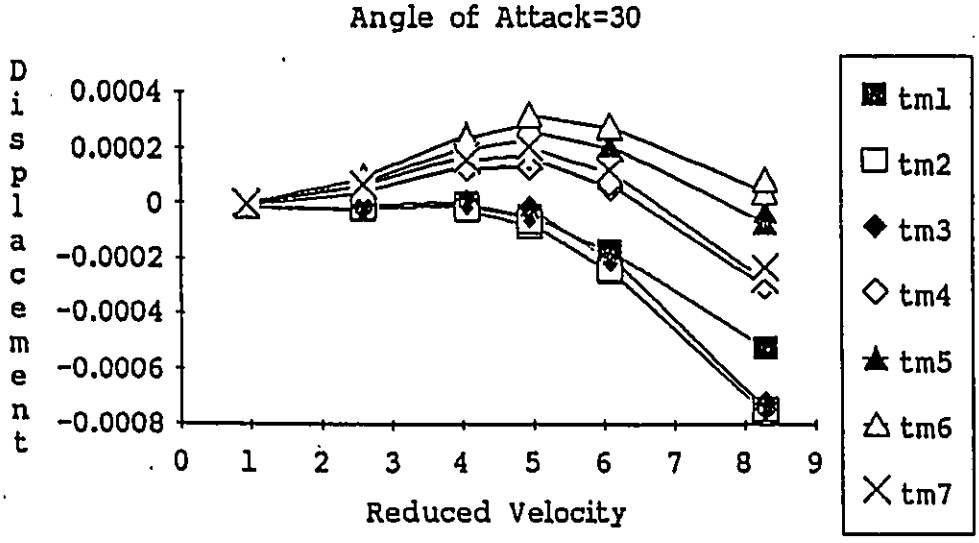

Fig.5.1 Mean Displacements vs. Reduced Velocity

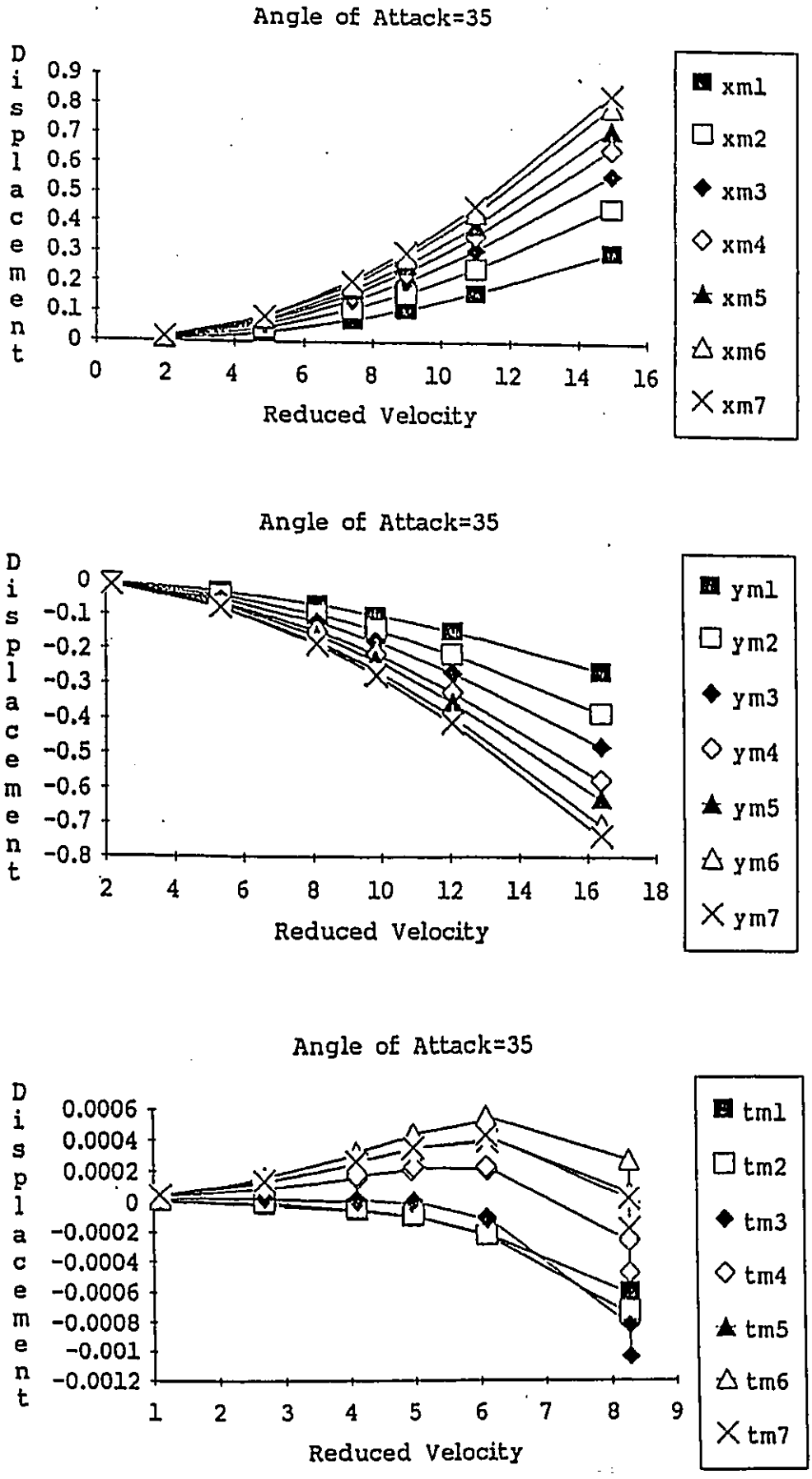

Fig.5.1 Mean Displacements vs. Reduced Velocity

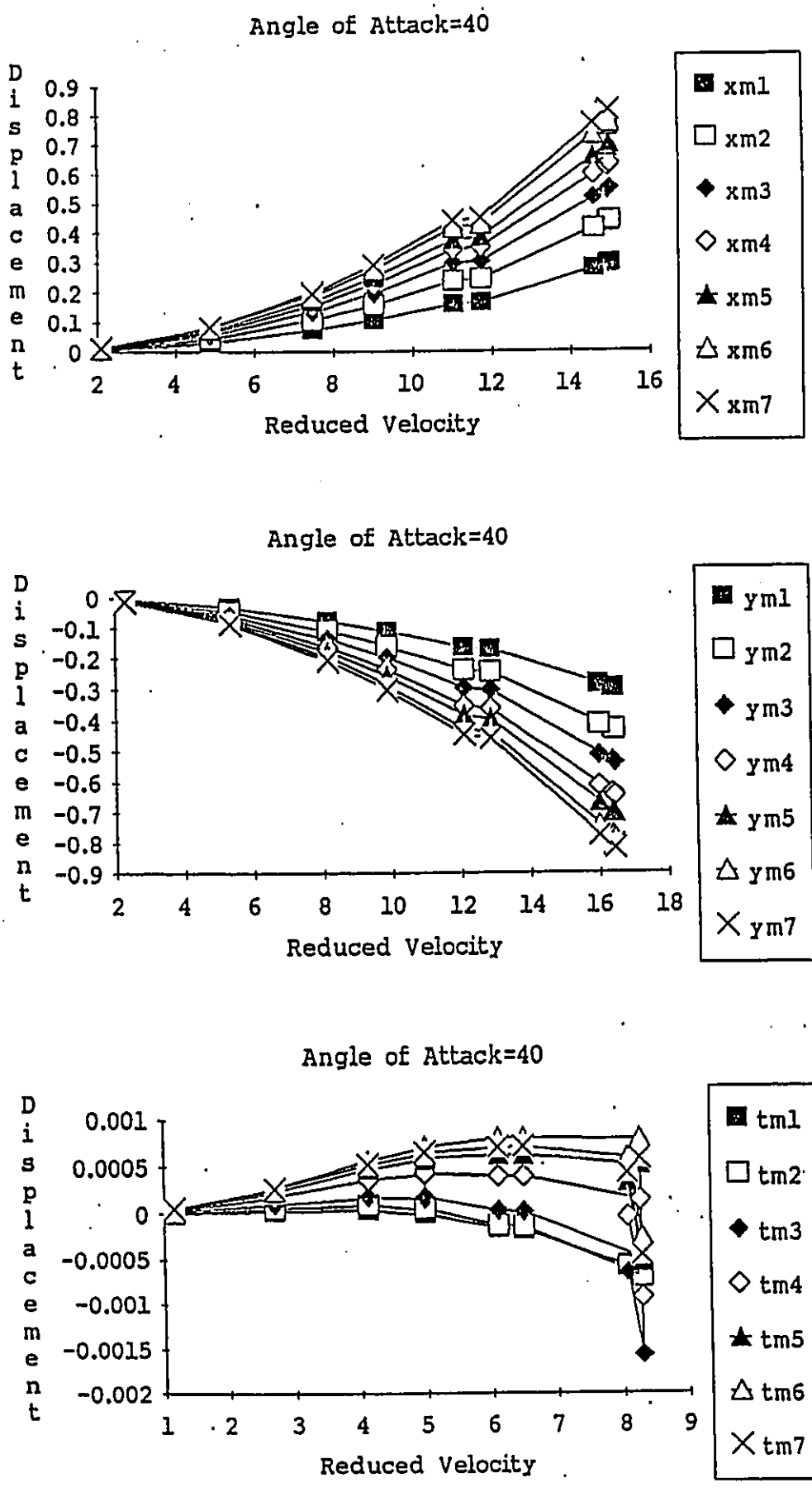

Fig.5.1 Mean Displacements vs. Reduced Velocity

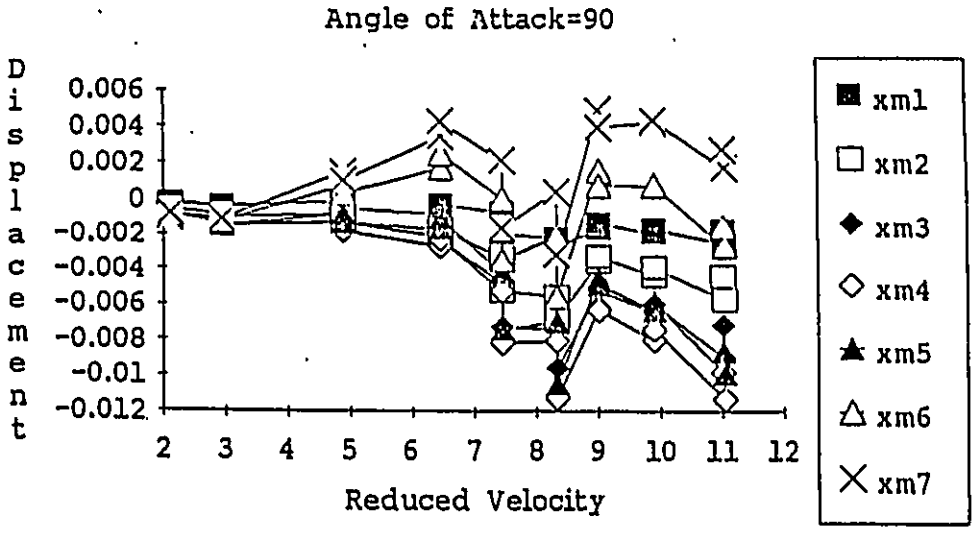

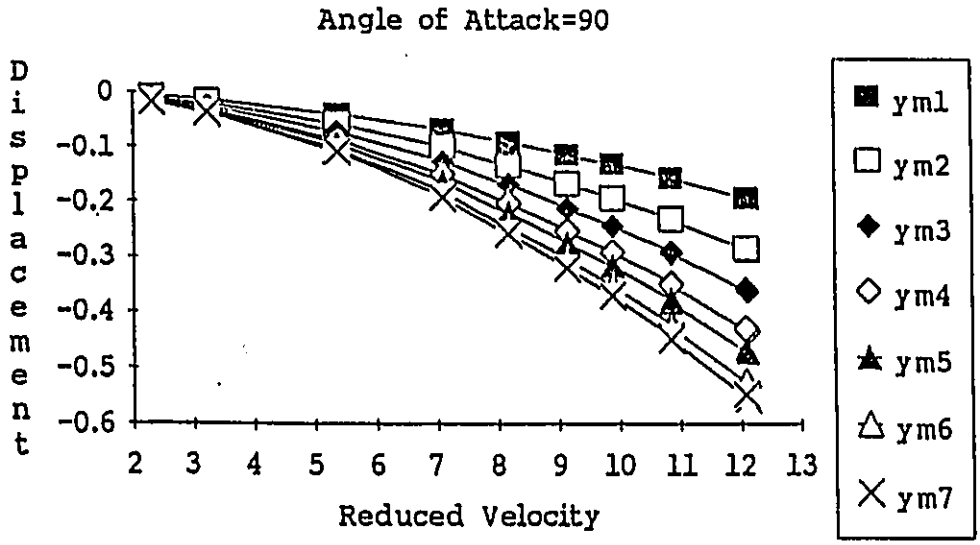

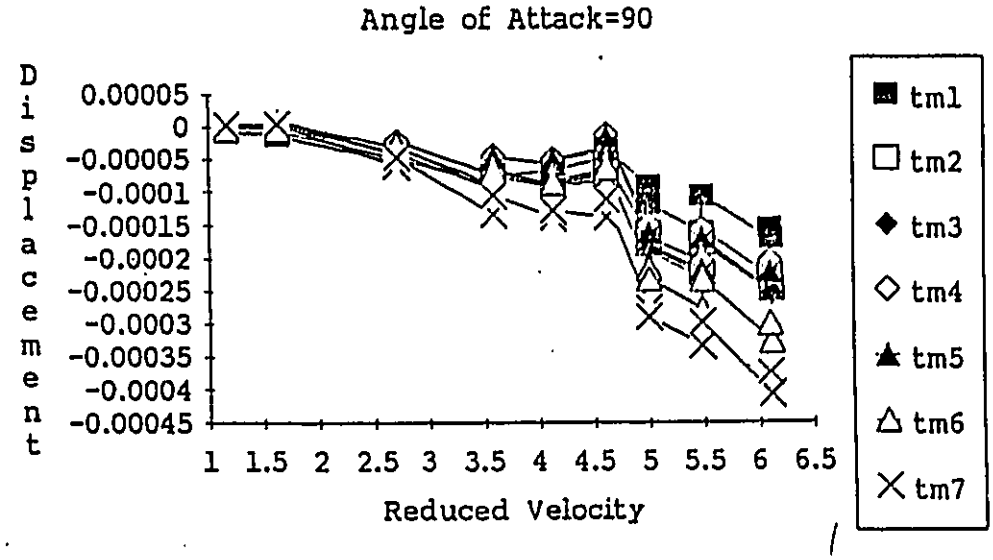

Fig.5.1 Mean Displacements vs. Reduced Velocity

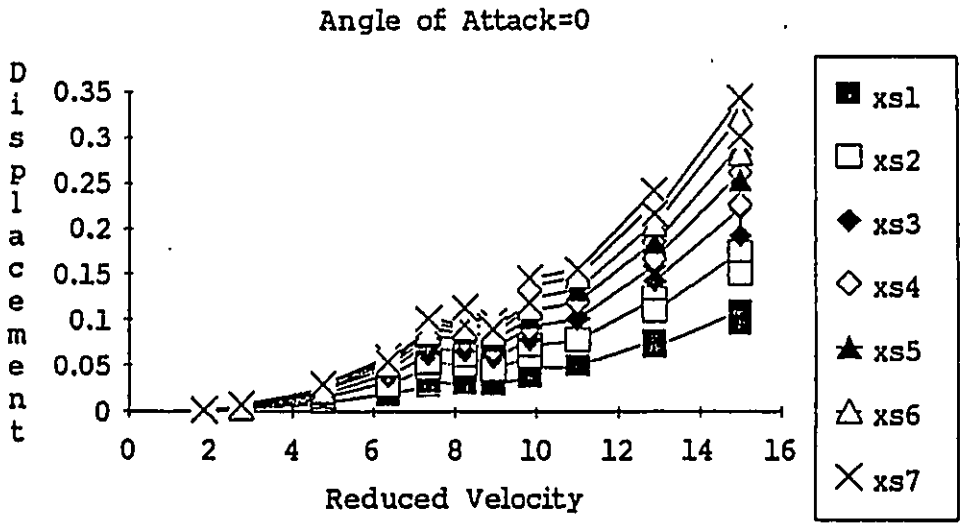

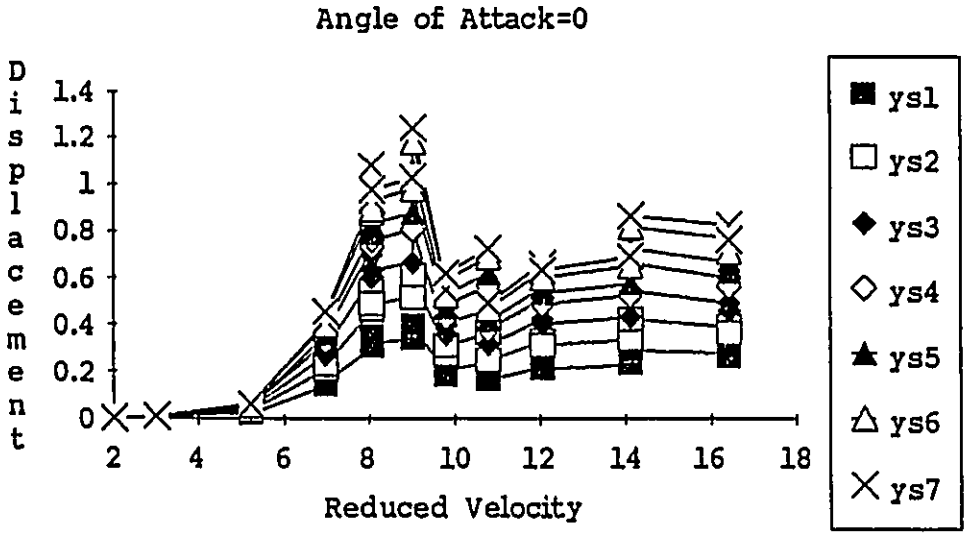

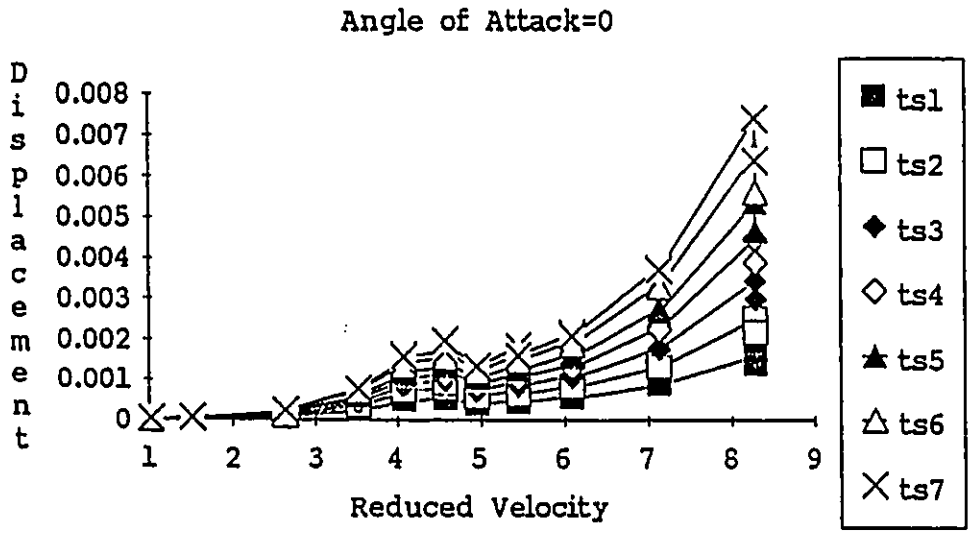

Fig.5.2 RMS Displacements vs. Reduced Velocity

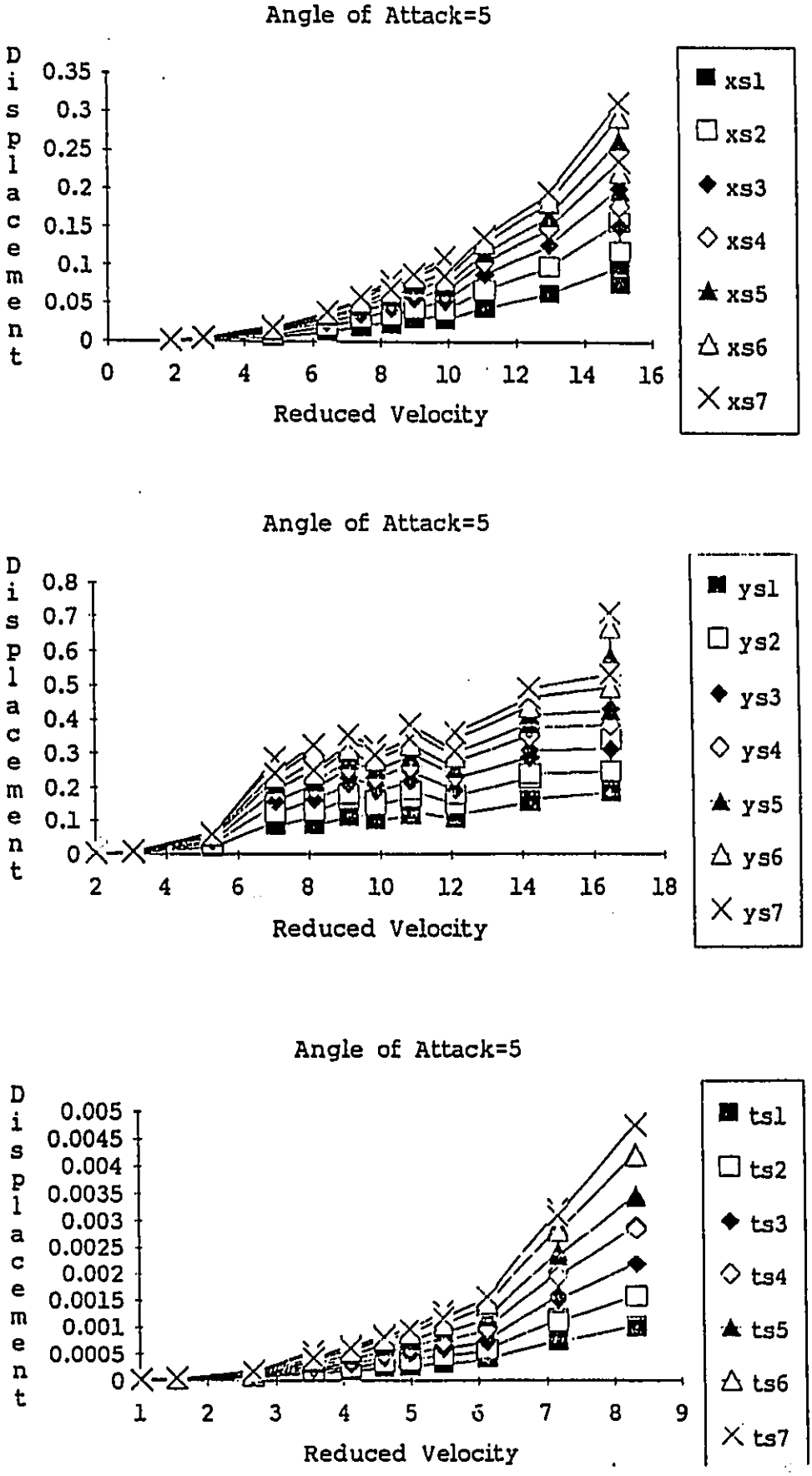

Fig.5.2 RMS Displacements vs. Reduced Velocity

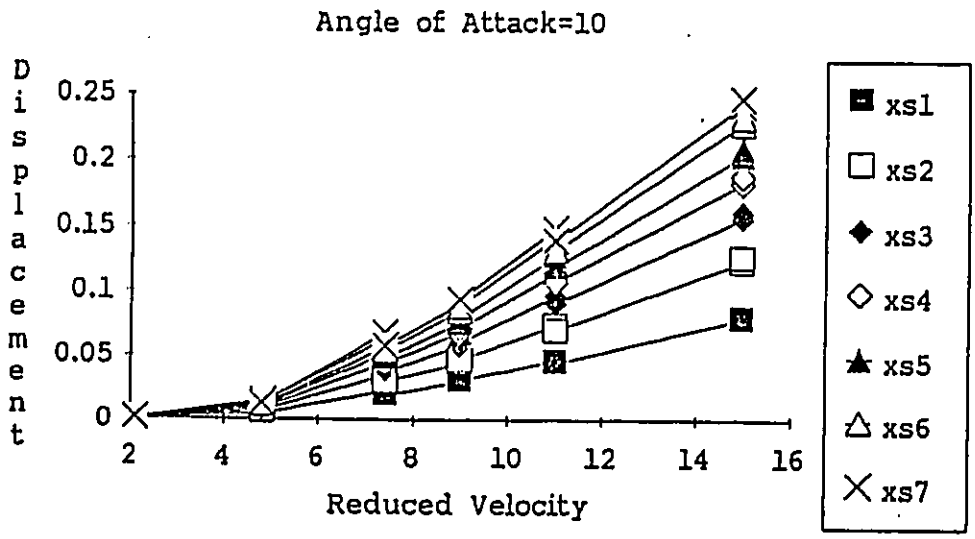

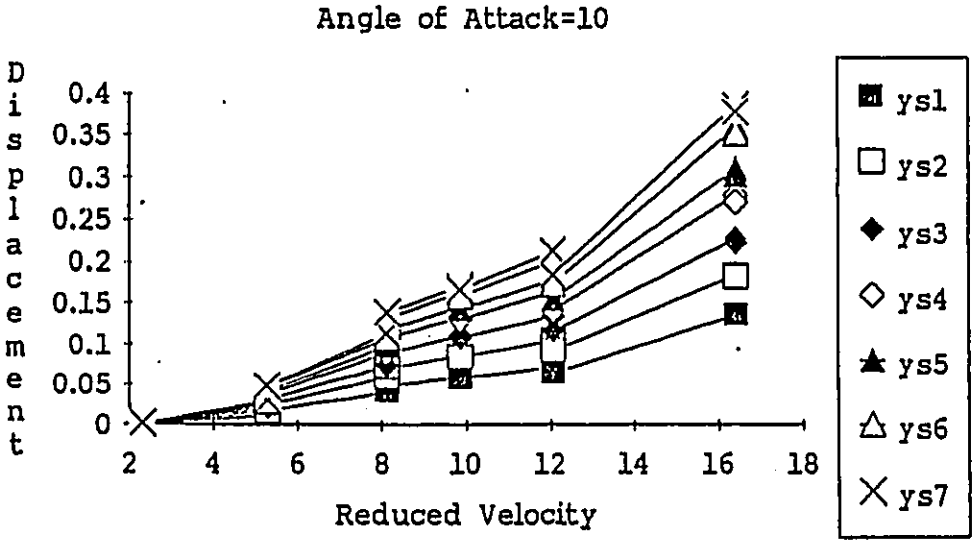

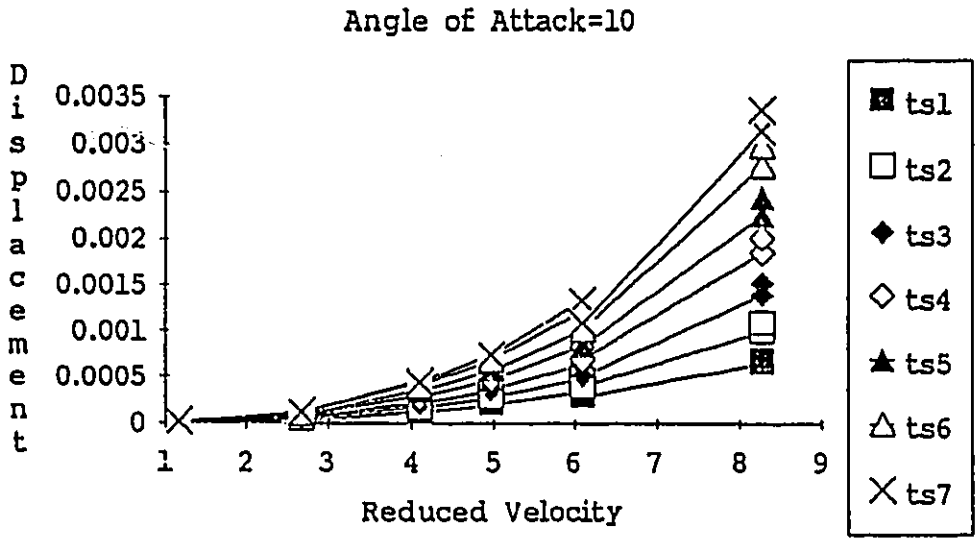

Fig.5.2 RMS Displacements vs. Reduced Velocity

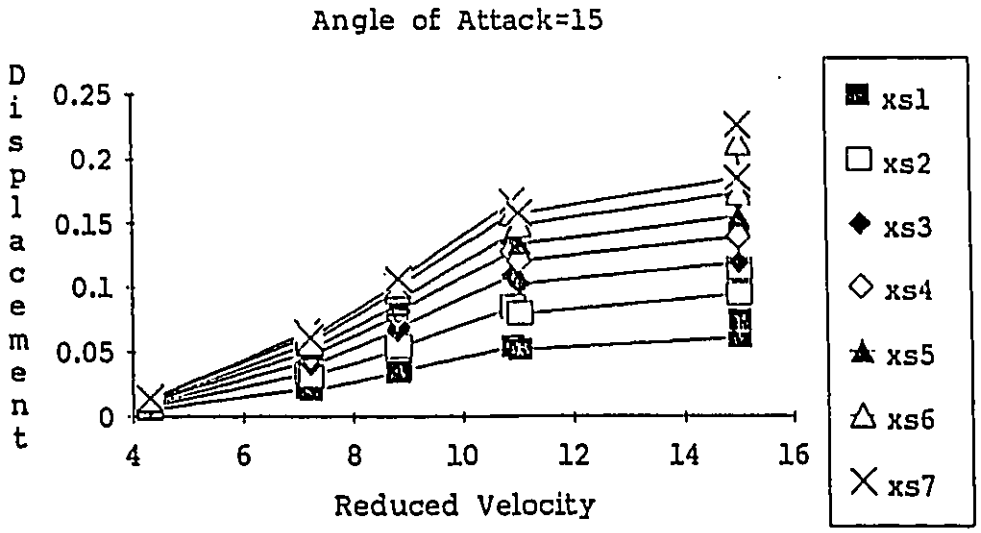

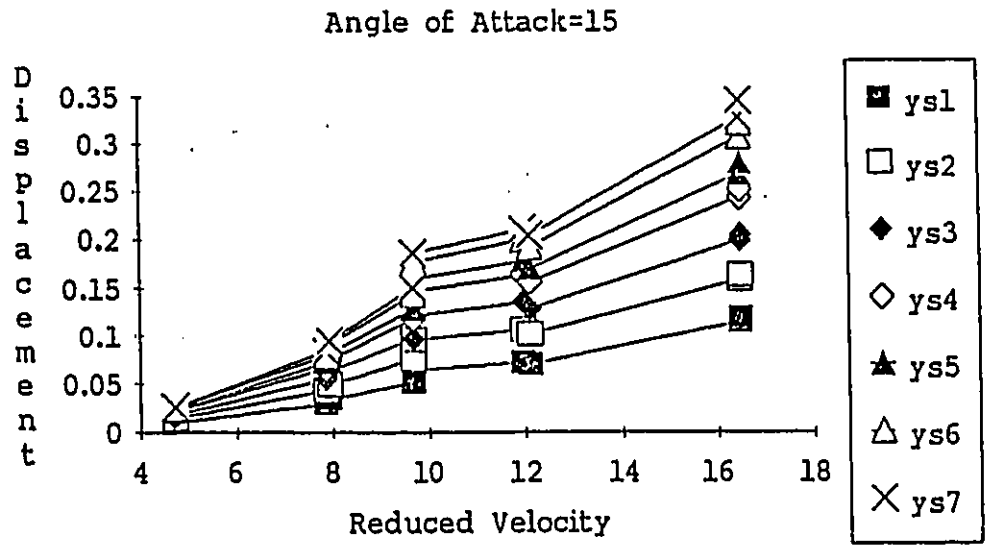

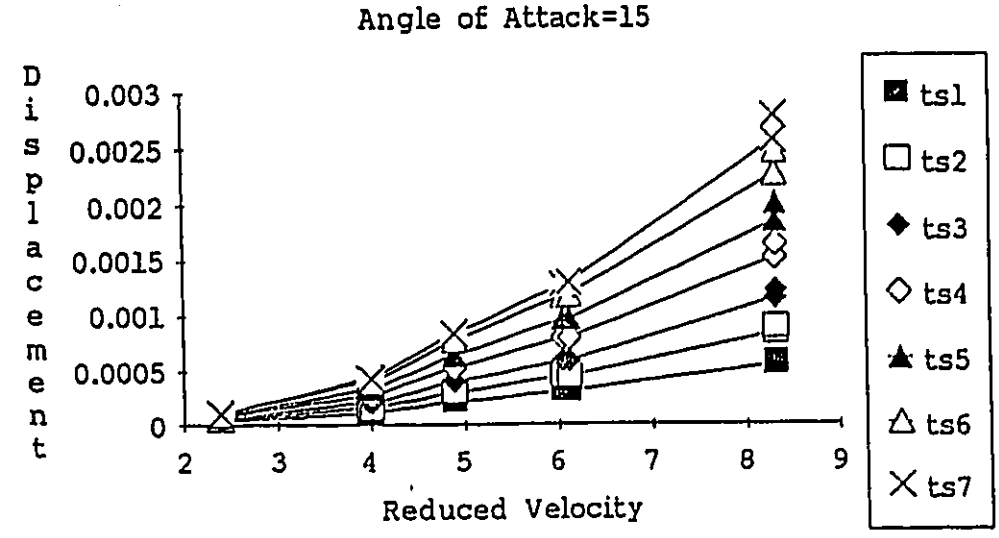

Fig.5.2 RMS Displacements vs. Reduced Velocity

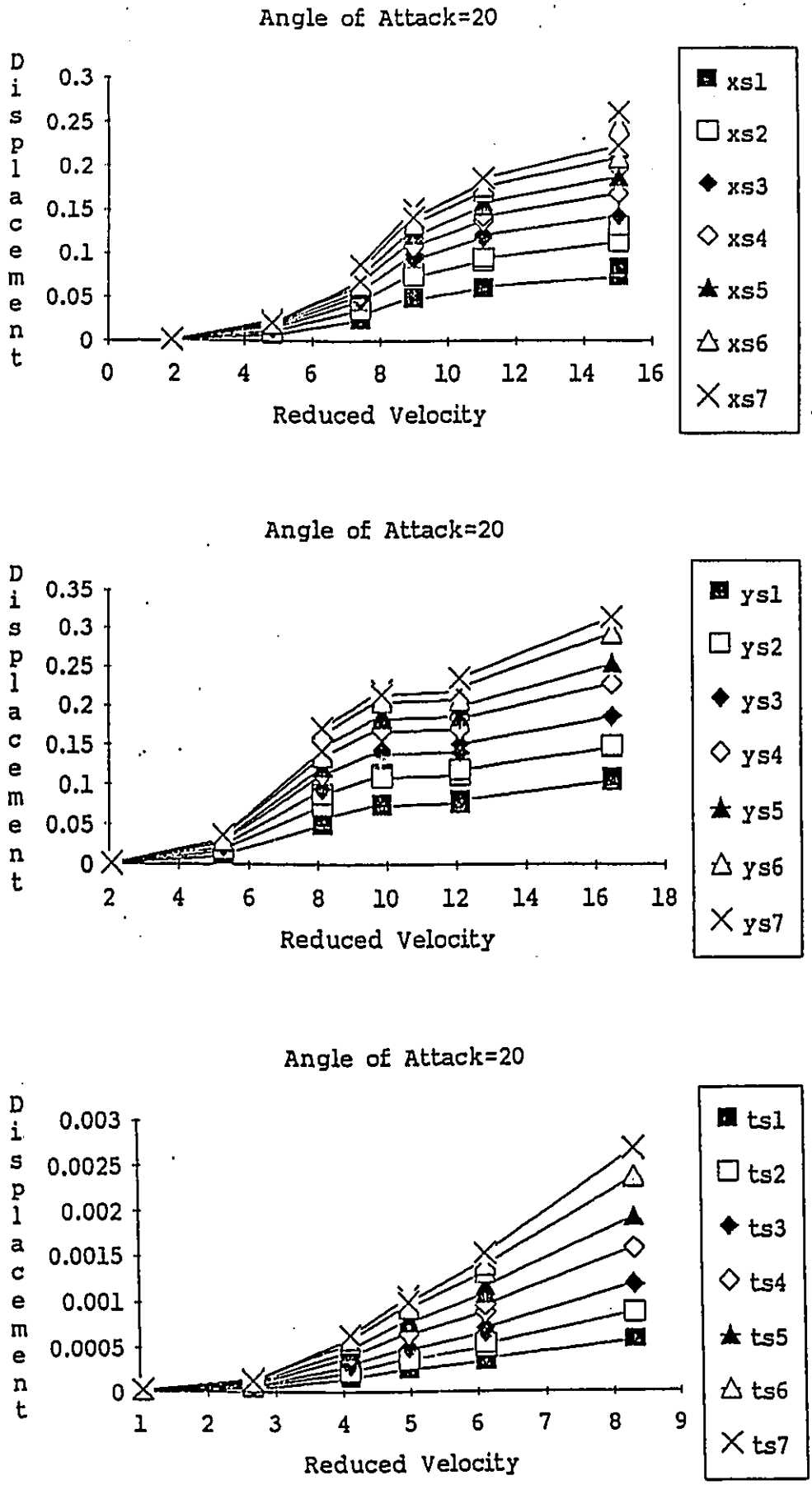

Fig.5.2 RMS Displacements vs. Reduced Velocity

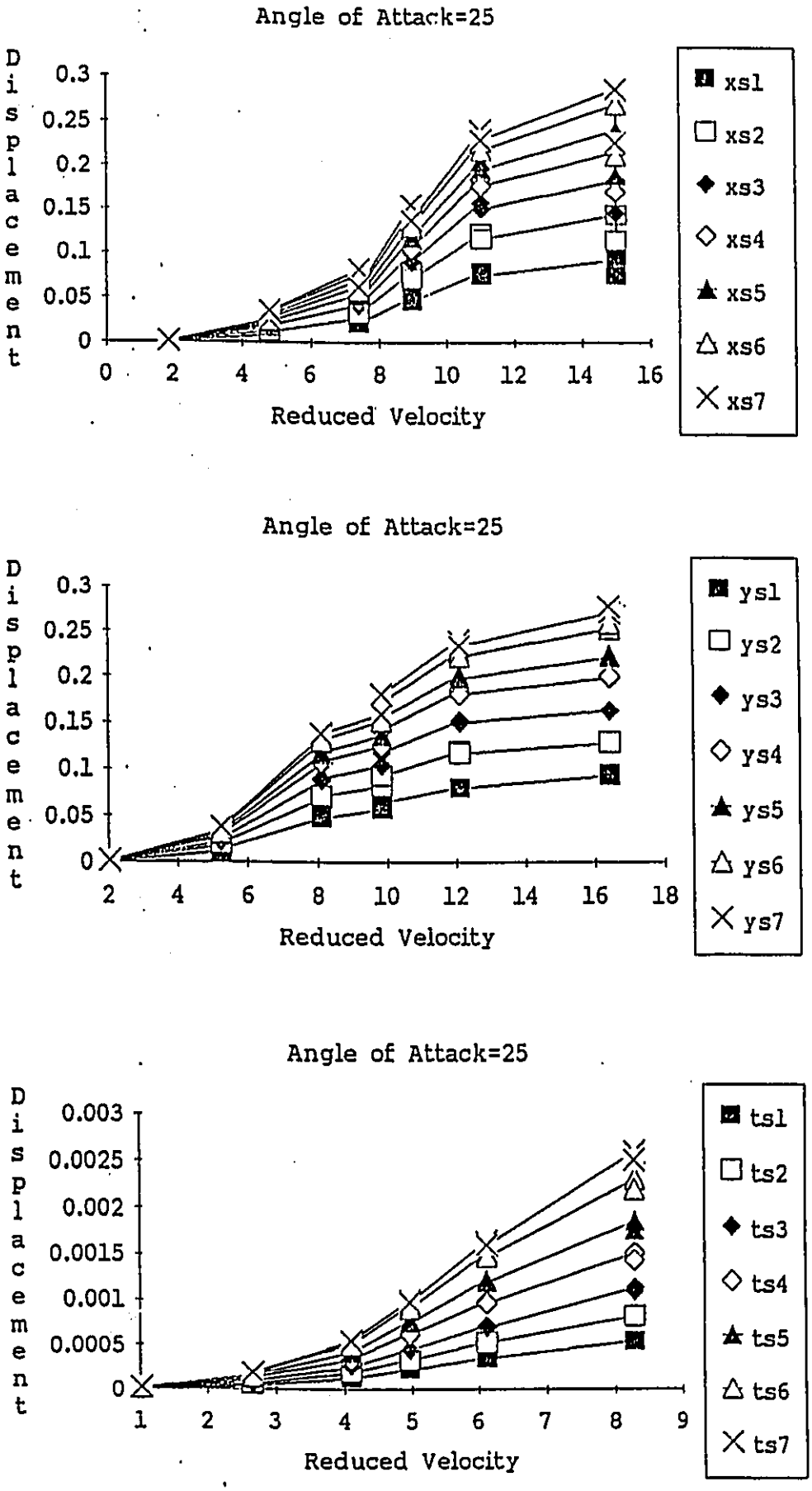

Fig.5.2 RMS Displacements vs. Reduced Velocity

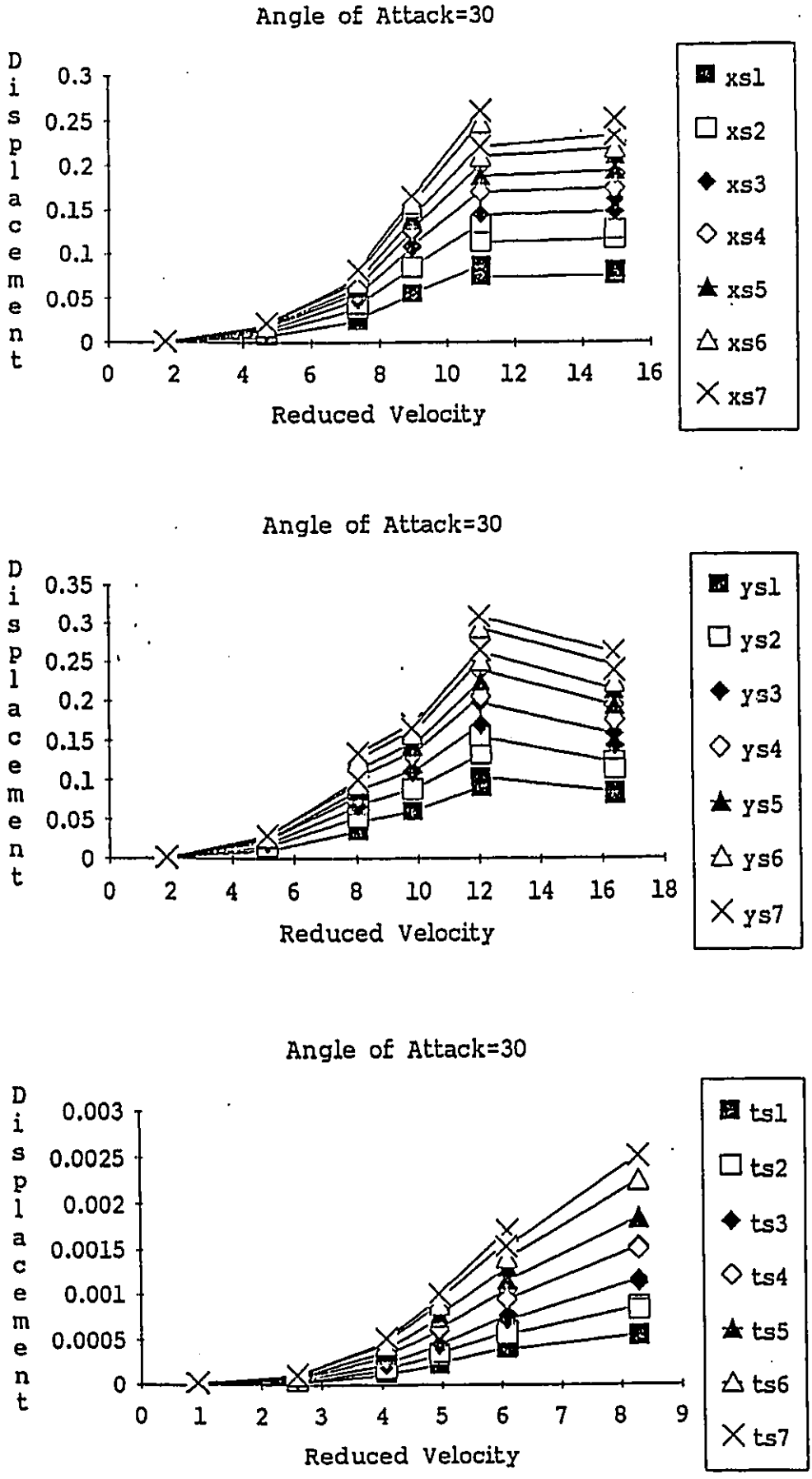

Fig.5.2 RMS Displacements vs. Reduced Velocity

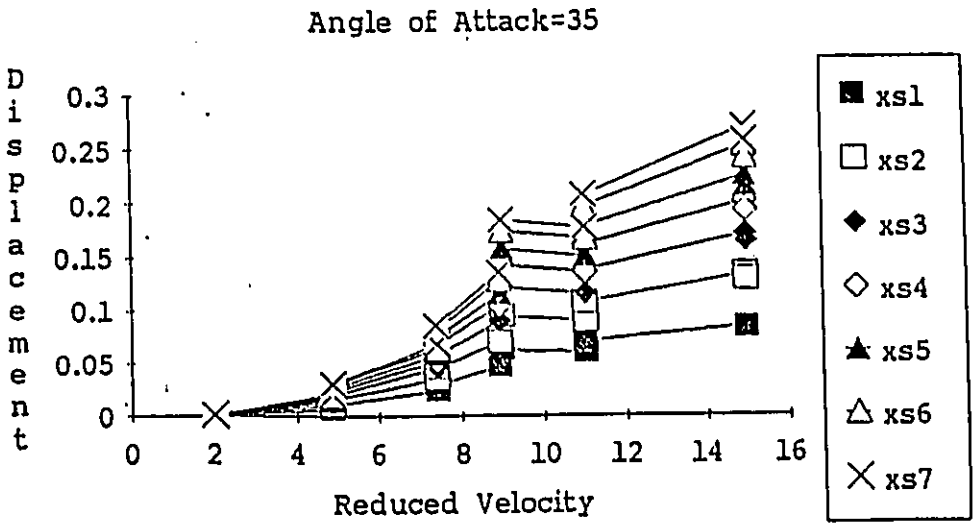

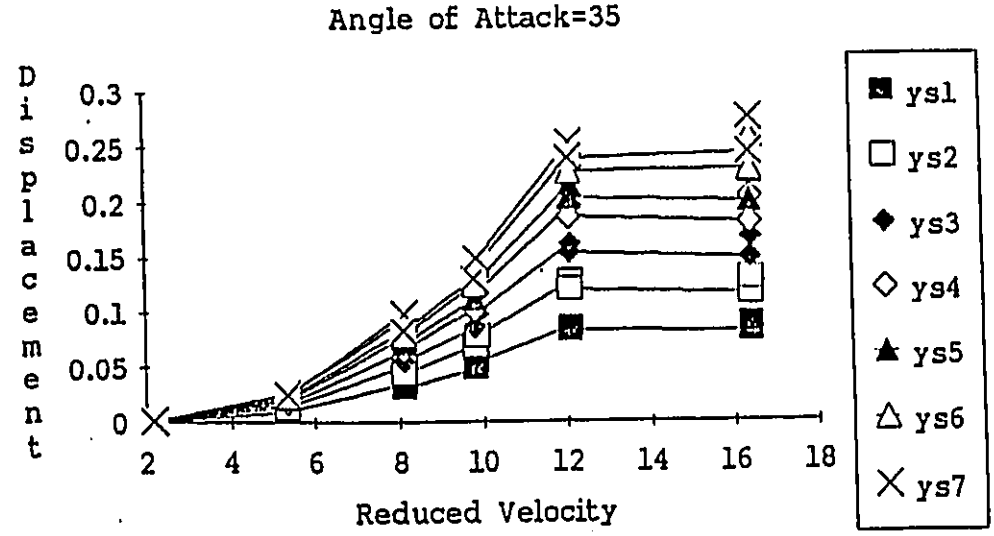

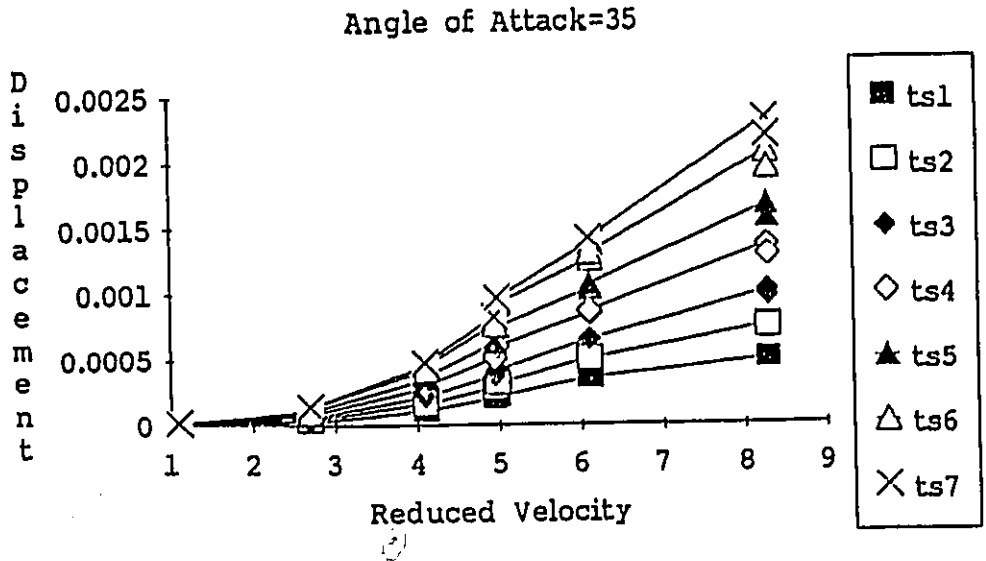

Fig.5.2 RMS Displacements vs. Reduced Velocity

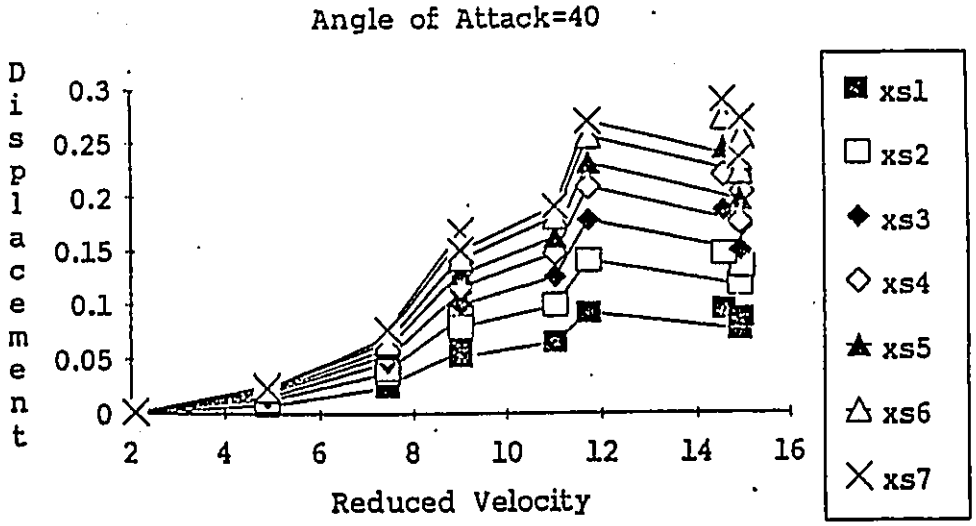

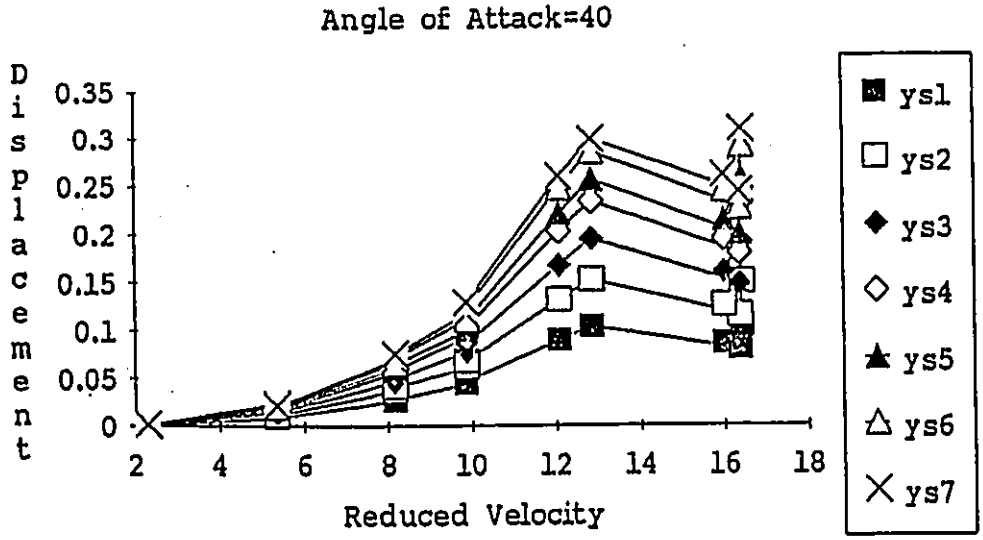

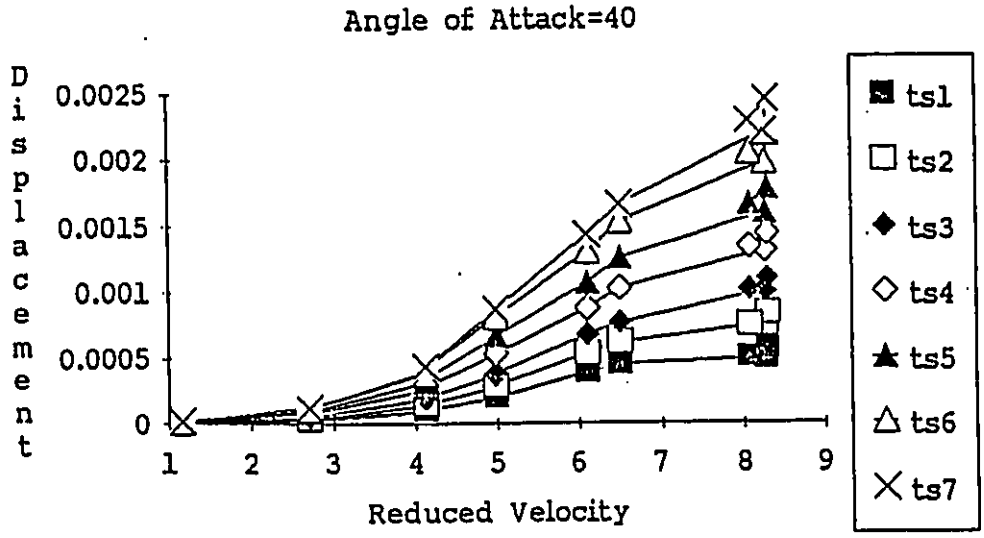

Fig.5.2 RMS Displacements vs. Reduced Velocity

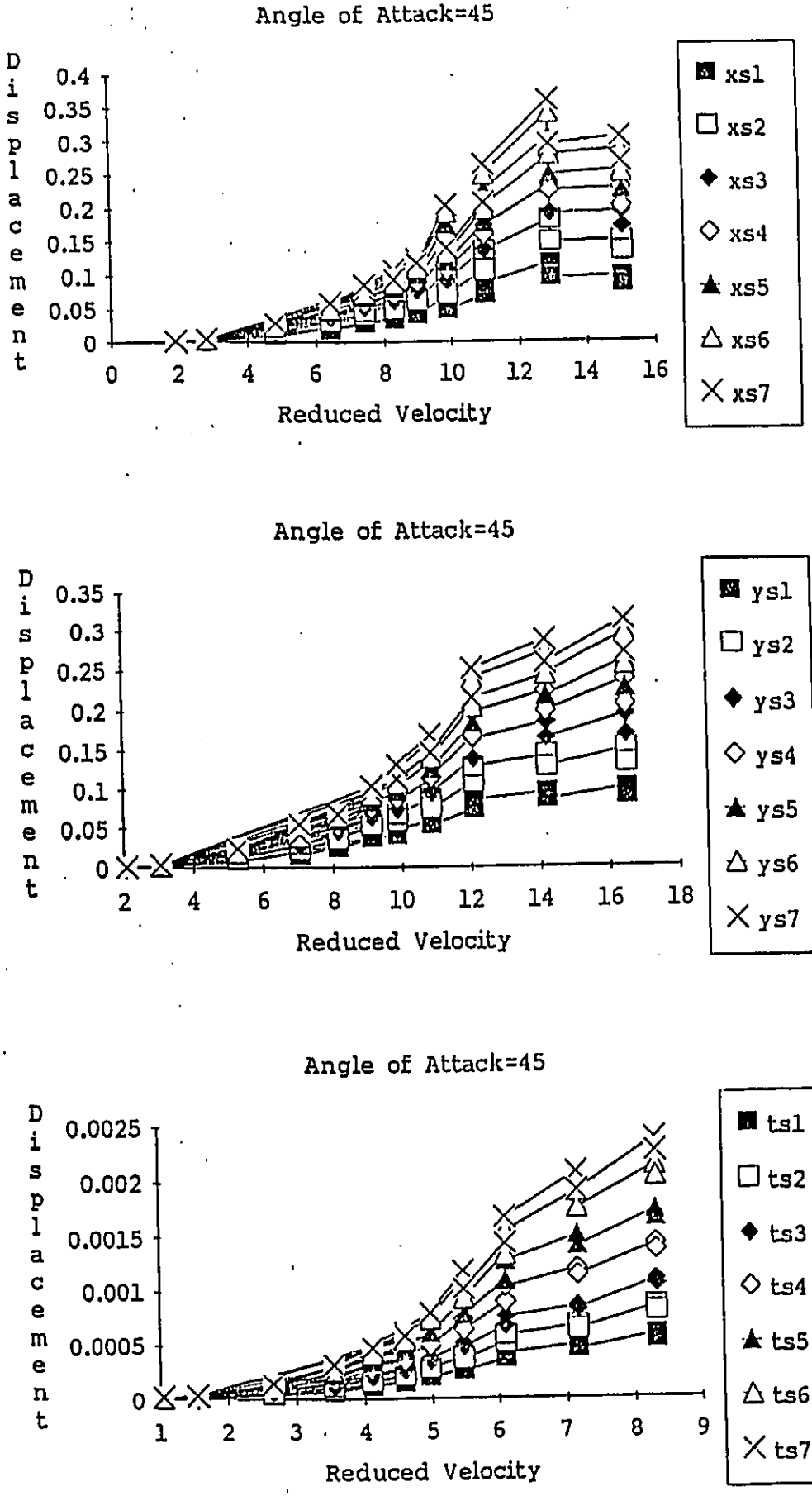

Fig.5.2 RMS Displacements vs. Reduced Velocity

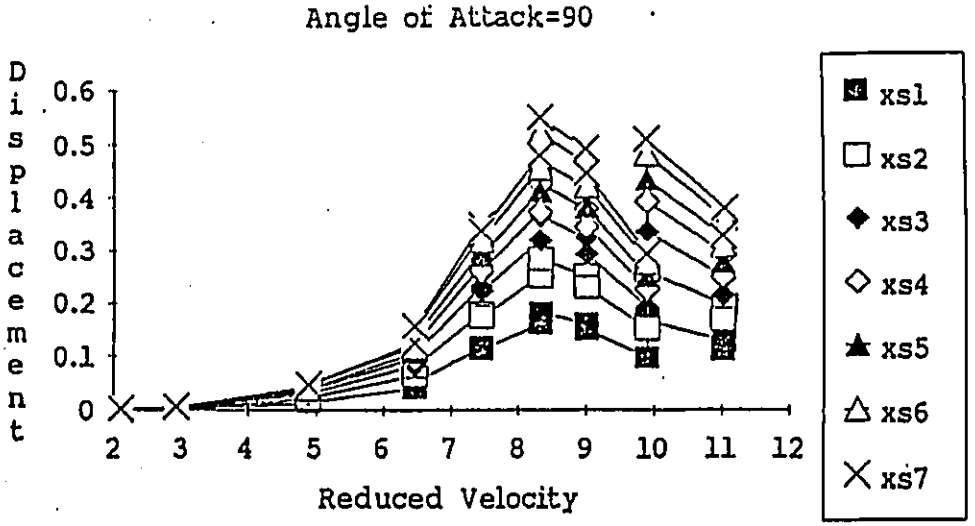

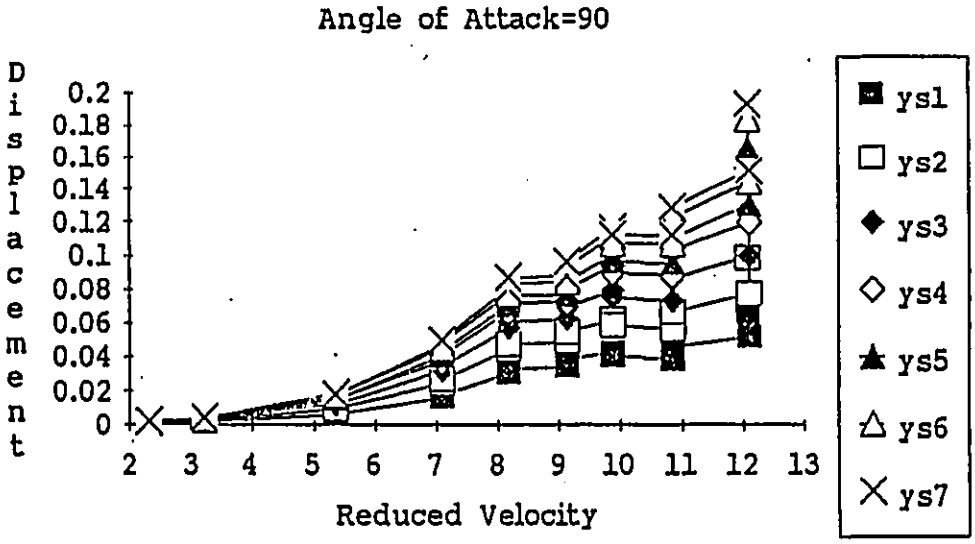

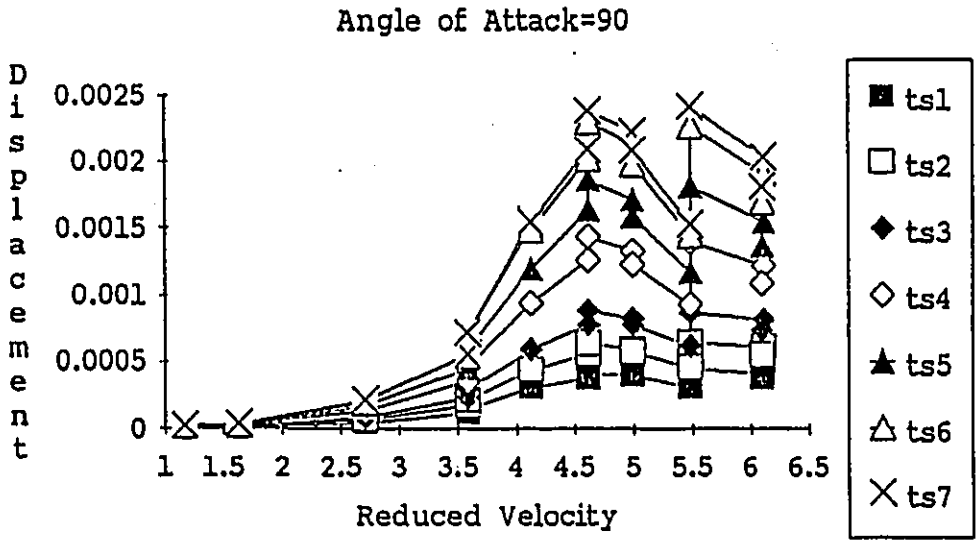

Fig.5.2 RMS Displacements vs. Reduced Velocity

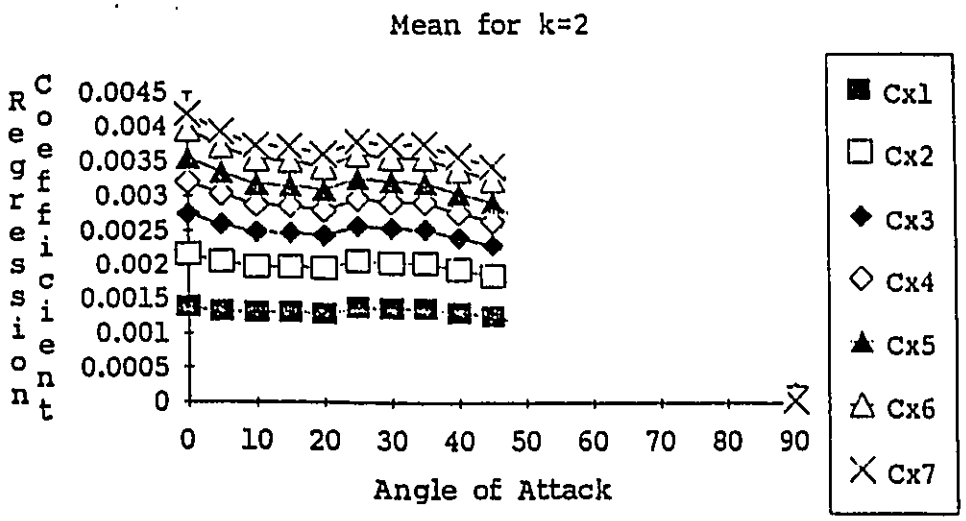

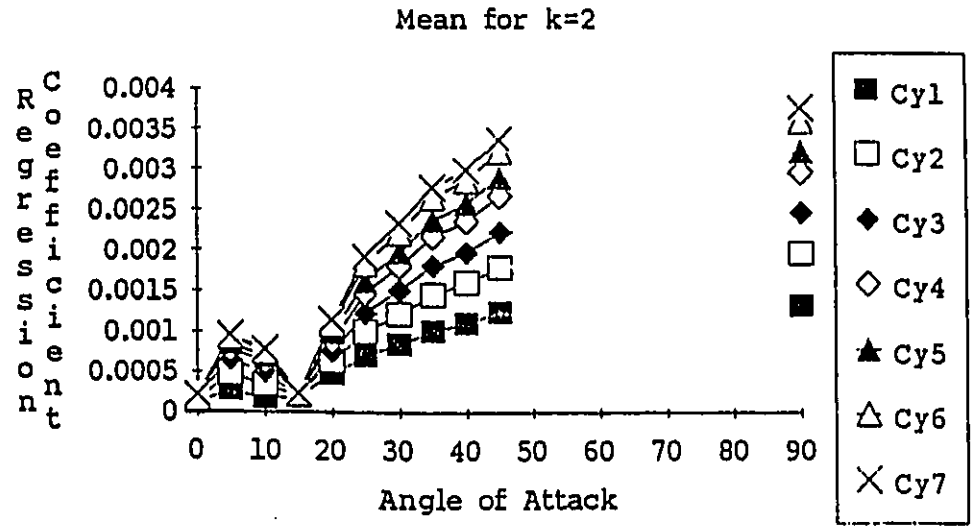

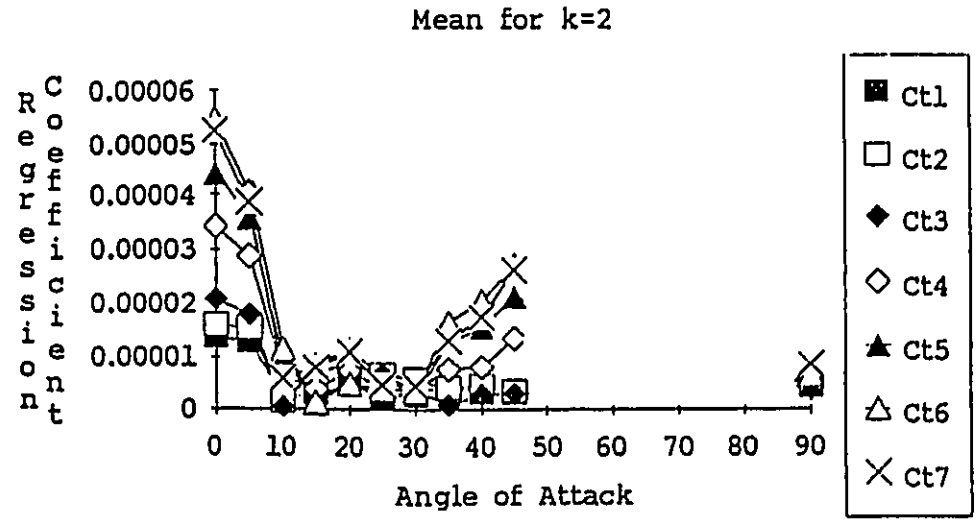

Fig.5.3 Relative Magnitude of Mean Response

(from [4.3])

Standard Deviation

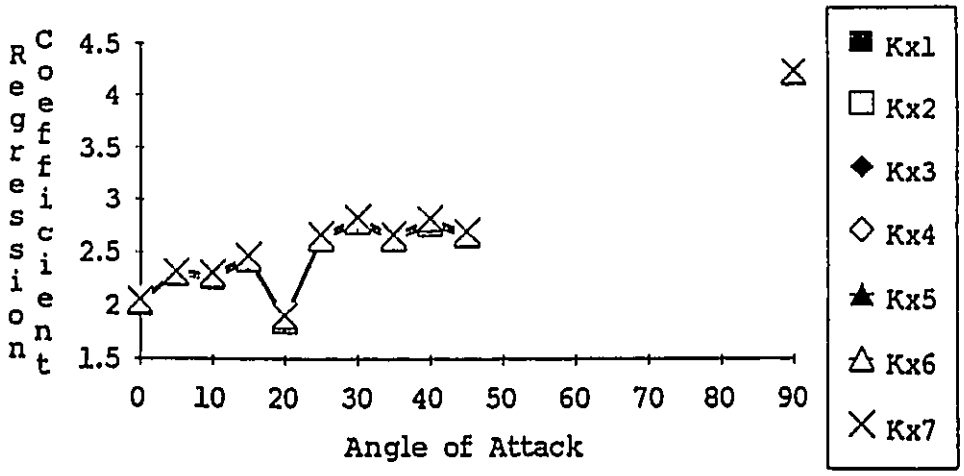

Standard Deviation

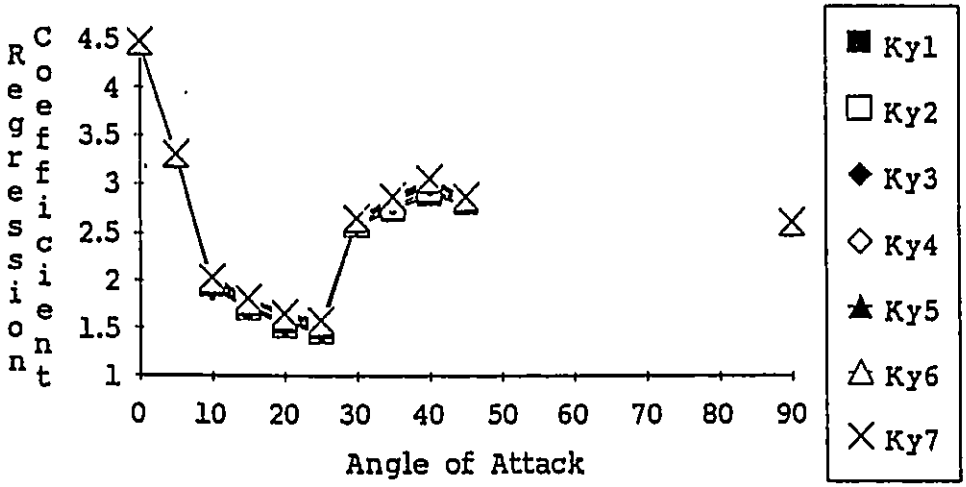

Standard Deviation

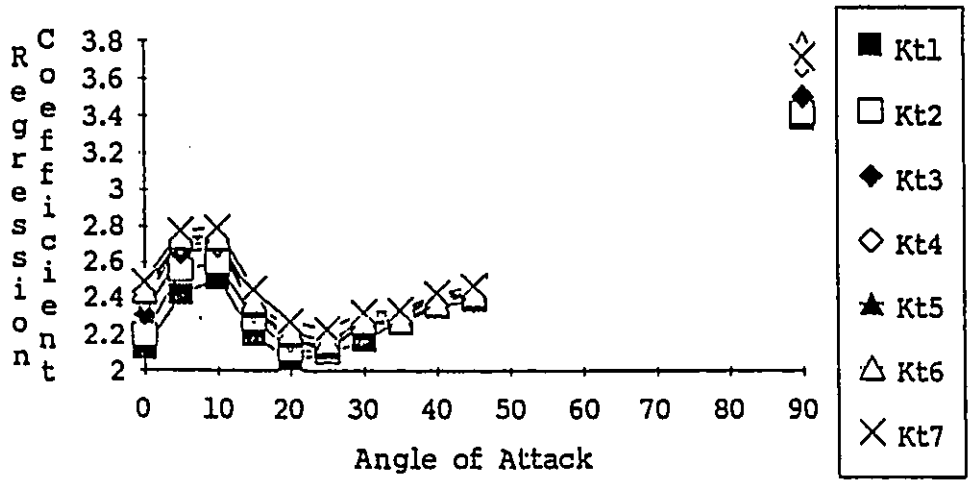

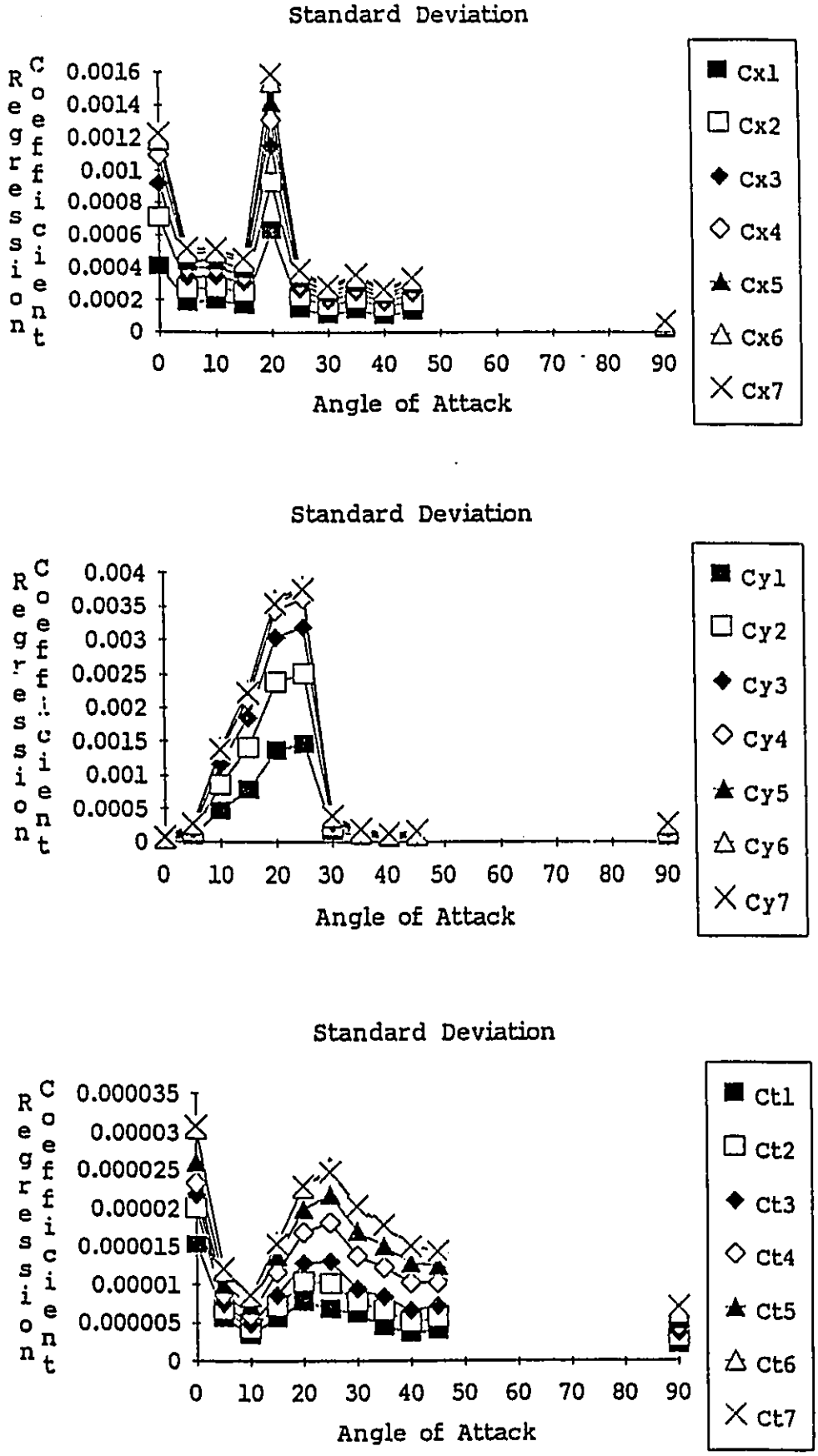

Fig.5.4 K and C Coefficients For RMS Response

(from [4.3])

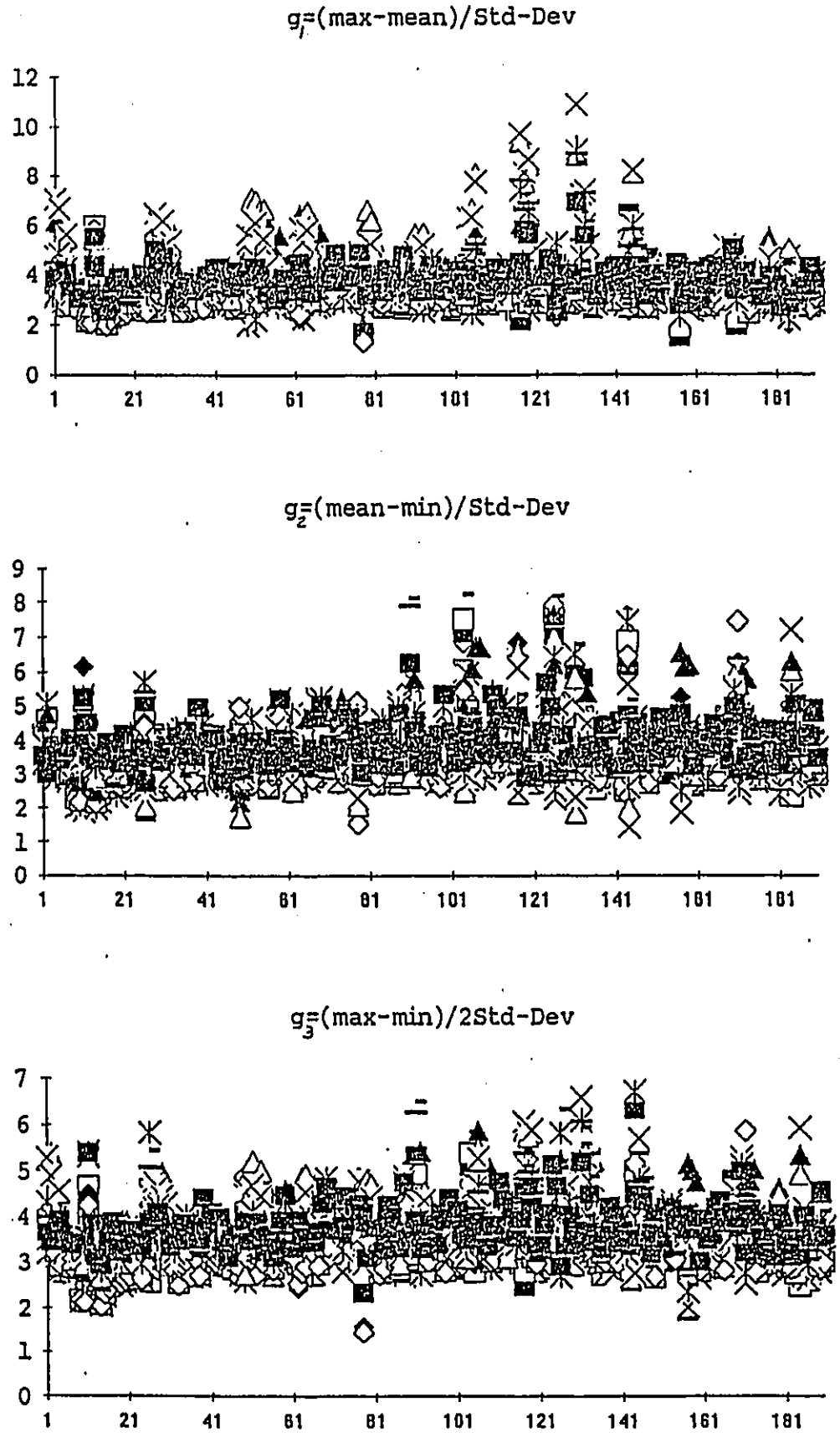

Fig.5.5 General Tendency of Peak Factors (from [4.3])

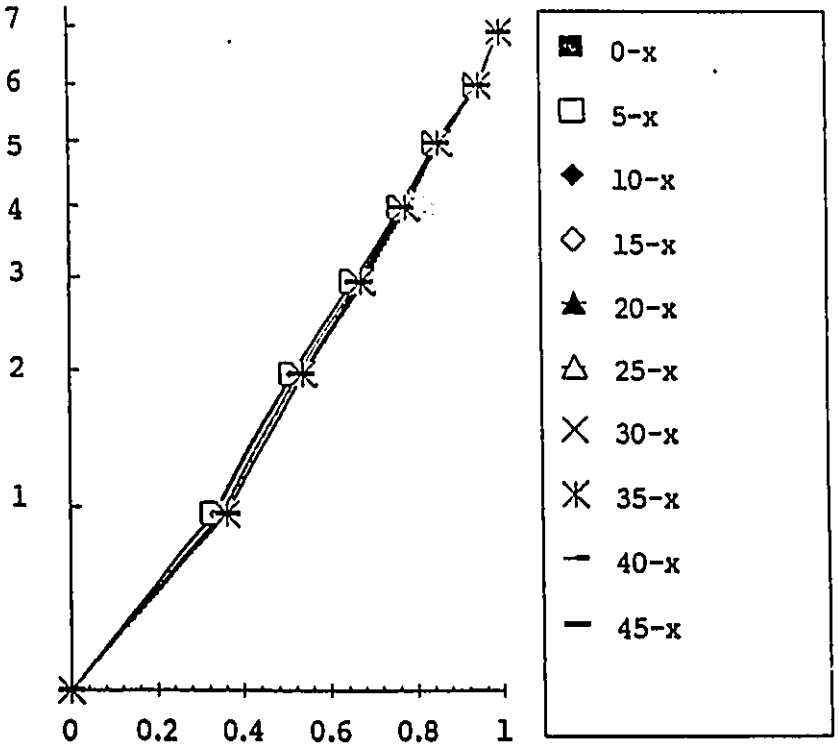

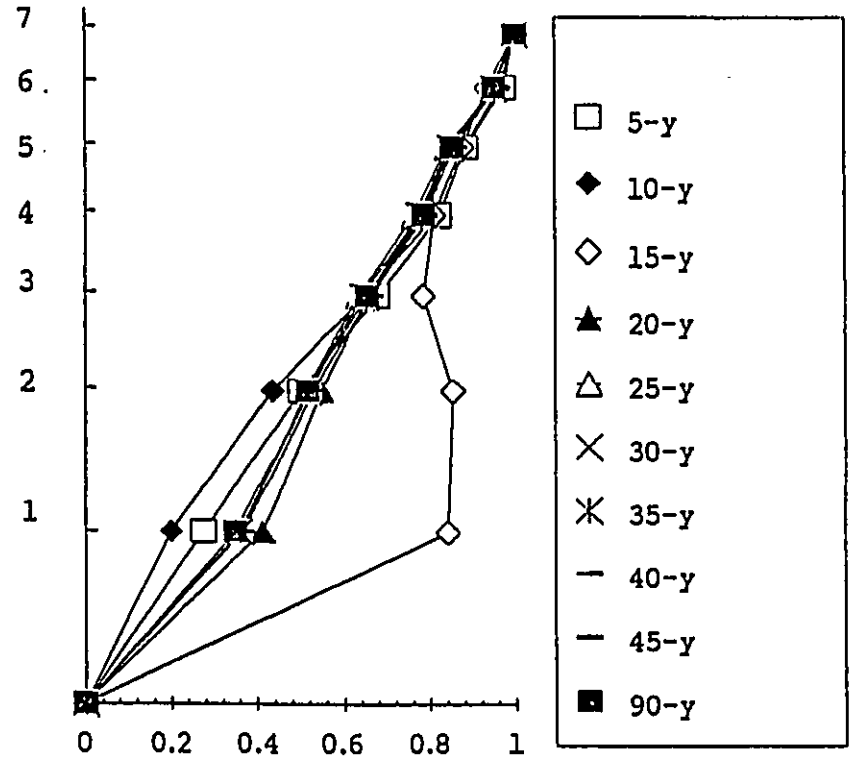

(from [4.3])

Fig.5.6 Response Mode Shape

Fig.5.7. Response Spectra

The following 11 pages show the measured response spectra for each azimuth angle in the highest tested wind speed for each run. Each page has spectra in three directions; X, Y and torsion. The spectra are given in dimensionless form by multiplying frequency and dividing by the variance. For each spectrum, the peak reading and corresponding frequency and the variance are also listed. These figures are from [4.3].

Run- 103 Point- 13

Angle of Attack- 0 · Wind Speed- 28.090 (m/s)

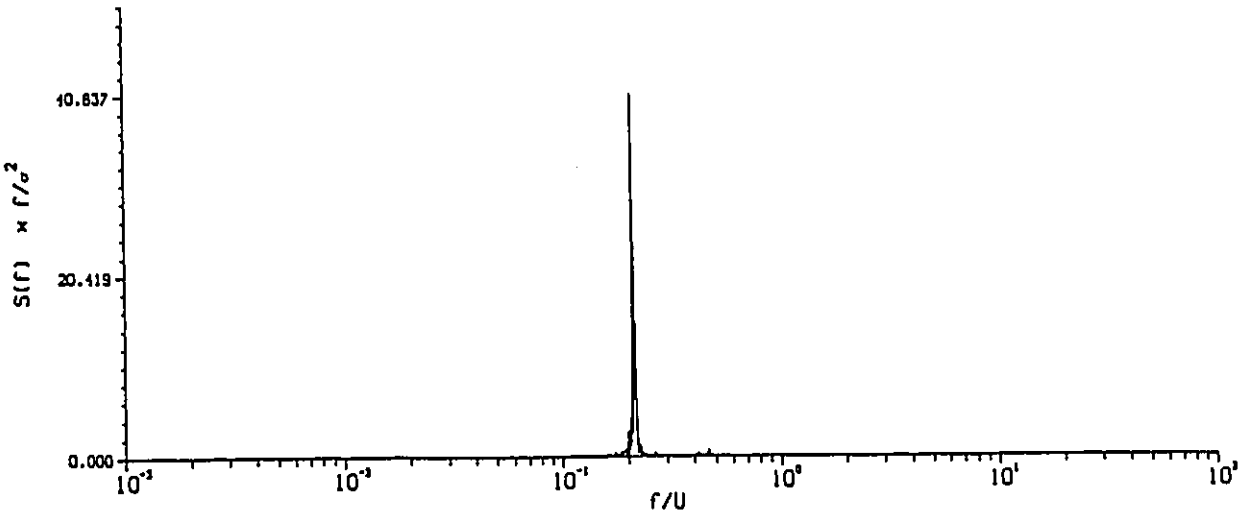

X Power Spectrum S(5.890)- 0.82044 σ²- 0.118331

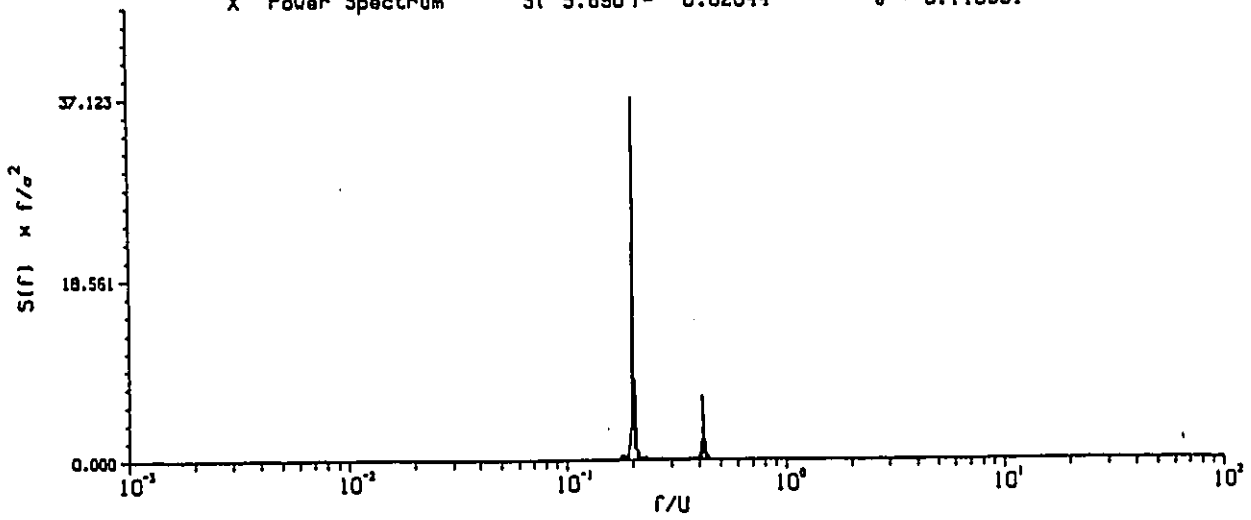

Y Power Spectrum S(5.676)- 4.45709 σ²- 0.681517

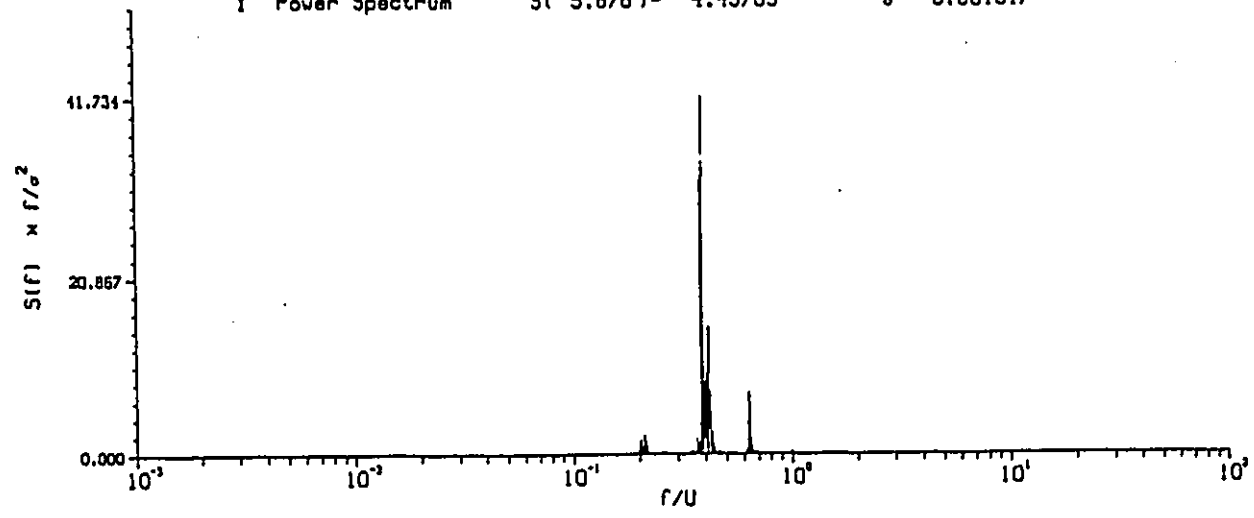

T Power Spectrum S(10.925)- 0.00021015 σ²- 0.000055014

Run- 108 Point- 11

Angle of Attack- 5 Wind Speed- 28.230 (m/s)

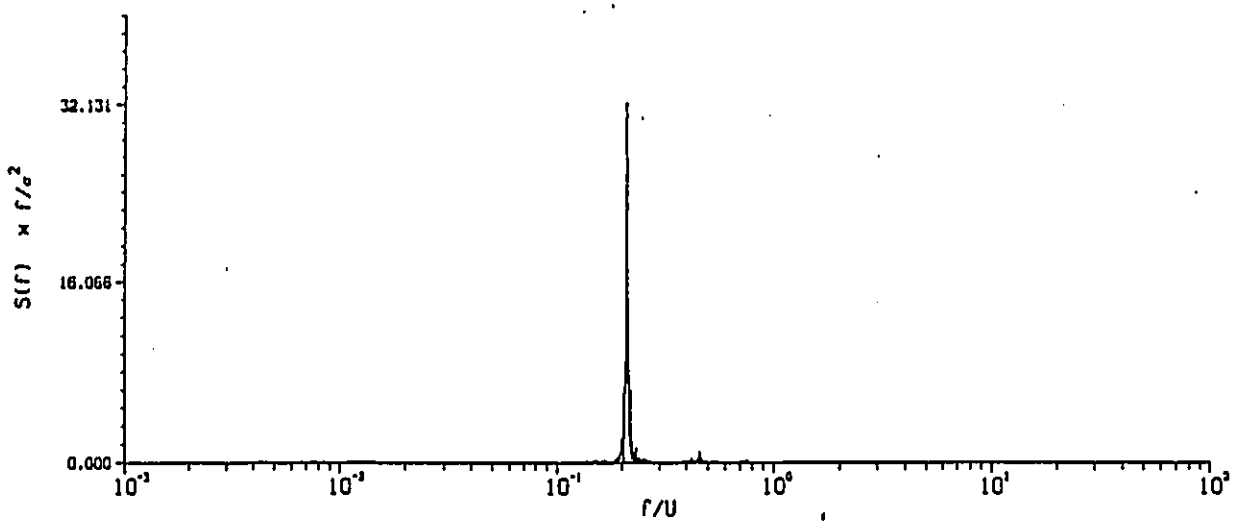

X Power Spectrum S(5.920)= 0.529054 σ^2= 0.0974823

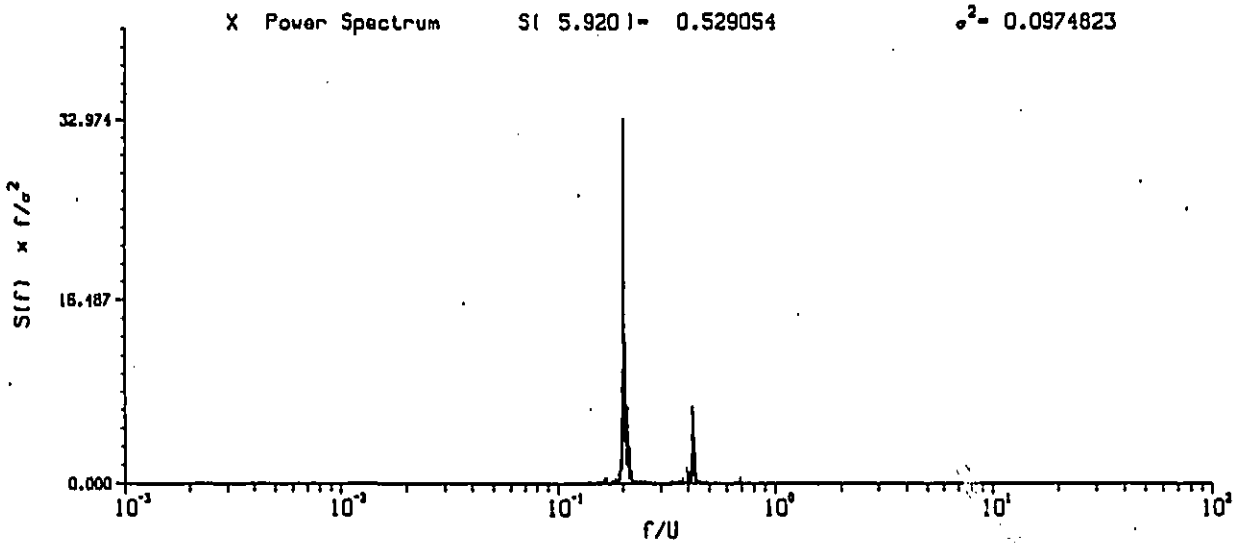

Y Power Spectrum S(5.676)= 1.63327 σ^2= 0.281155

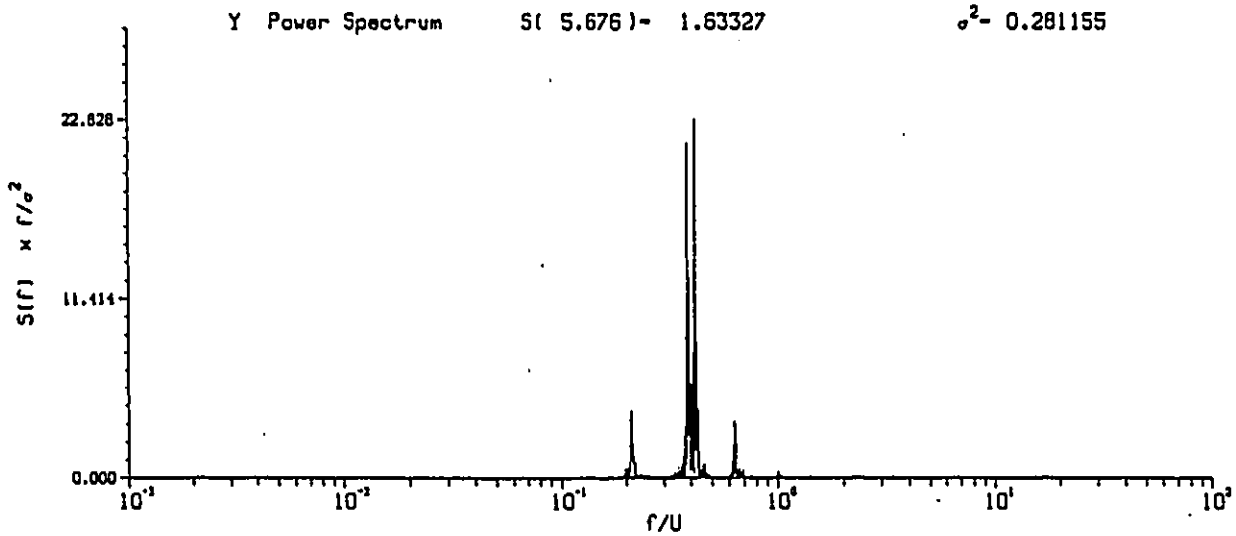

T Power Spectrum S(11.810)= 0.0000438678 σ^2= 0.0000226952

Run- 129 Point- 11

Angle of Attack- 10 Wind Speed- 28.043 (m/s)

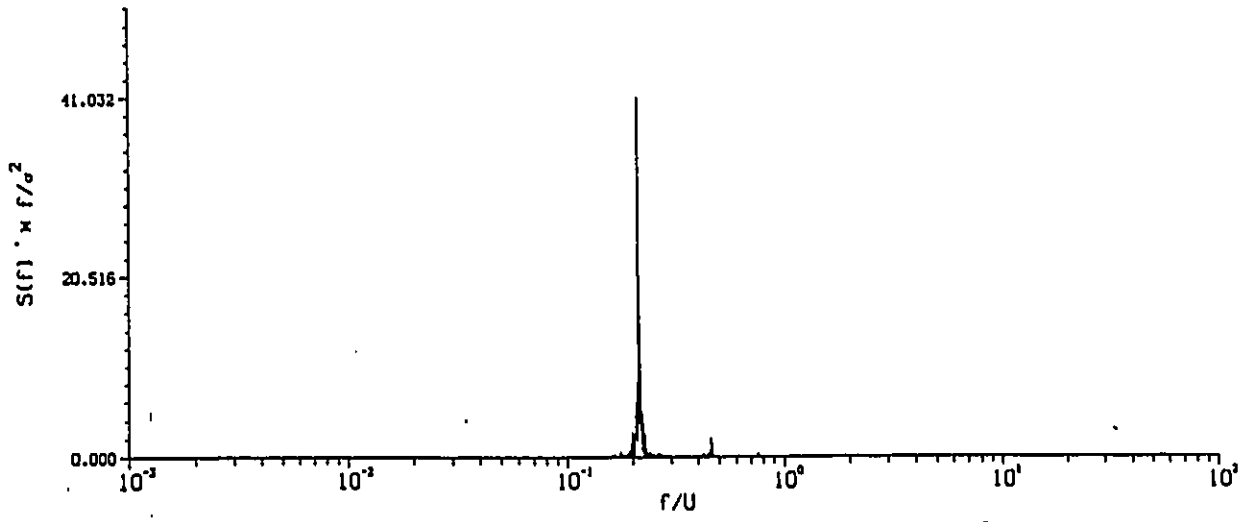

X Power Spectrum S(5.981)= 0.403485 σ^2= 0.0588176

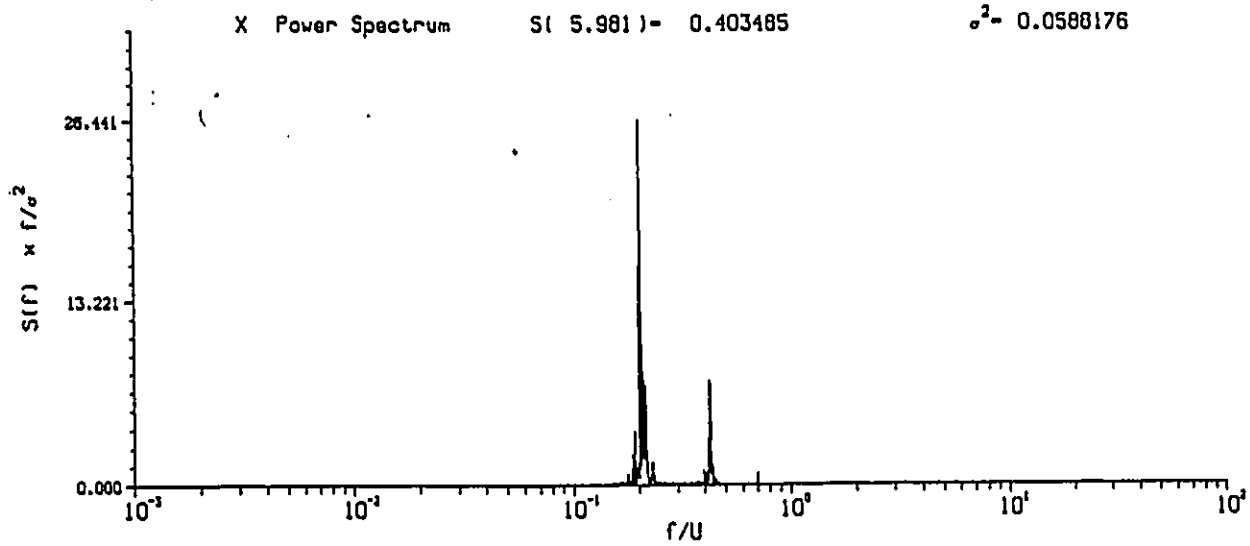

Y Power Spectrum S(5.676)= 0.696121 σ^2= 0.149439

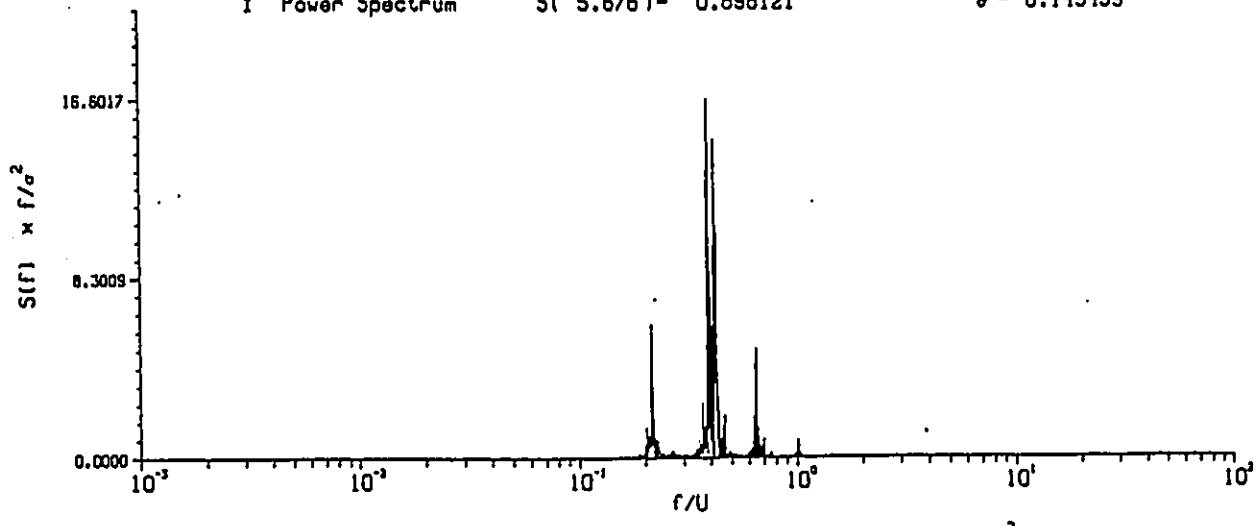

T Power Spectrum S(10.986)= 0.000014971 σ^2= 0.00000990717

Run- 118 Point- 11

Angle of Attack- 15 Wind Speed- 28.153 (m/s)

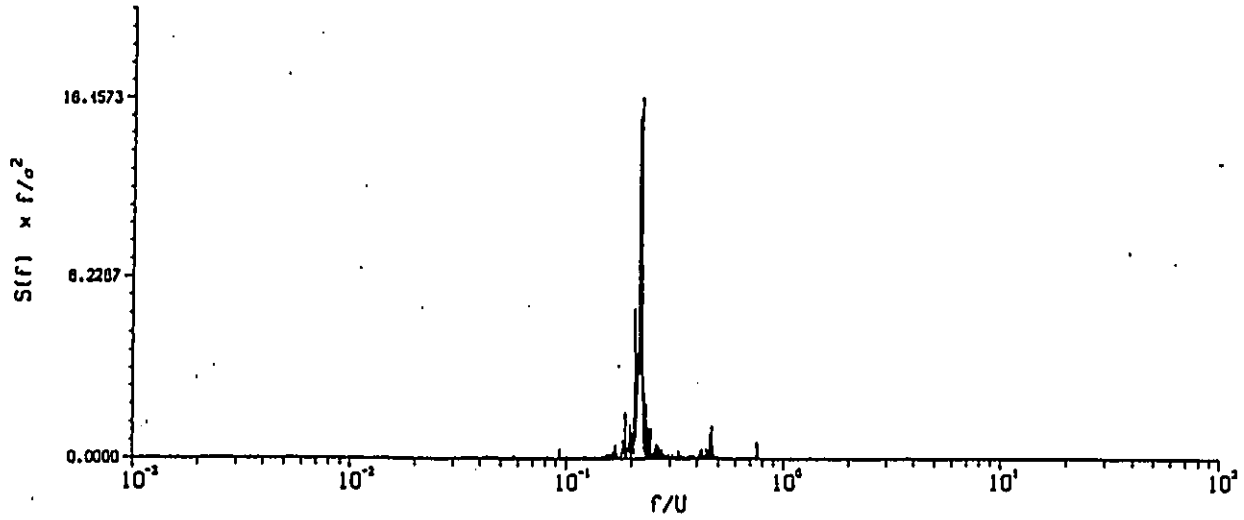

X Power Spectrum S(6.287)- 0.0894346 σ²- 0.0341636

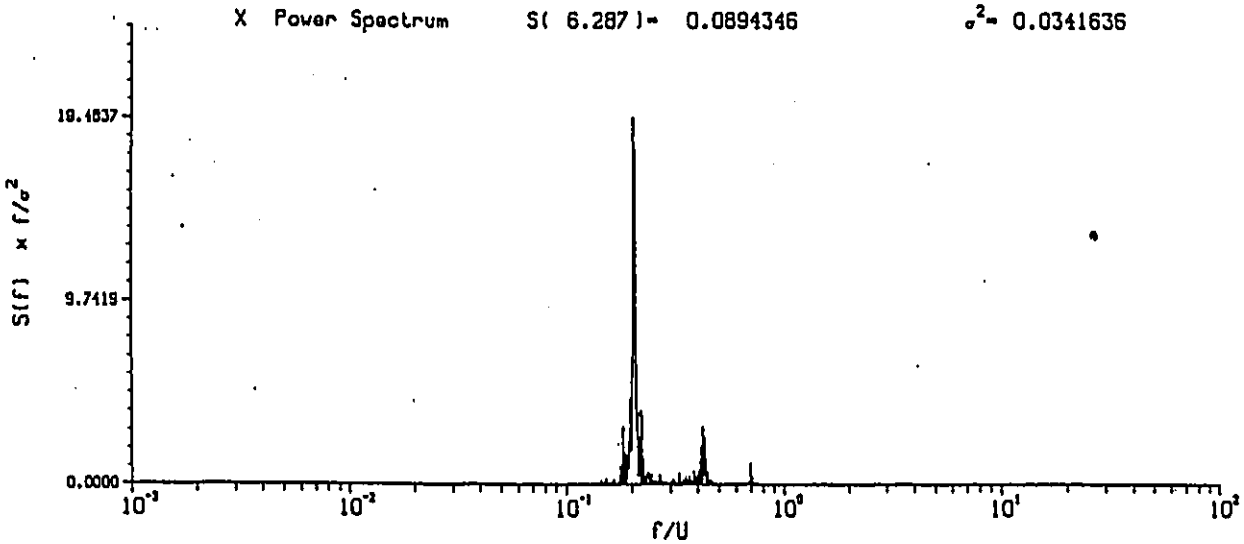

Y Power Spectrum S(5.707)- 0.367392 σ²- 0.107609

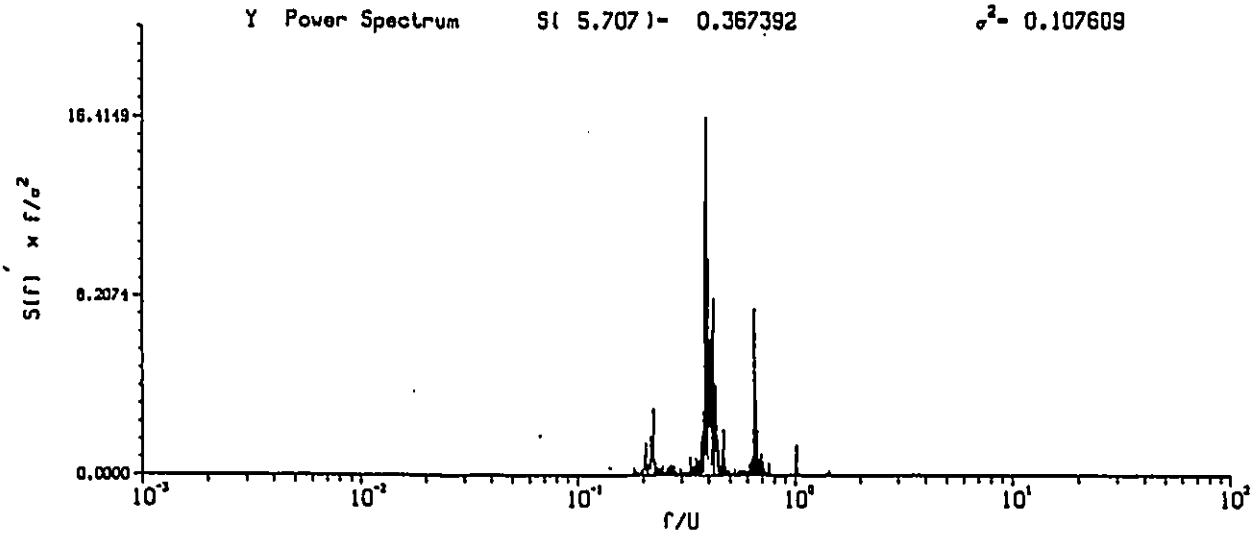

T Power Spectrum S(11.047)- 0.00000992916 σ²- 0.00000668242

Run= 116 Point= 11

Angle of Attack= 20 Wind Speed= 28.165 (m/s)

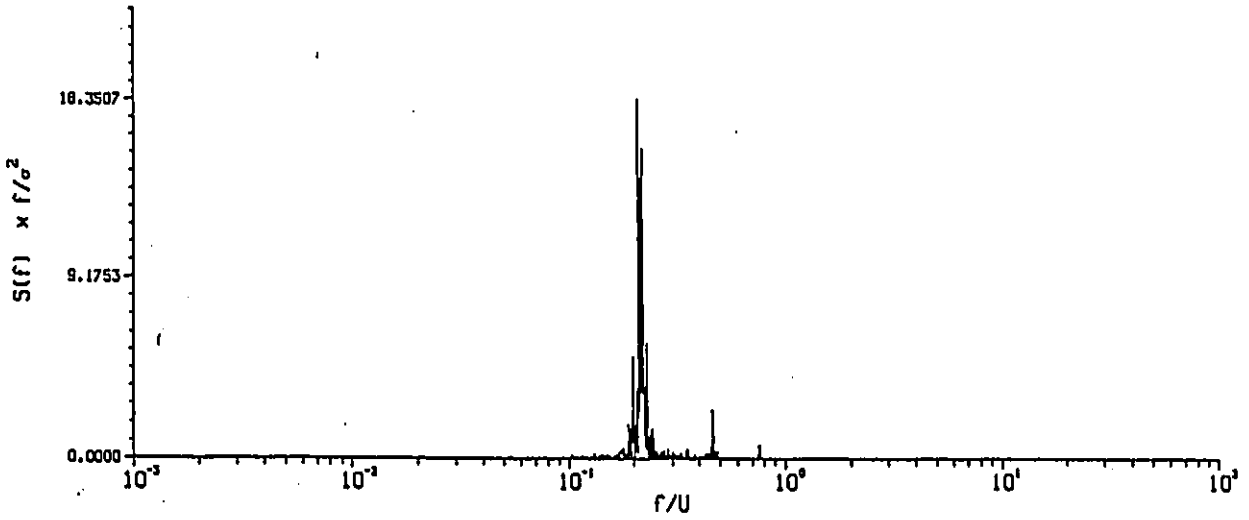

X Power Spectrum S(5.920)= 0.153442 σ^2= 0.0495045

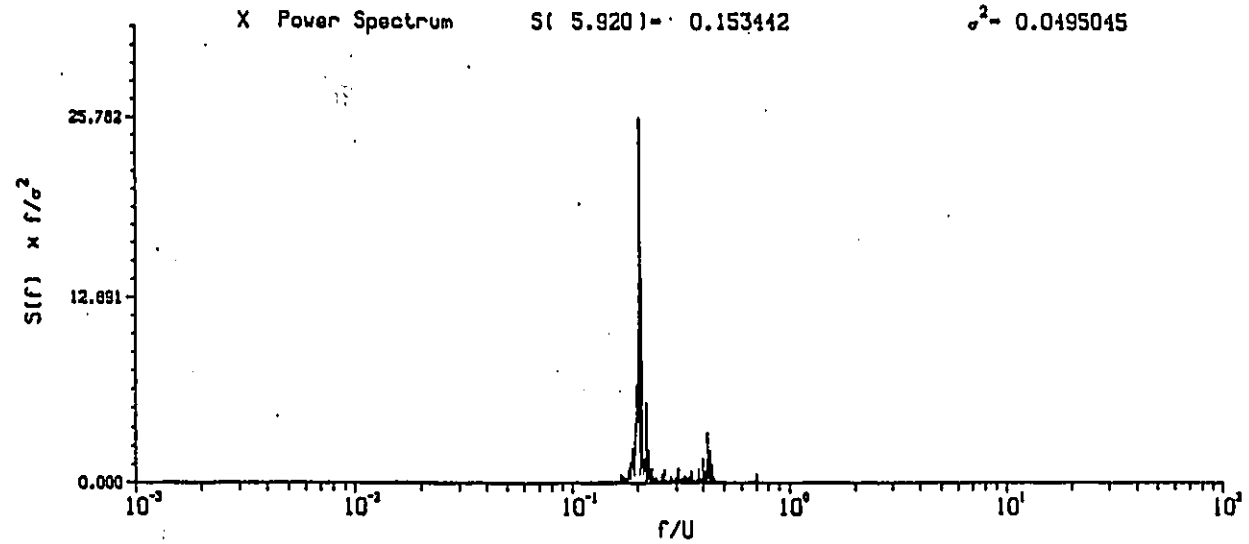

Y Power Spectrum S(5.798)= 0.433155 σ^2= 0.0974168

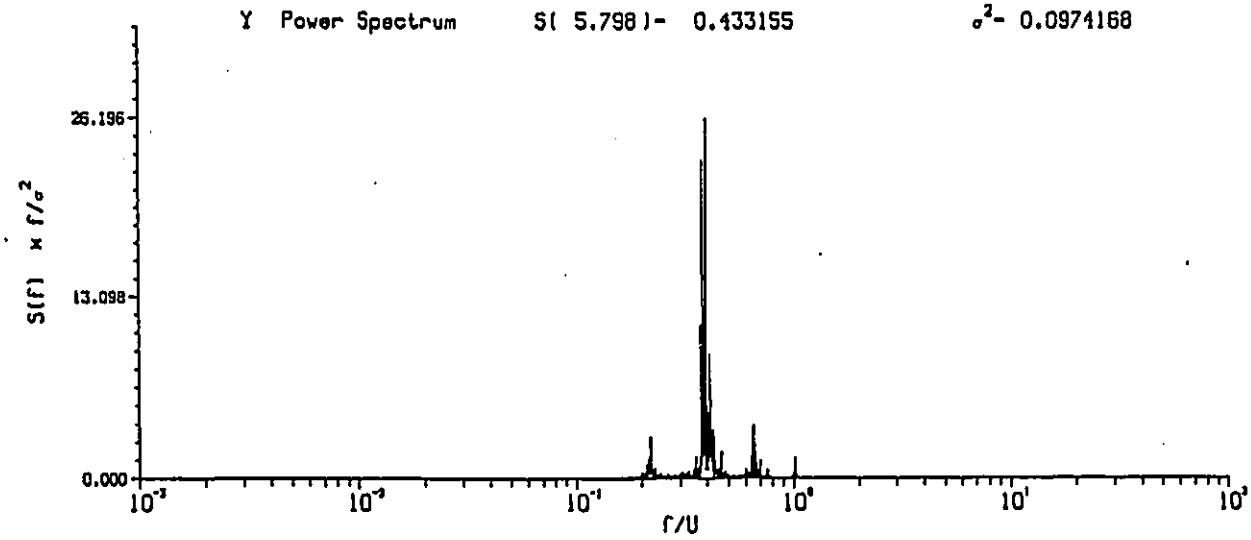

T Power Spectrum S(11.231)= 0.0000164604 σ^2= 0.00000705676

Run- 127 Point- 3

Angle of Attack- 25 Wind Speed- 28.094 (m/s)

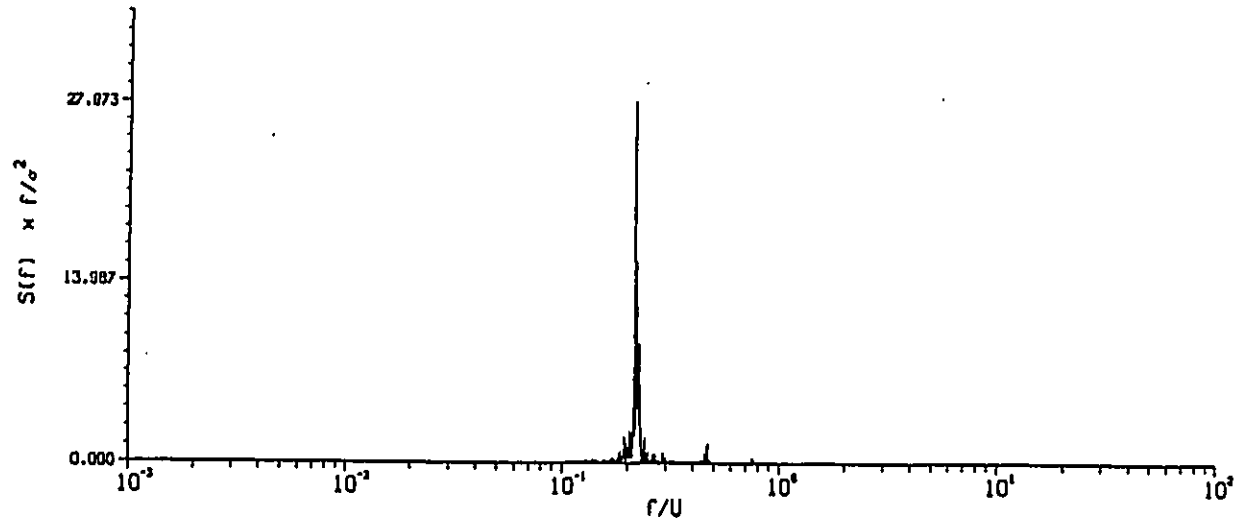

X Power Spectrum S(6.073)= 0.377262 σ^2= 0.0819036

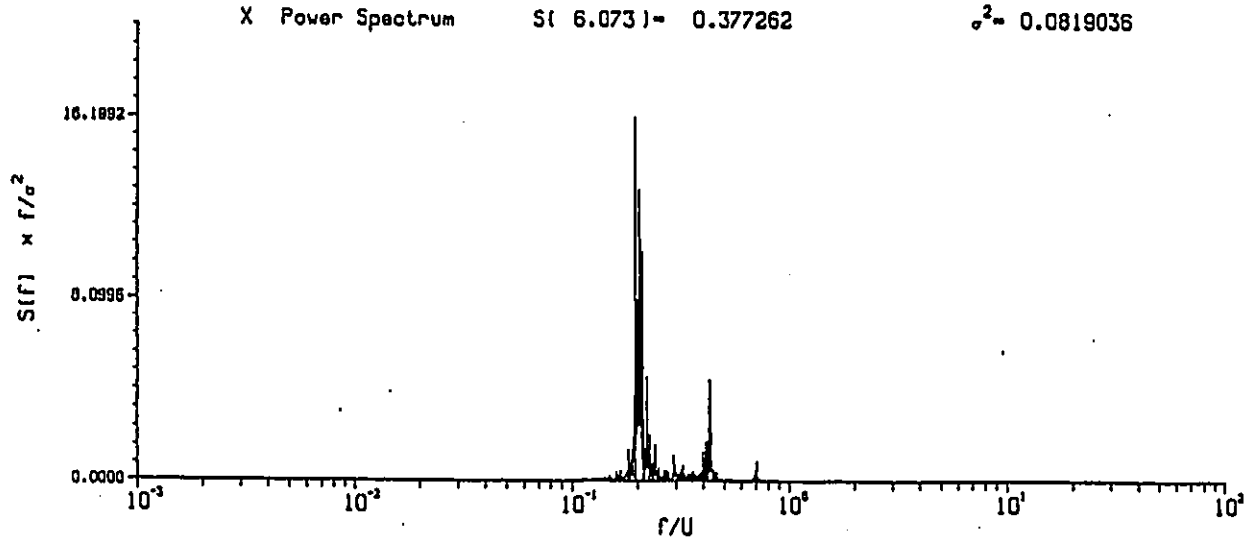

Y Power Spectrum S(5.463)= 0.216638 σ^2= 0.073054

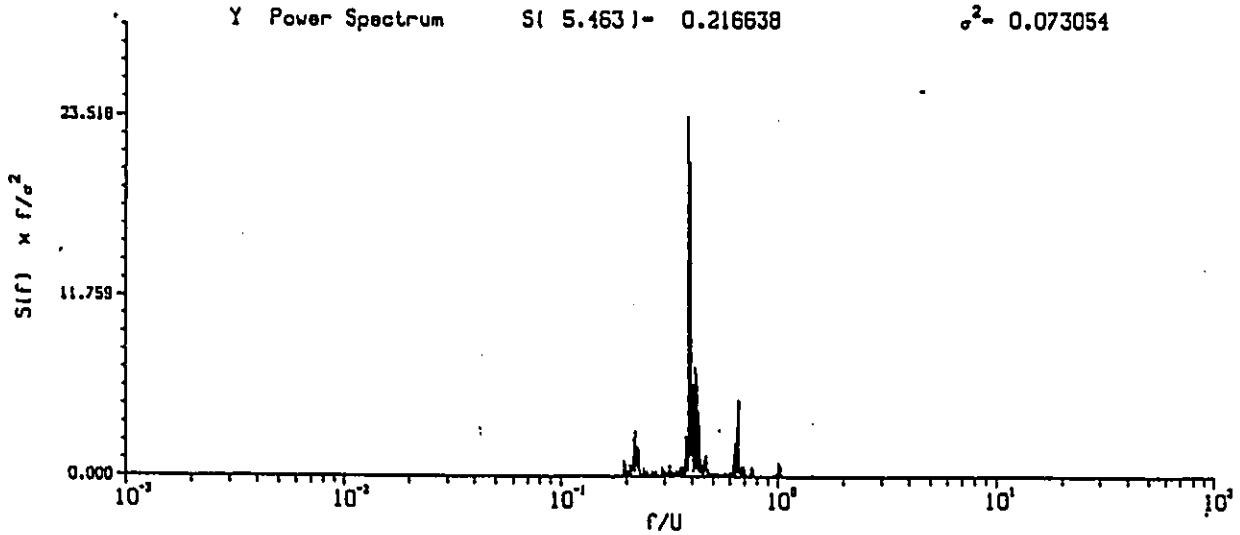

I Power Spectrum S(10.803)= 0.0000146467 σ^2= 0.0000067281

Run- 120 Point- 11

Angle of Attack- 30 Wind Speed- 28.064 (m/s)

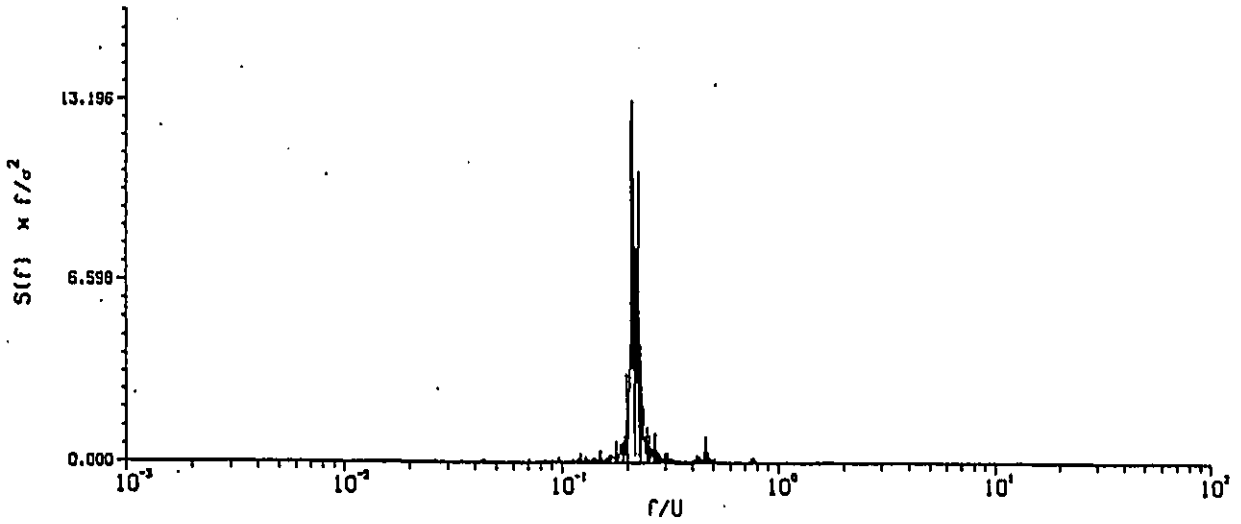

X Power Spectrum S(5.951)= 0.1202 σ^2= 0.0542057

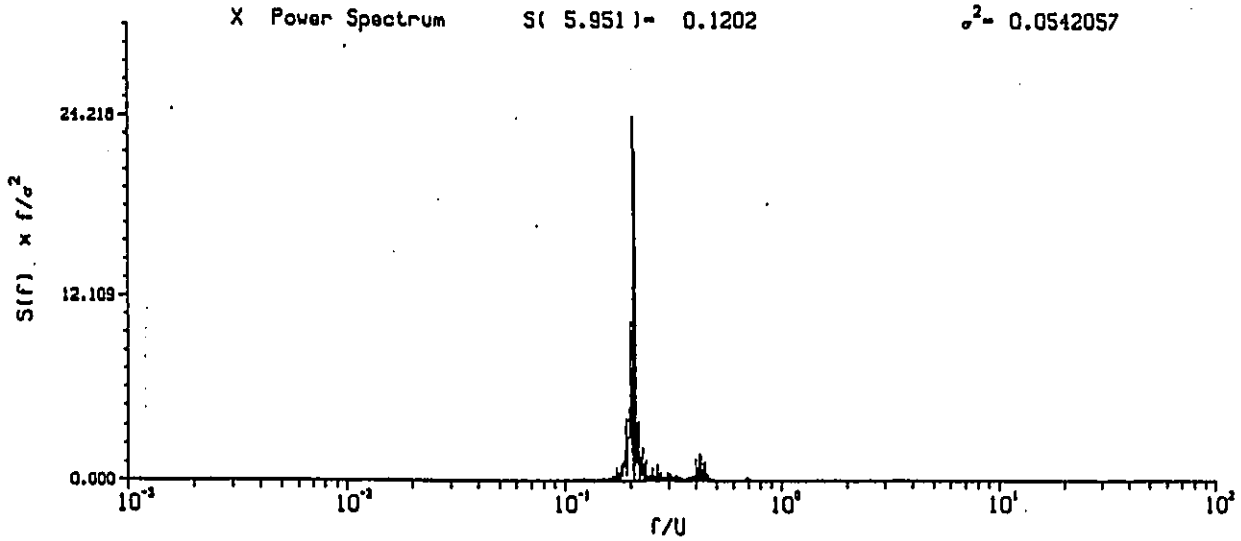

Y Power Spectrum S(5.768)= 0.286161 σ^2= 0.0681541

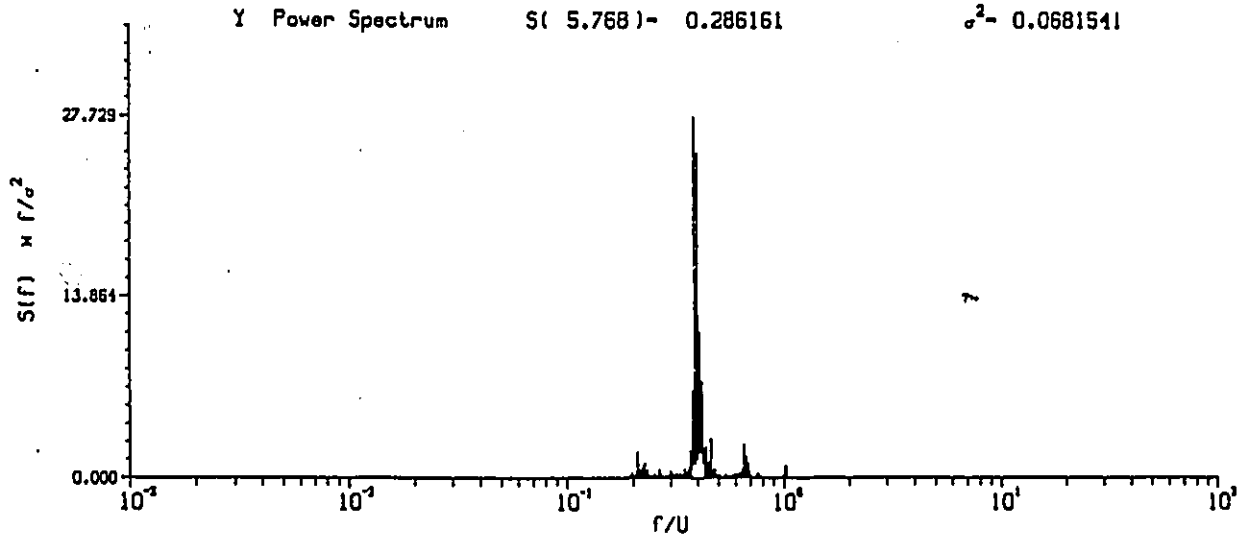

T Power Spectrum S(10.864)= 0.000016253 σ^2= 0.000006368

Run- 131 Point- 11

Angle of Attack- 35 Wind Speed- 28.031 (m/s)

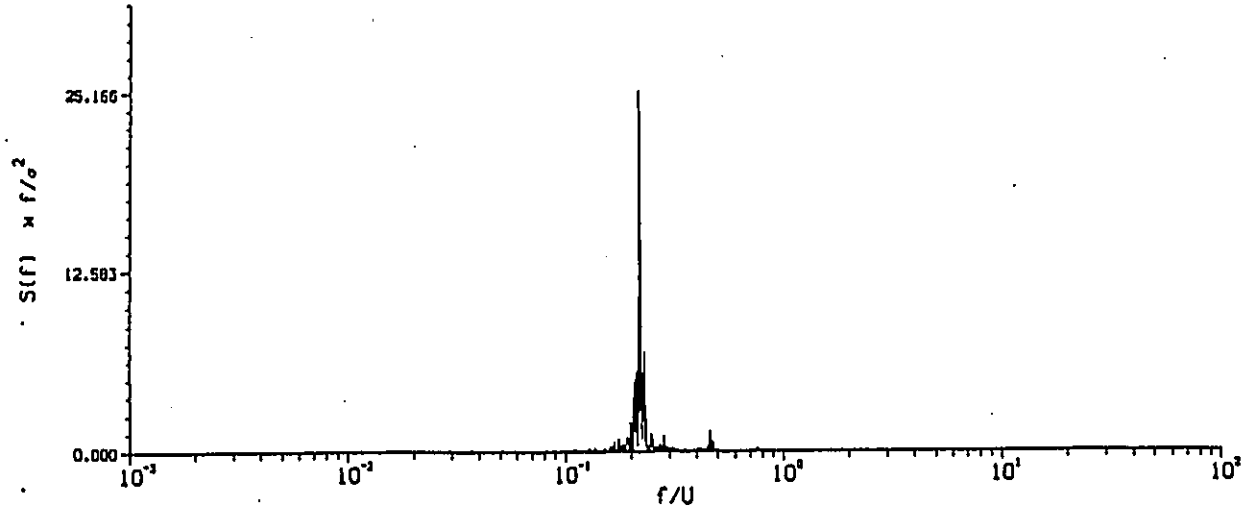

X Power Spectrum S(6.134)= 0.300057 σ^2= 0.0731373

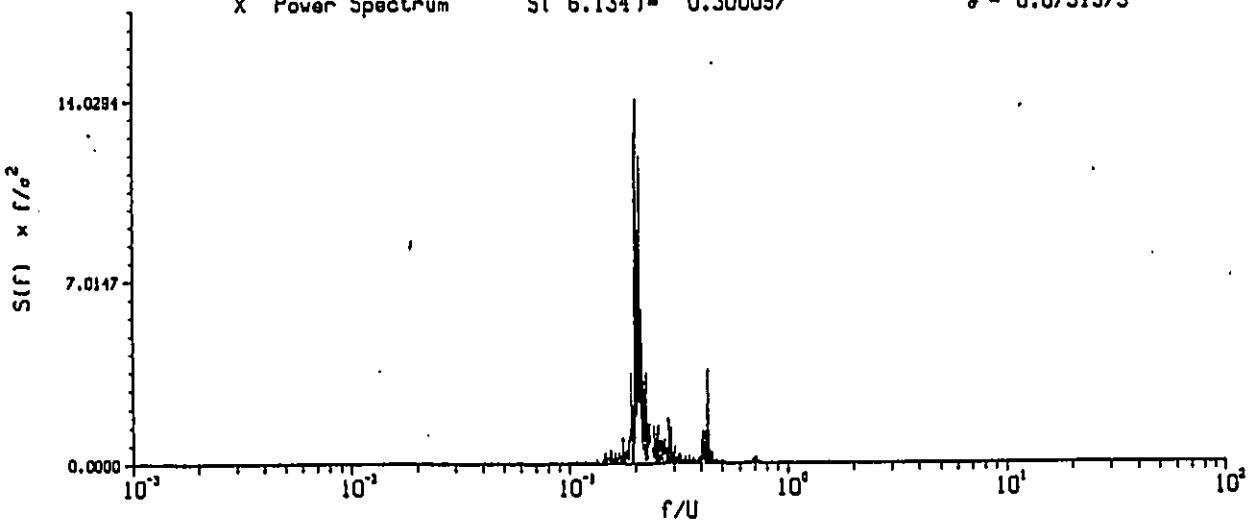

Y Power Spectrum S(5.676)= 0.148918 σ^2= 0.060252

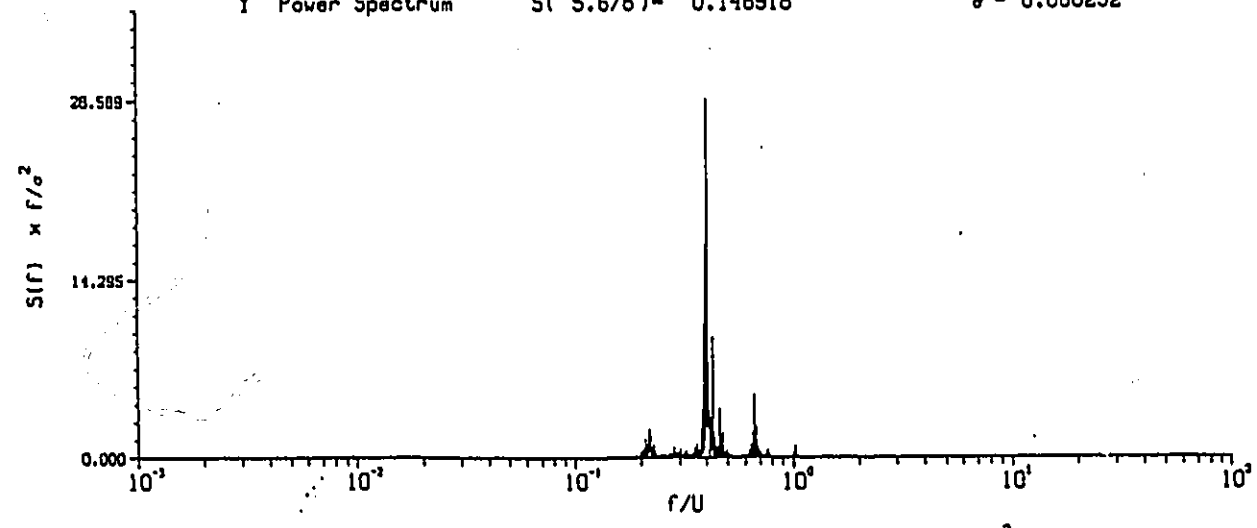

T Power Spectrum S(11.414)= 0.0000136958 σ^2= 0.0000054677

Run- 133 Point- 11

Angle of Attack- 40 Wind Speed- 27.997 (m/s)

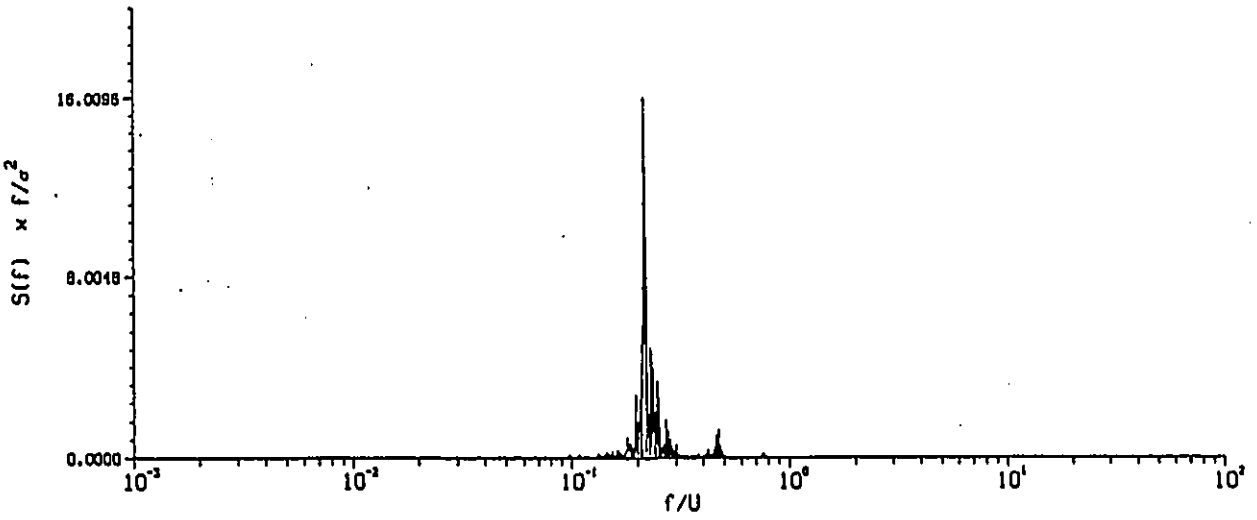

X Power Spectrum S(6.104)= 0.146521 σ²= 0.0558596

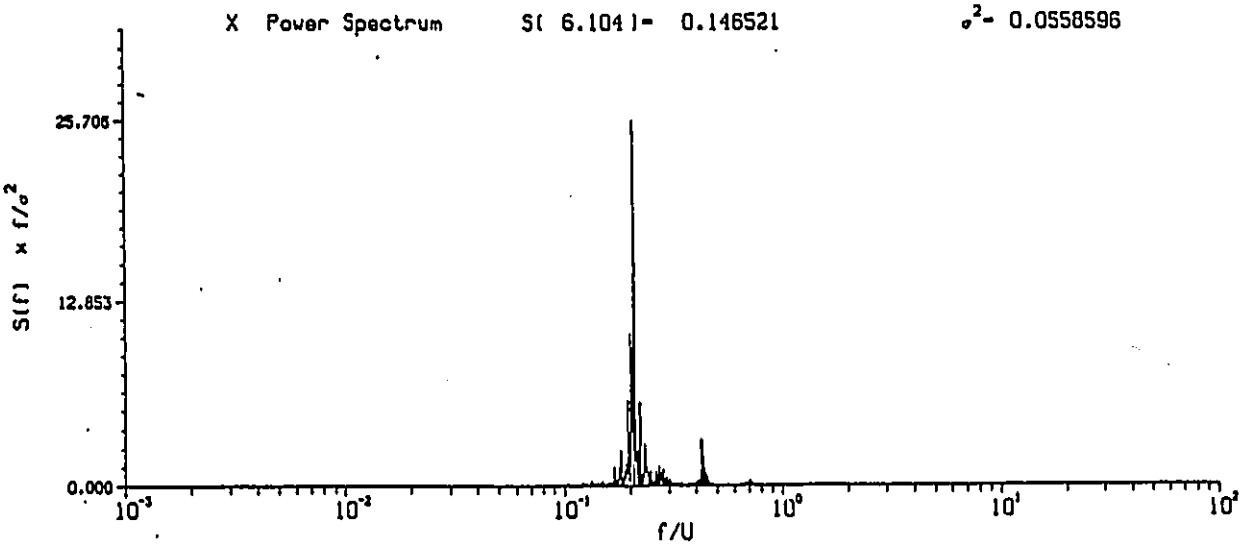

Y Power Spectrum S(5.829)= 0.261995 σ²= 0.0594072

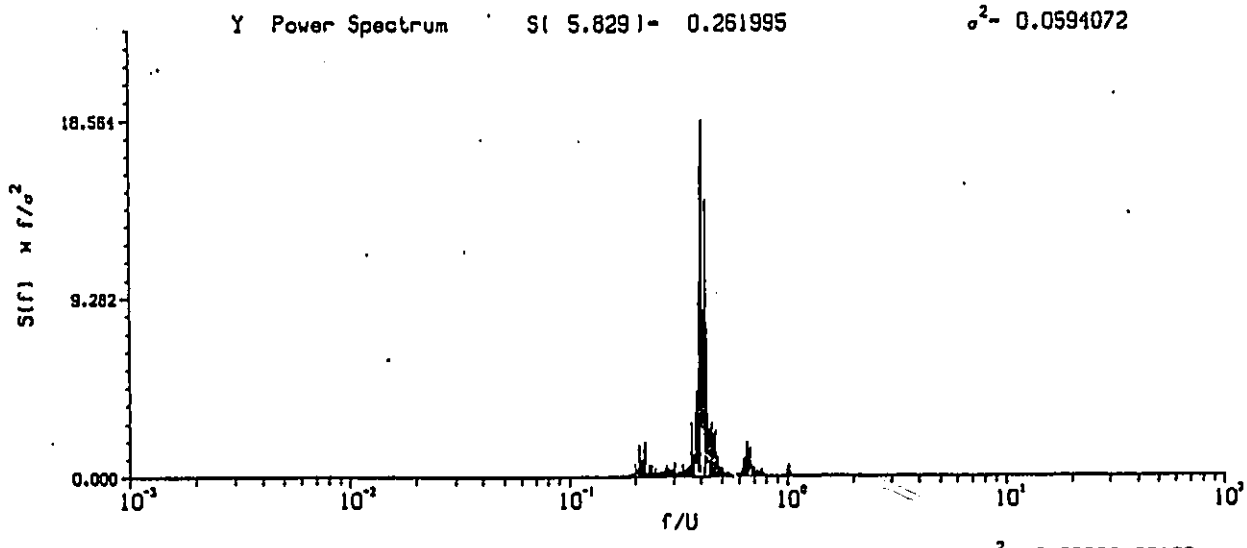

T Power Spectrum S(11.414)= 0.00000800541 σ²= 0.00000492192

Run- 114 Point- 14

Angle of Attack- 45 Wind Speed- 28.210 (m/s)

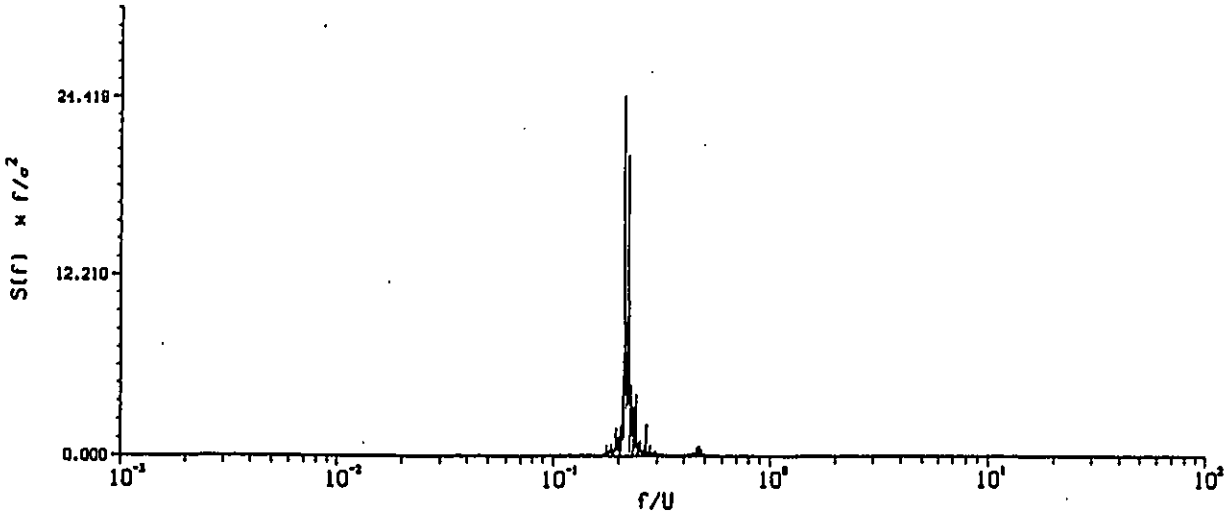

X Power Spectrum S(6.012)= 0.379427 σ^2= 0.0934142

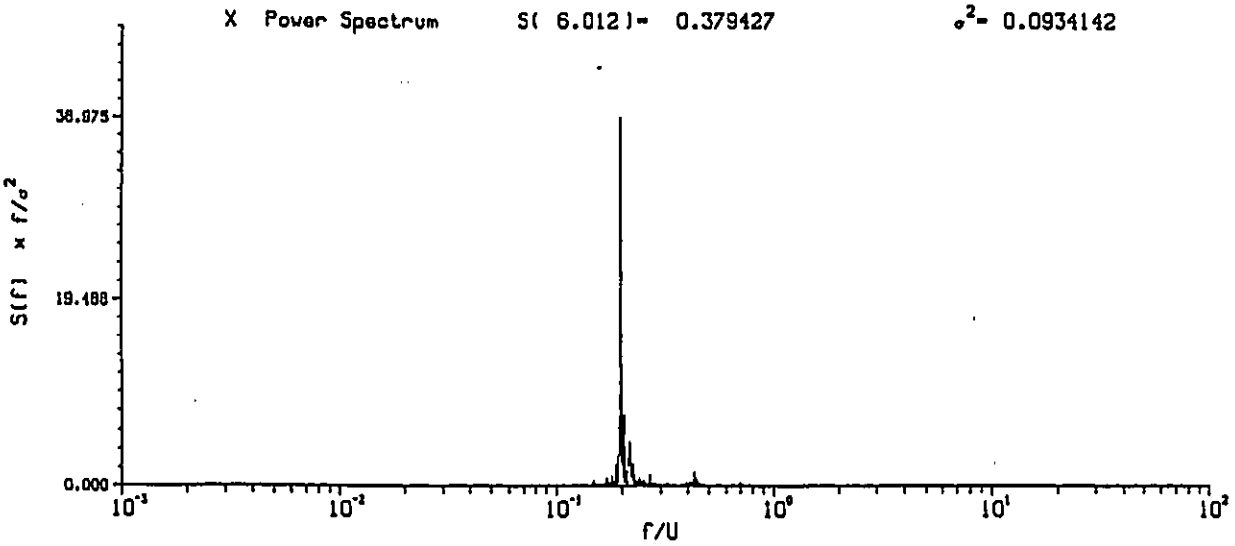

Y Power Spectrum S(5.585)= 0.686315 σ^2= 0.098342

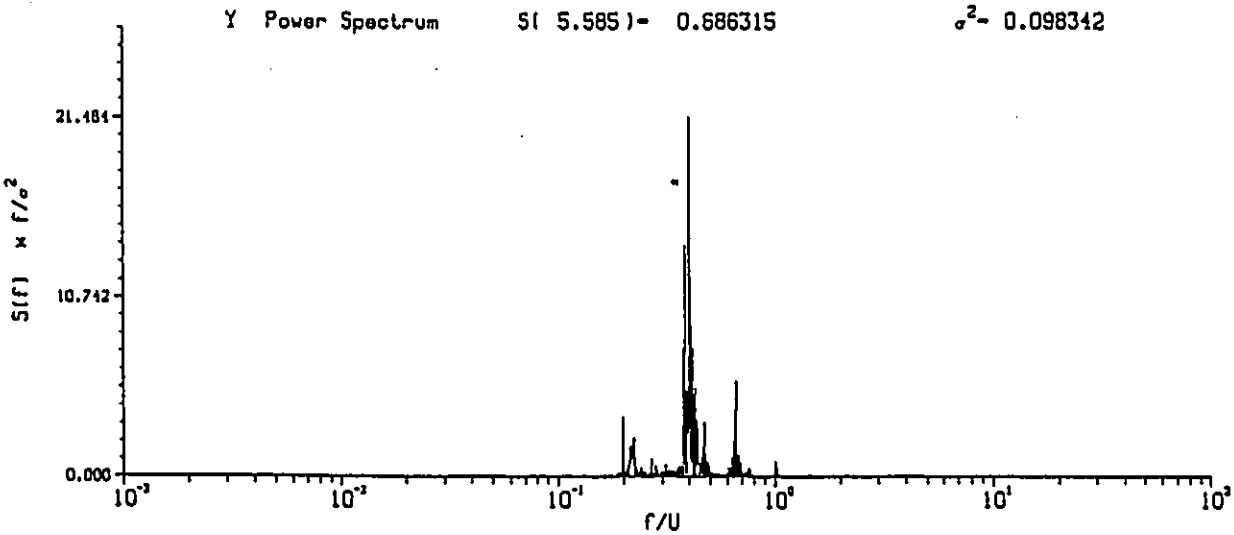

T Power Spectrum S(11.322)= 0.0000107427 σ^2= 0.00000566149

Run- 137 Point- 5

Angle of Attack- 90 Wind Speed- 20.697 (m/s)

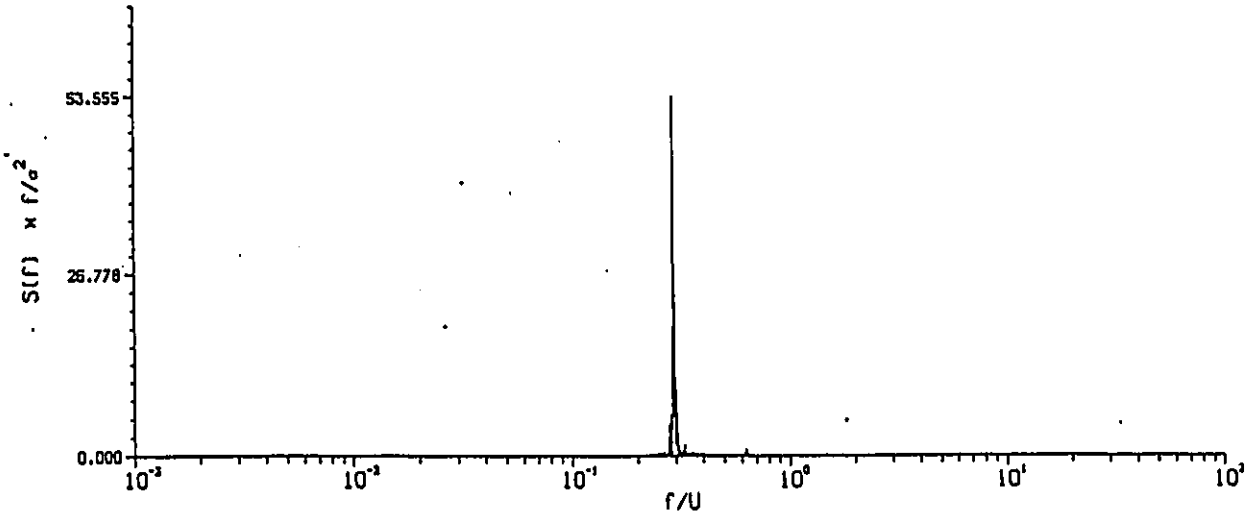

X Power Spectrum S(6.134)= 1.2484 σ^2= 0.142987

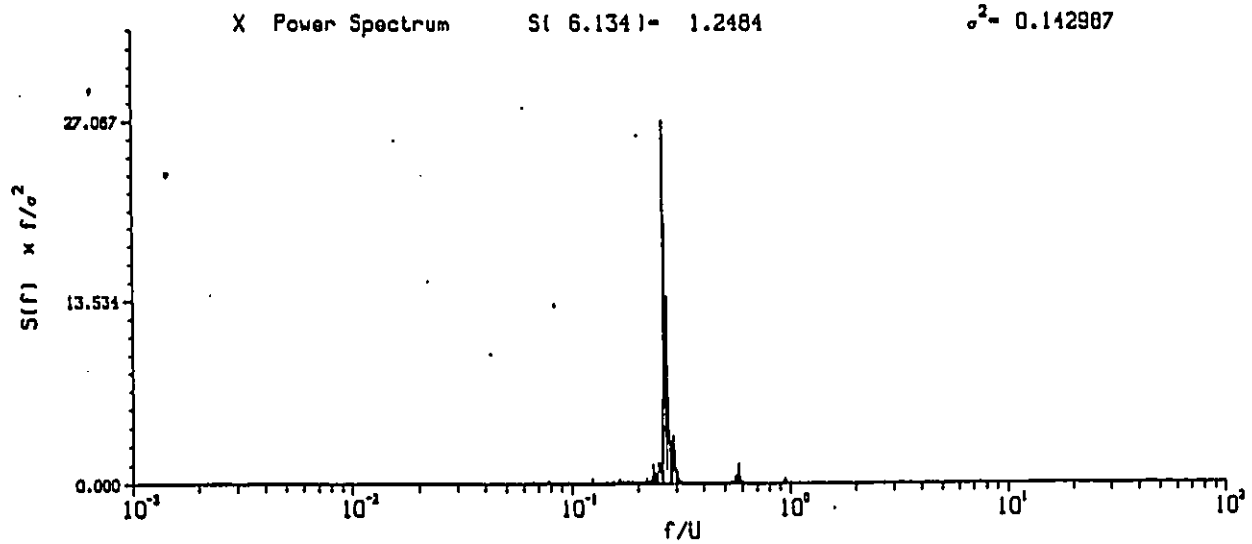

Y Power Spectrum S(5.463)= 0.113675 σ^2= 0.0229418

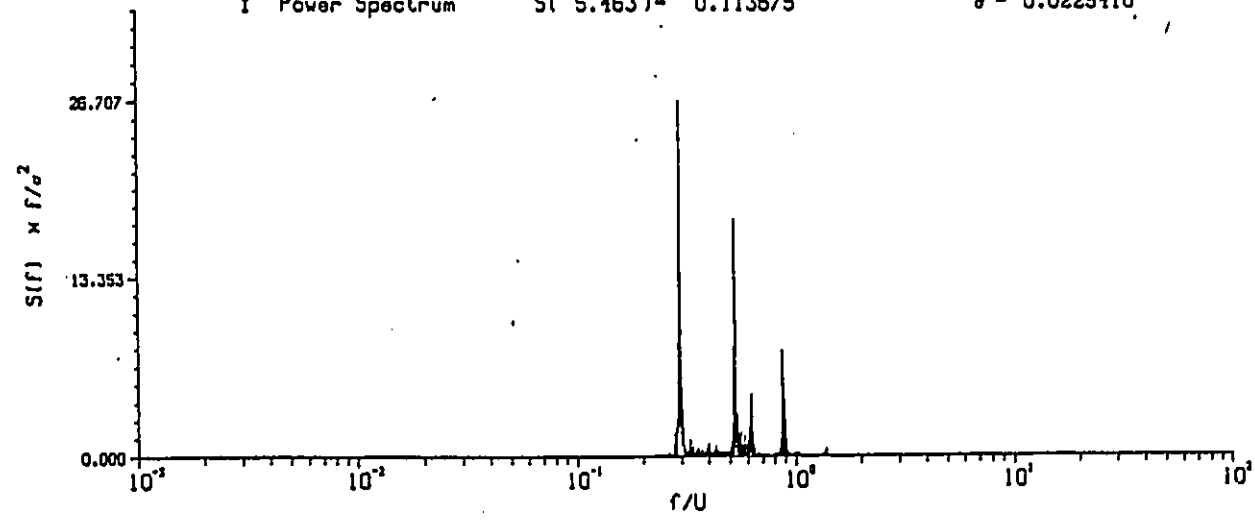

T Power Spectrum S(6.134)= 0.0000179861 σ^2= 0.00000413109

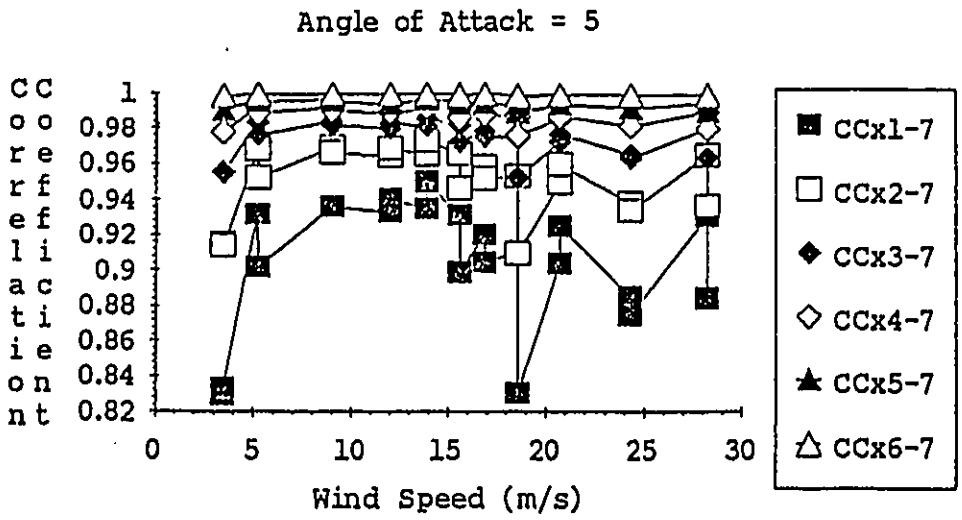

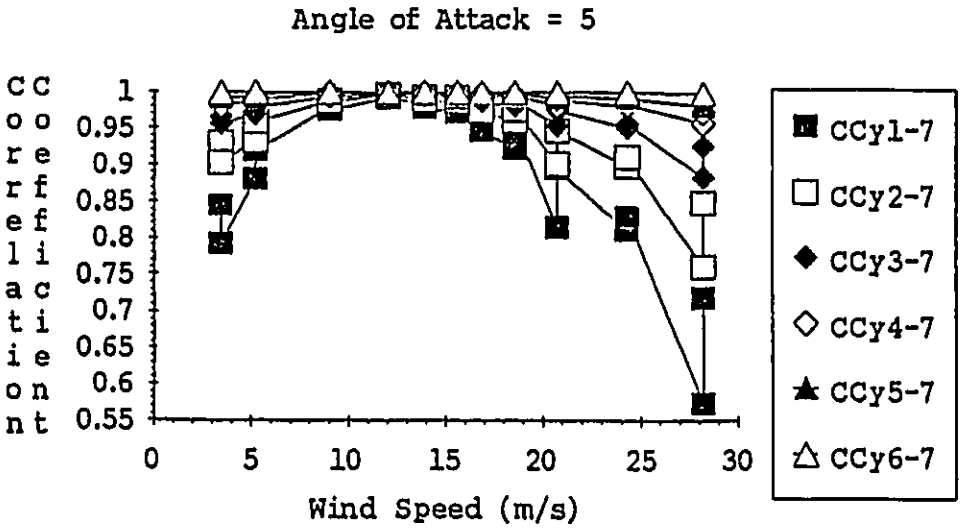

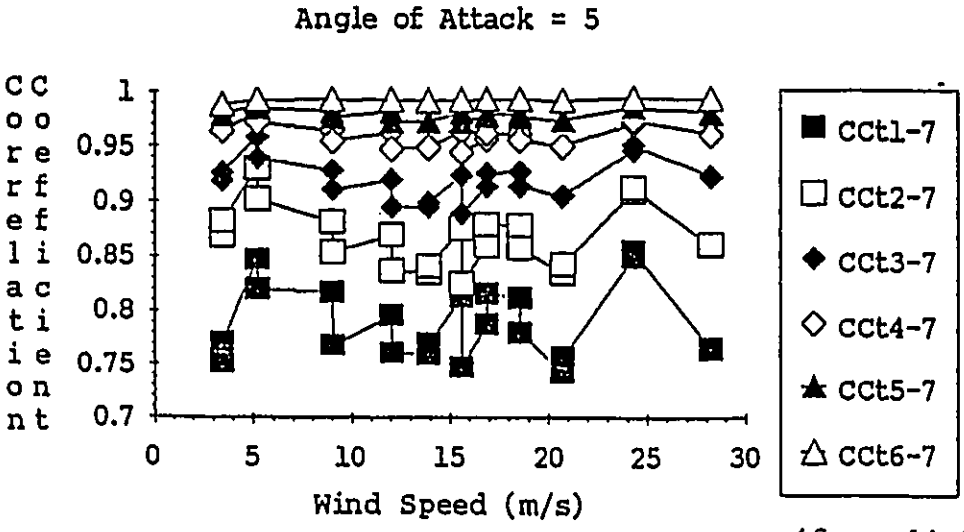

(from [4.3])

Fig.5.8 Vertical Correlation of Response

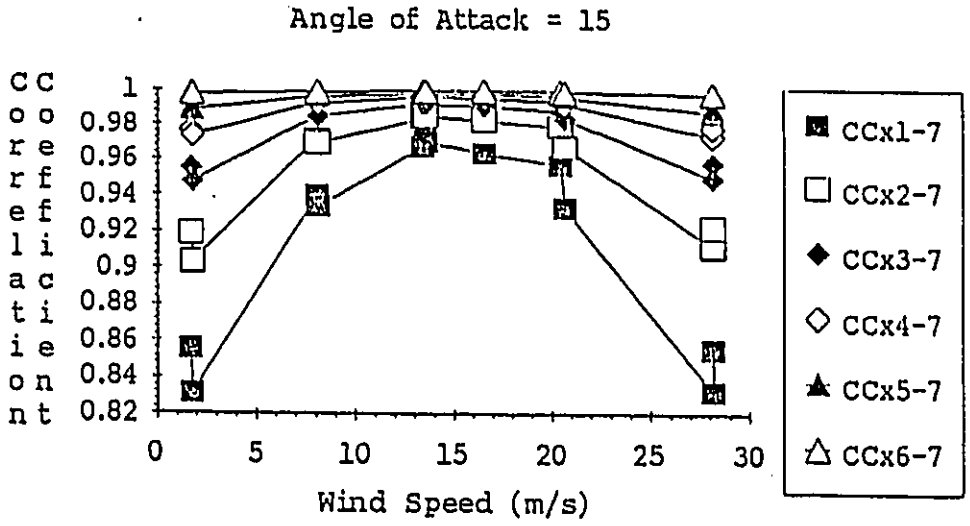

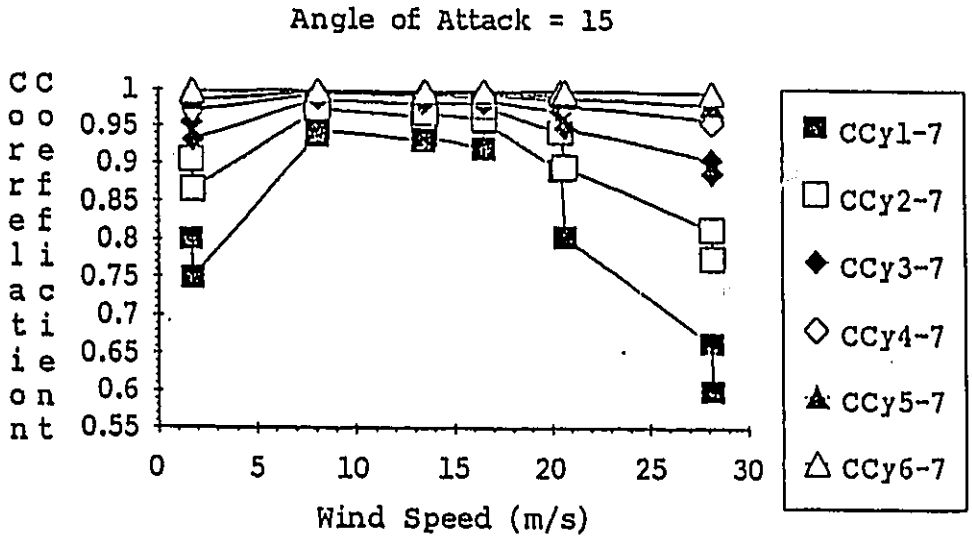

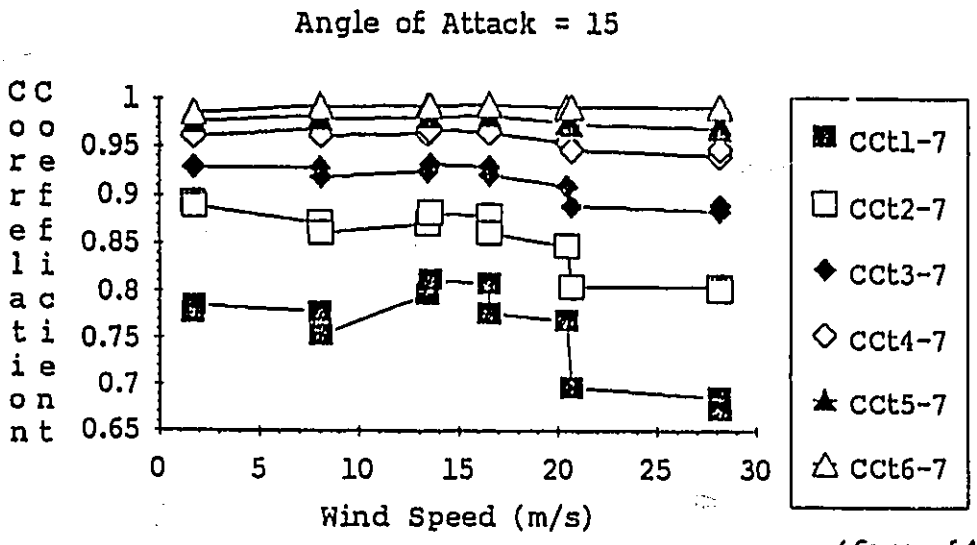

(from [4.3])

Fig.5.8 Vertical Correlation of Response

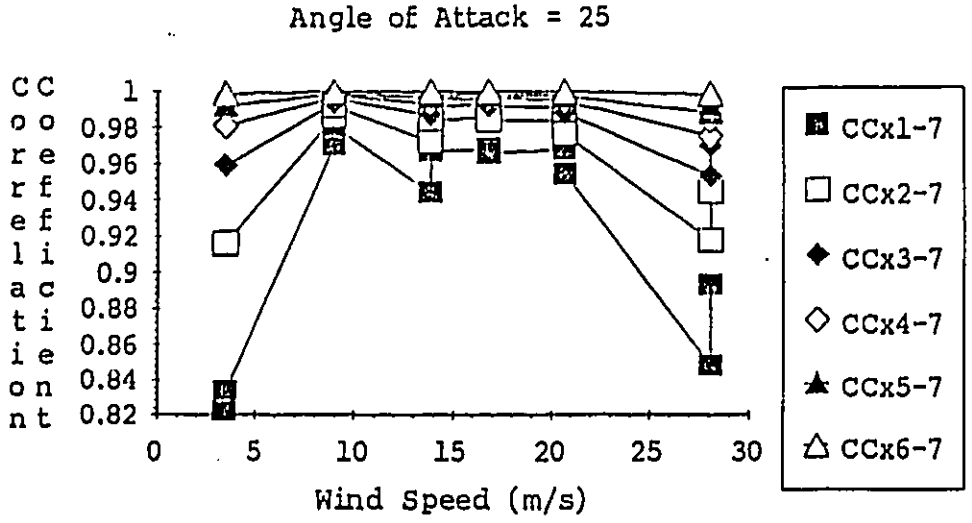

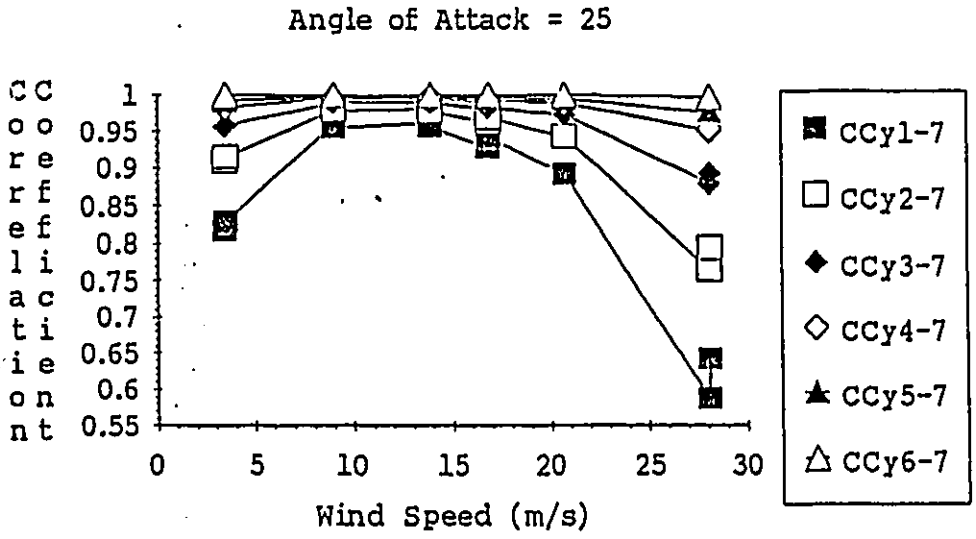

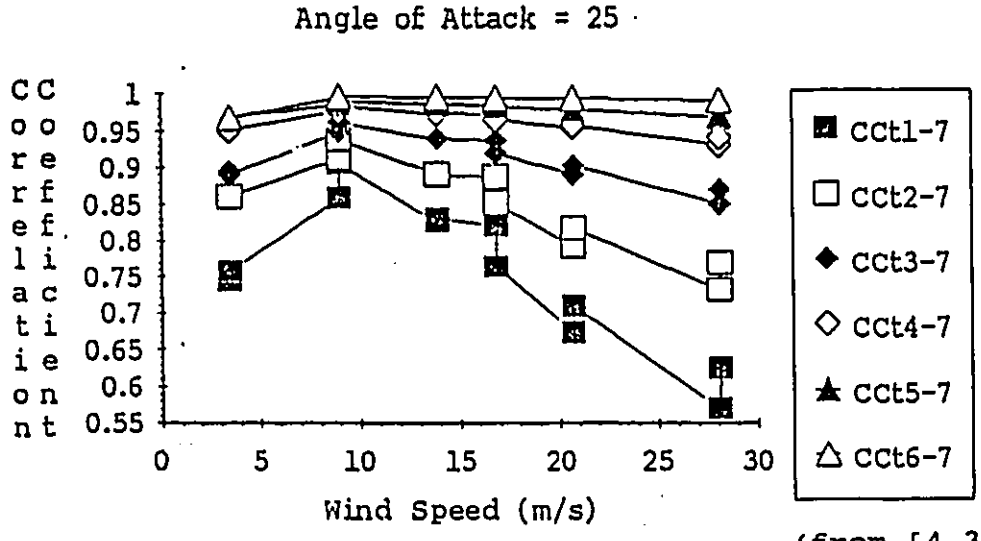

(from [4.3])

Fig.5.8 Vertical Correlation of Response

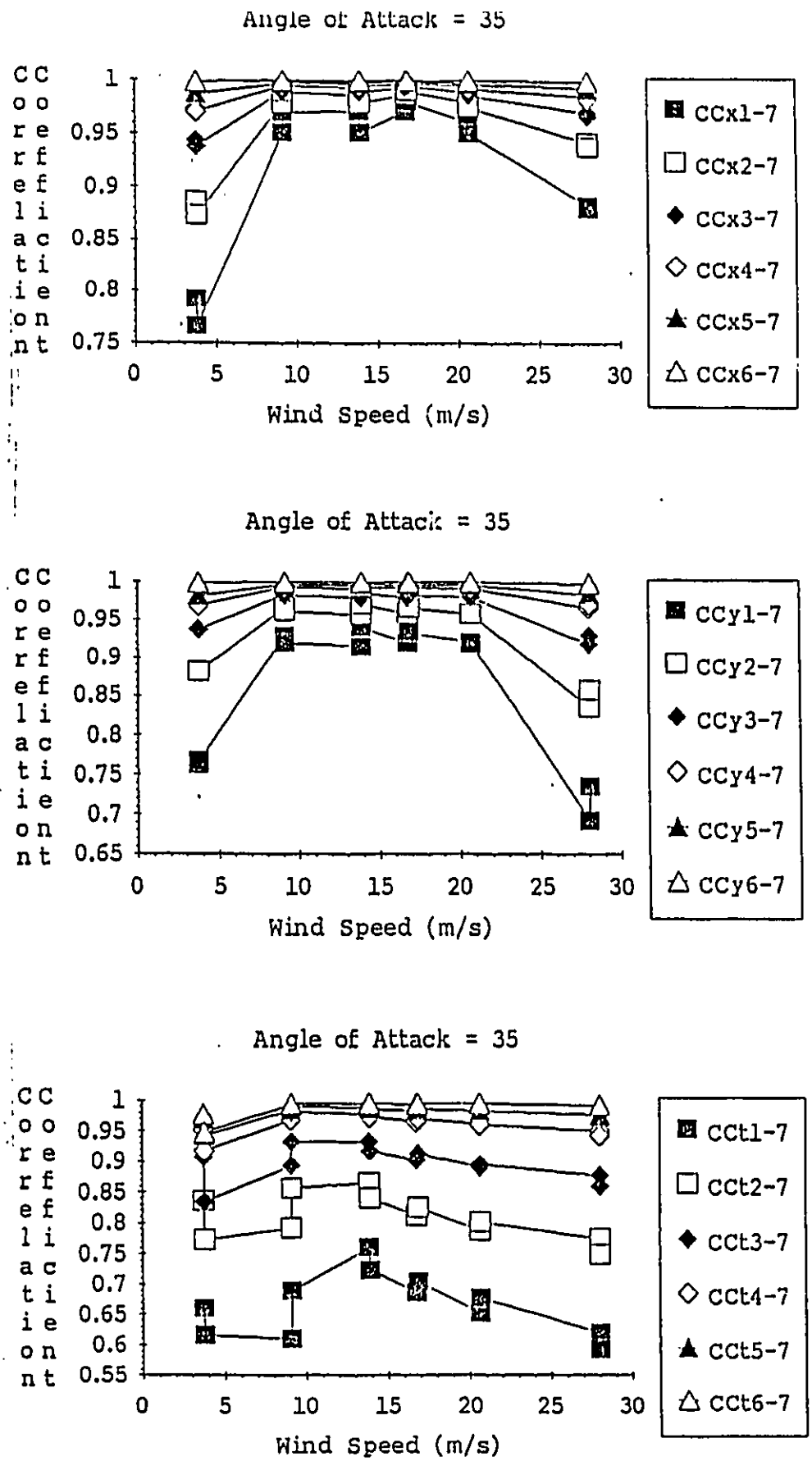

(from [4.3)

Fig.5.8 Vertical Correlation of Response

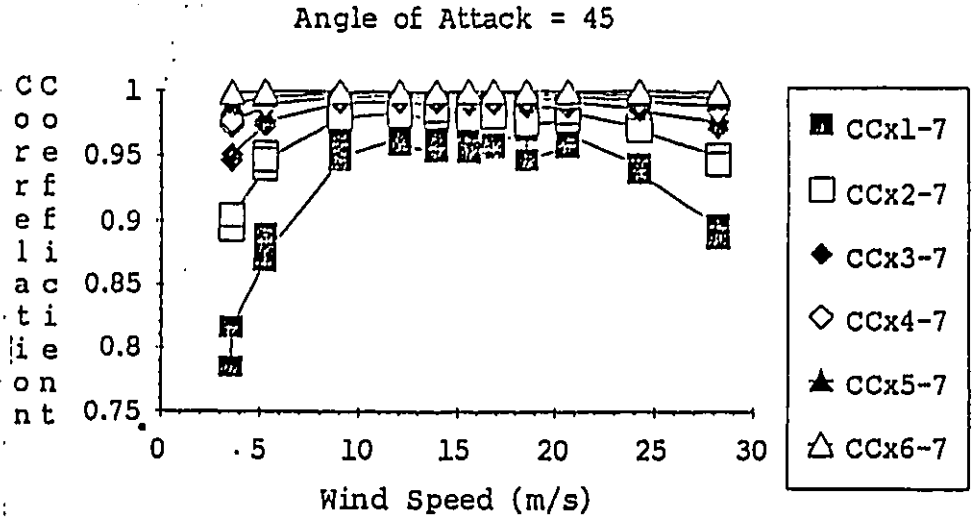

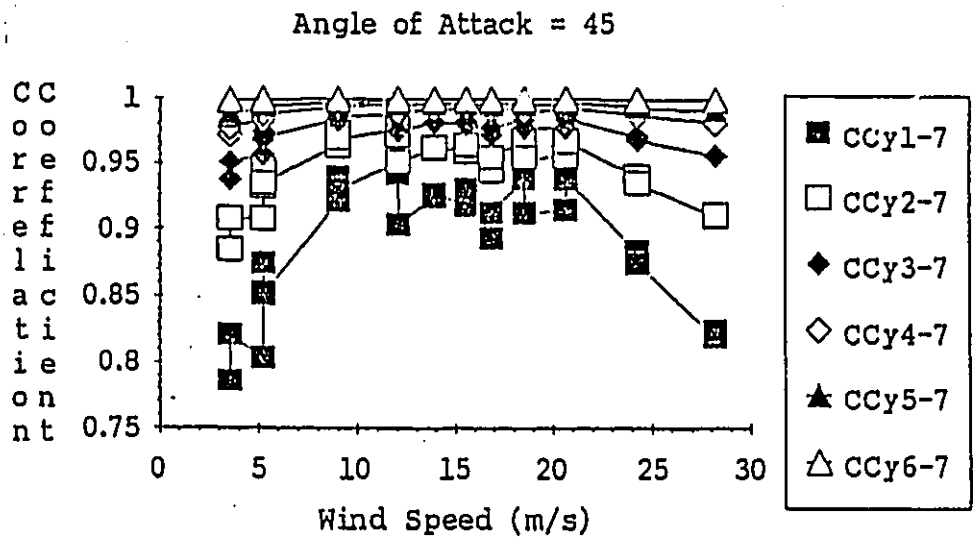

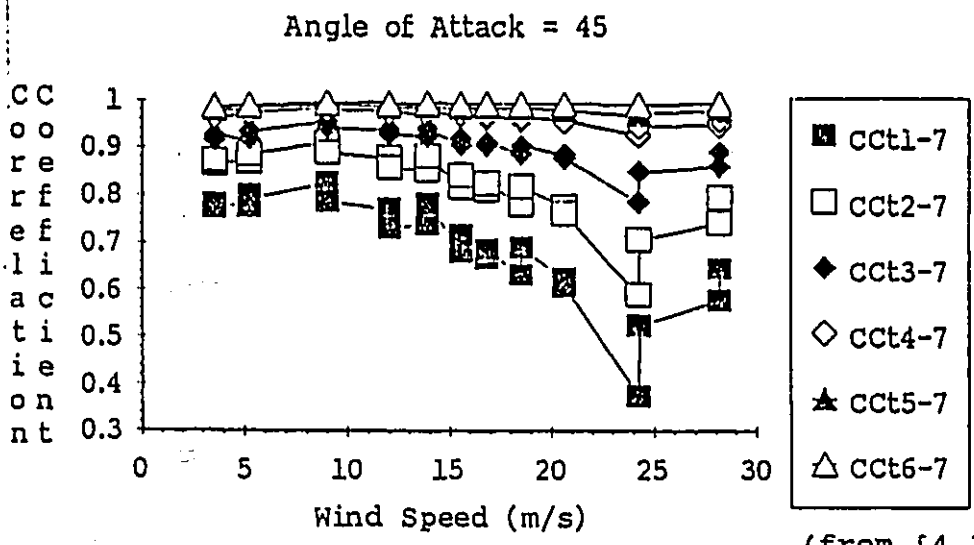

(from [4.3])

Fig.5.8 Vertical Correlation of Response

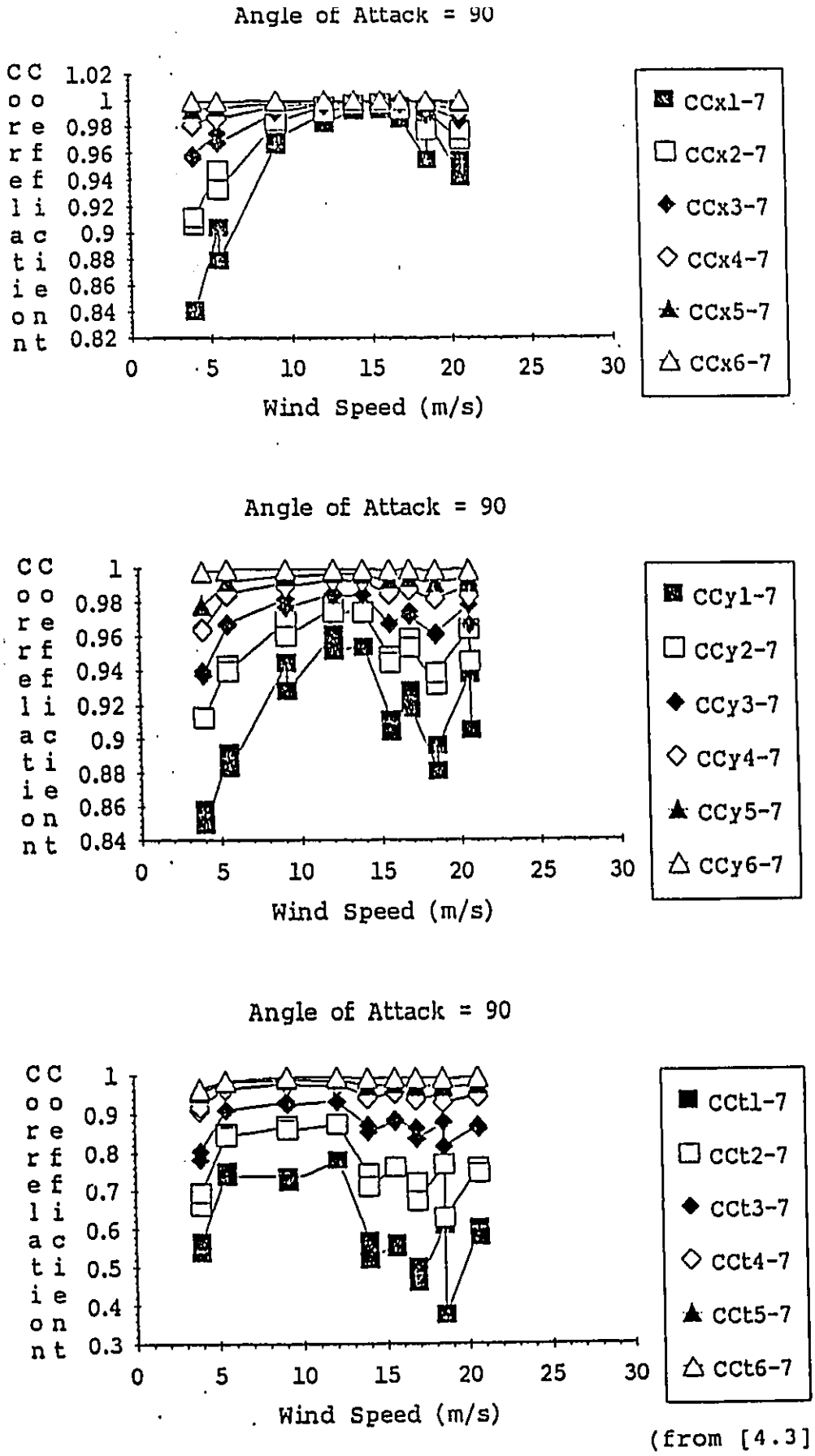

(from [4.3])

Fig.5.8 Vertical Correlation of Response

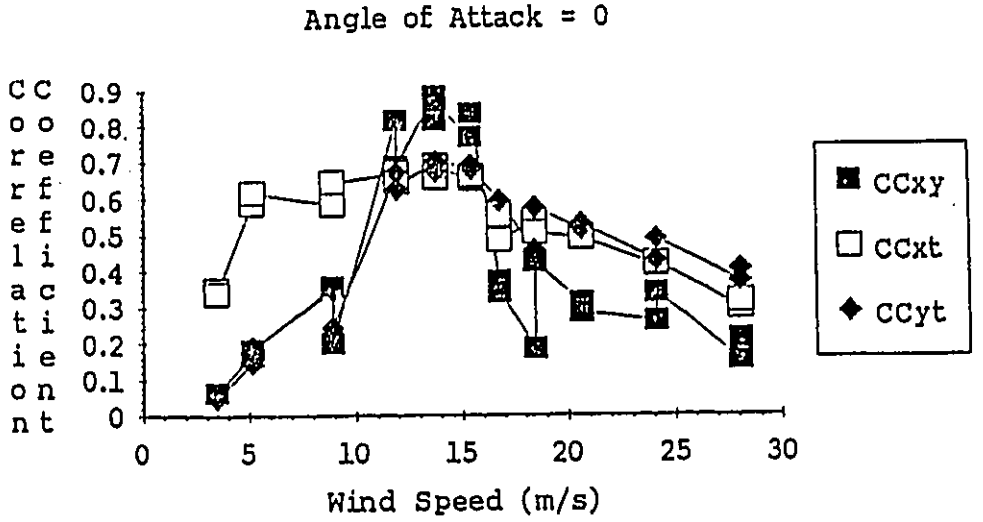

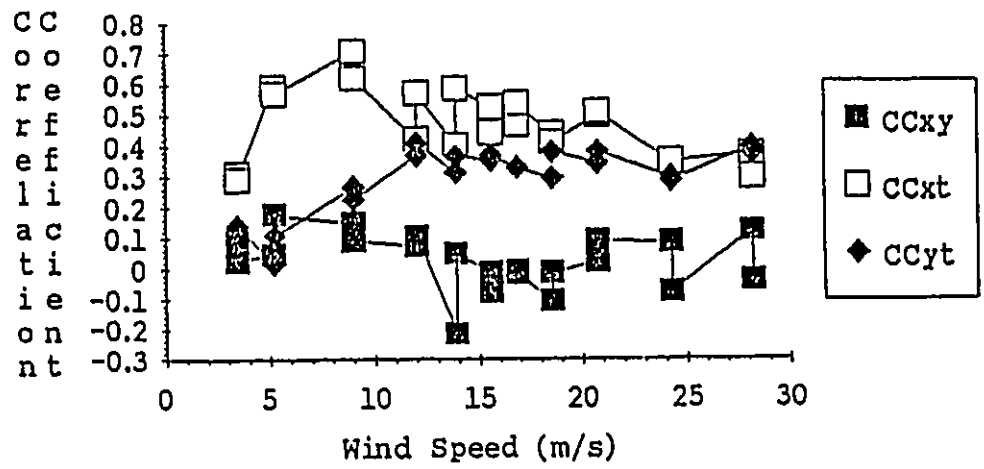

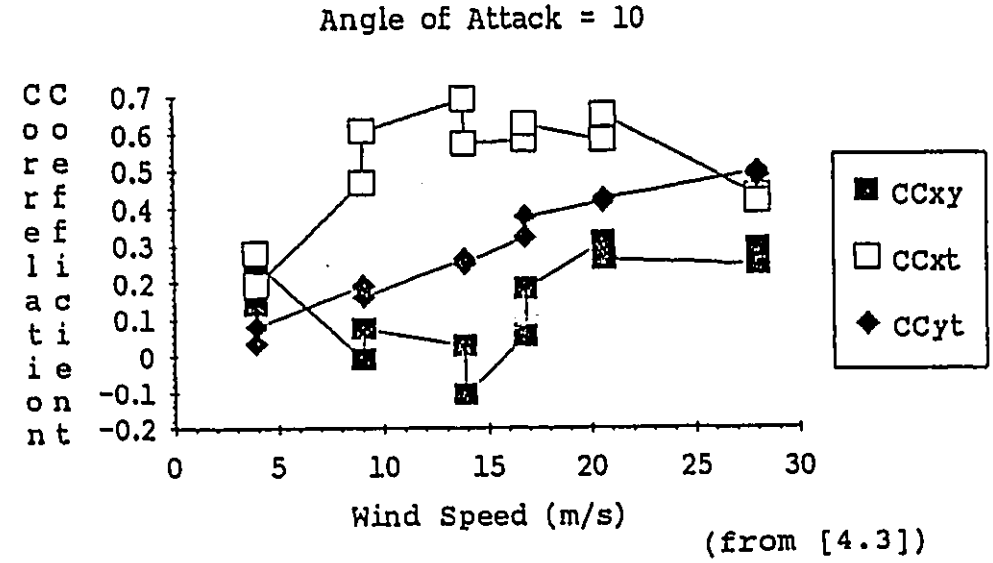

(from [4.3])

Fig.5.9 Correlation between Mode

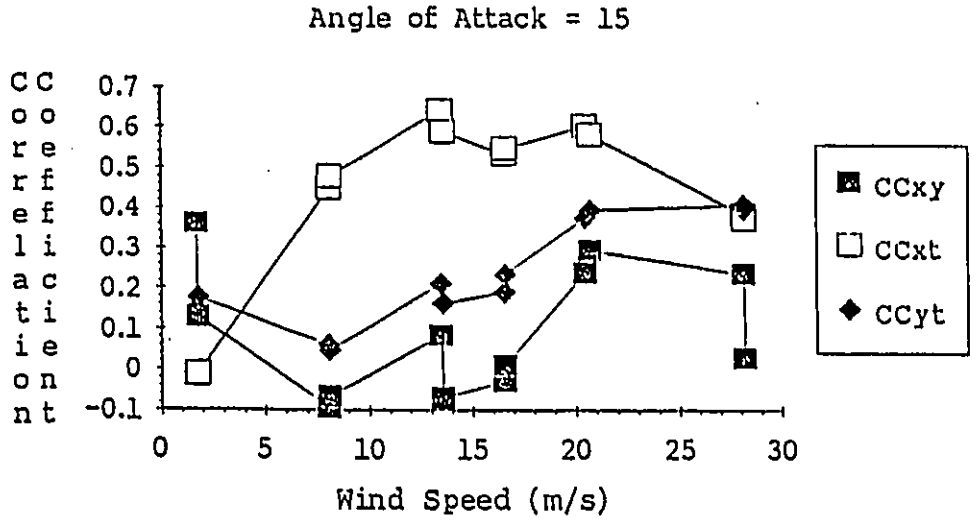

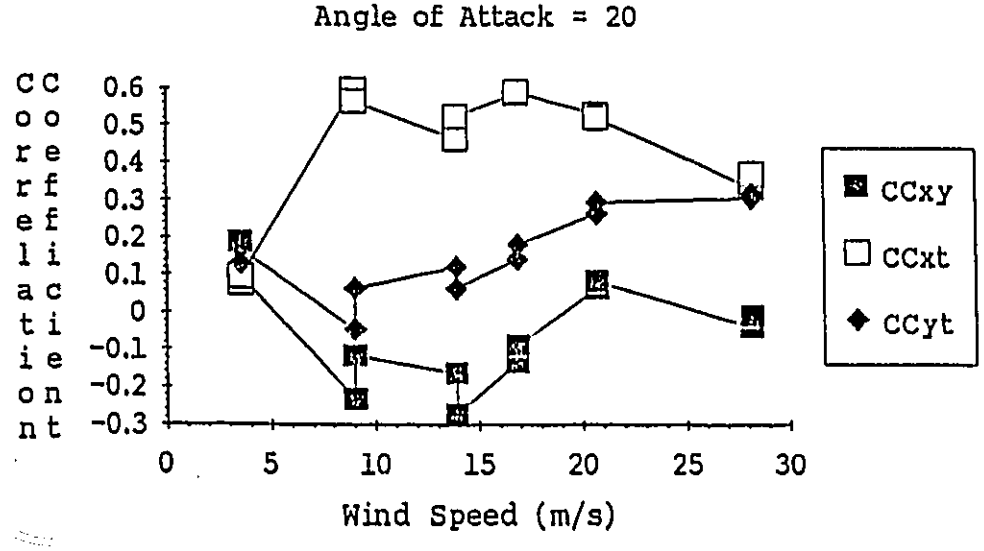

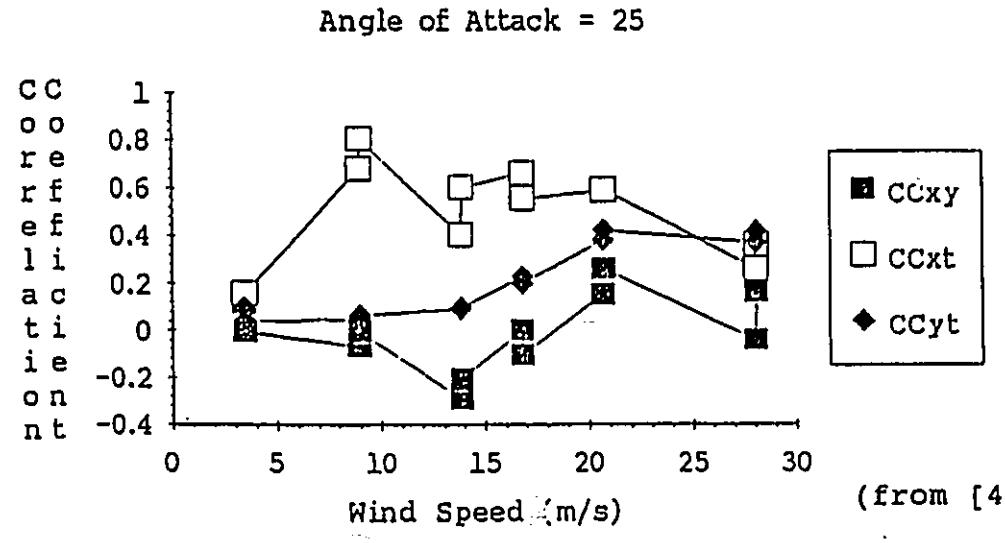

(from [4.3])

Fig.5.9 Correlation between Modes

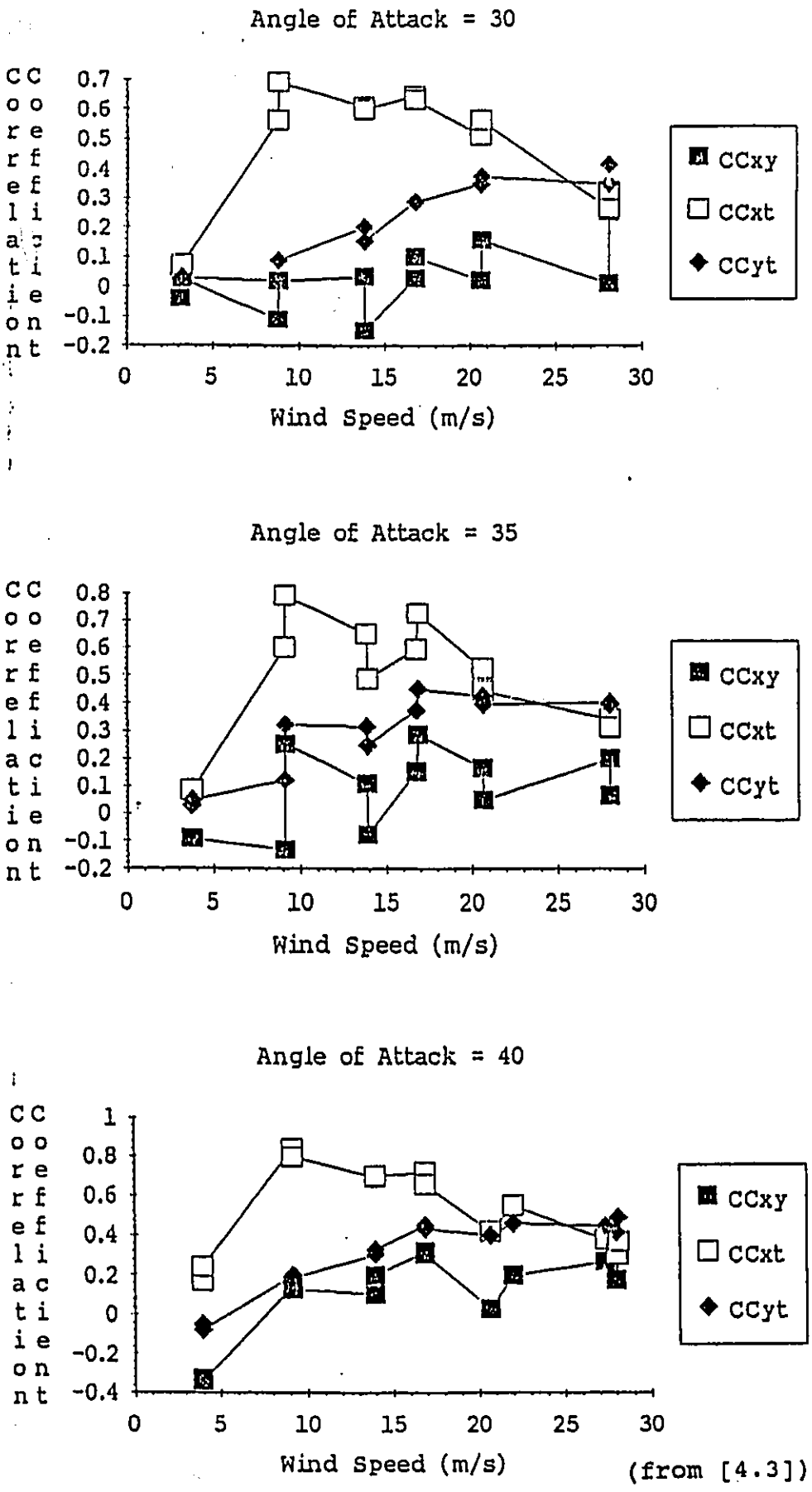

(from [4.3])

Fig.5.9 Correlation between Modes

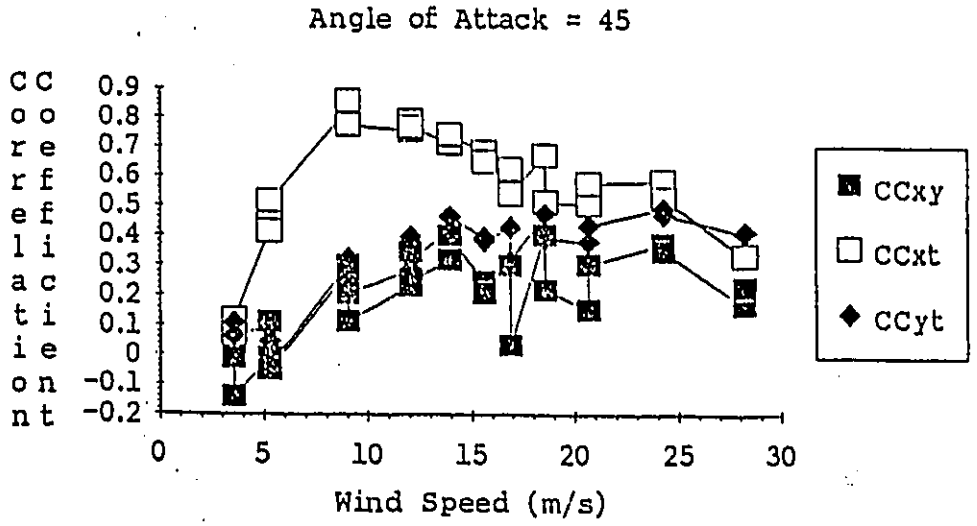

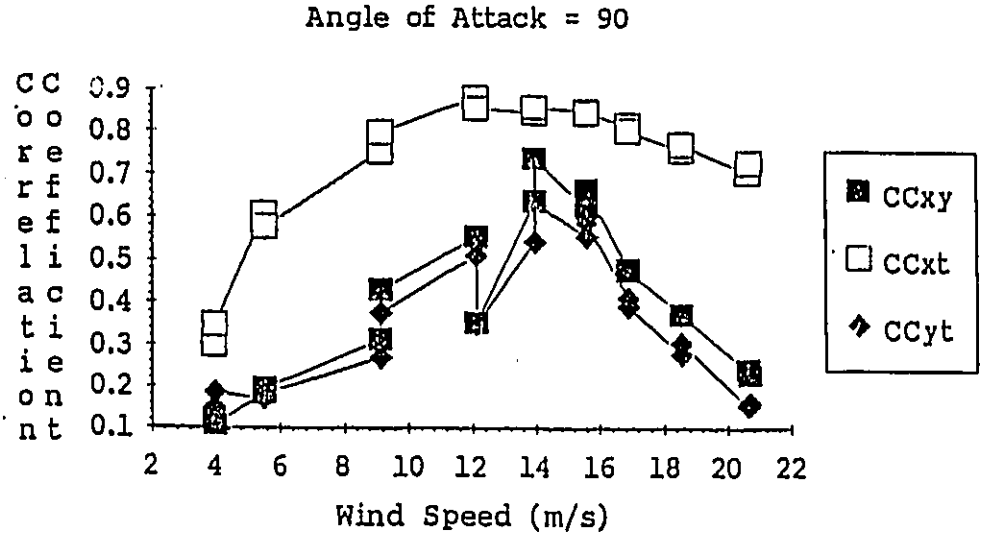

(from [4.3])

Fig.5.9 Correlation between Modes

Fig.5.10. Response Autocorrelation Function

The following 11 pages show the response autocorrelation for each azimuth angle in the highest tested wind speed for each run. Each page has three autocorrelation; X, Y and torsion. These autocorrelation function were obtained by applying the inverse Fourier Transform on the spectra which were analysed by using Fast Fourier Transform method. These figures are from [4.3]

Run- 103 Point- 13

Angle of Attack- 0 Wind Speed- 28.090 (m/s)

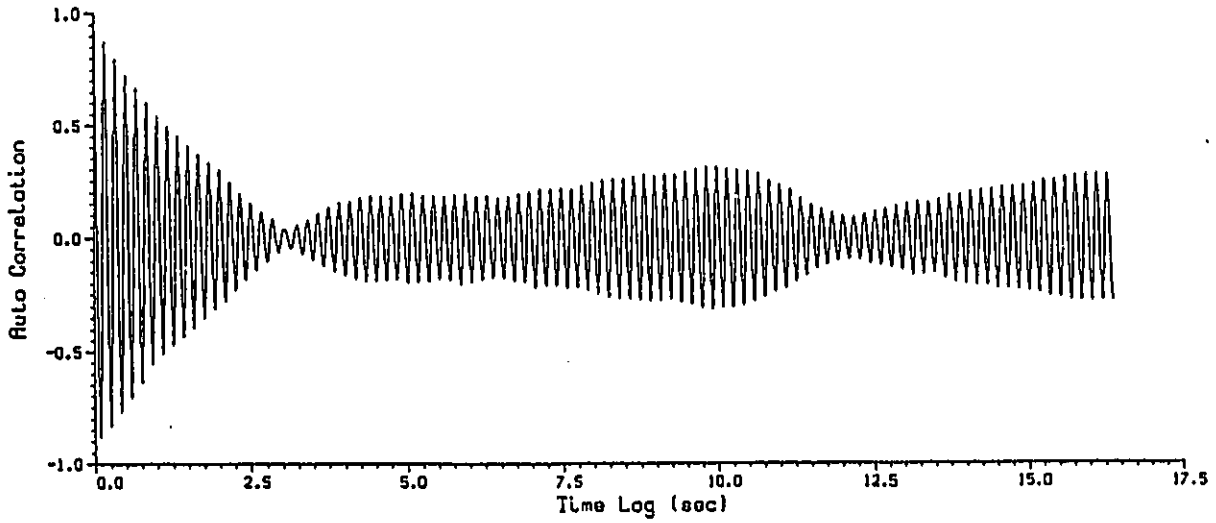

X Direction

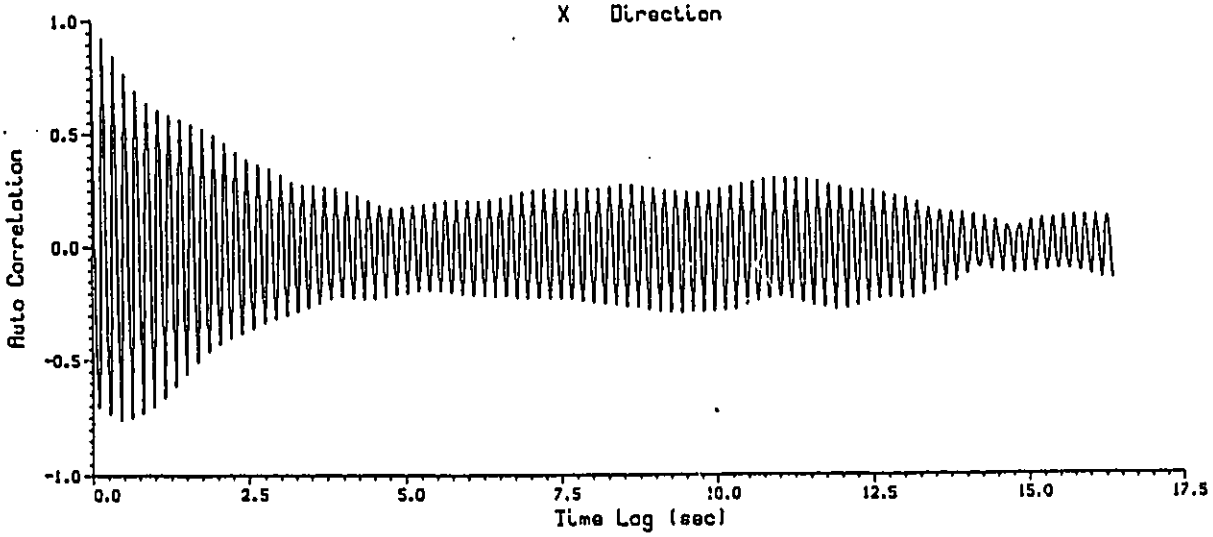

Y Direction

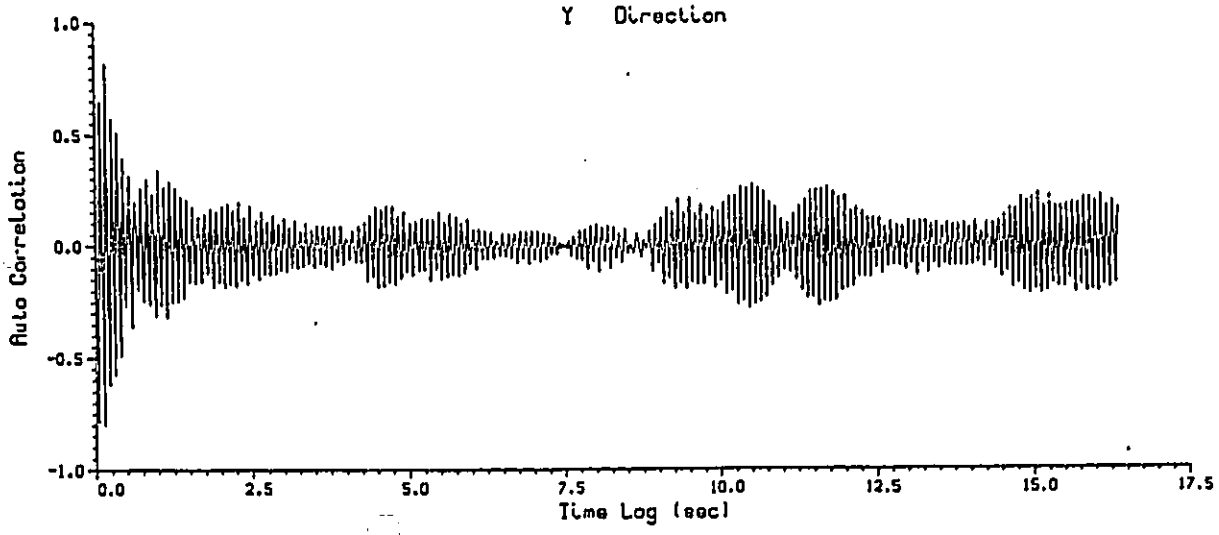

T Direction

Run- 108 Point- 11

Angle of Attack- 5 Wind Speed- 28.230 (m/s)

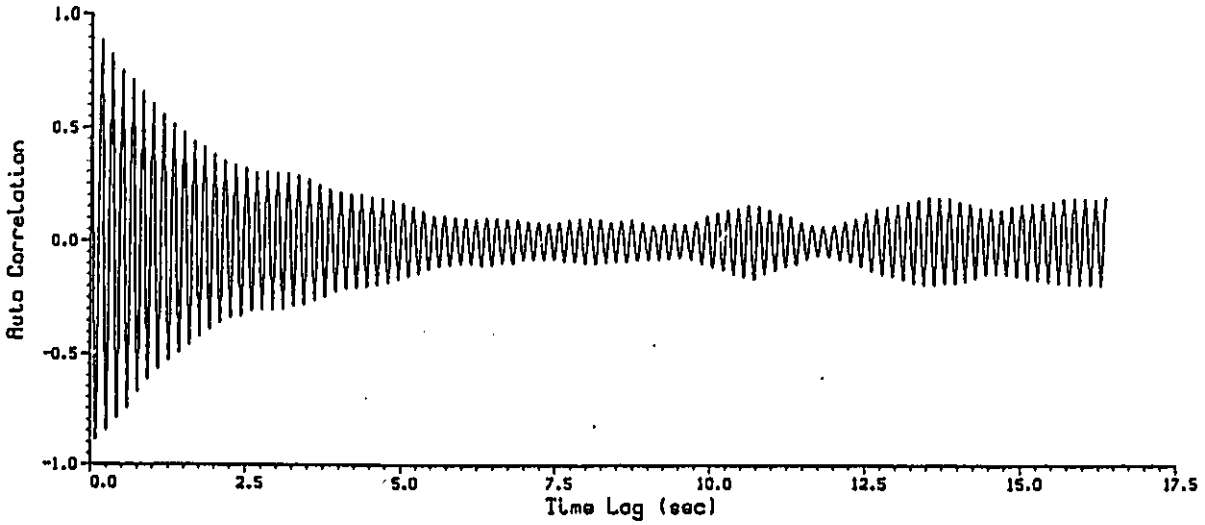

X Direction

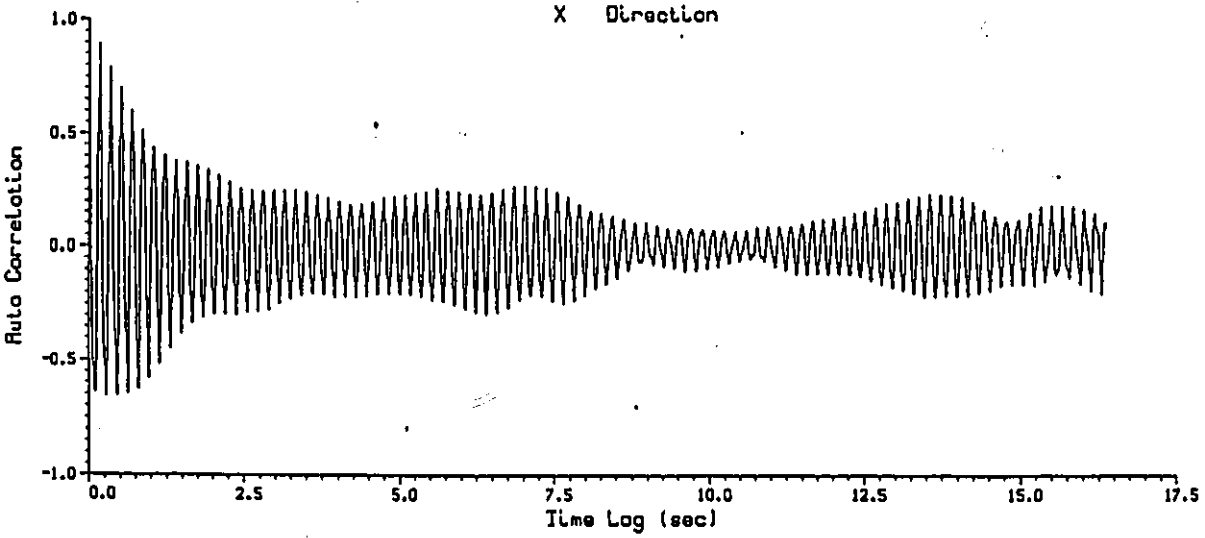

Y Direction

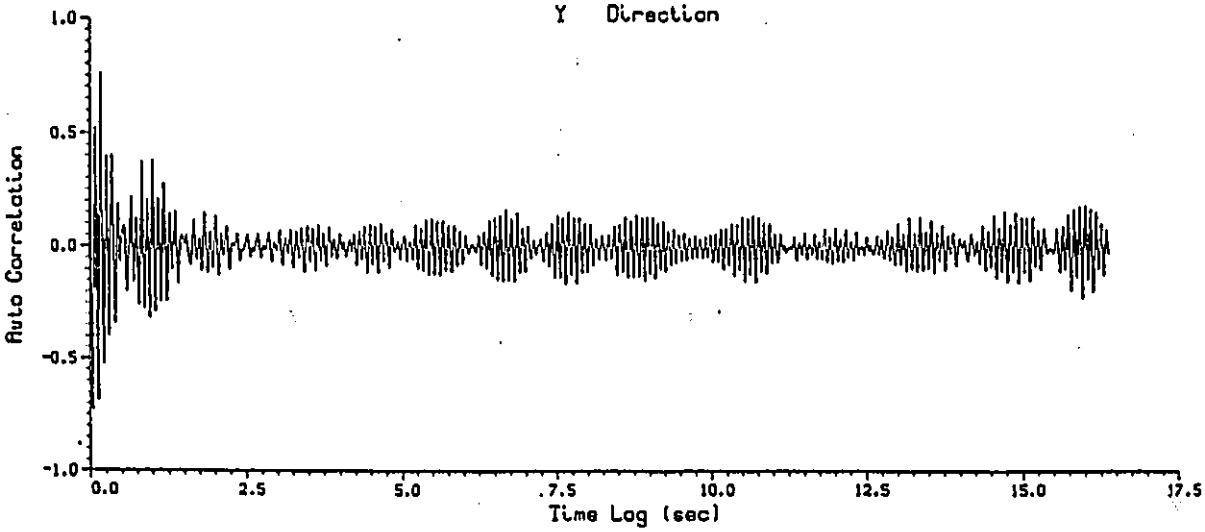

T Direction

Run- 129 Point- 11

Angle of Attack- 10 Wind Speed- 28.043 (m/s)

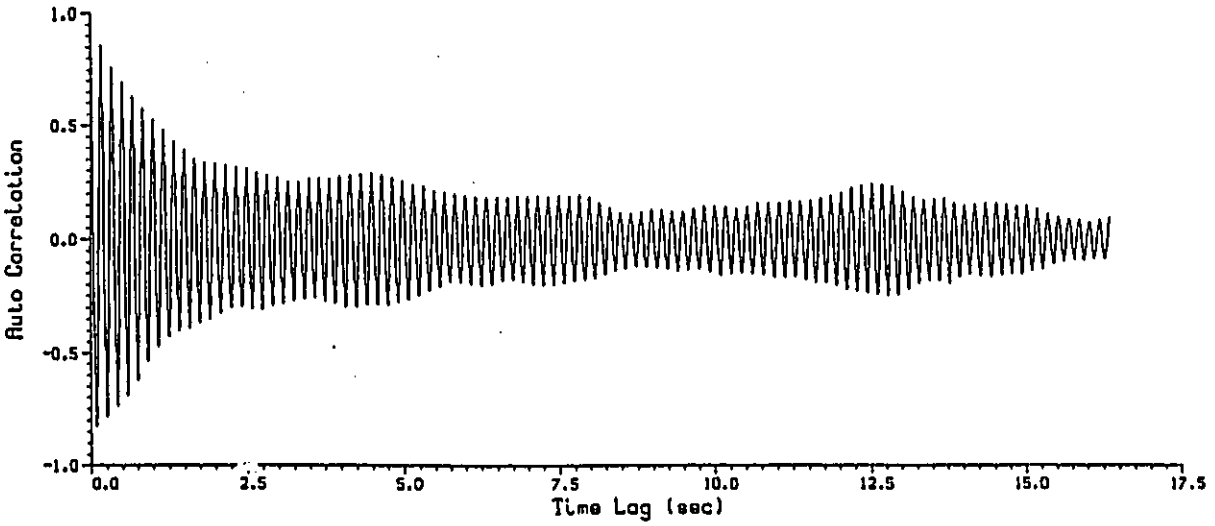

X Direction

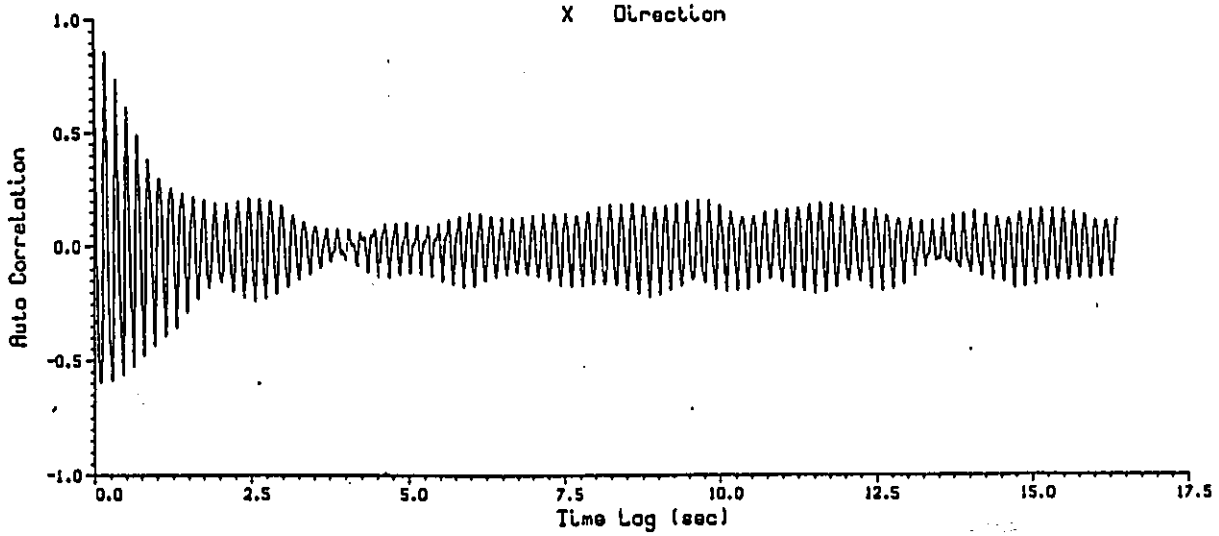

Y Direction

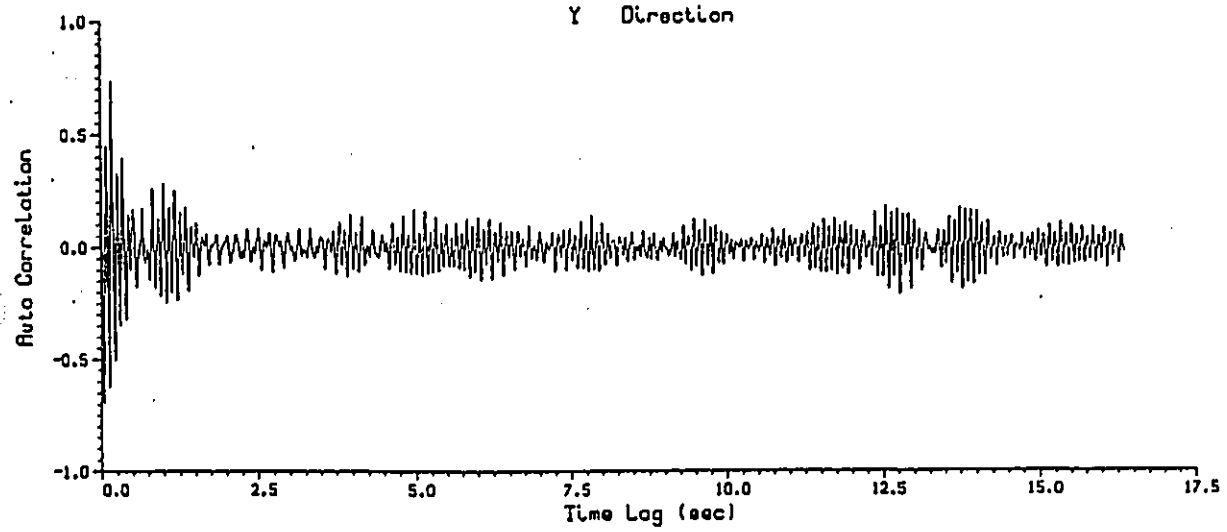

T Direction

Run- 118 Point- 11

Angle of Attack- 15 Wind Speed- 28.153 (m/s)

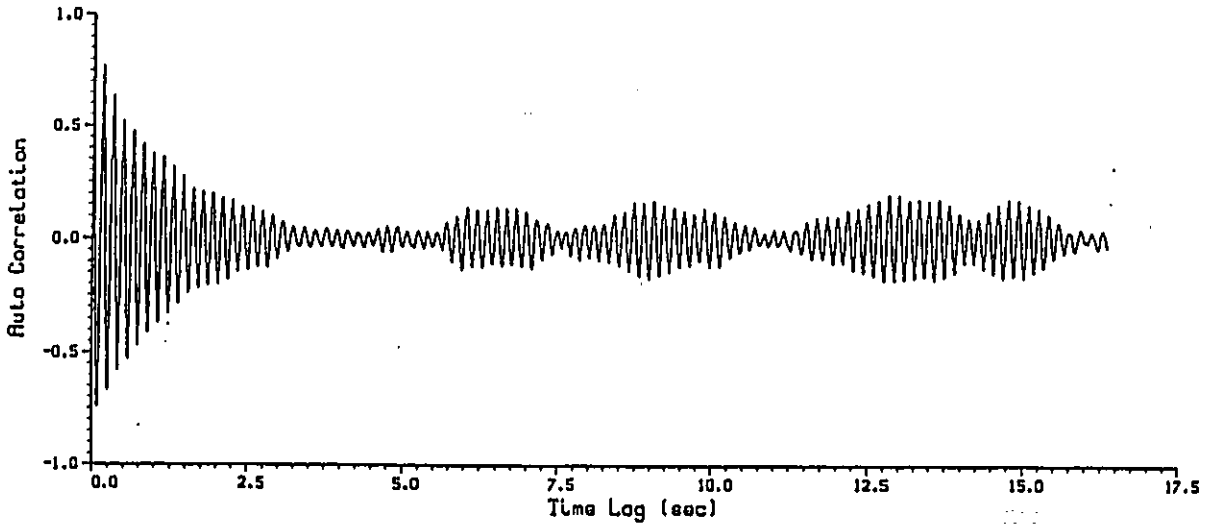

X Direction

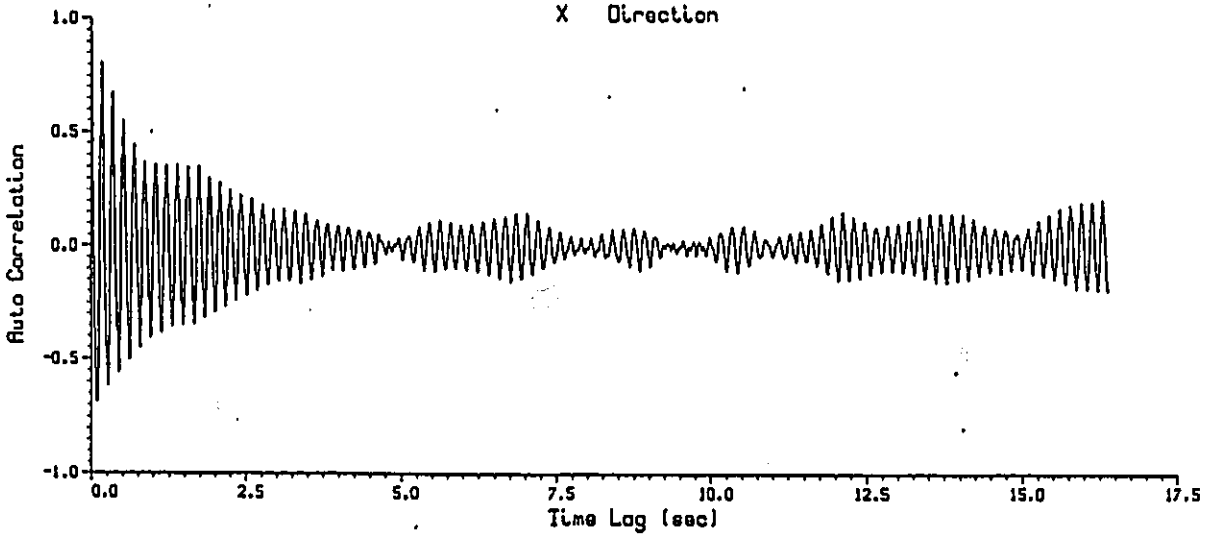

Y Direction

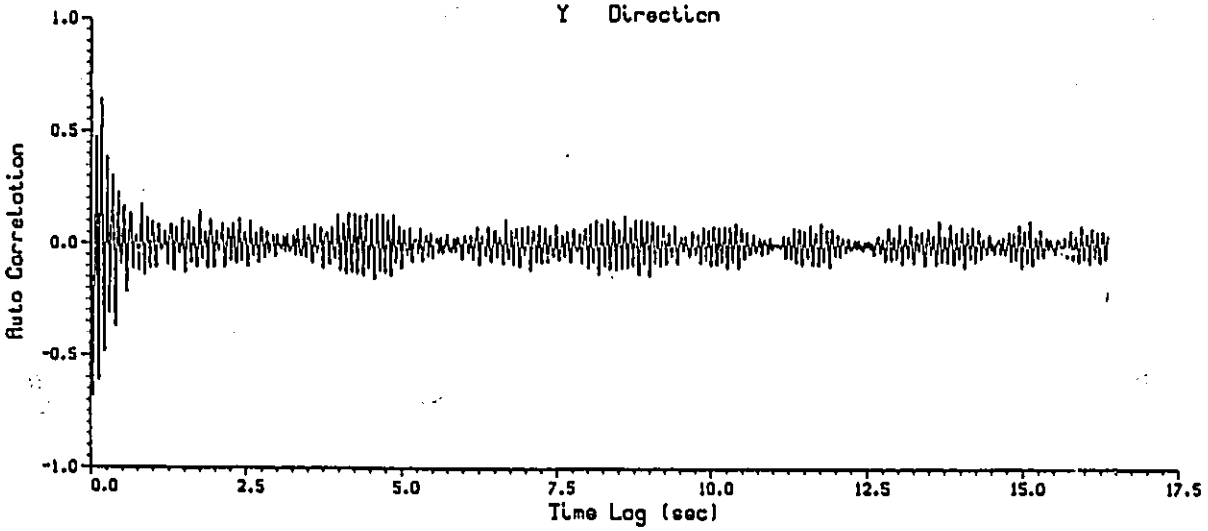

T Direction

Run- 116 Point- 11

Angle of Attack- 20 Wind Speed- 28.165 (m/s)

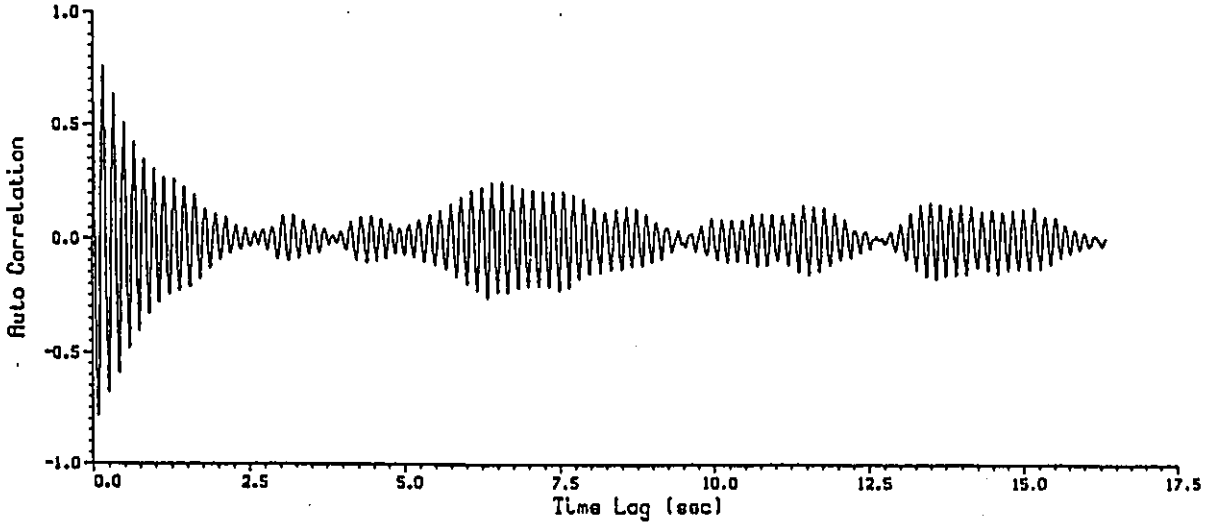

X Direction

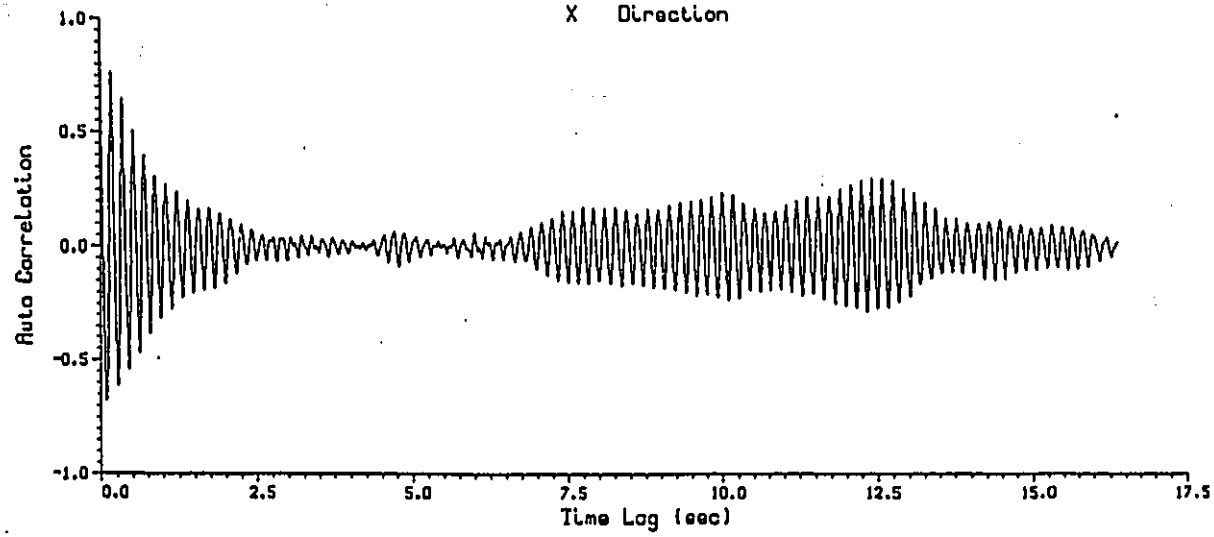

Y Direction

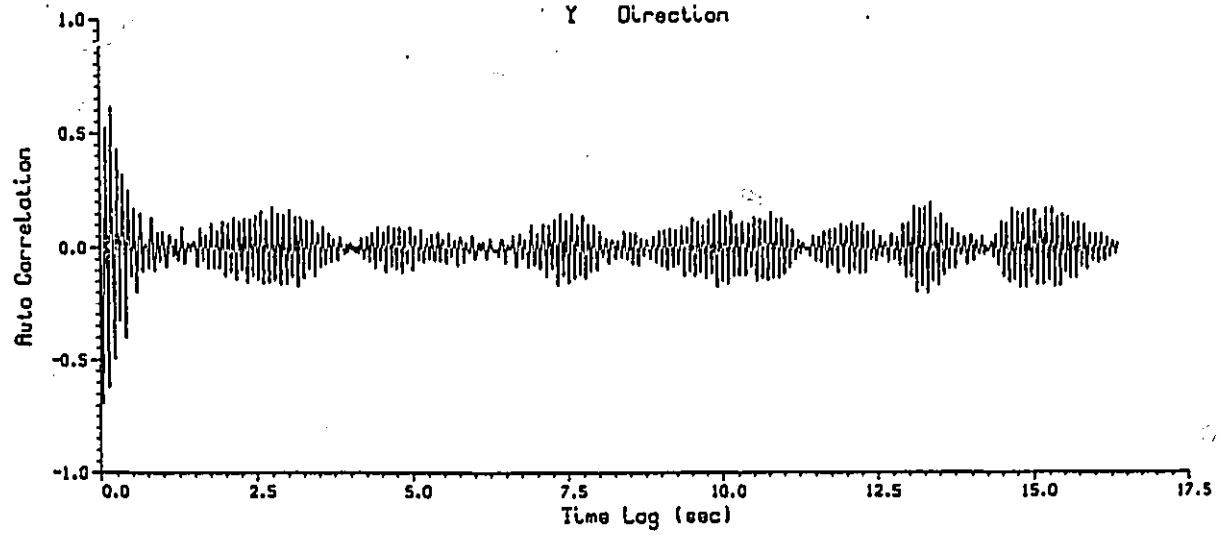

T Direction

Run- 127 Point- 3

Angle of Attack- 25 Wind Speed- 28.094 (m/s)

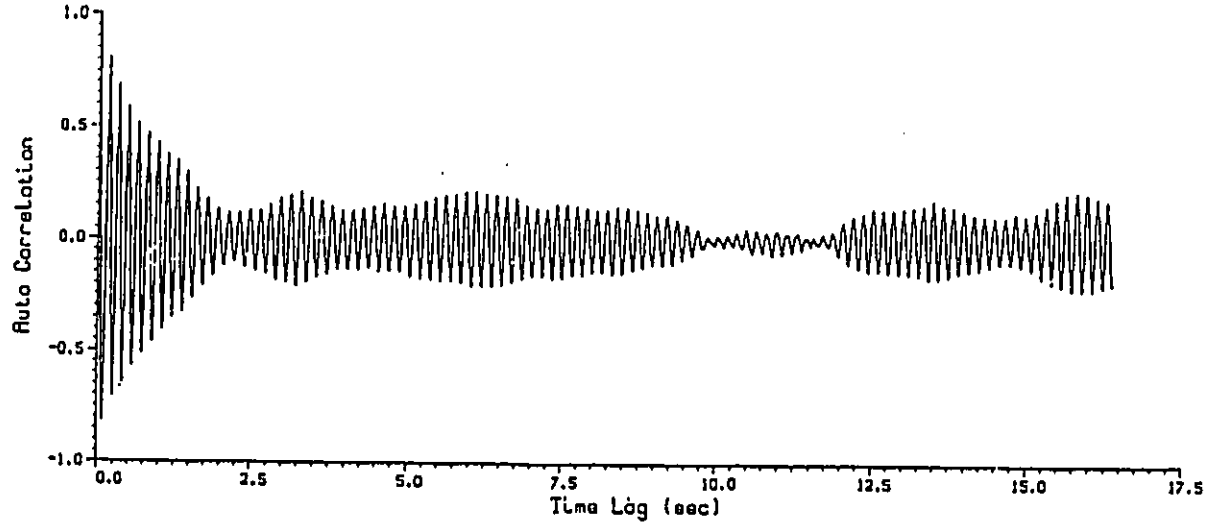

X Direction

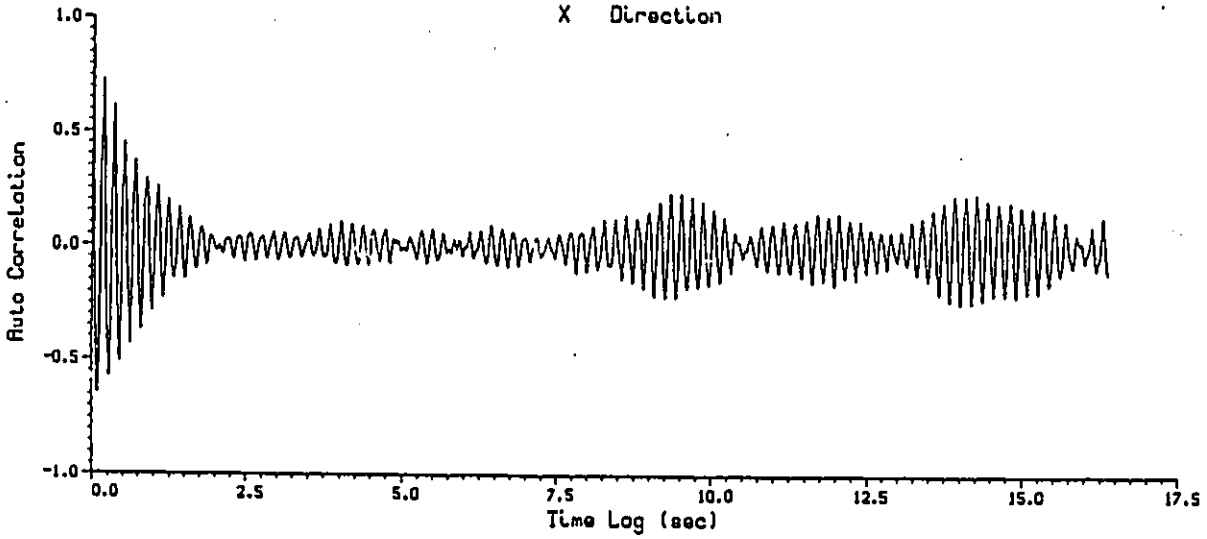

Y Direction

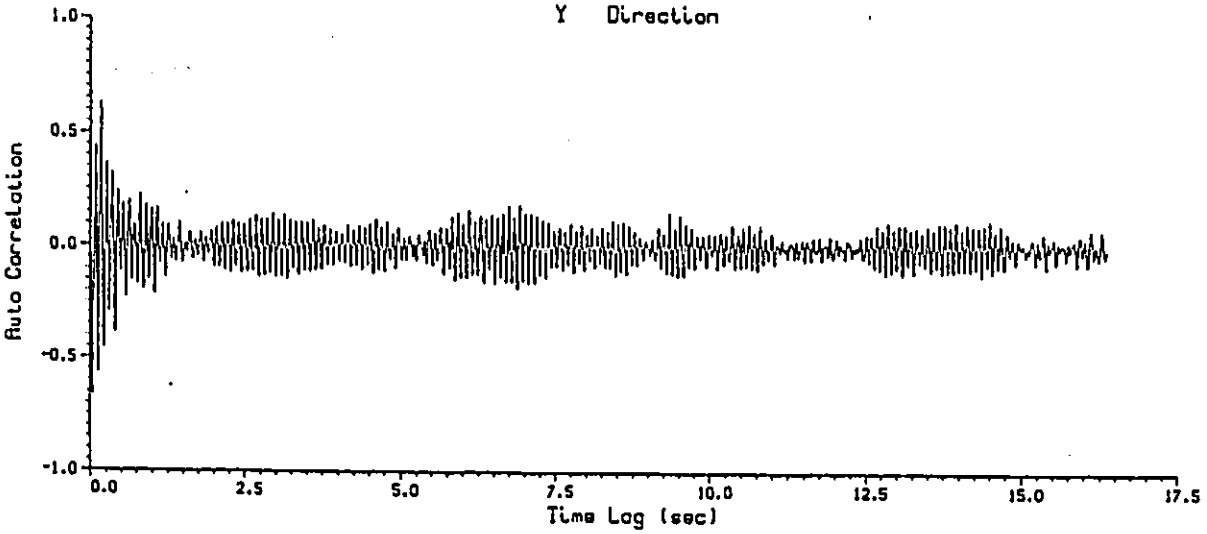

T Direction

Run- 120 Point- 11

Angle of Attack- 30 Wind Speed- 28.064 (m/s)

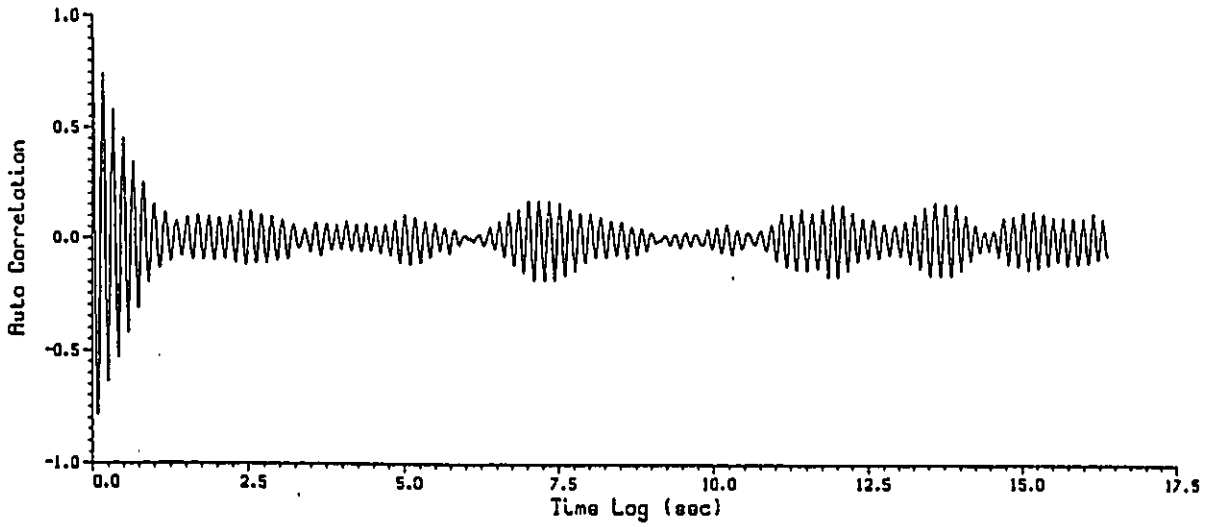

X Direction

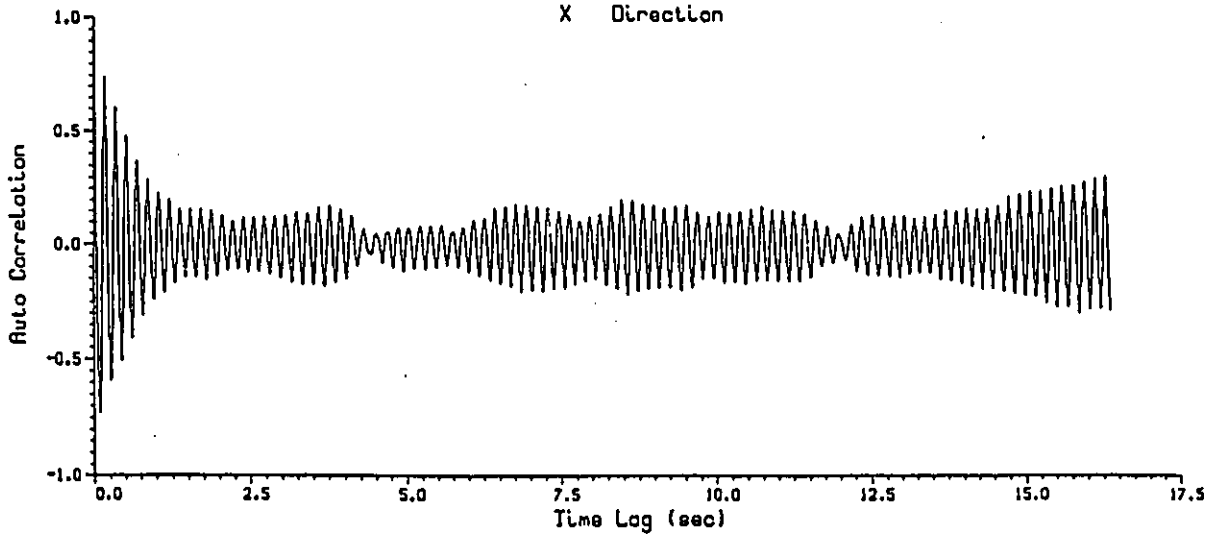

Y Direction

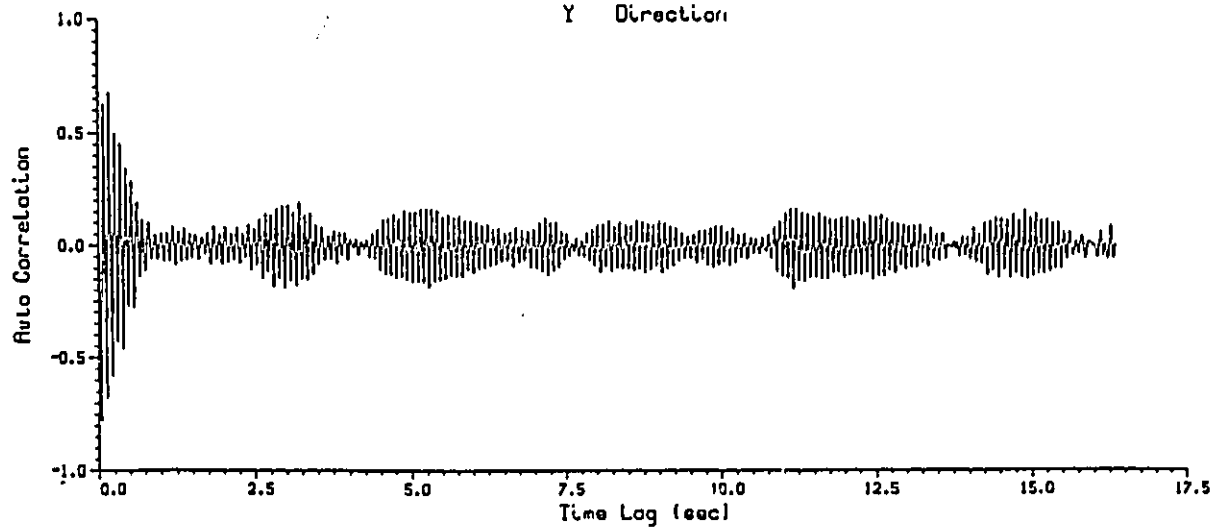

T Direction

Run- 131 Point- 11

Angle of Attack- 35 Wind Speed- 28.031 (m/s)

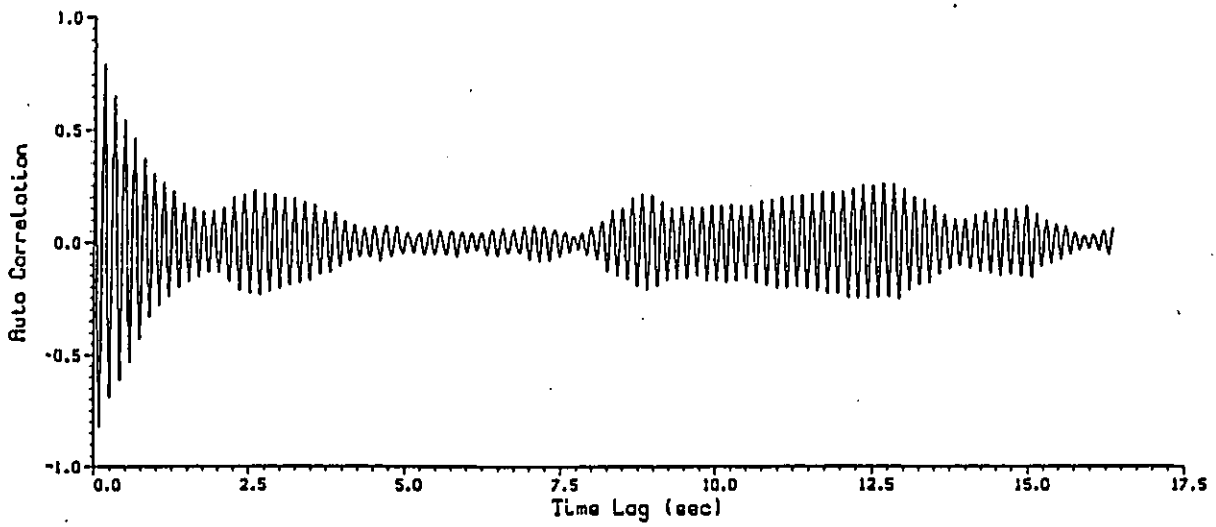

X Direction

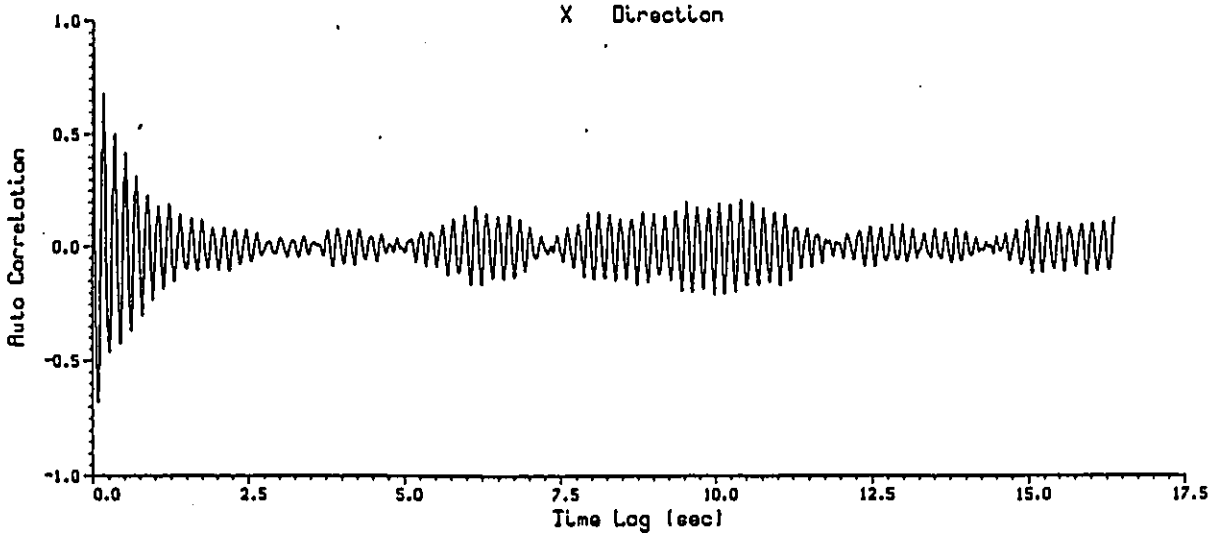

Y Direction

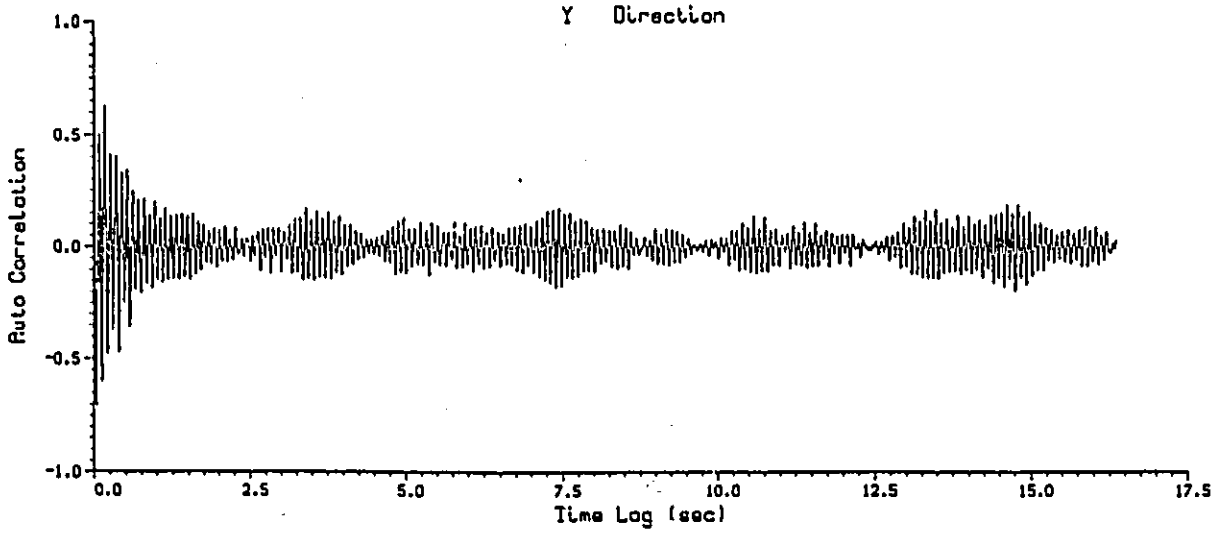

T Direction

Run- 133 Point- 11

Angle of Attack- 40 Wind Speed- 27.997 (m/s)

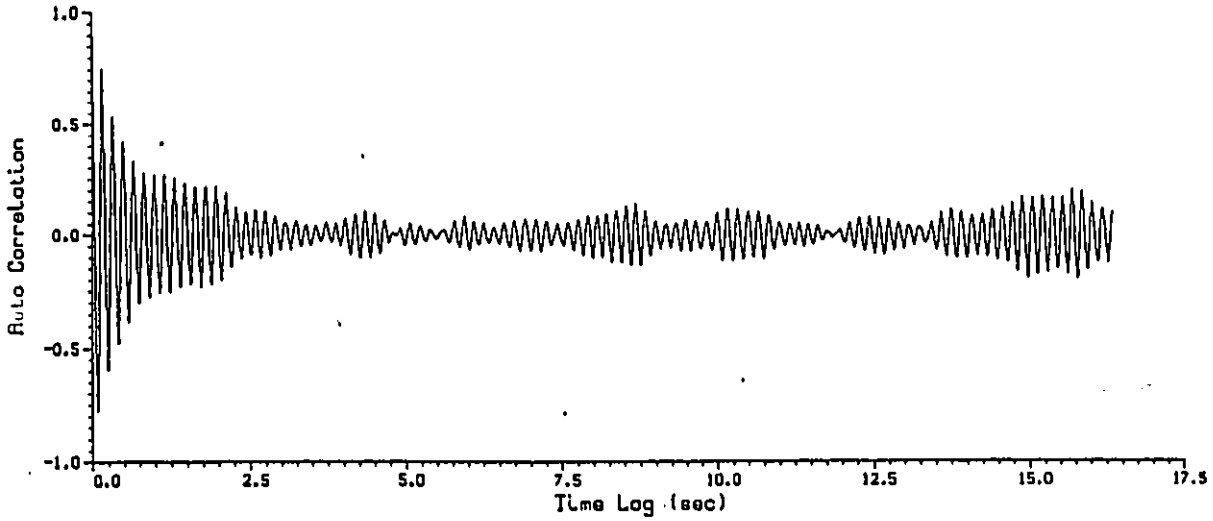

X Direction

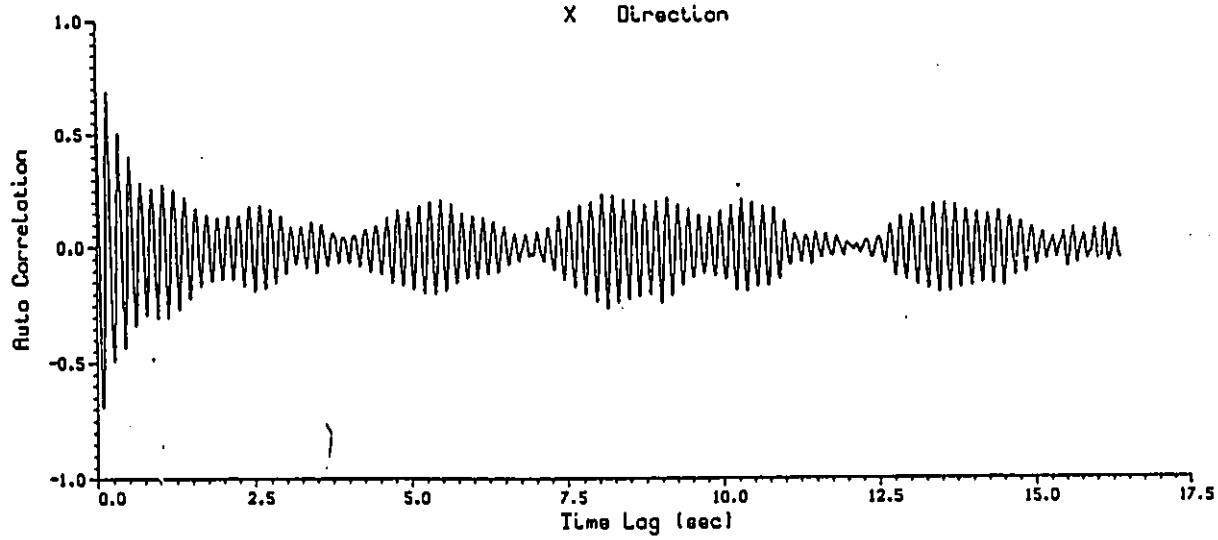

Y Direction

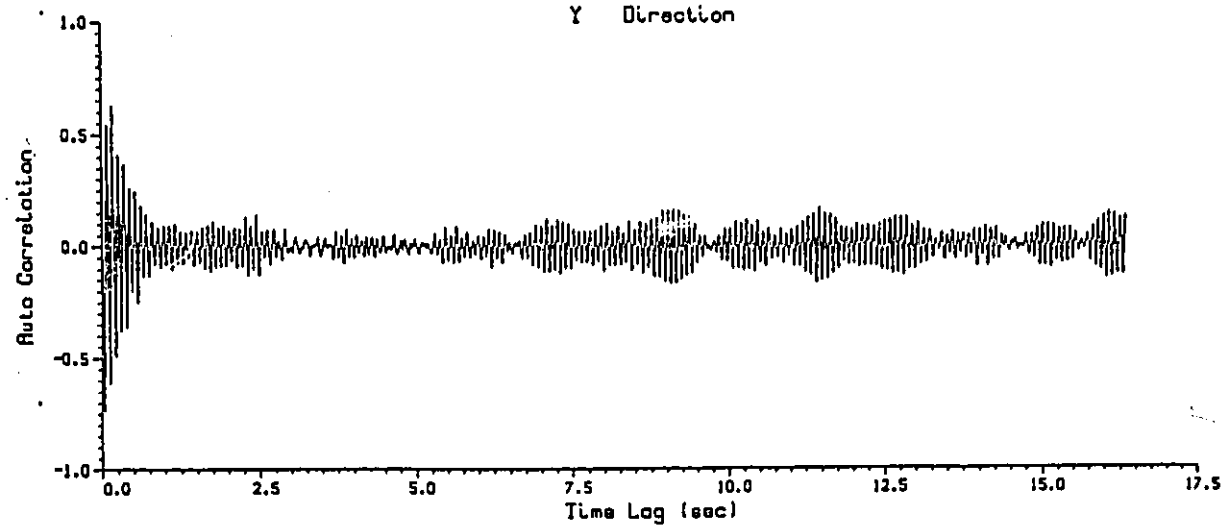

T Direction

Run- 114 Point- 14

Angle of Attack- 45 Wind Speed- 28.210 (m/s)

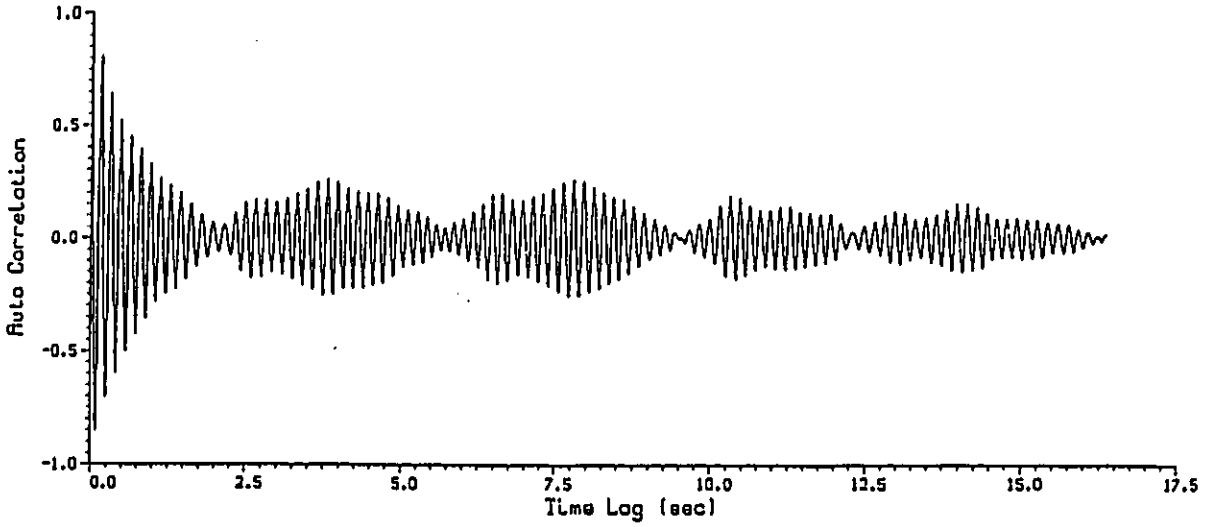

X Direction

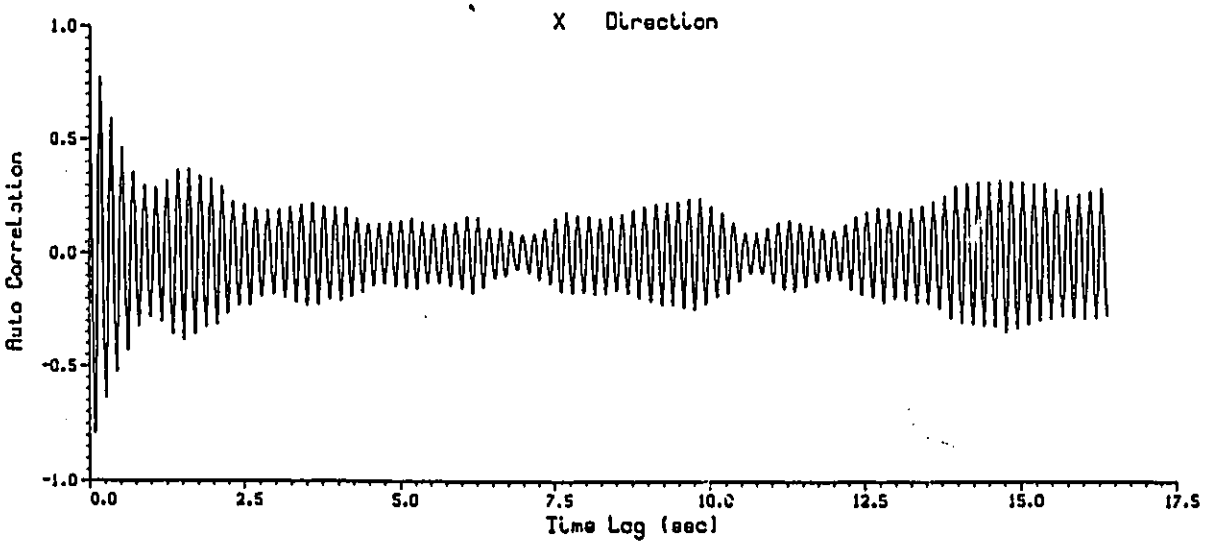

Y Direction

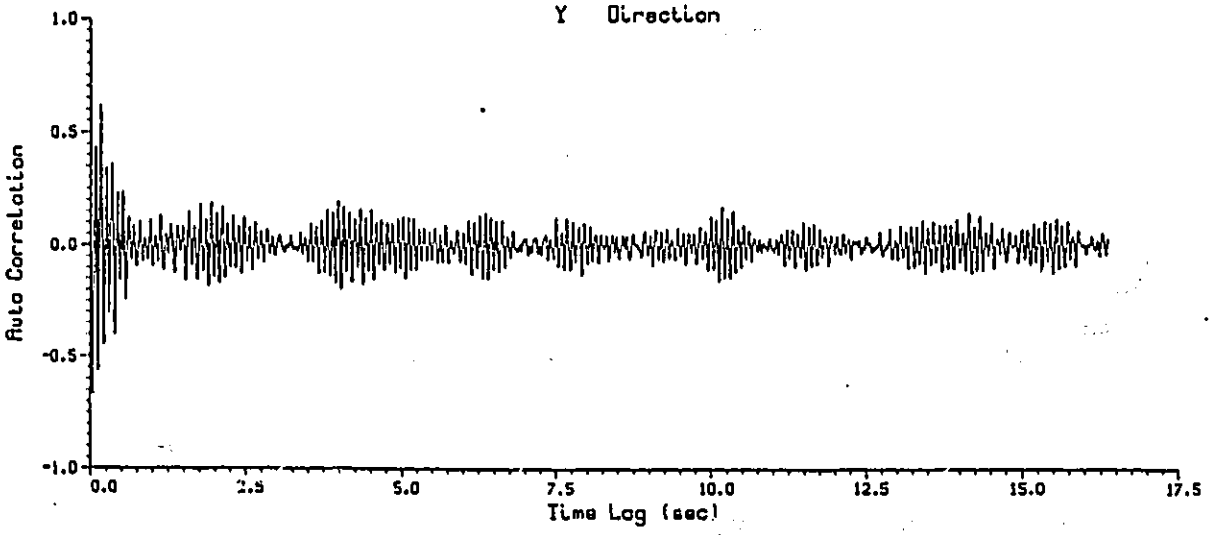

T Direction

Run- 137 Point- 5

Angle of Attack- 90 Wind Speed- 20.697 (m/s)

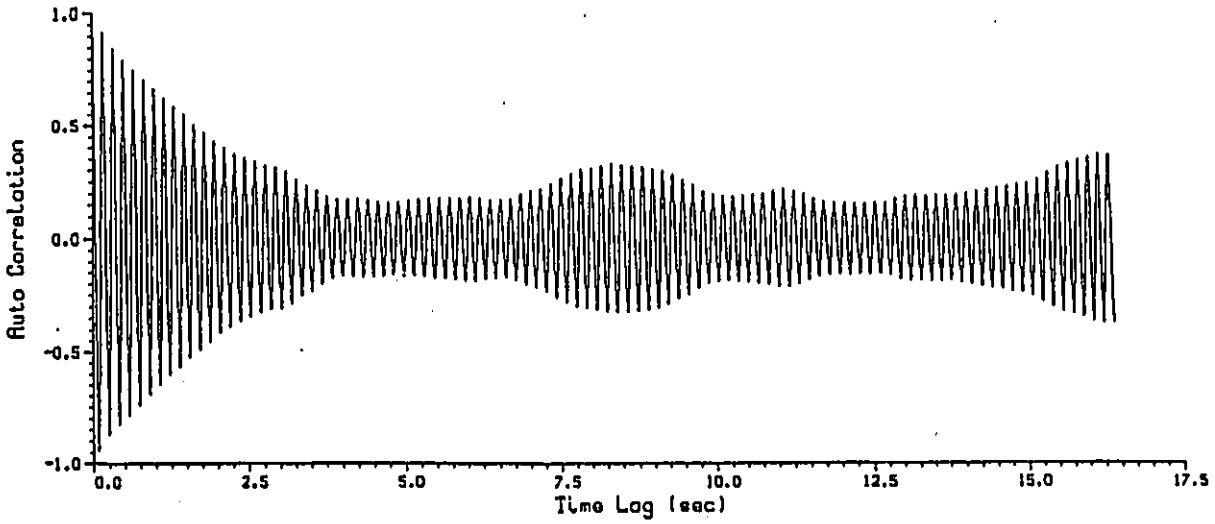

X Direction

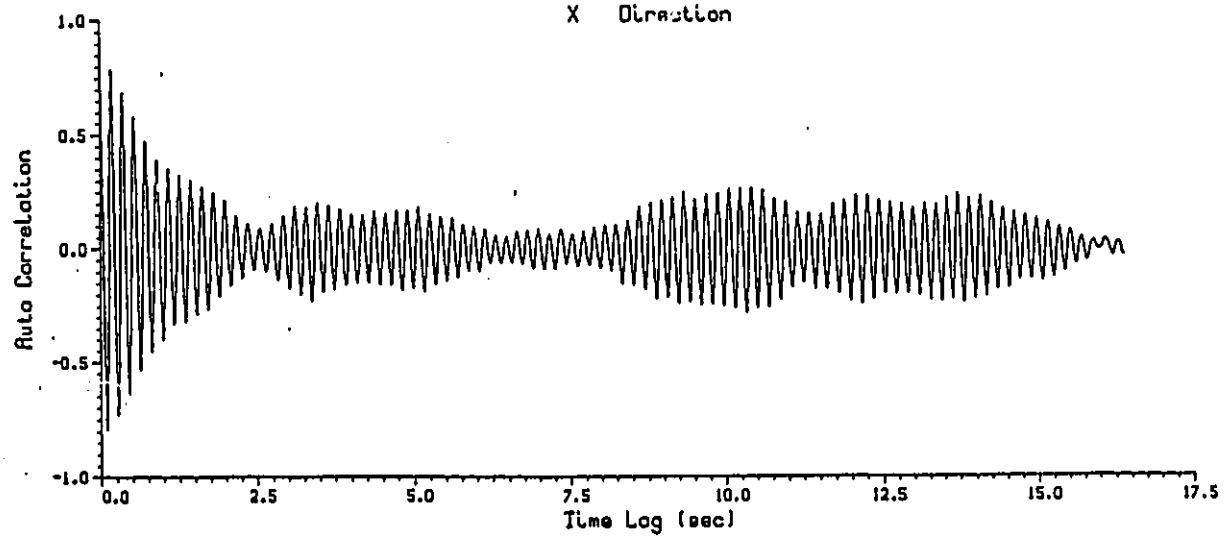

Y Direction

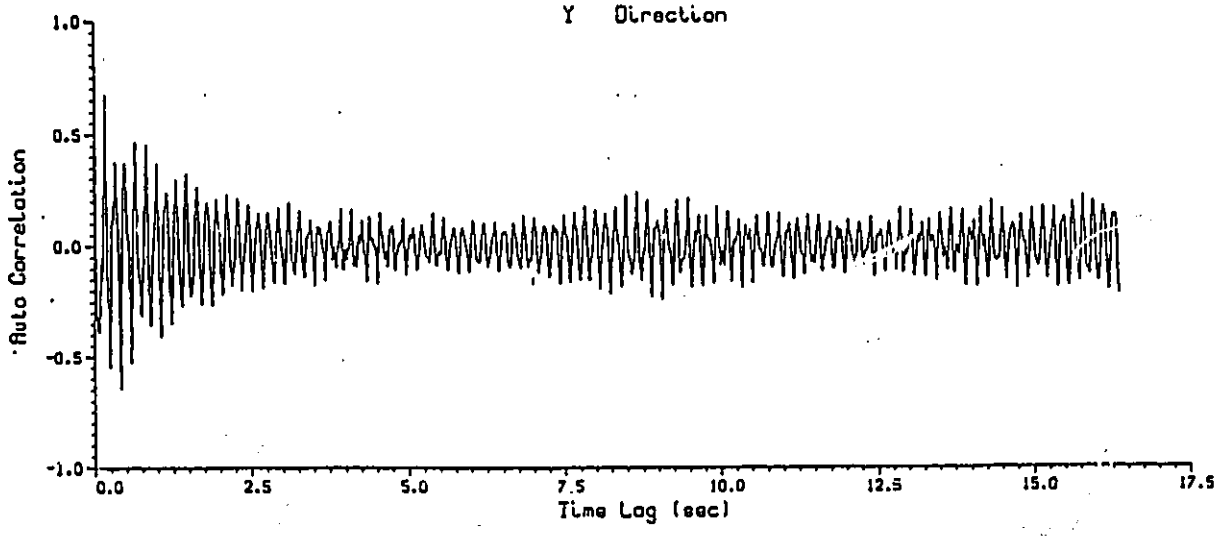

Z Direction

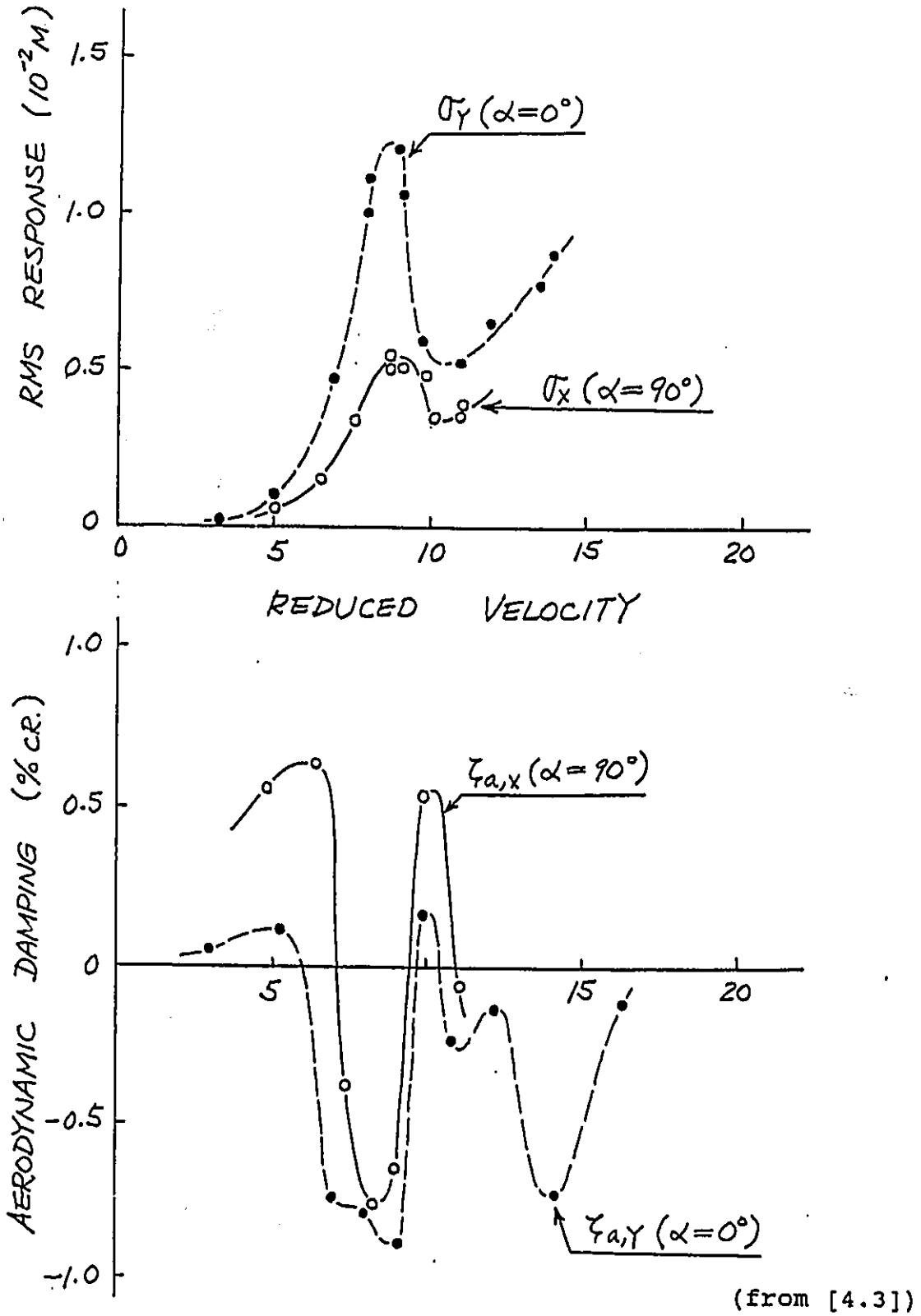

(from [4.3])

Fig.5.11 Aerodynamic Damping

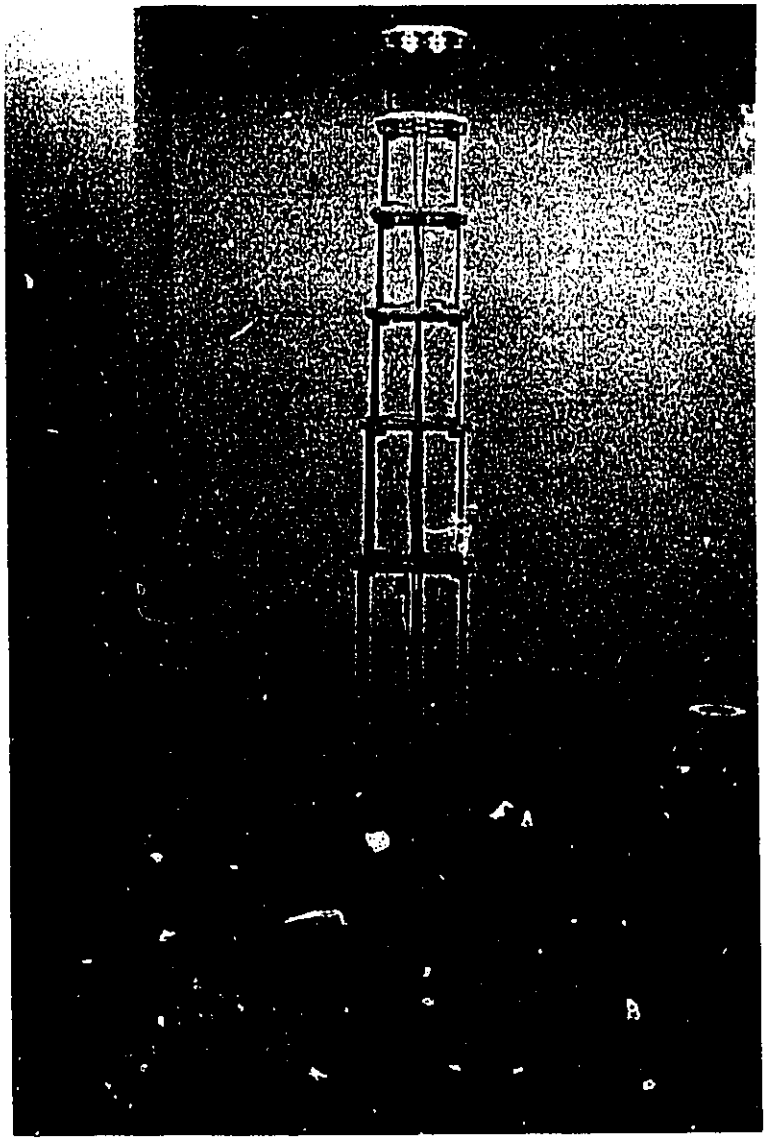

Photo.4.1 Assembled Frame of the Model

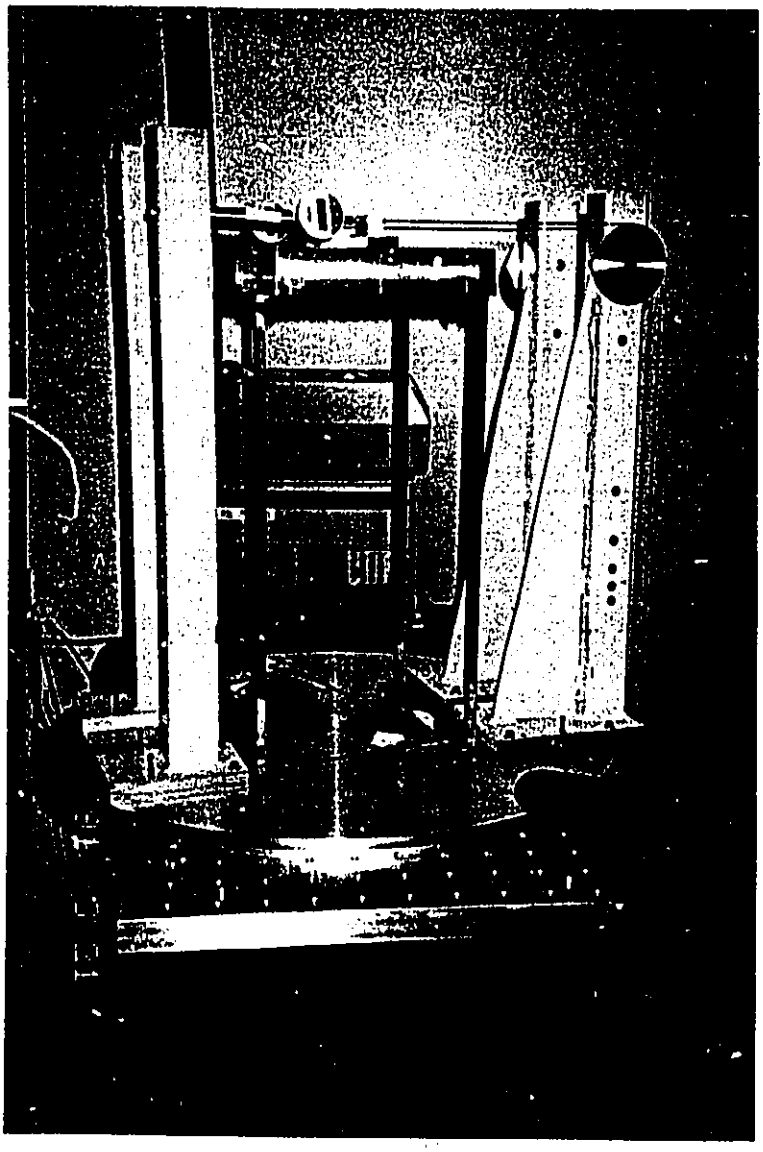

Photo.4.2 Static Calibration

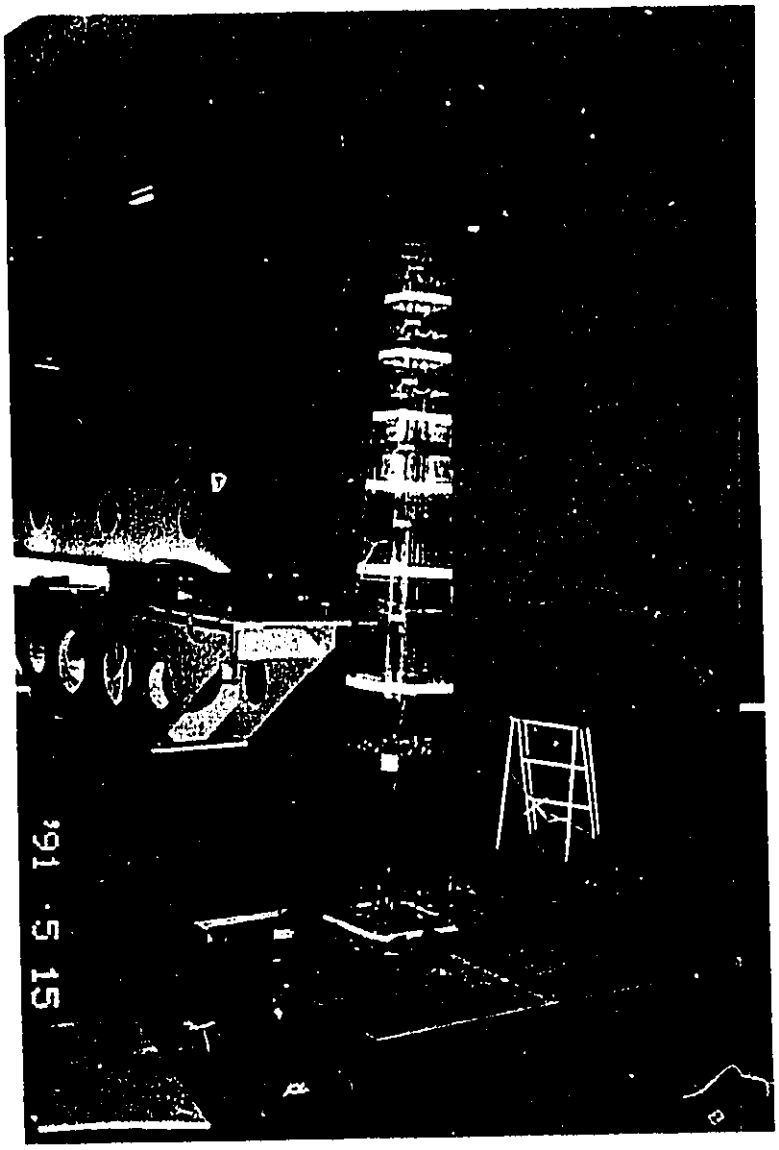

Photo.4.3 Dynamic Calibration

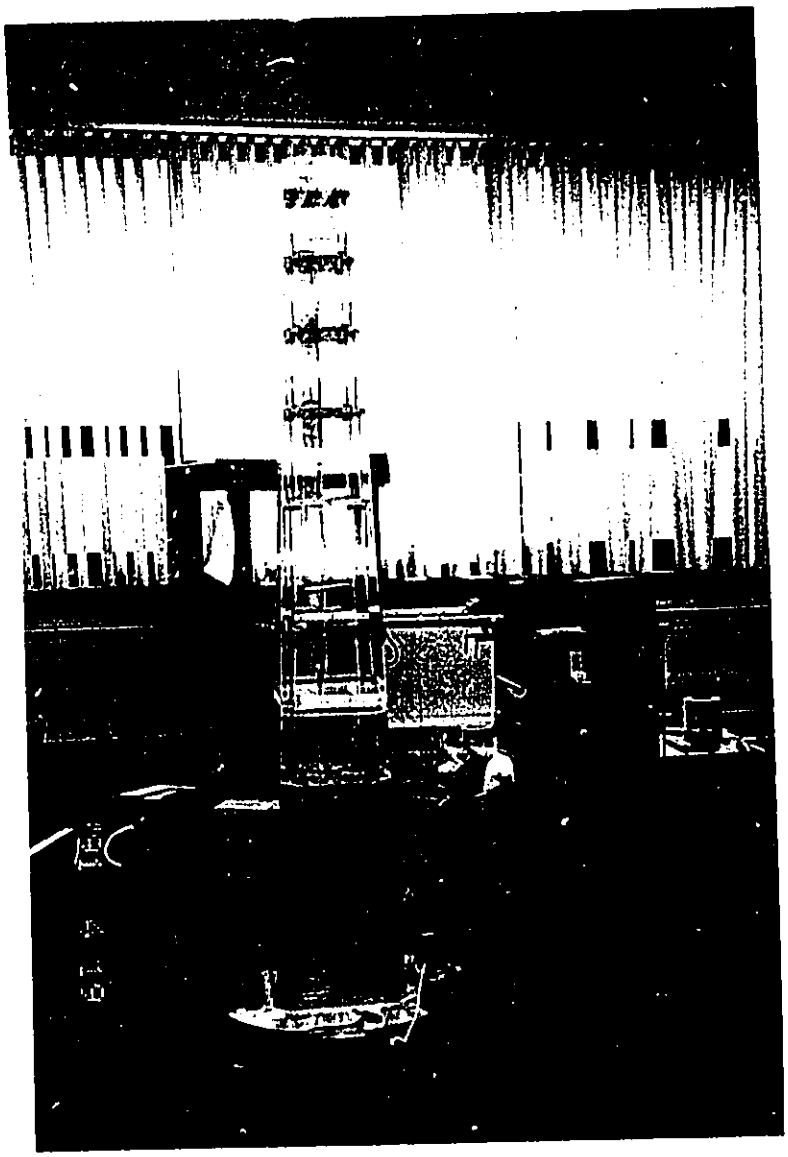

Photo.4.4 Set-up for Dynamic Calibration

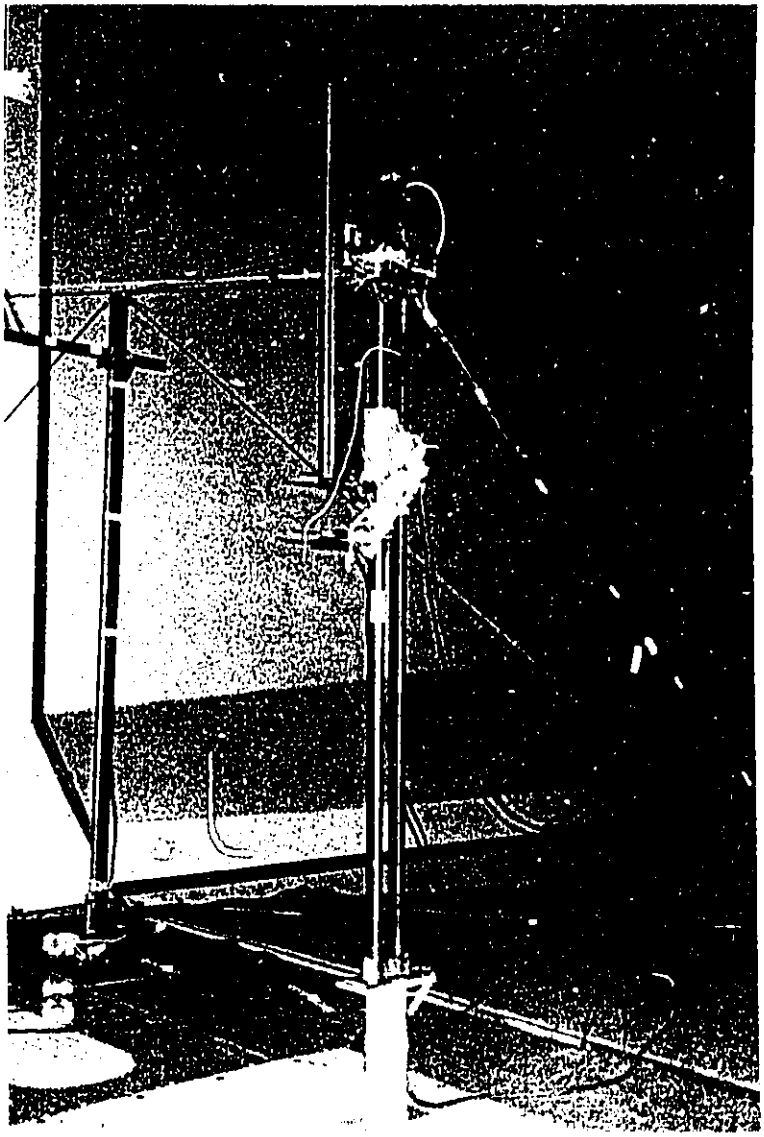

Photo.4.5 Set-up for Flow Measurement

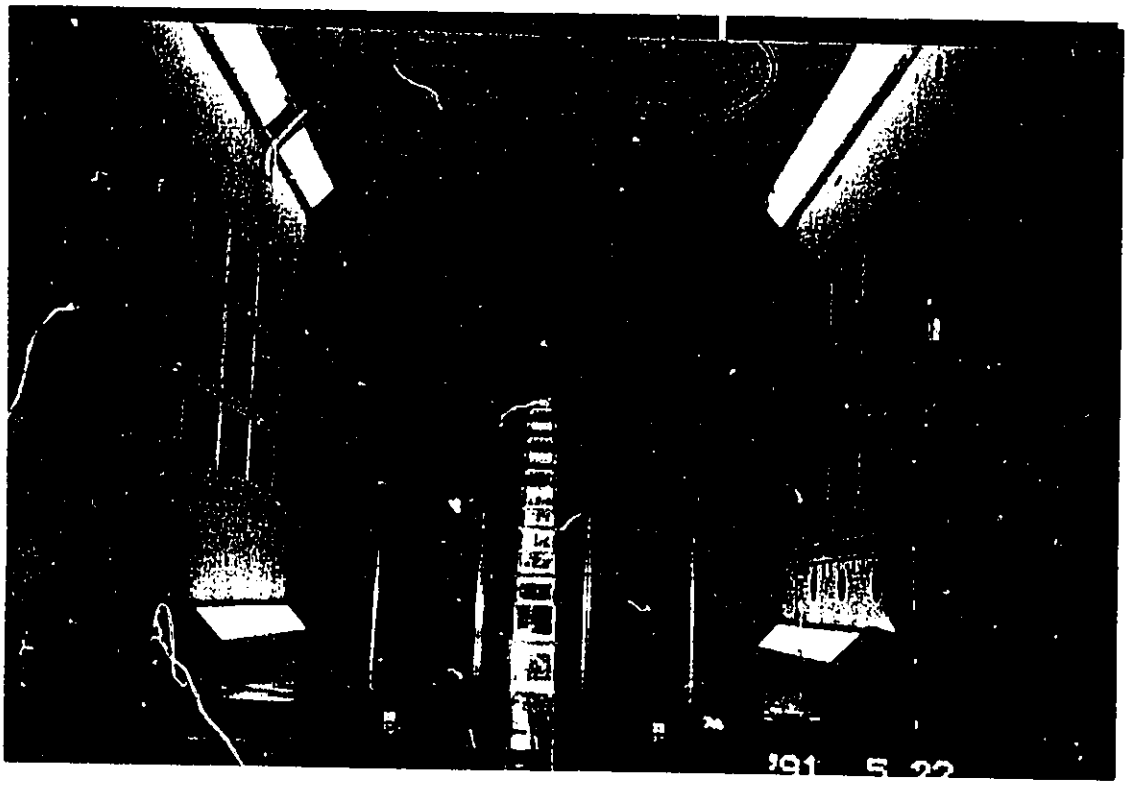

Photo.4.6 Model in the Wind Tunnel Test Section

Appendix A: WIRE RESISTANCE STRAIN GAUGES

A.1 General Principle

In 1856, Lord Kelvin discovered the principle on which the electrical resistance strain gauge is based [A.1]. For the resistance R of a uniform wire with lenght L, cross-sectional area A and the specific resistance r is given by

$$R = rL/S \tag{A.1}$$

By taking the differentials of (A.1)

$$dR/R = dr/r + dL/L - dS/S \tag{A.2}$$

As a first approximation, r and A can be assumed to be nearly constant. Then (A.2) can be reduced to

$$dR/R = dL/L \tag{A.3}$$

Following the discussion above, it is easily understood that by attaching a strain gauge to a beam (or a column) as shown in Fig.A.1, its surface strain can be detected by measuring the change of its electrical resistance.

A.2 Wheatstone Bridge

To study the strains in a beam when it is subjected to a bending moment, as shown in Fig.A.2, the Wheatstone bridge shown in Fig.A.3 can be employed. This circuit can be used to determine both static and dynamic strain gauge readings and the sensitivity of measurement is high.

The principle of the operation is to measure dE when the bending moment M is applied. Actually, the behaviour of this circuit, under initial balance conditions is

$$dE = V[R_1R_2/(R_1+R_2)^2] \times (dR_1/R_1 - dR_2/R_2 + dR_4/R_4) \tag{A.4}$$

If there is no difference in gauge characteristics, (A.4) becomes

$$dE = V\ (dR/R) \tag{A.5}$$

Applying (A.3), it becomes

$$dL/L = dE/V \tag{A.6}$$

Thus, by finding dE, the strain in the bent beam can be found.

A.3 Circuits for the Present Study

The strain gauge bridge system used in this experiment is shown in Fig.A.4, which is a derivative of the Wheatstone Bridge circuit.

Four strain gauges on each column made one bridge. The strain output was arranged to show a positive value when the floor mass swayed in positive X- or Y-direction. The name of the strain gauges was given with subscripts i and j where i means the floor number (i=1-7) and j is the column number (j=1-4). The displacement of each floor relative to the floor below was given by

$e_{i1} + e_{i3}$ = displacement in X-direction

$e_{i2} + e_{i3}$ = displacement in Y-direction

$-e_{i1} - e_{i2} + e_{i3} + e_{i4}$ = angle in torsion

Reference:

A.1 Fluege, L.(ed.), Handbook of Engineering Mechanics, McGraw-Hill.

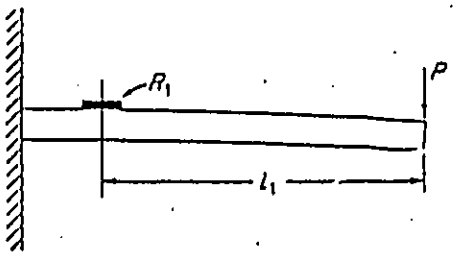

Fig.A.1 Strain Gauge mounted on a Beam

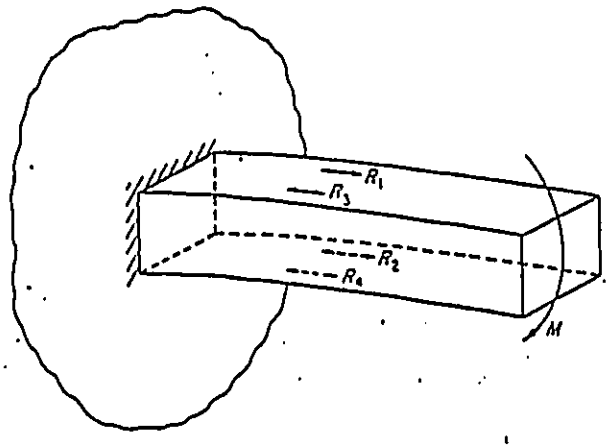

Fig.A.2 Position of four gauges employed on a beam in bending

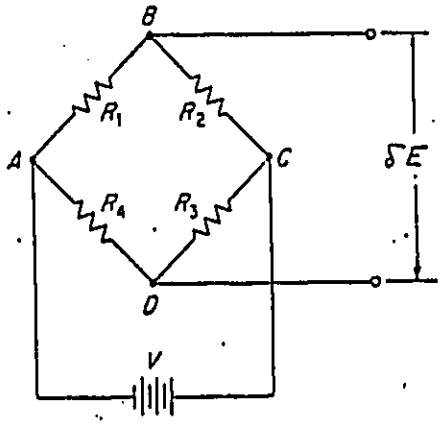

Fig.A.3 The Wheatstone bridge circuit

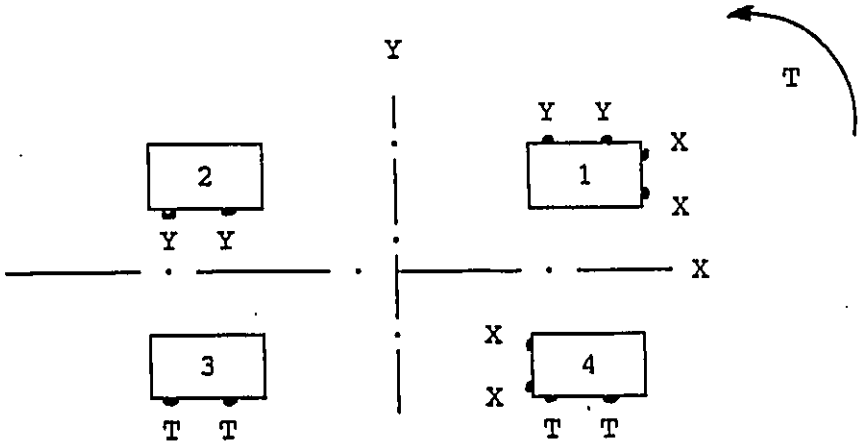

Fig.A.4 Position of Strain Gauges

Appendix B: MEASUREMENT OF MOMENT OF INERTIA

The moment of inertia was measured using a rotating pendulum shown in Fig.B.1. Strings were attached to the four corners of the top plate and the floor as shown in the figure. The restoring moment against any rotation A_t for this case is provided by the moment of a component of the gravitational force on the mass given as follows:

$$Mg(a/L)A_t a = Mga^2A_t/L \qquad (B.1)$$

where
- M : total floor mass
- g : acceleration due to gravity
- a : distance from the centre of gravity to each string
- L : effective length of each string
- A_t: angle of rotation

For the free rotation of the pendulum the equation of motion is given by

$$J_t A_t + Mg(a^2/L)A_t = 0 \qquad (B.2)$$

where J_t : polar mass moment of inertia around z-axis.

The natural circular frequency w_o, hence, is given by

$$w_o^2 = a^2Mg/L/J_t = aL/rg \qquad (B.3)$$

where $r = J_t/M$: radius of gyration

The natural period T_o is given by the inverse of the natural frequency. If M, a and L are given and T_o is measured, the polar mass moment of inertia can be determined from the following equation:

$$J_t = Mga^2/Lw^2 \qquad (B.4)$$

The first test was done with the 1st floor mass. For the convenience of the experiment, the other floors were placed on top of the first floor for the measurement. For

example, for the measurement of the 7th floor, following values were used for the calculation:

1st floor mass : M_1 = 10.885 kg
7th floor mass : M_7 = 0.658 kg
bolts for attachment : M_b = 0.111 kg

and L : 280.7 cm
a : 14.3 cm

The natural period was determined from the avarage of 100 cycles of vibration. These were

With the first floor : T_1 = 3.28 sec
With the 1st and 7th floors : T_{1+7} = 3.22 sec

Applying (B.4) J_{t1} = 2103.4 kg cm»
J_{t7} = 45.68 kg cm»

The design values for these floors were 2,100.7 kg-cm^2 and 49.52 kg-cm^2, respectively.

In case of the first floor mass the measured result is fairly close to the design value. For the seventh floor mass, however, the error is rather large, which is probably related to the way the experiment was set up. Though the polar mass moment of inertia for the first floor mass has an error of only 0.2% relative to its absolute value, this error which is included in the measurement for the seventh mass, is as large as 9.3% for the sevens floor mass whose absolute value is only 2.2% of the first mass. Nevertheless this calibration showed that the polar mass moment of inertia of each floor was found to be without significant error.

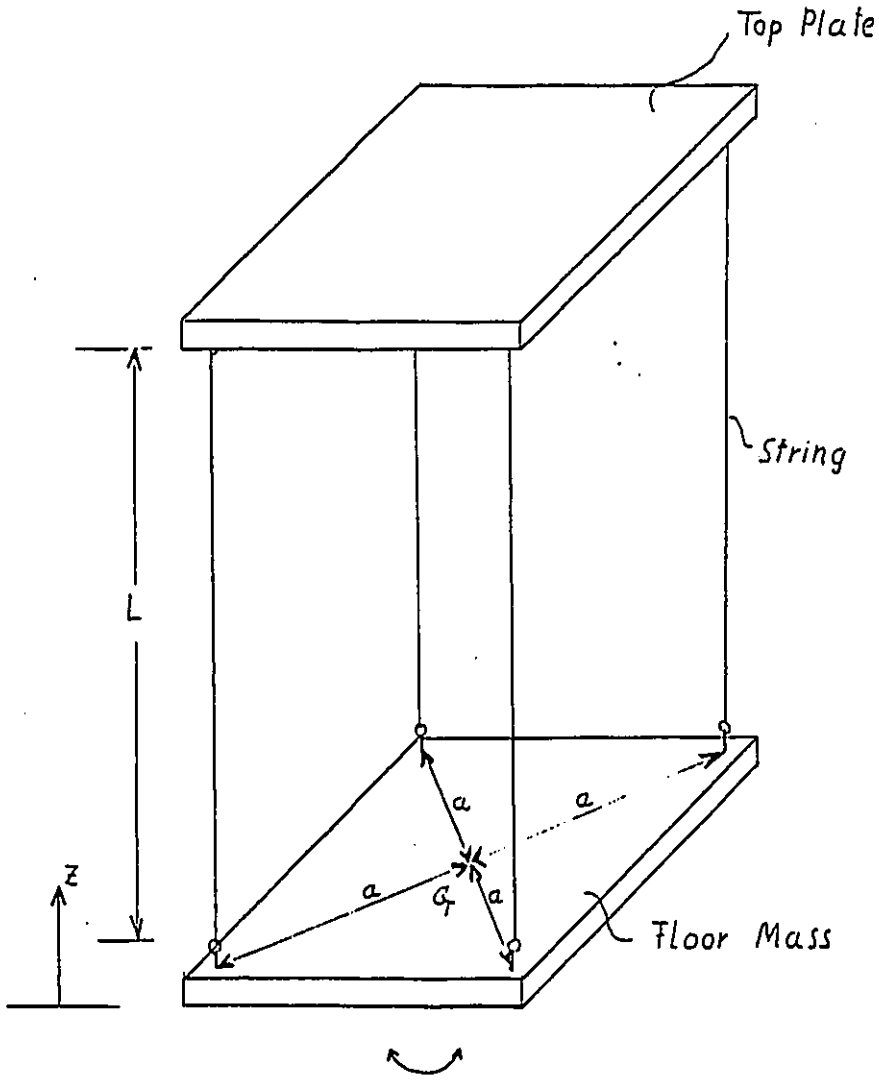

Fig.B.1 Pendelum to measure the Mass Moment of Inertia

Appendix C: COMPUTER PROGRAM FOR FFT ANALYSIS

The computer program in this appendix was written in Fortran for the main frame computer at the University of Ottawa. The program operates Fourier analysis of the time history data provided to calculate spectral density functions. It also calculate the autocorrelation functions by applying the Inverse Fourier Transform. Both parts of the program use the FFT algorithm given in Ref.D.1. For the plotting of the results, the display subroutine available with the main frame was used.

Reference:

D.1 Osaki, Y., Introduction to Spectral Analysis of Earthquake Motions, Kajima Press, Tokyo, 1976.

```
C CONVERTION (BINARY TO ASCII CODE), STATISTICS & FFT                          CON00010
C SAVES INTO 5 FILES (CORRELAT NRC-STAT NEW-STAT SPEC AUTOC)                   CON00020
C  NS  - NUMBER OF SAMPLES PER CHANNEL                                         CON00030
C  NL  - NUMBER OF LEVELS ON BUILDING                                          CON00040
C  NSL - NUMBER OF CHANNELS PER LEVEL ON BUILDING                              CON00050
C  NC  - TOTAL NUMBER OF CHANNELS                                              CON00060
C  N - NUMBER OF PROCESSED DATA AND INPUT DATA FOR FFT                         CON00070
C  ND2 - NUMBER OF OUTPUT DATA OF SPEC AND AUTOCORR                            CON00080
                                                                               CON00090
      PARAMETER (NL=7,NC=23,NS=30100,N=2**14,ND2=N/2+1)                        CON00100
      IMPLICIT REAL*4 (A-H,M,O-Z)                                              CON00110
      DIMENSION SUMX(NL),SUMXX(NL),AVE(NL),VAR(NL),RMS(NL)                     CON00120
      DIMENSION MAX(NL),MIN(NL),MAXPK(NL),MINPK(NL),GUST(NL)                   CON00130
      DIMENSION COV(NL),SUM(NL),CC7(NL)                                        CON00140
      DIMENSION X(N),F(ND2),G(ND2),R(ND2)                                      CON00150
      INTEGER*2 REPORT,RUN,TARE,POINT                                          CON00160
      INTEGER*2 ACHAN,ARATE,I4SCNS,I2RAY(NC)                                   CON00170
      REAL*4 MEANS(NC),STDVS(NC),PPKS(NC),NPKS(NC)                             CON00180
      REAL*4 XSWAY(NL,N),YSWAY(NL,N),TORSN(NL,N),DUMMY(NL,NS)                  CON00190
      CHARACTER*1 BUF*230                                                      CON00200
                                                                               CON00210
C *** GET STATISTICS FROM BINARY FILE                                          CON00220
      READ (1) REPORT,RUN,TARE,POINT                                           CON00230
      READ (1) ACHAN,ARATE,I4SCNS                                              CON00240
      READ (1) BUF                                                             CON00250
      READ (1) BUF                                                             CON00260
      K=ACHAN                                                                  CON00270
      READ (1) (I2RAY(I),I=1,K)                                                CON00280
      READ (1) (I2RAY(I),I=1,K)                                                CON00290
      READ (1) (I2RAY(I),I=1,K)                                                CON00300
      READ (1) (MEANS(I),I=1,K)                                                CON00310
      READ (1) (STDVS(I),I=1,K)                                                CON00320
      READ (1) (PPKS(I),I=1,K)                                                 CON00330
      READ (1) (NPKS(I),I=1,K)                                                 CON00340
                                                                               CON00350
C WIND SPEED                                                                   CON00360
      WRITE (3,*) 'AIR DENSITY (KG/M^3)'                                       CON00370
      READ (2,*) RO                                                            CON00380
      IF (MEANS(22).LT.0) GOTO 3                                               CON00390
      QMODL=0.97044*MEANS(22)                                                  CON00400
      VGRAD=SQRT(2.*(MEANS(22)*4.2490498E-3)/(RO/515.8032))/3.2808             CON00410
      VMODL=SQRT(2.*(QMODL*4.2490498E-3)/(RO/515.8032))/3.2808                 CON00420
    3 IF (MEANS(23).LT.0) GOTO 4                                               CON00430
      VH=SQRT(2.*(MEANS(23)*4.2490498E-3)/(RO/515.8032))/3.2808                CON00440
                                                                               CON00450
C WRITE HEADINGS AND STATISTICS OF WHOLE DATA INTO NRC-STAT FILE                CON00460
    4 WRITE (5,90) RUN,POINT,VMODL,RO                                          CON00470
      WRITE (17,90) RUN,POINT,VMODL,RO                                         CON00480
      WRITE (18,90) RUN,POINT,VMODL,RO                                         CON00490
      WRITE (19,90) RUN,POINT,VMODL,RO                                         CON00500
      WRITE (20,90) RUN,POINT,VMODL,RO                                         CON00510
      WRITE (5,100) 'QM  ',MEANS(22),MEANS(23),VGRAD,VMODL,VH                  CON00520
      WRITE (5,100) 'QS  ',STDVS(22),STDVS(23)                                 CON00530
      WRITE (5,100) 'QMAX',PPKS(22),PPKS(23)                                   CON00540
      WRITE (5,100) 'QMIN',NPKS(22),NPKS(23)                                   CON00550
```

```
                                                                      CON00560
      DO 5 J=7,9                                                      CON00570
      IF (J.EQ.7) THEN                                                CON00580
      IBG=1                                                           CON00590
      K=19                                                            CON00600
      WRITE (5,100) 'XM   ',(MEANS(I),I=IBG,K,3)                      CON00610
      WRITE (5,100) 'XS   ',(STDVS(I),I=IBG,K,3)                      CON00620
      WRITE (5,100) 'XMAX',(PPKS(I),I=IBG,K,3)                        CON00630
      WRITE (5,100) 'XMIN',(NPKS(I),I=IBG,K,3)                        CON00640
      END IF                                                          CON00650
      IF (J.EQ.8) THEN                                                CON00660
      IBG=2                                                           CON00670
      K=20                                                            CON00680
      WRITE (5,100) 'YM   ',(MEANS(I),I=IBG,K,3)                      CON00690
      WRITE (5,100) 'YS   ',(STDVS(I),I=IBG,K,3)                      CON00700
      WRITE (5,100) 'YMAX',(PPKS(I),I=IBG,K,3)                        CON00710
      WRITE (5,100) 'YMIN',(NPKS(I),I=IBG,K,3)                        CON00720
      END IF                                                          CON00730
      IF (J.EQ.9) THEN                                                CON00740
      IBG=3                                                           CON00750
      K=21                                                            CON00760
      WRITE (5,100) 'TM   ',(MEANS(I),I=IBG,K,3)                      CON00770
      WRITE (5,100) 'TS   ',(STDVS(I),I=IBG,K,3)                      CON00780
      WRITE (5,100) 'TMAX',(PPKS(I),I=IBG,K,3)                        CON00790
      WRITE (5,100) 'TMIN',(NPKS(I),I=IBG,K,3)                        CON00800
      END IF                                                          CON00810
    5 CONTINUE                                                        CON00820
                                                                      CON00830
C ***** SETTING OF DATA TO BE PROCESSED AND INITIALIZATION OF FFT *****CON00840
C     NBEG=1                                                          CON00850
      NBEG=(I4SCNS-N)/2                                               CON00860
      NEND=NBEG+N-1                                                   CON00870
                                                                      CON00880
C INDEX IND=100 for Fourier Spectrum                                  CON00890
C       IND=010 for Power Spectrum                                    CON00900
C       IND=001 for AutoCorrelation                                   CON00910
C IND IS ADDIBLE: IND=101(100+001) Fourier Spectrum & AutoCorrelation CON00920
                                                                      CON00930
      IND=011                                                         CON00940
      SFREQ=500.                                                      CON00950
      DT=1./SFREQ                                                     CON00960
                                                                      CON00970
C SKIP & READ TIME SERIES FROM BINARY FILE                            CON00980
      DO 10 J=1, NBEG-1                                               CON00990
       READ (1) (DUMMY(I,J),DUMMY(I,J),DUMMY(I,J),I=1,NL)             CON01000
   10 CONTINUE                                                        CON01010
                                                                      CON01020
      DO 20 K=NBEG,NEND                                               CON01030
       J=K-NBEG+1                                                     CON01040
       READ (1) (XSWAY(I,J),YSWAY(I,J),TORSN(I,J),I=1,NL)             CON01050
   20 CONTINUE                                                        CON01060
                                                                      CON01070
C CALCULATION & OUTPUT OF STATISTICS, POWER SPECTRUM & AUTOCORRELATION CON01080
C     SUMX, SUMXX, MEAN, RMS, MAX, MIN, POSPEAK, NEGPEAK              CON01090
      DO 30 II=7,9                                                    CON01100
```

```
      IF (II.EQ.7) THEN                                                 CON01110
         WRITE(17,*) 'X'                                                CON01120
         WRITE(18,*) 'X'                                                CON01130
         WRITE(19,*) 'X'                                                CON01140
      END IF                                                            CON01150
      IF (II.EQ.8) THEN                                                 CON01160
         WRITE(17,*) 'Y'                                                CON01170
         WRITE(18,*) 'Y'                                                CON01180
         WRITE(19,*) 'Y'                                                CON01190
      END IF                                                            CON01200
      IF (II.EQ.9) THEN                                                 CON01210
         WRITE(17,*) 'T'                                                CON01220
         WRITE(18,*) 'T'                                                CON01230
         WRITE(19,*) 'T'                                                CON01240
      END IF                                                            CON01250
                                                                        CON01260
    DO 35 I=1,NL                                                        CON01270
      SUMX(I)=0.0                                                       CON01280
      SUMXX(I)=0.0                                                      CON01290
      MAX(I)=-10000.0                                                   CON01300
      MIN(I)=10000.0                                                    CON01310
    IF (II.EQ.7) THEN                                                   CON01320
      DO 40 J=1,N                                                       CON01330
         SUMX(I)=SUMX(I)+XSWAY(I,J)                                     CON01340
         SUMXX(I)=SUMXX(I)+XSWAY(I,J)**2                                CON01350
         IF (MAX(I).LT.XSWAY(I,J)) MAX(I)=XSWAY(I,J)                    CON01360
         IF (MIN(I).GT.XSWAY(I,J)) MIN(I)=XSWAY(I,J)                    CON01370
40    CONTINUE                                                          CON01380
    END IF                                                              CON01390
    IF (II.EQ.8) THEN                                                   CON01400
      DO 41 J=1,N                                                       CON01410
         SUMX(I)=SUMX(I)+YSWAY(I,J)                                     CON01420
         SUMXX(I)=SUMXX(I)+YSWAY(I,J)**2                                CON01430
         IF (MAX(I).LT.YSWAY(I,J)) MAX(I)=YSWAY(I,J)                    CON01440
         IF (MIN(I).GT.YSWAY(I,J)) MIN(I)=YSWAY(I,J)                    CON01450
41    CONTINUE                                                          CON01460
    END IF                                                              CON01470
    IF (II.EQ.9) THEN                                                   CON01480
      DO 42 J=1,N                                                       CON01490
         SUMX(I)=SUMX(I)+TORSN(I,J)                                     CON01500
         SUMXX(I)=SUMXX(I)+TORSN(I,J)**2                                CON01510
         IF (MAX(I).LT.TORSN(I,J)) MAX(I)=TORSN(I,J)                    CON01520
         IF (MIN(I).GT.TORSN(I,J)) MIN(I)=TORSN(I,J)                    CON01530
42    CONTINUE                                                          CON01540
    END IF                                                              CON01550
                                                                        CON01560
    RN=REAL(N)                                                          CON01570
    AVE(I)=SUMX(I)/RN                                                   CON01580
    VAR(I)=SUMXX(I)/(RN-1.)-SUMX(I)**2/(RN*(RN-1.))                     CON01590
    IF (VAR(I).GE.0.) RMS(I)=SQRT(VAR(I))                               CON01600
    MAXPK(I)=(MAX(I)-AVE(I))/RMS(I)                                     CON01610
    MINPK(I)=(MIN(I)-AVE(I))/RMS(I)                                     CON01620
    GUST(I)=(MAX(I)-MIN(I))/(2*RMS(I))                                  CON01630
    WRITE (17, 300) I,SUMX(I),SUMXX(I),AVE(I),RMS(I),MAX(I),MIN(I),     CON01640
   &MAXPK(I),MINPK(I),GUST(I)                                           CON01650
```

```
   35 CONTINUE                                                          CON01660
                                                                        CON01670
      DO 50 I=1,NL                                                      CON01680
        COV(I)=0.                                                       CON01690
        SUM(I)=0.                                                       CON01700
      IF (II.EQ.7) THEN                                                 CON01710
        DO 51 J=1,N                                                     CON01720
           XSWAY(I,J)=XSWAY(I,J)-AVE(I)                                 CON01730
           SUM(I)=SUM(I)+XSWAY(I,J)**2                                  CON01740
           X(J)=XSWAY(I,J)                                              CON01750
           IF (I.EQ.7) GOTO 51                                          CON01760
           COV(I)=COV(I)+(XSWAY(7,J)-AVE(7))*XSWAY(I,J)                 CON01770
   51   CONTINUE                                                        CON01780
      END IF                                                            CON01790
      IF (II.EQ.8) THEN                                                 CON01800
        DO 52 J=1,N                                                     CON01810
           YSWAY(I,J)=YSWAY(I,J)-AVE(I)                                 CON01820
           SUM(I)=SUM(I)+YSWAY(I,J)**2                                  CON01830
           X(J)=YSWAY(I,J)                                              CON01840
           IF (I.EQ.7) GOTO 52                                          CON01850
           COV(I)=COV(I)+(YSWAY(7,J)-AVE(7))*YSWAY(I,J)                 CON01860
   52   CONTINUE                                                        CON01870
      END IF                                                            CON01880
      IF (II.EQ.9) THEN                                                 CON01890
        DO 53 J=1,N                                                     CON01900
           TORSN(I,J)=TORSN(I,J)-AVE(I)                                 CON01910
           SUM(I)=SUM(I)+TORSN(I,J)**2                                  CON01920
           X(J)=TORSN(I,J)                                              CON01930
           IF (I.EQ.7) GOTO 53                                          CON01940
           COV(I)=COV(I)+(TORSN(7,J)-AVE(7))*TORSN(I,J)                 CON01950
   53   CONTINUE                                                        CON01960
      END IF                                                            CON01970
                                                                        CON01980
        CALL SPAC(N,X,N,DT,IND,F,G,R,ND2,NFOLD,DF)                      CON01990
        DO 55 J=1,3280                                                  CON02000
          DUMMY(I,J)=G(J)                                               CON02010
   55   CONTINUE                                                        CON02020
        DO 60 J=1,ND2                                                   CON02030
          K=J+ND2                                                       CON02040
          DUMMY(I,K)=R(J)                                               CON02050
   60   CONTINUE                                                        CON02060
                                                                        CON02070
   50 CONTINUE                                                          CON02080
                                                                        CON02090
      WRITE (18,500) 'VARIANCE',(VAR(I),I=1,7)                          CON02100
C WRITE POWER SPECTRUM UNTIL F=100HZ (N=3280)                           CON02110
C     NFOLD = 8193      DF = 0.0305                                     CON02120
      DO 70 J=1,3280                                                    CON02130
      WRITE (18,600) (DUMMY(I,J),I=1,NL)                                CON02140
   70 CONTINUE                                                          CON02150
C WRITE AUTOCORRELATION                                                 CON02160
      DO 75 J=ND2+1,2*ND2                                               CON02170
      WRITE (19,700) (DUMMY(I,J),I=1,NL)                                CON02180
   75 CONTINUE                                                          CON02190
      DO 80 I=1,6                                                       CON02200
```

```
      CC7(I)=COV(I)/SQRT(SUM(I)*SUM(7))                                 CON02210
C     COV(I)=COV(I)/(RN-1.)                                             CON02220
   80 CONTINUE                                                          CON02230
      WRITE (20, 350) (CC7(I),I=1,6)                                    CON02240
C     WRITE (20, 350) (COV(I),I=1,6)                                    CON02250
   30 CONTINUE                                                          CON02260
                                                                        CON02270
C COVARIANCES & CORRELATION COEFFICIENTS FOR TOP FLOOR (N=7)            CON02280
      SUMXY=0.                                                          CON02290
      SUMXT=0.                                                          CON02300
      SUMYT=0.                                                          CON02310
      SUMX2=0.                                                          CON02320
      SUMY2=0.                                                          CON02330
      SUMT2=0.                                                          CON02340
      DO 85 J=1,N                                                       CON02350
       SUMXY=SUMXY+XSWAY(7,J)*YSWAY(7,J)                                CON02360
       SUMXT=SUMXT+XSWAY(7,J)*TORSN(7,J)                                CON02370
       SUMYT=SUMYT+YSWAY(7,J)*TORSN(7,J)                                CON02380
       SUMX2=SUMX2+XSWAY(7,J)**2                                        CON02390
       SUMY2=SUMY2+YSWAY(7,J)**2                                        CON02400
       SUMT2=SUMT2+TORSN(7,J)**2                                        CON02410
   85 CONTINUE                                                          CON02420
C     COVXY=SUMXY/(RN-1.)                                               CON02430
C     COVXT=SUMXT/(RN-1.)                                               CON02440
C     COVYT=SUMYT/(RN-1.)                                               CON02450
      CCXY=SUMXY/SQRT(SUMX2*SUMY2)                                      CON02460
      CCXT=SUMXT/SQRT(SUMX2*SUMT2)                                      CON02470
      CCYT=SUMYT/SQRT(SUMY2*SUMT2)                                      CON02480
                                                                        CON02490
      WRITE (20,350) CCXY,CCXT,CCYT                                     CON02500
                                                                        CON02510
   90 FORMAT ('RUN=',I3,'  POINT=',I2,'  VMODEL=',F7.3,                 CON02520
     & '  AIR DENSITY=',F7.3)                                          CON02530
  100 FORMAT (A4,7E16.8)                                                CON02540
  200 FORMAT (6X,'SUM(X)',9X,'SUM(XX)',12X,'MEAN',13X,'RMS',13X,        CON02550
     & 'MAX',13X,'MIN',8X,'POS PEAK',7X,'NEG. PEAK')                    CON02560
  300 FORMAT (I1,6E16.8,3F10.6)                                         CON02570
  350 FORMAT (6E16.8)                                                   CON02580
  500 FORMAT (A8,7E16.8)                                                CON02590
  600 FORMAT (7E14.6)                                                   CON02600
  700 FORMAT (7F12.8)                                                   CON02610
      STOP                                                              CON02620
      END                                                               CON02630
                                                                        CON02640
C ***********************************************************************CON02650
C  SUBROUTINE FOR FOURIER SPECTRA, POWER SPECTRA, and AUTOCORRELATION    CON02660
C ***********************************************************************CON02670
C             Pg. 130 in DR. OSAKI'S TEXTBOOK                           CON02680
C IMSL SUBROUTINE FOR FAST FOURIER TRANSFORMATION: FFT2C                 CON02690
                                                                        CON02700
      SUBROUTINE SPAC(N,X,ND1,DT,IND,F,G,R,ND2,NFOLD,DF)                CON02710
      PARAMETER (M=14)                                                  CON02720
      IMPLICIT REAL*4 (A-H,O-Z)                                         CON02730
      COMPLEX A(2**M)                                                   CON02740
      DIMENSION X(ND1),F(ND2),G(ND2),R(ND2),IWK(M+1)                    CON02750
```

```
                                                                      CONO2760
C Initialization                                                      CONO2770
      DO 110 I=1,N                                                    CONO2780
      A(I)=CMPLX(X(I),0.0)                                            CONO2790
  110 CONTINUE                                                        CONO2800
      NT=2                                                            CONO2810
  120 IF (NT.GE.N) GO TO 130                                          CONO2820
      NT=NT*2                                                         CONO2830
      GO TO 120                                                       CONO2840
  130 IF (NT.EQ.N) GO TO 150                                          CONO2850
      DO 140 I=N+1, NT                                                CONO2860
      A(I)=(0.0,0.0)                                                  CONO2870
  140 CONTINUE                                                        CONO2880
  150 NFOLD=NT/2+1                                                    CONO2890
      T=FLOAT(NT)*DT                                                  CONO2900
      DF=1.0/T                                                        CONO2910
      CALL FFT2C(A,M,IWK)                                             CONO2920
C     CALL FAST(NT,A,N,-1)                                            CONO2930
                                                                      CONO2940
C Fourier Spectrum                                                    CONO2950
      IF (IND.EQ.1) GO TO 180                                         CONO2960
      DO 160 K=1,NFOLD                                                CONO2970
      F(K)=CABS(A(K))*DT                                              CONO2980
  160 CONTINUE                                                        CONO2990
      IF (IND.EQ.100) RETURN                                          CONO3000
                                                                      CONO3010
C Power Spectrum                                                      CONO3020
      IF (IND.EQ.101) GO TO 180                                       CONO3030
      G(1)=F(1)**2/T                                                  CONO3040
      DO 170 K=2,NFOLD-1                                              CONO3050
      G(K)=2.0*F(K)**2/T                                              CONO3060
  170 CONTINUE                                                        CONO3070
      G(NFOLD)=F(NFOLD)**2/T                                          CONO3080
      IF(MOD(IND,10).EQ.0) RETURN                                     CONO3090
                                                                      CONO3100
C AutoCorrelation                                                     CONO3110
  180 DO 185 K=1,NT                                                   CONO3120
      A(K)=A(K)*CONJG(A(K))                                           CONO3130
  185 CONTINUE                                                        CONO3140
      DO 190 K=1,NT                                                   CONO3150
      A(K)=CONJG(A(K))                                                CONO3160
  190 CONTINUE                                                        CONO3170
      CALL FFT2C(A,M,IWK)                                             CONO3180
C     CALL FAST(NT,A,N,+1)                                            CONO3190
      DO 195 K=1,NT                                                   CONO3200
      A(K)=CONJG(A(K))/N                                              CONO3210
  195 CONTINUE                                                        CONO3220
      RO=REAL(A(1))                                                   CONO3230
      DO 200 J=1,NFOLD                                                CONO3240
      R(J)=REAL(A(J))/RO                                              CONO3250
  200 CONTINUE                                                        CONO3260
      RETURN                                                          CONO3270
      END                                                             CONO3280
C *************************************************                   CONO3290
C     SUBROUTINE FOR FAST FOURIER TRANSFORMATION                      CONO3300
```

```
C ****************************************************                CON03310
C             Pg.93 in DR. OSAKI'S TEXTBOOK                          CON03320
      SUBROUTINE FAST(N,X,ND,IND)                                    CON03330
      IMPLICIT REAL*4 (A-H,O-Z)                                      CON03340
      COMPLEX X(ND),TEMP,THETA                                       CON03350
      J=1                                                            CON03360
      DO 140 I=1,N                                                   CON03370
        IF (I.GE.J) GOTO 110                                         CON03380
          TEMP=X(J)                                                  CON03390
          X(J)=X(I)                                                  CON03400
          X(I)=TEMP                                                  CON03410
  110   M=N/2                                                        CON03420
  120   IF (J.LE.M) GOTO 130                                         CON03430
          J=J-M                                                      CON03440
          M=M/2                                                      CON03450
        IF (M.GE.2) GOTO 120                                         CON03460
  130   J=J+M                                                        CON03470
  140 CONTINUE                                                       CON03480
      KMAX=1                                                         CON03490
  150 IF (KMAX.GE.N) RETURN                                          CON03500
      ISTEP=KMAX*2                                                   CON03510
      DO 160 K=1,KMAX                                                CON03520
        THETA=CMPLX(0.0,3.141593*FLOAT(IND*(K-1))/FLOAT(KMAX))       CON03530
        DO 170 I=K,N,ISTEP                                           CON03540
          J=I+KMAX                                                   CON03550
          TEMP=X(J)*CEXP(THETA)                                      CON03560
          X(J)=X(I)-TEMP                                             CON03570
          X(I)=X(I)+TEMP                                             CON03580
  170   CONTINUE                                                     CON03590
  160 CONTINUE                                                       CON03600
      KMAX=ISTEP                                                     CON03610
      GOTO 150                                                       CON03620
      END                                                            CON03630
```

```
C ***************************************************************** SPE00010
C *   PLOTTING FFT DATA (POWER SPECTRUM)                          * SPE00020
C ***************************************************************** SPE00030
                                                                    SPE00040
      PARAMETER (N=2**14,NP=3280)                                   SPE00050
      IMPLICIT REAL*4 (A-H,O-Z)                                     SPE00060
      CHARACTER*64 T1,T2,T3,T4,TEXT,TXT                             SPE00070
      DIMENSION G(7,NP),F(NP),VAR(7),PX(NP),PY(NP)                  SPE00080
   70 FORMAT (7E14.6)                                               SPE00090
   80 FORMAT (A8,7E16.8)                                            SPE00100
   90 FORMAT (A4,I3,A8,I2,A9,F7.3,A14,F7.3)                         SPE00110
                                                                    SPE00120
      IALFA=45                                                      SPE00130
      DF=500./FLOAT(N)                                              SPE00140
      READ (18,90) T1,IRUN,T2,IPOINT,T3,VMODL,T4,RO                 SPE00150
      IF (VMODL.EQ.0.) THEN                                         SPE00160
        WRITE (6,*) 'WIND VELOCITY AT MODEL HEIGHT (M/S)'           SPE00170
        READ (5,*) VMODL                                            SPE00180
      ENDIF                                                         SPE00190
                                                                    SPE00200
      CALL ANYDEV                                                   SPE00210
C     CALL QMS                                                      SPE00220
      CALL HWROT ('AUTO')                                           SPE00230
      CALL HWSCAL ('SCREEN')                                        SPE00240
      CALL PAGE (8.5, 11.0)                                         SPE00250
      CALL BASALF ('STANDARD')                                      SPE00260
      CALL MIXALF ('L/CSTD')                                        SPE00270
      CALL MX3ALF ('INSTRU', '&')                                   SPE00280
      CALL MX4ALF ('L/CGREEK', '%')                                 SPE00290
      CALL PHYSOR (0.0, 0.0)                                        SPE00300
      CALL AREA2D (8.0, 10.5)                                       SPE00310
      CALL MESSAG ('R(UN= )$',100,3.5,10.5)                         SPE00320
      CALL INTNO (IRUN,'ABUT','ABUT')                               SPE00330
      CALL MESSAG ('   P(OINT= )$',100,'ABUT','ABUT')               SPE00340
      CALL INTNO (IPOINT,'ABUT','ABUT')                             SPE00350
      CALL MESSAG ('A(NGLE OF )A(TTACK= )$',100,1.5,10.0)           SPE00360
      CALL INTNO (IALFA ,'ABUT','ABUT')                             SPE00370
      CALL MESSAG ('   W(IND )S(PEED= )$',100,'ABUT','ABUT')        SPE00380
      CALL REALNO (VMODL,3,'ABUT','ABUT')                           SPE00390
      CALL MESSAG (' ((M/S))$',100,'ABUT','ABUT')                   SPE00400
      CALL ENDGR (0)                                                SPE00410
      YOR=7.                                                        SPE00420
                                                                    SPE00430
      DO 105 J=1,3                                                  SPE00440
        READ (18,'(A)') TEXT                                        SPE00450
        READ (18,80) TXT,(VAR(I), I=1,7)                            SPE00460
        F(1)=0.                                                     SPE00470
        AREA1=0.                                                    SPE00480
        DO 120 JJ=1,NP                                              SPE00490
          READ (18,70) (G(I,JJ), I=1,7)                             SPE00500
          IF (JJ.EQ.1) GOTO 120                                     SPE00510
          F(JJ)=F(JJ-1)+DF                                          SPE00520
C         PX(JJ)=F(JJ)*.3/VMODL                                     SPE00530
          PX(JJ)=F(JJ)/VMODL                                        SPE00540
C         PY(JJ)=G(7,JJ)                                            SPE00550
```

```
      PY(JJ)=F(JJ)*G(7,JJ)/VAR(7)                                        SPE00560
C     PY(JJ)=F(JJ)*G(7,JJ)                                               SPE00570
  120 CONTINUE                                                           SPE00580
                                                                         SPE00590
C     DO 125 JJ=3,NP                                                     SPE00600
C       AREA1=AREA1+(.5*(F(JJ)-F(JJ-1))*(G(7,JJ-1)+G(7,JJ)))            SPE00610
C 125 CONTINUE                                                           SPE00620
      PYMAX=-1000                                                        SPE00630
      PYMIN=+1000                                                        SPE00640
      DO 130 K=1,NP                                                      SPE00650
        IF (PY(K).LT.PYMIN) PYMIN=PY(K)                                  SPE00660
        IF (PY(K).GT.PYMAX) THEN                                         SPE00670
          PYMAX=PY(K)                                                    SPE00680
          NPEAK=K                                                        SPE00690
          IF (F(NPEAK).GT.59.) GOTO 140                                  SPE00700
        ENDIF                                                            SPE00710
  130 CONTINUE                                                           SPE00720
      NPP=NP                                                             SPE00730
      GOTO 150                                                           SPE00740
                                                                         SPE00750
  140 PYMAX=-1000                                                        SPE00760
      NPP=NPEAK-1                                                        SPE00770
      DO 145 KK=1,NPP                                                    SPE00780
        IF (PY(KK).GT.PYMAX) THEN                                        SPE00790
          PYMAX=PY(KK)                                                   SPE00800
          NPEAK=KK                                                       SPE00810
        ENDIF                                                            SPE00820
  145 CONTINUE                                                           SPE00830
                                                                         SPE00840
  150 CALL PHYSOR (1.5,YOR)                                              SPE00850
      CALL AREA2D (6.0,2.5)                                              SPE00860
      CALL HEIGHT( 0.08 )                                                SPE00870
      CALL MESSAG (TEXT,3,0.5,-.5)                                       SPE00880
      CALL MESSAG (' P(OWER )S(PECTRUM )$',100,'ABUT','ABUT')            SPE00890
      CALL MESSAG ('      S(()$',100,'ABUT','ABUT')                      SPE00900
      CALL REALNO (F(NPEAK),3,'ABUT','ABUT')                             SPE00910
      CALL MESSAG ('())= $',100,'ABUT','ABUT')                           SPE00920
      CALL REALNO (G(7,NPEAK),15,'ABUT','ABUT')                          SPE00930
      CALL MESSAG ('      %S)&E.8H.7(2)&EXHX(=)$',100,'ABUT','ABUT')     SPE00940
      CALL REALNO (VAR(7),15,'ABUT','ABUT')                              SPE00950
C     CALL MESSAG ('      A(REA= )$',100,'ABUT','ABUT')                  SPE00960
C     CALL REALNO (AREA1,15,'ABUT','ABUT')                               SPE00970
C     CALL XNAME ('(F)*B/U)$',100)                                       SPE00980
C     CALL YNAME ('S((F))$',100)                                         SPE00990
C     CALL YNAME ('S((F)) ( * F)$',100)                                  SPE01000
      CALL YNAME ('S((F)) ( * F/)%S)&E.8H.7(2)$',100)                    SPE01010
      CALL XNAME ('(F/)U$',100)                                          SPE01020
      CALL YTICKS (10)                                                   SPE01030
      CALL YAXANG (0.)                                                   SPE01040
      CALL XLOG (0.001,1.2,PYMIN,(PYMAX-PYMIN)/2)                        SPE01050
      CALL SETCLR ('MAGNETA')                                            SPE01060
      CALL CURVE (PX,PY,NPP,0)                                           SPE01070
      CALL RESET ('SETCLR')                                              SPE01080
      CALL RESET ('HEIGHT')                                              SPE01090
      CALL RESET ('YAXANG')                                              SPE01100
```

```
      CALL ENDGR (0)                                                SPE01110
      YOR=YOR-3                                                     SPE01120
  105 CONTINUE                                                      SPE01130
                                                                    SPE01140
      CALL ENDPL (0)                                                SPE01150
      CALL DONEPL                                                   SPE01160
      STOP                                                          SPE01170
      END                                                           SPE01180
```

```
C ***************************************************************** TIM00010
C *   PLOTTING FFT DATA (POWER SPECTRUM & AUTOCORELATION)          * TIM00020
C ***************************************************************** TIM00030
                                                                    TIM00040
      PARAMETER (N=2**14,NS=6857)                                   TIM00050
      IMPLICIT REAL*4 (A-H,O-Z)                                     TIM00060
      INTEGER*2 TARE,ACHAN,ARATE                                    TIM00070
      CHARACTER*64 TEXT,TXT                                         TIM00080
      DIMENSION T(N),G(7,NS),G1(N),G2(N),G3(N),G4(N),G5(N),G6(N),G7(N) TIM00090
   40 FORMAT (A21,A20)                                              TIM00100
   50 FORMAT (3I7,F13.7,I11,2I7)                                    TIM00110
   60 FORMAT (A5,7E17.8)                                            TIM00120
   70 FORMAT (2E17.8)                                               TIM00130
   80 FORMAT (I7,7E16.8)                                            TIM00140
      DT=1./500                                                     TIM00150
      IALFA=0                                                       TIM00160
                                                                    TIM00170
      CALL ANYDEV                                                   TIM00180
C     CALL OMS                                                      TIM00190
      CALL HWROT ('MOVIE')                                          TIM00200
      CALL HWSCAL ('SCREEN')                                        TIM00210
      CALL PAGE (8.5, 11.0)                                         TIM00220
      CALL BASALF ('STANDARD')                                      TIM00230
      CALL MIXALF ('L/CSTD')                                        TIM00240
      CALL MX3ALF ('INSTRU', '&')                                   TIM00250
      YOR=7.                                                        TIM00260
                                                                    TIM00270
      DO 105 J=1,3                                                  TIM00280
        READ (J,40) TEXT,TXT                                        TIM00290
        READ (J,'(A)') TXT                                          TIM00300
        READ (J,50) TARE,IRUN,IPOINT,VMODL,I4SCNS,ACHAN,ARATE       TIM00310
        READ (J,'(A)') TXT                                          TIM00320
        DO 101 K=1,4                                                TIM00330
          READ (J,60) TXT,D,D,D,D,D,D,D                             TIM00340
          READ (J,70) D,D                                           TIM00350
  101   CONTINUE                                                    TIM00360
        NBEG=(I4SCNS-N)/2                                           TIM00370
C       NBEG=1                                                      TIM00380
        NEND=NBEG+N-1                                               TIM00390
C       NEND=2*N                                                    TIM00400
        DO 102 II=1,NBEG-1                                          TIM00410
          READ (J,80) L,(G(I,II), I=1,7)                            TIM00420
  102   CONTINUE                                                    TIM00430
        T(1)=0.                                                     TIM00440
        VMAX=-1000.                                                 TIM00450
        VMIN=+1000.                                                 TIM00460
        DO 120 K=1,N                                                TIM00470
          IF (K.EQ.1) GOTO 110                                      TIM00480
          T(K)=T(K-1)+DT                                            TIM00490
  110     READ (J,80) L,G1(K),G2(K),G3(K),G4(K),G5(K),G6(K),G7(K)   TIM00500
            IF (G1(K).GT.YMAX) YMAX=G1(K)                           TIM00510
            IF (G1(K).LT.YMIN) YMIN=G1(K)                           TIM00520
            IF (G2(K).GT.YMAX) YMAX=G2(K)                           TIM00530
            IF (G2(K).LT.YMIN) YMIN=G2(K)                           TIM00540
            IF (G3(K).GT.YMAX) YMAX=G3(K)                           TIM00550
```

```
            IF (G3(K).LT.YMIN) YMIN=G3(K)                                TIM00560
            IF (G4(K).GT.YMAX) YMAX=G4(K)                                TIM00570
            IF (G4(K).LT.YMIN) YMIN=G4(K)                                TIM00580
            IF (G5(K).GT.YMAX) YMAX=G5(K)                                TIM00590
            IF (G5(K).LT.YMIN) YMIN=G5(K)                                TIM00600
            IF (G6(K).GT.YMAX) YMAX=G6(K)                                TIM00610
            IF (G6(K).LT.YMIN) YMIN=G6(K)                                TIM00620
            IF (G7(K).GT.YMAX) YMAX=G7(K)                                TIM00630
            IF (G7(K).LT.YMIN) YMIN=G7(K)                                TIM00640
  120   CONTINUE                                                         TIM00650
        XMAX=T(N)                                                        TIM00660
        CALL PHYSOR (2.00,YOR)                                           TIM00670
        CALL AREA2D (6.0,2.5)                                            TIM00680
        CALL HEIGHT( 0.08 )                                              TIM00690
        CALL MESSAG (TEXT,21,2.25,-.5)                                   TIM00700
        CALL XNAME ('T(IME (SEC))$',100)                                 TIM00710
        CALL YNAME ('D(ISPLACEMENT)$',100)                               TIM00720
        CALL XTICKS (10)                                                 TIM00730
        CALL YTICKS (10)                                                 TIM00740
        CALL YAXANG (0)                                                  TIM00750
        CALL GRAF (0.,'SCALE',XMAX,YMIN,'SCALE',YMAX)                    TIM00760
        CALL SETCLR ('MAGNETA')                                          TIM00770
C       CALL LEGLIN                                                      TIM00780
        CALL CURVE (T,G1,N,0)                                            TIM00790
        CALL DOT                                                         TIM00800
        CALL CURVE (T,G2,N,0)                                            TIM00810
        CALL CHNDSH                                                      TIM00820
        CALL CURVE (T,G3,N,0)                                            TIM00830
        CALL CHNDOT                                                      TIM00840
        CALL CURVE (T,G4,N,0)                                            TIM00850
        CALL DASH                                                        TIM00860
        CALL CURVE (T,G5,N,0)                                            TIM00870
        CALL CURVE (T,G6,N,0)                                            TIM00880
        CALL DOT                                                         TIM00890
        CALL CURVE (T,G7,N,0)                                            TIM00900
C       CALL LINEST (LEGPAK,170,8)                                       TIM00910
C       CALL LINES ('L(EVEL 1)$',LEGPAK,1)                               TIM00920
C       CALL LINES ('L(EVEL 2)$',LEGPAK,2)                               TIM00930
C       CALL LINES ('L(EVEL 3)$',LEGPAK,3)                               TIM00940
C       CALL LINES ('L(EVEL 4)$',LEGPAK,4)                               TIM00950
C       CALL LINES ('L(EVEL 5)$',LEGPAK,5)                               TIM00960
C       CALL LINES ('L(EVEL 6)$',LEGPAK,6)                               TIM00970
C       CALL LINES ('L(EVEL 7)$',LEGPAK,7)                               TIM00980
C       CALL MYLEGN (' ',1)                                              TIM00990
C       XL=XLEGND (LEGPAK,7)                                             TIM01000
C       YL=YLEGND (LEGPAK,7)                                             TIM01010
C       CALL LEGEND (LEGPAK,7,7.-XL,0.)                                  TIM01020
        CALL RESET ('SETCLR')                                            TIM01030
        CALL RESET ('HEIGHT')                                            TIM01040
        CALL RESET ('YAXANG ')                                           TIM01050
        CALL ENDGR (0)                                                   TIM01060
        YOR=YOR-3                                                        TIM01070
  105 CONTINUE                                                           TIM01080
                                                                         TIM01090
        CALL PHYSOR (0.0, 0.0)                                           TIM01100
```

```
      CALL AREA2D (8.0, 10.5)                                                  TIMO1110
      CALL MESSAG ('R(UN= )$',100,2.0,10.50)                                   TIMO1120
      CALL INTNO (IRUN,'ABUT','ABUT')                                          TIMO1130
      CALL MESSAG ('     P(OINT= )$',100,'ABUT','ABUT')                        TIMO1140
      CALL INTNO (IPOINT,'ABUT','ABUT')                                        TIMO1150
      CALL MESSAG ('     N= $',100,'ABUT','ABUT')                              TIMO1160
      CALL INTNO (N,'ABUT','ABUT')                                             TIMO1170
      CALL MESSAG ('     NBEG= $',100,'ABUT','ABUT')                           TIMO1180
      CALL INTNO (NBEG,'ABUT','ABUT')                                          TIMO1190
      CALL MESSAG ('A(NGLE OF )A(TTACK= )$',100,2.0,10.0)                      TIMO1200
      CALL INTNO (IALFA ,'ABUT','ABUT')                                        TIMO1210
      CALL MESSAG ('   W(IND )S(PEED= )$',100,'ABUT','ABUT')                   TIMO1220
      CALL REALNO (VMODL,3,'ABUT','ABUT')                                      TIMO1230
      CALL MESSAG (' ((M/S))$',100,'ABUT','ABUT')                              TIMO1240
      CALL ENDGR (0)                                                           TIMO1250
                                                                               TIMO1260
      CALL ENDPL (0)                                                           TIMO1270
      CALL DONEPL                                                              TIMO1280
      STOP                                                                     TIMO1290
      END                                                                      TIMO1300
```